The Influence of Electric Charge and Electric Fields on the Formation and Duration of Water Boules.

by

Jeremy Clive Ahern

Being a thesis submitted for the degree

of

Doctor of Philosophy

Brunel University

Department of Design and Systems Engineering

October 2003

The Influence of Electric Charge and Electric Fields on the Formation and Duration of Water Boules.

by

Jeremy Clive Ahern

Being a thesis submitted for the degree

of

Doctor of Philosophy

Brunel University

Department of Design and Systems Engineering

October 2003

ABSTRACT

Consideration is given to the conditions under which floating drops of water, here referred to as water boules, form, exist and coalesce. Particular emphasis is placed on the part played by electric charge and electric fields in these processes.

The literature is reviewed in terms of both the phenomenon of floating drops and of the development of hydrostatics, hydrodynamics and electrohydrodynamics as applicable to the subject. .

Experimental investigations to ascertain the boundary conditions to the influence of such electrical forces are described, together with observations of the connected electrical events. It is confirmed that boules will fail to form at all, *i)* under conditions of high humidity, and *ii)* in the presence of an electric field greater than a certain value. This is investigated experimentally, and shown to be approximately 34kV/m, this figure being about two-thirds that previously reported.

Boules traversing a plane water surface are demonstrated to acquire additional charge in the process. In the case of drops dispensed from a grounded source, forming boules and crossing a bulk water surface some 15cm wide, the additional charge gathered is significant. Boules of 0.055g mass were found to have a mean charge of 1.6×10^{-12}C on leaving a water surface, having arrived as drops with an average charge of 5.8×10^{-14}C. Possible charging mechanisms are discussed. The origin of the initial drop charge is considered, and measurements of this are presented from *(i)*, conventional Faraday cup determinations, and *(ii)*, induction methods applied to free-falling drops.

Experimental investigation of the time-dependent electrical records of the coalescence of a dispensed drop with a plane water surface shows the whole coalescence process to have a two-part form. This detail is commonly hidden within more conventional charge-transfer measurements. For the coalescences investigated experimentally an small initial event is shown to occur, involving a charge transfer in the range $1.2 – 4.8 \times 10^{-12}$C. Oscillograms taken from a large number of coalescences show this preliminary event to be a general feature of the coalescence process, with a number of such traces being appended to the thesis. This initial event is followed by a larger one where the signs of the signals from the drop and the bulk surface are opposite to those of the initial event, and whose potential magnitude is broadly in agreement with that anticipated by double layer disruption.

The interfacial potential difference necessary for the onset of instability and subsequent coalescence in the case of closely opposed drops is shown to be dependent on the relative humidity of the ambient air. Consideration is given to G I Taylor's equation describing the critical potential for the onset of instability between closely spaced drops, and this is shown experimentally to require correction for different humidities. It is demonstrated that the critical potential, V_c, at a relative humidity of 100% is approximately 50% of that at 40% RH. Possible reasons for this are discussed, drawing attention to the problem of establishing an accurate DC relative permittivity value for vapour-laden air in small interfacial gaps. The rôle of evaporation in modifying the system geometry is considered experimentally and theoretically, and shown to be significant only for humidities < 50%. The complex nature of the interface in the case of very small air-gaps is discussed, together with the implications of these investigations for the interfacial stability of a floating drop or boule system.

A theoretical model based on a consideration of the complex liquid-air-liquid interface as a capacitive system is developed, and shown to be in good agreement with practical observations. This model demonstrates that the parts played by electrical forces, together with environmental factors, are likely to be significant in terms of coalescence at stages prior to gap thinning to the point where London/van-der-Waals forces become dominant. Interfacial potentials are calculated in a boule system at a number of times between 0.1 and 10 seconds, and shown to be sufficient to promote instability and coalescence. Full data based on a number of values of instability potentials is appended to the thesis. Development of the model raises questions concerning the validity of currently accepted values both for interfacial stability in small gaps and for the relative permittivity of humid air in similar situations. Suggestions are made for future work in such areas, together with possible methodologies.

The phenomenon of floating water drops is therefore shown to be compatible with the general coalescence process, the event time being modified by such diverse factors as the impact energy with the surface, the ambient humidity and the magnitude of the initial drop charge. The latter is shown to be the dominant factor in the case of drops arriving on a clean surface with low kinetic energies, with the small charge inherent on any water drop being sufficient to produce potentials adequate to promote eventual instability.

DECLARATION

I declare that no part of the work referred to in this thesis has been submitted in support of an application for another degree or qualification in this or any other university or other institution of learning.

Jeremy C Ahern.

October, 2003.

DEDICATION

To the Memory of Bartolomeo Bizio,

Venetian natural philosopher and polymath, who in 1818 watched drops falling from his boatman's oars and floating on the Venice Lagoon, and wondered . . . .

FRONTISPIECE

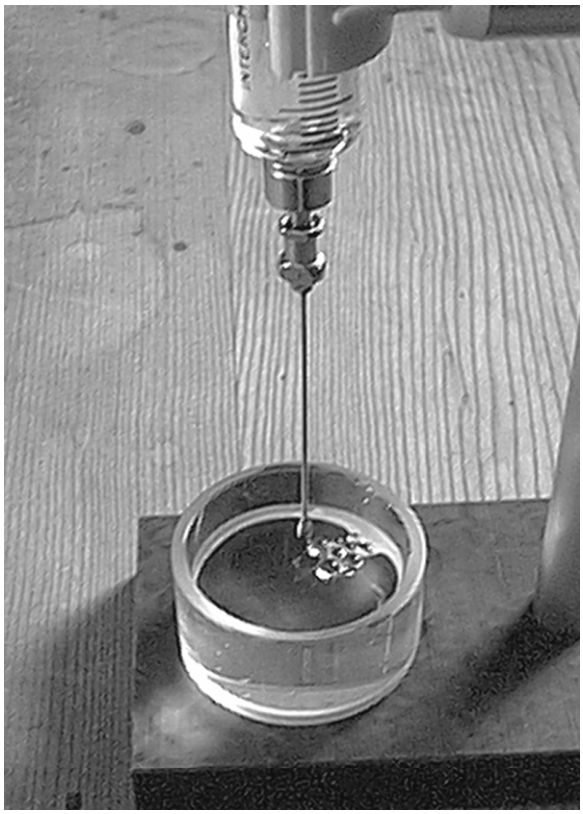

Frontispiece.

Water Boules.

"..un fenomeno ch'offrono in vari casi le gocciole cadenti sulla superfice di un liquido omologo.." *B. Bizio, 1818.*

ACKNOWLEDGEMENTS

On reaching the end of a piece of extended research such as is detailed in this thesis, one is deeply aware of the debt of gratitude that has been building up over time. In many cases assistance and encouragement has been both prolonged and consistent, whilst there have been other instances of brief chance meetings and conversations that have exercised a profound effect on the course of the research. To recall everything is both a difficult and perhaps unnecessary task. The present writer is therefore confining these acknowledgements to individuals and institutions who stand out in his memory as those without whom this research would either never have happened, or else been much the poorer.

_____

A particular debt of gratitude is owed to Professor Wamadeva Balachandran both for his initial encouragement of the research and for his continued wise counsel, involvement and enthusiasm throughout its course.

Dr. Colin Pounder of Ilkeston, Derbyshire, has been both a staunch friend and valued sounding-board for developing ideas throughout, as well as being a source of considerable encouragement to undertake the work.

Mrs Irena McCabe and Dr. Frank James, past and present librarians of the Royal Institution, were both kind and helpful in the search for early and obscure material, and in the loan of rare texts, such as Plateau's works, for private reading.

The staff of the British Library and the Document Supply Centre gave great assistance in helping to trace early serials and in providing copies of papers from all periods.

Yale University Library microfilmed the only known extant copy of Leidenfrost's works.

Professor Henri Gibert of the Embassy of France in London gave useful assistance in obtaining material on Boutigny from the Bibliothéque Nationale.

The Instrument Loan Pool (EPSRC) at the Rutherford Appleton Laboratory made available a Memrecam C^3 and a Kodak 4050 High-speed Video system at different times, and Dr. Adrian Walker of the Loan Pool kindly explained their intricacies.

Dr. Anatol Jaworek of the Institute of Fluid Flow Machinery in Gdansk kindly sent copies of earlier Soviet papers.

Finally, the writer would like to record his deepest thanks to his wife, Mave, for her constant affectionate support, and her cheerful toleration over some years not only of her husband's frequent preoccupation, but also of the sprawling domestic laboratory in which most of the experiments here recorded were performed.

CONTENTS

Table of Contents.

1 GENERAL INTRODUCTION, THESIS STRUCTURE AND CONTRIBUTIONS TO KNOWLEDGE.

1.1 General introduction.

When drops of water fall on a water surface they normally coalesce with it seemingly instantly, merely adding their volume to the bulk. It is, however, not uncommon for coalescence to be delayed for a short period, ranging from a small but perceptible fraction of a second to maybe one or two seconds, during which time the impinging droplet remains suspended on the liquid surface. Occasionally the circumstances of its fall cause the droplet to be almost stationary but more commonly it will dart rapidly across the surface prior to its eventual coalescence.

These floating drops occur not infrequently in everyday life. They are often apparent, for example when a tap drips into a metal sink, or when spray from a fountain or cascade splashes into the pool below. Figure 1.1 illustrates the former of these situations.

Figure 1.1. Floating drops traversing a water surface in a damp sink.

The phenomenon is strangely counter-intuitive. One expects splashes and one expects bubbles, but the sight of actual drops of water apparently floating on water seems somehow disturbing!

These small ephemeral droplets can appear possessed of some sort of life of their own. When present in numbers they either bounce and recoil from one another in a fascinating manner, or coalesce to produce larger and slower drops whose career is often subsequently brief.

Throughout this research the term ‘boule’ is used interchangeably with ‘floating drop’, and this nomenclature, by way of apology, requires some explanation.

The term ‘boule’ is not new in the context of floating drops. It was first coined by Hickman in 1964 [40] with reference to the relatively monster floating drops that he was producing on a superheated liquid surface by a careful reflux condensation of drops that fell a small distance slowly down a rod and formed themselves into one giant floating drop. Hickman explained that his derivation of ‘boule’ was a borrowing from the synthetic-gem makers, who use this word to describe a large single crystal pulled slowly from a fused mass.

The present research is concerned with the diminutive floating droplets that occur at more ambient temperatures, but the term ‘boule’ is extended in this thesis to cover these. Anyone who has watched – or participated in – a game of Petanque will see the fanciful comparison between the interactions of the silvery steel boules on a dusty Petanque court and those floating droplets a-top a water surface. It is therefore with this allusion to the delightful French pass-time in mind, and in affectionate acknowledgement of the part played by early French investigators of the phenomenon, that the term is used!

The mechanism by which boules can remain aloft has been of intermittent interest for nearly two centuries. Early references to the phenomenon are both scarce in number and surprisingly late in appearance, the first that could be established after an exhaustive search being from Bizio, a Venetian philosopher in 1818 [11]. By the end of the

nineteenth century, however, it had become generally accepted that an entrained air-film separated the drop from the surface, coalescence being inhibited until this had drained to the point where the contiguous water surfaces could come into contact.

It was reported by Stong in 1973 [57] that water boules were impossible to form in the presence of an electric field of greater than a certain magnitude, and it was this observation that added impetus to the present writer's interest in the phenomenon, which, developing over a period of time, led to the present research.

It was perhaps inevitable that an investigation of this type should involve a more-than-ordinary amount of practical experimental work. As well as the notorious difficulties involved in taking findings from one topic in electrohydrodynamics and blindly applying them in another, there was a large number of situations for which straightforward data was simply not available in a useful form. Practical investigative work has therefore formed a large part of this research. In general this is described in detail in the relevant places, the only exception to this rule being the block description of the principal methods used in generating streams of droplets for boule formation. The majority of the apparatus used has been of the writer's own design and construction, a process whose frustrations in terms of time consumed have been amply repaid by insight gained.

1.1.1 Aims and Objectives of the Research.

The primary object of the research was to investigate the mechanisms by which boules may form, and which lead to their eventual coalescence. In particular attention has been devoted to the environmental and electrical factors that influence both the formation and duration of water boules, and to the ways in which these factors may differ in both type and magnitude from those associated with the 'normal' coalescence process. Certain parameters such as humidity and the presence of electric fields had been reported by previous workers as exercising a modifying influence over boule formation and maintenance, and the present research has aimed to quantify these effects more accurately, and to build a descriptive model to explain them.

1.2. The Structure of the Thesis.

Following necessary front matter and the writer's grateful acknowledgements to individuals and organizations, the main body of the thesis comprises a total of nine chapters, together with short Appendices containing information and data relevant to the research, but which was inappropriate to include in the main body of the text. The work concludes with a Bibliography listing reference works used during the course of the research and details of individual published papers cited, together with a list of the present author's publications.

There now follows a brief description of the content and scope of the main chapters of the thesis.

1.2.1 Review of literature relevant to water boules.

Chapter 2 presents a review of the principal literature either directly relating to, or generally relevant to, floating drops. Direct material is very limited, and what is presented here is the fruit of a detailed search of both individual institutional libraries in the UK and abroad, together with the currently available electronic datasets. With the notable exception of JSTOR, whose electronic archive includes all Royal Society serials of both the 'Philosophical Transactions' and the 'Proceedings' from their inception, electronic databases are generally confined to material from the last twenty years or less. Whilst many research topics would be very adequately served by such a resource the long time-span over which the contributory threads of the present subject have been woven has meant that much investigation of paper copies of serials has had to be undertaken. In one case this entailed the tracking down and microfilming the only known copy of an early work, which is a salutory reminder of the fragility of knowledge. Several important early papers are of Continental origin and unavailable in English translation, which has given the writer the interesting task of refreshing his small language skills, largely forgotten! Assistance was, however, sought in the translation of Ivchenko and Muradyan's paper [111] from the Russian.

The format of Chapter 2 is substantially chronological. An artificial break is made at the start of the twentieth century by which time the understanding of capillarity and of the influence of electric forces had reached a stage broadly recognisable today. Up to the middle part of the nineteenth century it is important to recognise that interpretation of interfacial events such as those producing boules was largely hampered by a general lack of understanding of capillary forces and of the concept of surface tension. The development of these topics is also briefly reviewed, as lending insight into contemporary thought. This aspect of the review makes no pretence at completeness, but exists to give a context for the main topic. At the start of the twentieth century the scope of the review narrows to focus more specifically on the twin topics of floating drops and the general coalescence process. These are treated under two principal headings: first, (2.3.2), on issues principally of a hydro- or thermohydro- dynamic nature, and extending reference to the part played by surfactants (2.3.3), and secondly, (2.3.4), on the development of electrostatic and electrohydrodynamic considerations. The chapter concludes with summary tables giving the chronological order of key developments as relevant to the research (Table 2.1) and those landmark events in the literature of floating drops and boules (Table 2.2).

1.2.2. Methods of boule production and initial investigations.

Chapter 3 divides into two main parts. The first (3.1) is concerned with the development of methods of boule production for laboratory studies. After a review of the principal methods by which water boules may be formed the two principal methods used throughout the research are described. A ‘launcher’, deriving ultimately from Rayleigh’s investigations into colliding water drops [9], and which may be usefully used to provide a stream of droplets of medium velocity appropriate to glancing impact with a water surface, is described, together with a so-called ‘gentle placement’ technique developed from the methods used by Meunier [13] and Tomlinson [15].

The second part of this chapter (3.2) is concerned with a number of initial experiments that were performed with the twofold purpose of confirming some of the previous results reported from sometimes amateur sources, and for allowing the writer the

opportunity to become familiar with the general ‘feel’ of the phenomena involved. This section of the chapter opens with an initial demonstration (3.2.1) that there is no appreciable matter exchange between boule and bulk surface, perhaps the simplest experiment that can be performed. Methods of establishing cleanliness of the bulk water surface are described, and there then follows (3.2.2-3) experimental work to confirm Stong’s report [57] of the extinction of a stream of water boules in an electric field, and to measure the field-strength at which this occurred.

There follows (3.2.4) an investigation of the extension of boule duration by vibration of the bulk surface, reported by Walker [58]. This is developed to allow for duration times of many minutes, and it is shown that careful manipulation of the standing-wave pattern on the surface allows the boule to be effectively completely stationary.

The chapter concludes by posing a series of questions whose answers would point to a more complete understanding of the part played by electrical forces in both ‘normal’ coalescence and in the delayed coalescence that is, in effect, a definition of the boule system.

1.2.3. Water molecules and the electrical double layer.

Chapter 4 focuses on background material connected with the structure of water molecules and the development of the theory of the electrical double layer. The basic formulation of water in discussed in Section 4.1, with reference to the isotopes of both hydrogen and oxygen. Spatial relationships between molecular orbitals in water are described, together with the electrostatic model of a water molecule as developed by Bjerrum [65].

The concept of the electrical double-layer is introduced (4.2) and a short developmental history of the topic given, concentrating on the early model of Helmholtz [67] and the subsequent refinements to this theory by Gouy [68], Chapman [69] and Stern [70]. This initial review is extended (4.2.1) to a consideration of the electrical double layer at a

gas/liquid interface, and the establishment of the value of the ζ-potential by McTaggart [74], Alty [76] and Chalmers and Pasquill [77].

There follows (4.3) a listing of the principal drop-charging mechanisms, which is succeeded by considerations of charging by disruption of the double layer (4.3.1) and disruption at an orifice, contact and induction charging (4.3.2)

The effect of electric fields and charging on surface tension is considered in Section 4.4. The work of Efimov et al [82], Sato, Kudo and Saito [83] and Schmidt, Hurd and Snavely [84] is cited in this connexion, and it is shown that at charge levels relevant to this research the change in surface tension is insignificantly small. The chapter concludes with a summary (4.5).

1.2.4. Charges transferred by boules, falling and disrupted drops.

Chapter 5 is concerned in its entirety with experimental investigations and issues arising from them. The initial section describes experiments to measure the charge on boules of a specific size that have traversed a horizontal water surface and fallen from its edge, and to compare these charges with those on the droplet stream which provided the boules. It is shown that the traversing action causes the drops to develop charges some two orders of magnitude greater than that found on the initial droplets.

The source of these droplets was grounded, and projected them in a rising arc through the air, prior to their falling into the Faraday cup used for charge measurement. Charges transferred by these drops were therefore compared with those from drops falling vertically from a grounded source into the same cup (5.2.2), and these were found to be in fair agreement. The method, however, has greater uncertainty attached to it than that used in the previous experiment, chiefly arising from the difficulty of establishing a reliably uniform field over a small distance.

Double-layer disruption has already been discussed as a charge source in Chapter 4, and the charges found in the last two experiments were therefore compared with those

which the same sized drops showed on falling through a shielded tube, transferring charge by induction (5.3). These charges are shown to be less by a factor of between two and four times than those measured when the drops were disrupted by splashing into a collecting cup. Possible causes of the discrepancies between the two methods are discussed.

Section 5.4. considers the additional charge that boules had been shown to gather after crossing and leaving a water surface. Possible charging mechanisms are considered, and the dynamics of the situation are shown to be extremely complex, but whilst no firm conclusion can be reached regarding the actual mechanism responsible, a matter-transfer mechanism operating in the highly dynamic and active environment of the system interface is postulated, being referred to for convenience as 'trans-phase charging'. Investigation of the possible mechanism operating is referred to further investigation.

The final section of this chapter (5.5) briefly introduces the conceptual model of the boule system as a capacitor. The general form of the interfacial profile of such a system is known, and if the drop carries a charge relative to the surface, then the intervening air-film forms the dielectric layer in what is effectively a capacitor. In the case of water boules, the 'electrodes' may be considered as conductive, and the fast charge-relaxation time of water ensures uniform surface charge distribution. This concept is developed further in Chapter 8 to produce a practical model of the boule system.

1.2.5. Electrical events accompanying coalescence.

Chapter 6 reports on an investigation into the electrical events that accompany coalescence. In these investigations potential rather than charge is monitored, as this allows for time-dependency to be considered. An experiment carried out early in the research is described (6.1), in which the voltage signal from water in a container was observed as a drop from a grounded needle coalesced with the surface. This showed surprisingly a large amplitude (100 – 400mV) and corresponded with the duration of the coalescence, and investigation was extended to consider signals from both the

originating needle and the ‘well’ containing the bulk liquid, which exhibited considerable symmetry. These initial experiments were then refined (6.2.1) into a series of experiments (6.2.2) where both signal channels were monitored, together with a simultaneous high-speed video record. The high potentials previously recorded were reduced by use of platinum electrodes, and the rationale for their use is discussed. Two novel events are described as a result of these experiments. First, a small electrical event at the moment of coalescence, separate from the principal one associated with bulk matter-transfer is recorded, and, second, the appearance on the video record of a small asperity at the point of coalescence is noted and discussed.

The geometry and film-drainage of approaching liquid surfaces is considered, together with the formation of the dimpled interface, with particular reference to the work of Frankel and Mysels [88] concerning the variation with time of the maximum and minimum thicknesses of the air film. The interpretation of the video record described earlier in the chapter is discussed in the light of this work. The chapter concludes with a short summary of the principal findings.

1.2.6. The effect of humidity variation on the critical coalescence potential between two closely-spaced drops.

Chapter 7 is devoted to an experimental investigation of the effect of humidity variation on the critical coalescence potential between two closely-spaced drops. It had become apparent from the observations of previous workers such as Tomlinson [15], Mahajan [32] and Prokhorov [35] that boule-formation was affected by conditions of high humidity, and a series of experiments was undertaken to investigate whether humidity variation had any discernable effect on the potential difference necessary between two drops to promote their instability and coalescence.

An introduction (7.1) reviews the topic briefly, and focus is then drawn (7.2) to the work of Prokhorov [35] and Lindblad [104], and their principal findings summarized (Table 7.1). Attention then moves (7.3) to an investigation undertaken to assess the rôle of humidity variation in this respect.

Sections 7.3.1. to 7.3.5. describe the design of the experimental arrangements made in some detail, and section 7.4. the practical method employed in their use. A main section (7.5) of experimental results obtained follows, including subsidiary results (7.6) of an investigation of evaporative effects on the drops under investigation. The main results show that increasing humidity exerts a significant influence on the critical coalescence potential, and these are discussed (7.7) in the light of Taylor's earlier investigations [105] into the topic, which had ignored any humidity influence. It is demonstrated (7.8) that for a given geometry a correction factor may be applied to Taylor's work [128]. In order to make a more general correction to Taylor's expression for the critical coalescence potential the rôle of permittivity is considered. The mixed-dielectric nature of vapour-laden air is described, and a hypothetical curve produced to demonstrate how the critical coalescence potential would be brought much closer into line with recorded observations if the permittivity of air in small interfaces were to rise with humidity.

1.2.7. Coalescence dynamics of water boules and system model.

Chapter 8 considers the coalescence of water boules. Following a brief introductory section the chapter opens (8.2) with a consideration of the effects of both air entrainment and impact as they relate to the non-coalescence of boules which had traversed a surface and left it carrying a higher charge than that necessary to produce coalescence in static or slow-moving systems. Jayaratne and Mason's work [54] is cited to demonstrate that bouncing is only inhibited by charges several orders of magnitude greater than those found on 'charged' boules, and that the interfacial profile is significantly modified in such cases, being considerably thicker. The section ends with a summary of relevant data (Table 8.1)

The concept of a capacitive model of the boule system, briefly mentioned in Chapter 5 is then developed (8.3). Preliminary consideration is given to the simplest possible model, consisting of a buoyant spherical drop on a liquid surface, and separated from it by an interstitial air-film of uniform thickness. The possible capacity of such a system is shown to be excessively high. This simplistic model is then replaced by one based on

the known interfacial profile of such a system, and the time-dependent equations of Frankel and Mysels [88] are used to generate maximum and minimum air-gap thicknesses over a time-range for a boule system of the size principally investigated (8.3.2, 8.3.3).

Consideration is then given to modelling the interfacial profile of the air-gap at different times, and to the calculation of its resulting capacity. Whilst the complex and changing geometry of the interface make precise definition of the curvature extremely difficult, it is argued that a profile of generally elliptical curves allows for a good approximation. The capacitance is calculated in two different ways. The first attempt (8.3.4) treats the system as equivalent to a parallel plate capacitor, whose plates are separated by a distance equal to the average of the gap. This is shown to be erroneous by failing to consider the extremities of the system, where capacitance is greatest because separation is least. A second calculation is then made (8.3.5), which both divides the profile into a series of concentric annular discs and extends the radial limit of the capacitor to allow for the not inconsiderable edge effect.

From these calculations a curve of capacitance variation with time (i.e. as the gap profile changes) is drawn.

Section 8.3.6 demonstrates that as both the charge on the drop forming the upper ‘plate’ and the capacity of the system are known, then the effective interfacial potential may be found. Figures for this over a period of 10 seconds are presented for drops carrying charges *i)* equivalent to that on a drop from a grounded source and *ii)* that on a charged boule.

The chapter continues to consider instability at air/water interfaces (8.4). Following a brief review of earlier work, the investigations of Taylor [105] and Taylor and McEwan [124], together with the more recent ones of Eow et al [126, 127] are focused upon. Instability between both convex/convex and plano/convex interfaces is considered, but it is pointed out that the data available is that for comparatively large interfaces, and should be applied cautiously in the case of much smaller ones.

A realistic figure for the instability limit in the boule system is hypothesized, and on this basis instability in the model is determined. The model demonstrates that despite rising capacitance due to the draining of the air-film, the closest points of the capacitor converge even more rapidly, and in consequence instability can occur at these points.

The time-dependent interfacial fields arising from drops with a range of initial charges is then calculated (8.5), and the resulting figures applied to the model to obtain maximum duration times for the system. Because of the questionable nature of the exact interfacial field-strength necessary to promote coalescence in such a system values are computed for a range of interfacial fields. Summary data are presented in tabular form (Table 8.5), and the entire dataset in Appendix 5.

The chapter concludes with an interpretation of the data as applied to the model, and with reference to the field-enhancement which would in practice occur as a result of charge distribution variations at the interfacial surfaces. It is shown that these will result in an effective shortening of the system dwell-time as a result of the increased interfacial field at the most sensitive part of the interface.

1.2.8. Summary and recommendation for further study.

Chapter 9 summarizes the work in the research, presenting the most important findings in order, concluding with recommendations for further study. Five principal and pivotal areas are identified and suggestions made in each case for possible approaches to the problem.

1.3 Contributions to knowledge.

As a result of this research the following contributions to knowledge are claimed.

1. The inhibiting effect of an electric field upon the formation of boules previously reported by Stong [57] is confirmed and the magnitude of that

limiting field is shown to be lower than the figure reported at that time (Sections 3.2.2, 3.2.3).

2. It is demonstrated that some charging mechanism applies to boules traversing a water surface, resulting in their charge enhancement by some two orders of magnitude (Section 5.1).

3. The electrical processes accompanying drop/surface coalescence are shown to consist of two phases. Time-dependent analysis has shown that there is a small preliminary event at the onset of coalescence, and that this initial event is followed by a sign-reversed main event as the coalescing drop undergoes complete disruption (Section 6.2.2). Visual evidence is presented for a disturbance on the plane surface coincident with onset (Section 6.4 and Appendix 4).

4. It is demonstrated that the critical coalescence potential between two closely-spaced drops is humidity dependent, and that the magnitude of this potential decreases with increasing humidity (Sections 7.5.1, 7.5.3). This may be accommodated for specific geometries by the application of a correction factor, but in general terms it is shown to bring into question the previous assumption that the relative permittivity of the vapour-laden interface between two drops in close proximity is that of either free space or dry air (Section 7.8). It is shown that a permittivity > 8.854×10^{-12}F/m is necessary to adjust the interfacial force balance in existing expressions describing the critical coalescence potential.

5. It is shown that the interface between a boule and a bulk surface may be modelled as having a variable time-dependent capacity. This capacitive element is shown to have geometric characteristics that result in rising capacity during film-drainage being accompanied by a proportionally greater reduction in the minimum interfacial gap, with a consequent rise in field gradient at the capacitive rim. The model demonstrates that this rise allows the field gradient to rise to levels sufficient to promote

instability and consequent coalescence (Section 8.2.5). The model is shown to give realistic conformity to measured values of external field, given some uncertainty concerning the exact values for the interfacial instability potential and the interfacial relative permittivity (Sections 8.2.6 to 8.4).

2 A REVIEW OF THE LITERATURE RELEVANT TO WATER BOULES AND FLOATING DROPS.

2.1 Introduction

This chapter presents an historical review of the literature relating to the several aspects of the coalescence process as it applies to floating drops or boules, with eventual particular emphasis on the influence of electric charges and forces. This latter area is historically relatively recent, but earlier work leading to a fuller understanding of the effects of electric fields and charges on liquids, as well as of the development of the hydro- and thermohydrodynamics of the liquids themselves, is important for the insight it lends to the primary subject of this research. This review covers some of the normal coalescence processes and those variant conditions, causing phenomena such as floating drops, which present themselves under certain favourable conditions.

The earliest work was qualitative and observational, descriptive of phenomena but without the means either of quantitative measurement or of theoretical interpretation. It is, however, of considerable interest in demonstrating just how long the knowledge of many phenomena has existed, as well as for the picture it paints of the observational acuity of the earlier experimenters. Many, if not most, of the basic phenomena concerning the effects of an electric field or electric charge upon liquids had been observed at least in part by the middle part of the eighteenth century, and the early records of these give us a profound insight both into contemporary scientific agendas, as well as the bases for the development of subsequent theoretical work.

So that some order may be imposed upon the several contributory threads, the topics are considered in the following sequence.

1. Early history (to the end of the 19th Century) of, *(i)*, the effect of electricity on charged liquid bodies, *(ii)*, floating drops and boules, and, *(iii)*, aspects of the development of concepts of capillarity and surface tension in respect of coalescence.

2. The development of the understanding of coalescence and its anomalies from the beginning of the 20th Century to the present, with an emphasis on the developing relevant electrohydrodynamics.

2.2 Early history of the topic.

2.2.1 The Effects of Charged Bodies on Liquids.

That an electric field could have an effect upon a liquid was realized early in the history of electricity. The first reliable reference is to be found in William Gilbert's great work, ***De Magnete*** of 1600, [1] where he notes the effect of a piece of charged amber upon water drops. His words give unequivocal evidence of his observations:

> *"Hence it is probable that amber exhales something peculiar that attracts the bodies themselves, and not the air. It plainly attracts the body itself in the case of a spherical drop of water standing on a dry surface; for a piece of amber held at a suitable distance pulls toward itself the nearest particles and draws them up into a cone; were they drawn by the air the whole drop would come toward the amber".*

In the middle of the seventeenth century Sir Thomas Browne takes up the theme, and in his curious and compendious ***Pseudodoxia Epidemica***, published in 1646 [2], refers to Gilbert's observations, and extends them to include oils. Speaking of bringing charged amber close to oil, he states:

> *"It will likewise attract oyl it self, and if it approacheth unto a drop thereof, it becometh conical, and ariseth up unto it . . ."*

The origin of his knowledge of the effect of an electrically charged body on oil is unclear. It may be a result of Browne's own experiments, or he may have gleaned it from the ***Philosophia Magnetica*** of Niccolò Cabeo which was published in 1629. Certainly after the publication of the ***Pseudodoxia*** the phenomenon became widely known. Tyndall, during his Christmas Lectures delivered at the Royal Institution in 1875-6, [3] referred to the attraction of oil as *". . . the experiment of the Florentine*

Academicians", suggesting an alternative origin. The Accademia del Cimento, however, was founded only in 1657, surviving just ten years, and Browne's own reference predates this by almost a decade. Origins notwithstanding, the experiment, capitalizing as it does on the long relaxation time of oils and their relatively high viscosities, both of which factors help to render the pulling of the oil into threads and cones more readily visible, remained a popular elementary demonstration well into the twentieth century.

Little of moment was added to the subject until the second quarter of the eighteenth century, when Stephen Gray reported first on the attraction of a soap bubble by a charged rod [4], and subsequently on a rather more detailed series of experiments with water surfaces [5]. This latter publication described first the charging by induction of a small quantity of water held in a dish upon an insulated stand, with a subsequent concavity forming upon the surface when repelled by a like charge brought close to it, and then of the effect observed upon bringing an electrified rod near the surface of water held in a very small insulated container, such that the water meniscus was above the container's rim. As well as noting, with Gilbert, the formation of a cone at the water surface, Gray also repeated the experiment in the dark and observed a visible corona, accompanied by a noise described as;

> *"a snapping noise, almost like that when the fingers are held near the* (charged) *tube, but not quite so loud, and of a more flat sound."*

Repeating the experiment in bright sunlight Gray noted that, on bringing a charged glass tube close to the water surface, small droplets were evolved, and,

> *"that sometimes there would arise a very fine stream of water from the vertex of the cone, in the manner of a fountain, from which there issued a fine steam, or vapour, whose particles were so small as not to be seen; yet it is certain it must be so since the under side of the tube was wet, as I found when I came to rub the tube again; and I have since found, that although there does not always arise that cylinder of water, yet there is always a stream of invisible particles thrown on the tube, and sometimes to that degree as to be visible on it."*

Gray's words are quoted at length, as they leave little room for doubt that in these finely observed experiments he was recording the same phenomenon of electrohydrodynamic

atomization that had to wait for more than a century and a half to be investigated quantitatively and theoretically by such investigators as Rayleigh, Zeleney and Taylor.

Gilbert and Gray are perhaps the greatest – certainly amongst the most widely known – of the observers of the effects of a charged body on liquids during the early phase of electrical history. Others, however, made significant contributions, and these are worthy of recall.

The Abbè Nollet of the Royal Academy of Sciences in Paris was a dominant figure in European electrical research in the middle of the eighteenth century, and he experimented with drops of water issuing from an insulated container, demonstrating the coalescence of drops into a continuous stream when charged, and making observations of the effect of varying the orifice size. [6] Additionally, he made measurements of the rates of flow of water from an orifice with both charged and uncharged streams, and, in a sequence of over a hundred individual experiments, concluded that the rate of emission was greater when the water is charged. He also observed that if the orifice were sufficiently large *". . . greater than three lines . ."* (i.e. ¼ inch), and uncharged water allowed to issue from it in a stream, then charging it sufficiently highly caused the stream to diverge into several individual jets (Figure 2.1.*a*). Nollet extended his work to speculate that electric charge might modify the transport of liquids in plants and animals, performing experiments to compare water loss in birds and mammals when charged with their equivalent uncharged rates. Interestingly, these general researches were further extended to embrace the effect of electric charge on the speed of germination of seeds, with the result that he claimed that the presence of charge promoted both germination and quality of growth – an idea that has been the subject of intermittent investigation ever since! (Figure 2.1*b*)

Also in 1747, John Ellicott independently presented a paper to the Royal Society [7] in which, like Nollet, he described an experiment demonstrating the coalescence of water drops issuing from a syphon in a reservoir attached to the prime conductor of an electrical machine. He observed that upon ceasing to turn the machine the stream of water instantly returned to a dripping mode, this abrupt change doubtless aided by the relatively fast leakage to earth of contemporary insulators. Ellicott was also well aware

of the rise of liquids in capillary tubes, and experimented with charging water into which capillary tubes had been inserted, to see if a change in the level of capillary rise might be detected. This he failed to do, but his work is perhaps the first conscious effort to consider the effect of charge upon surface tension.

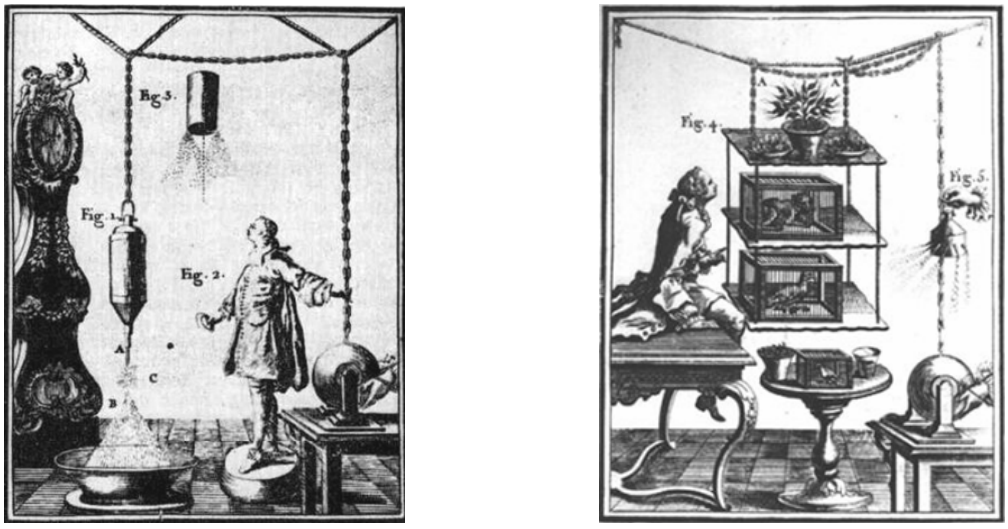

Figure 2.1. The Abbé Nollet's experiments on *(a, left)* electrostatic spraying, and, *(b, right)* the effects of electrification on the water-loss in animals and the growth of plants. *(From Recherches sur les Causes Particulieres des Phenomenes Electriques, par l'Abbe Nollet, 1753).*

Like Nollet, therefore, Ellicott investigated the rate of flow of water issuing from a small orifice both when charged and when grounded. His account leaves one with the distinct impression that he was seeking an explanation beyond the simple observation of the difference caused by the presence or absence of charge, and was moving towards a notion that the charge had a specific effect in modifying some physical property of the liquid. By implication this would mean its surface tension, although the concept of this had yet to evolve. Ellicott further observed the repulsion between falling drops in a more powerful electric field, a phenomenon that had to wait for a further hundred and thirty years for Rayleigh's explanation.

Fashions in scientific research applied in the eighteenth century, as today, and after about 1750 the philosophers' electrical interests turned to other matters. Franklin's work stimulated a spate of investigations into atmospheric electricity, and this was partly paralleled, and then overshadowed, by growing interest in matters of tribo-charging and

charge induction. These were doubtless encouraged by the beginnings of more quantitative research made possible both by the new electrometers of such men an Henly and Bennet, and, towards the end of the eighteenth and early into the nineteenth centuries, by the evolving theoretical work of such men as Cavendish, Poisson, Coulomb and Green. Within this period, however, aspects of Henly's work demonstrating the transport of charge by water drops advanced electrohydrodynamic knowledge significantly. In a wide-ranging series of experiments [8] he recorded both the emission of charged drops from a capillary and the conducting nature of water vapour, and moreover noted the effects of water temperature on the conductivity of the surrounding air. In doing so he made, if somewhat unwittingly, what is probably the first specific connexion between humidity and the conductivity of the air.

Throughout the first half of the nineteenth century interest in voltaic electricity was in the ascendent, in parallel with a growing understanding of electrochemistry. This, together with the rise of electromagnetism, chiefly following Faraday's pioneering work in both fields, dictated the principal areas of electrical research. Interest in the effects of electric charge on liquids therefore went generally into eclipse, and, with very few exceptions, it was not until the experimental work of Rayleigh in the third quarter of the nineteenth century that more of significance was contributed.

Rayleigh's contribution to knowledge proved pivotal to the subject area to the extent that today many of his writings are still frequently cited as a kind of 'root of title' in electro-hydrodynamical research.

In a well-known paper of 1879, ***"On the Influence of Electricity on Colliding Water-Drops"*** [9], Rayleigh described the moderating influence of weak electric fields on two droplet streams impinging upon one another. Uncharged drops will rebound from one another, whilst even very weak fields are shown to produce coalescence. (Increasing the fields beyond a certain point, however, leads to sufficiently high charges on the drops that they repel each other, a circumstance observed by Ellicott, and accurately interpreted by Rayleigh).

The significance of Rayleigh's paper on the present research is two-fold. First it established, albeit qualitatively, that a charge difference between colliding drops will promote coalescence, and that the required quantity of charge is very small. He quoted the potential difference of a single Grove cell (~ 2.0v) as imparting an adequate charge to promote coalescence between the experimental drops. Secondly, the normality of rebound between uncharged colliding drops, which may be considered to have clean surfaces, together with the implied 'buffering' effect of entrained air, is of considerable interest in the context of the present research. In addition, Rayleigh noted the effect of surfactants upon coalescence, and the impossibility of producing rebounds between colliding drops if they contained such a material.

The century concluded with a second paper by Rayleigh [10] in which he again addressed the topic, and speculated on the mechanism that might promote coalescence between two electrified streams of droplets. Two possible causes were examined. The first considered the possibility of direct electrical discharge – a spark – across the intervening small air gap between the drops. This he rejected on the basis of contemporary knowledge of the potentials necessary to initiate such a discharge. The second explanation suggested introduced the important concept of instability, and moved research towards a consideration of the hydrodynamic instabilities operating in such a circumstance. These, it was argued, would be increased because of small charge differences, and, whilst the viscosity of the trapped air would be sufficiently high to render its complete expulsion unlikely over the event duration, the opposing liquid surfaces would develop corruscations, resulting in some extreme localized thinning of the gap. Small dust-motes or airborne particulates would then be able to bridge the gap, causing coalescence.

Rayleigh recognized that a large increase in field-strength would be established by the geometry of such aspereties, but seems to have stopped short of considering conclusively that either these high local potential gradients might be adequate to disrupt the liquid surface and produce matter transferrence, or that adhering surface particulates from dust motes might similarly act as discharge points.

This, then, represents in broad terms the understanding of the effects of charge upon liquids at the close of the nineteenth century.

2.2.2 Floating Drops and Boules.

Perhaps strangely for a phenomenon that most people must have sometime witnessed, there is no apparent early reference to floating drops or water boules. Amongst the ancients, neither Aristotle nor Lucretius mention it nor the later mediaeval philosophers such as Grosseteste and Bacon, and in the early years of the Age of Enlightenment even the indefatigably curious Sir Thomas Browne passes it by. The first traceable reference to floating drops appears to be in a paper by the Venetian, Bartolomeo Bizio, [11] written in 1818. In this he described watching drops of water falling from his boatman's oars on to the surface of a lagoon. Bizio reproduced the phenomenon in the laboratory, and extended the range of liquids producing boules of different liquids including alcohol, ammonia and mercury. (This latter success is worthy of note, given the rapid rate of contamination of a mercury surface in air.) He also recorded the first known observation of boules being produced during filtration processes, as drops of filtrate splashed into the receiving vessel.

The paper is interesting both for its phenomenological observations and also for its author's comment on the lack of previous references to the phenomenon, a situation which an extended search of the indices of long-established serial publications such as the *Philosophical Magazine*, the *Philosophical Transactions*, Poggendorf's *Annalen* and the *Comptes Rendus*, together with earlier Continental sources, confirms.

Bizio speculated on the cause of the floating drops, but with an inadequate understanding of the nature of liquid surfaces. He concluded, in part as a result of correspondence with his contemporary Bellani, [11, *p280.*] that the surface of a liquid must be covered by a pellicle of some sort, adding some quality of resilience to the surface of drops. Although such conjecture is long since untenable, it affords an interesting insight into contemporary ideas of capillarity and surface tension.

A period of some silence on the topic then ensued, until broken by Sire [12] in 1853, in a communication in which he observed the extended duration of ether boules, attributing their greater longevity to the volatility of ether, with a resulting copious vapour layer acting as a suspending cushion between the surfaces.

Meunier continued the Continental monopoly of the subject by publishing in 1863 an important Note [13], ***De la Forme Globulaire que les Liquides et le Gaz peuvent prendre sur leur propre Surface***. (A translation is to be found in Appendix 1.) Like Bizio, Meunier expressed his surprise at the lack of reference to the phenomenon in the literature. He gave the results of some detailed experimental observations of boules of water, alcohol and glacial acetic acid. He also recorded, as had Bizio before him, the formation of boules during the slow process of filtration, and likened their general appearance to the Leidenfrost drops with which his French contemporary Boutigny was then engaged [14].

Meunier's technique for producing boules was to dip a glass rod into the liquid, withdraw it carefully, and allow some of the adhering liquid to fall upon the surface. He made the interesting observation that success in this was best assured by floating a thin layer of the experimental liquid upon a substrate of a denser liquid with which it was immiscible. By projecting alcohol boules on an alcohol surface coloured with tincture of iodine, he was able to demonstrate that prior to coalescence there is no liquid contact between the boule and the bulk liquid. He also records the ejection of material, forming a smaller secondary boule during the coalescence of the first boule with the surface. Observations of this phenomenon were continued to include colliding boules, and to note the production of as many as five or six secondaries upon eventual coalescence with the bulk surface.

In discussing his findings, Meunier compared boules with the air bubbles evolved by gently warming aerated water, and concluded that the mechanism of their production was in some way a product of interphase forces acting between the liquid and its vapour.

In the same year (1863) Tomlinson of King's College, London, [15] extended Meunier's work to include boules of essential oils, concentrating on oils of turpentine and eucalyptus. He made three principal observations, the latter two of which prove to have considerable relevance to the present research:

i) that freshly distilled turpentine produced boules of longer duration that older stock;

ii) that boule formation is suppressed by conditions of high humidity;

iii) that there are extensive streaming currents within the boule, demonstrated by dusting boules with lycopodium powder and observing their movements to show the convection-type currents.

Tomlinson also observed that whilst boules of fatty oils are impossible to produce at room temperatures, they happen with comparative ease at elevated ones (refined fish-oil at 320°C being quoted), and that this material used as a bulk liquid would also support boules of other oils, water and ether at this temperature.

Tomlinson's paper is interesting in two respects. First, it is apparent, especially in his treatment of liquid drops supported on a high-temperature substrate as described, that he wished to interpret boules as a form of the 'spheroidal state', a concept forwarded by Boutigny [14] as a development of the observations and writings of Leidenfrost [16]. There is little doubt that he was working towards an interpretation of the phenomenon of floating drops as part of a 'spheroidal state' process operating throughout an extended temperature range, i.e. without consideration of the critical Leidenfrost Point. In this respect he was at little variance with his contemporary Meunier, and the emphasis that both researchers placed on the 'spheroidal state' makes an interesting comment on contemporary concepts of phase states. Secondly, Tomlinson interpreted his observation of the streaming currents within the boule as being corroboration of the Marangoni effect. In later investigations he veered towards considerations of wetting and of interfacial tensions between liquids, and, although the phenomenon in question was subsequently alluded to, he did not develop it further.

References to true boules in the nineteenth century conclude with a Note of 1882 by Reynolds [17], in which he pointed out the necessity for surface cleanliness before boules would form, and described a simple technique for obtaining a temporarily clean water surface. This entailed dusting the surface with flowers of sulphur and then splashing drops of water on it to form a new clean surface, this being indicated by the sulphured surface being driven back. The concluding sentence of his Note contains the curious comment;

> *". . .whatever may be the cause of this suspension* (i.e. floating drops) *it depends only on the surface of the water being pure, and not at all on the temperature or condition of the air,"*

This remark seems strangely at odds with Tomlinson's investigations, where the environmental constraints of temperature and humidity were carefully monitored and their respective influences noted, and with the experimental evidence he offered for the difficulty of forming boules in humid conditions.

A passing reference should also be made to a paper by Maltézos [18]. Whilst not strictly concerning boules as defined, it is nonetheless of some interest. He discussed small drops - *microglobules* - of mercury being floated on the surface of water, olive oil or petroleum. This phenomenon was correctly explained in terms of interfacial tensions extant between the two liquids and air, considered in pairs in turn, and demonstrates the development and acceptance of what are now considered to be the classical interpretations of interfacial forces in this situation.

2.2.3 The Development of Concepts of Surface Tension.

A detailed review of the literature chronicling the development of contemporary concepts of capillarity and surface energy would be voluminous in its own right, and the task here is to give but a brief outline of the principal developments up to the turn of the twentieth century.

The skin-like behaviour of liquid surfaces, and in particular that of water, had been known since antiquity, and the first attempts at explanation, alluded to above, treated

the surface as if covered with some pellicle, thus imparting a type of exterior film on the liquid surface, and, in the case of small drops, forming a containing bag. This concept very slowly gave way as new ideas were brought to bear on the question. The new instruments of thermometers and barometers, developed in the seventeenth century, brought familiarity with capillary tubes, and with it wider knowledge of the rise of the meniscus where a wetting liquid surface touched the bore of the tube, or of meniscus depression in the case of a non-wetting liquid such as mercury. The concept of *cohesion* arose, and with it the first attempts at measuring the cohesive forces at work at a liquid/solid boundary.

Hauksbee published two papers in the early years of the eighteenth century which contain the first accounts of any detailed investigation of capillary rise. In the first of these, of 1710, [19], he gave a description of two glass plates formed into a narrow wedge, with a film of oil of orange between them. In a second paper of two years later [20], he gave the results of more detailed investigations of the form of the curve taken by the oil film, and recorded what is probably the first experimental data concerning this.

Following Hauksbee's death in 1713 the investigation of capillary rise was extended by Jurin. In two papers, published in 1717 and 1719 [21, 22], he discussed the rise of the water level in a capillary tube as a function of the cohesive forces, and derived a relationship stating that the capillary rise is inversely proportional to the tube radius. (It is interesting to note that he was initially led to these investigations in an attempt to produce perpetual motion by making an unequal-armed syphon of tapering bore. Whilst he was phlegmatic about his failure in this endeavour, the episode well illustrates the deeply engrained hope – not totally extinct even today – that such an outcome might be possible!)

Investigators such as Hauksbee and Jurin were essentially considering the problem from a purely hydrostatic viewpoint, and real progress was not made until the old static picture of liquids and gases was displaced by the evolution of thermodynamic theory and by the rise of the Kinetic theory of matter. The theoretical models of Young [23] and Laplace [24], and their later development by Gauss [25], took some time to take

effective root, but the result was that Tomlinson, for example, had available to him an understanding totally denied to Bizio half a century before. Maltézos' explanation of his 'microglobules' reflects very clearly the development of knowledge throughout the century. By the end of the nineteenth century Plateau's work on surface tension and capillary forces [26] was widely known, and what we now view as the classical hydrodynamics of these phenomena had been firmly established.

Two excellent summaries, both from the 1870s, record the development of knowledge of surface forces. The first, written as a review paper in 1873 by Van der Mensbrugge [27], concentrates on the development of surface dynamics from the close of the eighteenth century. This cited the work of many Continental *savants*, many regrettably relatively unknown in England. The second, far better known account, is James Clerk Maxwell's article on 'Capillary Action' [28] written for the Ninth Edition of the *Encyclopædia Britannica*, and published in 1876. As well as tracing a history of the topic this article provided a concise but succinct mathematical analysis of surface tension and surface forces, to the extent that it is still a valuable reference a century and a quarter later.

One cannot leave the nineteenth century without making mention of two publications, each of which exercised considerable influence on the study of hydrodynamics and the phenomena of liquid surfaces. The first of these was the appearance in book form, of a series of Christmas Lectures given in 1889 at the Royal Institution by C.V. Boys entitled "***Soap Bubbles and the Forces that Mould Them***" [29]. This little volume, as well as having considerable charm, represents an excellent, if popular, summary of the state of contemporary knowledge and understanding of the topic. Furthermore, it may be argued that its appearance did much to ensure that the phenomena it described became a part of the canon of the school science teaching then evolving under the influence of such men as John Tyndall and Sylvanus Thompson, and hence established within the framework of 'necessary knowledge' for students.

Finally, reference must be made to the work of A.M. Worthington. His researches into the dynamics of splashes covered much of the last decade of the century, and his various published papers were summarized in ***'A Study of Splashes'*** issued in 1908 [30]. This

contained the first effective high-speed photographs of splashes and coalescence events, and allowed their analysis in a way hitherto unknown.

Both of these writers seem to form a natural conclusion to the century. Each was an experimentalist of great skill and dedication, and each brought new techniques to bear on his topic, laying foundations both for future work and of experimental methodologies that were to develop throughout the twentieth century.

2.3 Work on Floating Drops and Coalescence from the beginning of the Twentieth Century.

2.3.1 Introduction.

The close of one century and the start of another is an arbitary event in the way that it touches upon progress and research, and in an historical review a division of this sort is at best a compiler's convenience: the landmarks of a subject's history pay no heed to the Calendar. In the present case, however, it happens that something of a hiatus occurs in the development of boules as a topic of research, and there was nothing of consequence produced for nearly fifty years after Reynold's observations of 1882. (In passing it is interesting to note that this was also a period of considerable activity and development in the areas both of fluid dynamics and of surface science, and the lack of research activity into floating drops during this time may well explain the paucity of reference to the phenomenon in most standard texts, with only Adam, 1930 [31] having been found to make a passing note). This relatively long period of silence in respect of the subject of the present research is important for more than just its mere existence. The inevitable outcome was that when interest again began, albeit sporadically, it was through a scientific approach quite different from that which had guided the work of the nineteenth century philosophers.

Old investigative phenomenology, qualitative by nature and concerned more with revealing 'the wonders of the world' had given way to a far more rigorous,

mathematically-based theoretical determinism, and the old, 'holistic' physics or Natural Philosophy had divided into a range of sub-disciplines. The result is that the literature of the topic was now disseminated across several discrete subject areas, however blurred their boundaries might become at their margins.

In consequence, it is more convenient – and useful – to review the literature of floating drops during the twentieth century under two headings; those that treat the phenomenon in purely hydrodynamic or thermohydrodynamic terms, and those that investigate the effects of electrical fields and charges, i.e. electrohydrodynamic considerations. There will, of course, be occasions when the distinction between these two camps cannot be clearly drawn, but the device is useful in helping to focus on the background development of the present research.

2.3.2 Developments of a mainly Hydro- or Thermohydro-dynamic Nature.

Work in the first half of the twentieth century was almost exclusively aimed at investigations into the entrained air-film between two drops, or between a drop and a bulk liquid surface. The first publication of any moment was in 1930, when Mahajan published a paper [32] presenting experimental evidence that the stability of floating drops, and hence their longevity, is governed by the drainage rate of the air-film between them. In a further paper [33] Mahajan reported on the ease with which boules might be formed at high altitudes when they could not be formed at sea-level. Further evidence of the importance of this air-film was supplied by Benedicks and Sederholm, who in 1944 [34] reported that floating drops could not be formed *in vacuo*.

These results were, however, largely qualitative, and the first serious attempt to consider the dynamics of the situation was made by Prokhorov in 1954, when he published a paper [35] on an investigation into the form of the entrained air-film, and the way in which its drainage is modified by the extent to which the surrounding air is saturated with the liquid vapour – in the case of water by the relative humidity of the surrounding atmosphere. Details of Prokhorov's findings are examined more closely in Chapter 7 during a consideration of the effects of relative humidity on the potential difference

between drops needed to produce instability and coalescence, and it is sufficient here to state his principal conclusion, that for conditions of humidity deficit, i.e. relative humidities below 100%, there is a chance of boules forming, but that at saturation coalescence is effectively certain.

This result is interesting in that it refuted Reynold's assertion [17] that environmental considerations other than surface cleanliness are unimportant in boule formation, and supported Tomlinson's findings of 1863 [15] that boules could not be formed under conditions of very high humidity. It is one of the principal purposes of the present research to demonstrate that under these conditions electrical, as well as these environmental, hydro- and thermohydrodynamic considerations, play a significant rôle in determining coalescence.

One further contribution during the 1950s was made by Baird in 1959 [36], who considered the formation of inverse bubbles, sometimes referred to as 'antibubbles', in which a small globule of liquid surrounded by a thin air-film is induced to remain in the body of a bulk volume of the same liquid. This process generally involves the use of surfactants of some sort, and is largely outside the scope of the present research, but the work is interesting in that it reported that the minimum air-film thickness for the stability of an inverse bubble is of the order of 300nm, and that with the particular surface agents used coalescence always occurred before the air-film had thinned to the point where first-order interference of the illumination source could be obtained. (For sodium D lines, $\lambda/4 = 147.3$ nm). The use of surfactants in promoting boule formation will be discussed later in the light of recent work in the field. Baird concluded that the eventual rupture of the air-film was the result solely of van der Waals forces acting across its thickness, a viewpoint which requires reconsideration in the light of the present research.

1960 saw the publication, within a few days of one another, of two papers of considerable importance for the topic, if for different reasons. The first of these was by Scriven and Sternling [37], and was in the form of a review of the Marangoni effect. This short but scholarly review traced the history of the Marangoni effect, the variation in local interfacial tension and consequent surface activity brought about by small

variations in material composition or of temperature. The topic was traced from its original explanation by J. Thompson, (brother of Sir W. Thompson) in 1855 [38] to the claim to its discovery made by Marangoni in 1871, which resulted in his name being 'attached' to the phenomenon. Scriven and Stenling's paper is of importance in the present context because it served to re-focus contemporary minds on the local surface convective movements resulting from small temperature differences.

The second paper of 1960 was by Schotland [39] and describes experimental results obtained for collisions of small (200 - 800μm diameter) water drops with a water surface, in this case a surface produced by over-filling glass tubes in the range 6 - 30mm diameter to produce either a flat surface or one with a required radius of curvature. In a preliminary discussion Schotland considered the question of falling raindrops and their collision efficiency, *C*, which statistically must lie within the range $0 < C < 1$, designing his apparatus such that all drops collided with the surface, i.e. $C = 1$.

The initiation of coalescence for drops in equilibrium with their vapour was shown to depend on the following non-dimensional relationships,

$$\pi_1 = \rho_D V_N^2 D / \gamma \tag{2.1}$$

and,

$$\pi_2 = \rho_M / \rho_D \tag{2.2}$$

where ρ_D is the drop density, ρ_M the medium density, γ the surface tension, V_N the normal component of the impact velocity, and D the drop diameter, connected by the functional relationship,

$$f(\pi_1, \pi_2) = 0 \tag{2.3}$$

π_1 is therefore proportional to the ratio of the kinetic energy of the drop to the energy needed to deform the surface of the liquid target, and π_2 is the density scale factor.

Schotland's findings are important in two respects: first, they formed a hydrodynamic basis upon which other researchers built, and, second, his experimental technique took steps to ensure the electrical neutrality of both the falling drops and the surface upon

which they impinged. This second circumstance requires some amplification. Rayleigh [9] had demonstrated the effect of very small electric fields in promoting coalescence, and Schotland was one of the first workers to recognise the relevance of this. However, in the light of evidence presented in Chapter 5, it is doubtful whether drop neutrality was completely achieved in these experiments, or, indeed, is ever truly achievable.

Following Schotland's work a change of emphasis may be found in the general literature of the subject: the emerging science of electrohydrodynamics began to assert itself, and some polarization of interests is discernible. It should therefore be borne in mind that some bifurcation of the literature emphasis now occurred, the more electrohydrodynamical aspects of this being dealt with in the following section.

The term 'boule' first appeared in a paper by Hickman, 1964 [40] where he used the term to describe large floating drops, generated by a reflux distillation process, on the top surface of a superheated bulk of the same liquid within a closed apparatus. The formation of the boule was attributed to the activity of the vapour-film separating it from the mother liquor. This vapour film, referred to by Hickman as the shroud, has minimum thickness at its base (lowest point), where the hydraulic pressure of the supported boule is greatest and vapour mobility least, and its maximum at the rim where the vapour velocity is greatest and the effective pressure difference to the atmosphere is zero. The mother liquor was superheated to between 2 and 5ºC above normal boiling point, heating being from the sides, by means of an annular heating mantle. Figure 2.2 details the boule and bulk liquid diagrammatically.

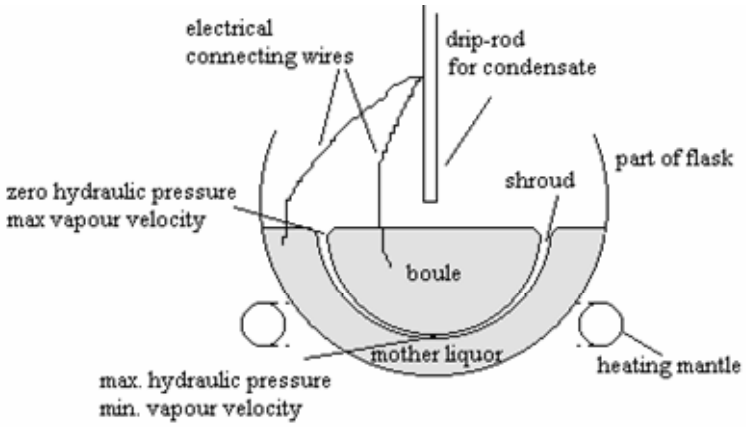

Figure 2.2. Hickman's experimental arrangements.

In a subsequent paper Hickman [41] and his co-workers extended this work to include a wide variety of inorganic and organic liquids, including fluorocarbons, in order to test the hypothesis that boule formation is a function of the vapour layer activity, and does not stem from idiosyncratic surface or chemical properties of any specific liquid. The apparatus was further refined both for ease of use and for ease of operational photography, and an easily-made version of this latter form was described by Stong in 1974 in the "Amateur Scientist" Department of *Scientific American* [42]. Some considerable detail was given of measurements of the vapour-layer, or shroud, thickness, both in terms of experimental technique and of results obtained. In the case of large boules formed above superheated liquid, where the liberation of vapour without ebullution is prolific, vapour-layer thicknesses in the range 25 - 40μm were measured – considerably higher than those associated with floating drops at ambient temperature. (Typically < 2μm).

Drawing on Prokhorov's work, Hickman sought to explain the phenomena of boule formation and maintenance in Marangoni terms, i.e. of the 'pumping' effects within the vapour-layer brought about by small inequalities of surface temperature and consequent convection. Figure 2.3, taken from Hickman et al, 1967 [41] illustrates these convection currents and the resulting vapour pumping in the vapour-layer.

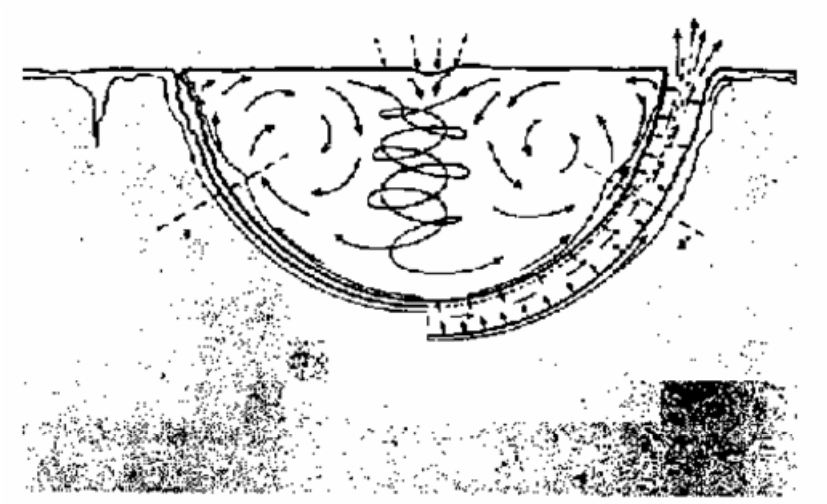

Figure 2.3. Convection currents and inferred vapour exchanges between a boule and its supporting liquid. *(From Hickman et al, 1967 [41])*

Hickman's work, whilst principally qualitative and experimental, is also of importance for the point that he consistently made that, in order to produce large boules successfully, it is imperative that the condensate on the drip-rod, the boule itself and the mother liquor should be at zero electrical potential. In his first paper [40] some detail was given of brief experiments made with a small range of potential differences between boule and bulk liquid, and the findings of these are appropriate to the next section of this review.

In a short paper of 1995 [43], Dell'Aversana, Monti and Gaeta commented on ground-based and microgravity instances of non-coalescence due to Marangoni flow at liquid interfaces observed in liquid bridges of silicone oils. (The microgravity results came from the D2 Spacelab mission.) This paper gave qualitative detail of the results of a number of experiments involving both pairs of liquid drops at different temperatures being forced together, and drops in shear against a moving liquid surface under isothermal conditions. Perhaps the most significant aspect of this paper in the context of the present research is the categorical statement that whilst a number of different oils, together with organics such as *epthane*, *iso-propanol* and *fluorinert FC-75* exhibited Marangoni flow water did not, neither was it possible to observe non-coalescence under either the non-isothermal or isothermal (shear) conditions described.

Considerations of the effects of Marangoni currents within drops were further extended by Dell'Aversana and his co-workers at the *MARS* (Microgravity Advanced Research and Support) Centre in Naples, in a series of papers and articles between 1996 and 1998. [44 - 46]. These all investigated the non-coalescence either of drops of silicone oils of different temperatures which were physically forced together, or of a drop held against a rotating bath of the same liquid to produce conditions of interfacial shear. Convective onset was made visible by reflecting laser light off the drops and liquids, which contained small (~5μm) glass microspheres, and using CCD cameras to monitor magnified images.

In the case of drops of 5*cSt* silicone oil held on the end faces of opposed heated rods, the critical temperature differential, ΔT_c, to inhibit immediate coalescence was found to be 3.0 ±1.0ºC. Whilst these findings are interesting, their immediate applicability to the

present research is limited, mainly by the considerable differences between silicone oils, being non-polar and of low surface activity, compared with water and aqueous solutions. Of more relevance is the work of Dell'Aversana's group that focussed on shear conditions, which were carried out under isothermal conditions, and where the maintenance of the air-film between the liquids is a consequence of their relative motion.

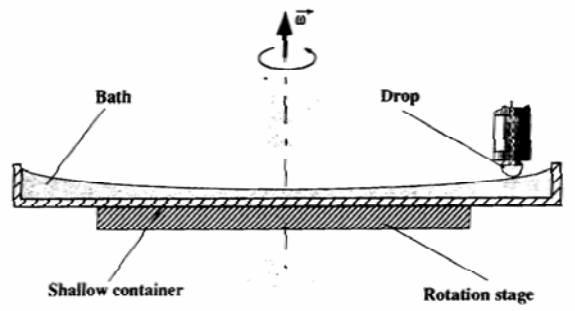

Figure 2.4. Rotating isothermal arrangement *(From Dell'Aversana et al, 1996 [44])*

A shallow container, partly filled with silicone oil, was placed on a rotating stage (see Figure 2.4.) and a drop-dispenser arranged above it as shown, such that the position of the drop might be anywhere along the bath radius. This gave tangential velocities between the drop and the bulk surface variable between zero (drop at the centre) and 35 cm/s. At low relative velocities coalescence occurred, but this was suppressed as the relative velocity was increased, and the pendent drop impressed was shown to leave a definite wake on the moving surface.

It was further found that if tracers in the drop were observed the onset of motion within the drop could be seen when it was still some tangible distance above the rotating surface, and that this activity increased as the drop was lowered towards the surface. Dell'Aversana's group concluded that these observations suggested that airflow dragged by the moving surface contributed to the non-coalescence phenomenon.

At a differential velocity of 35 cm/s the capillary number, Ca_s, and the Reynolds number Re_s, were respectively calculated to be,

$$Ca_s = \frac{\mu U}{\gamma} = 0.081 \qquad (2.4)$$

and,

$$\mathrm{Re}_s = \frac{Ua}{\nu} = 105 \qquad (2.5)$$

where ν is the kinematic viscosity, μ the absolute viscosity (ν x density), γ the surface tension and U the relative velocity. These compare with calculated Ca_s and Re_s numbers of 0.0525 and 68 respectively for static drops brought together in the thermocapillary experiments referred to previously.

Findings from the isothermal experiments with a velocity difference between the drop and the bulk liquid have implications for water boules traversing a water surface, and will be discussed later in the thesis.

Conditions of shear were further investigated by Nahmias, Téphany and Méjanelle working at IUT d'Orsay and in a communication of 1997 [47] they reported on further experiments on silicone oils under shear conditions, the bulk liquid being set in motion by a magnetic stirrer. Free drops of oil were then introduced on to the surface, and migrated under rotational forces to the centre of the vortex formed where they remained for several minutes before coalescing. Multiple drops introduced coalesced with one another, forming a large drop sufficient to distort the vortex shape, until continuing additions caused a partial coalescence with the bulk liquid, reducing the mass of the central floating drop. On stopping the rotating action and allowing the bulk liquid to settle a drop could be induced to float for about half a minute before coalescing. This effect was noted to a lesser degree with certain other oils, but not with water, glycerol, pure sulphuric acid or castor oil.

In a follow-up letter in 1999 [48] Téphany and Nahmias reported on extensions to their experiments to include the effects of reduced ambient air pressure. These showed that a reduction of air pressure increased the drop lifetime. Their results are displayed graphically in Figure 2.5.

This result is perhaps surprising, although it accords with the findings of Mahajan [33] that boules might be formed more easily at high altitudes, and hence under reduced pressure. This issue will be discussed further when the question of humidity effects is discussed in Chapter 7, as the reduction of specific humidity both with altitude and with decreasing temperature is significant.

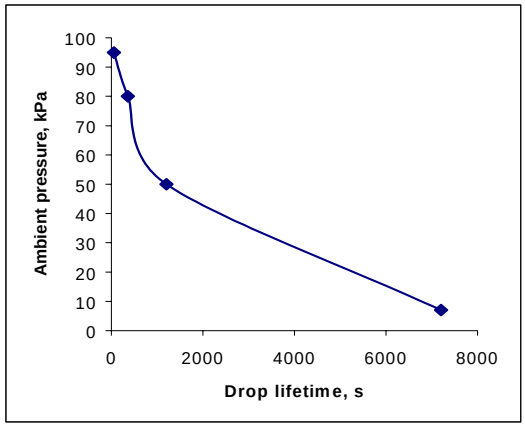

Figure 2.5. Plot of Téphany & Nehmias' drop duration results.

Calculations of the critical air-film thickness in these investigations made by Téphany and Nehmias, based on a drop duration equation (2.6) derived from the application of Reynold's equation to the parameters of their experiment.

$$t_c = \frac{\mu r^5 \Delta\rho g}{4\sigma^2} \frac{1}{h_c^2} \qquad (2.6)$$

where t_c is the time to coalescence, r the drop radius, $\Delta\rho$ the liquid/air density difference, σ the surface tension, μ the absolute liquid viscosity, and h_c the critical air-film thickness. Equation (2.6) by re-arrangement becomes,

$$h_c = \sqrt{\frac{\mu r^5 \Delta\rho g}{4\sigma^2 t_c}} \qquad (2.7)$$

Substitution of the experimental values obtained suggested that the limiting critical thickness of the air-film for coalescence was some 0.15 μm. Certain simplifications to the situation had, however, been made. In making this calculation it was assumed that *a)* the drop was spherical, and, *b)* the surfaces behave as immobile solids, both of which assumptions should be treated with extreme caution.

Thermal Marangoni effects have been most recently considered by Savino, Paterna and Lappa, 2003 [49] who have extended previous studies by mapping the thermal gradients between a drop and a surface using a sensitive infra-red camera to image heat transfer from a relatively hotter liquid pool to a drop suspended upon it. The authors developed a physical and mathematical model to explain their findings, obtaining a reasonable correlation with observation for oil-on-oil systems, but an unsatisfactory outcome for a water-on-oil system. This outcome has to be evaluated in the light of the statement by Dell'Aversana *et al*, 1995, [43], than Marangoni currents are not observable in water.

2.3.3 The Influence of Surfactants.

Some attention has recently been paid to the way in which coalescence may be extensively modified by the use of surfactants. In a recent (2001) study Amarouchene, Christobal and Kellay [50] reported on experimental investigations into the critical height from which falling water drops doped with surfactant fail temporarily to coalesce with a similarly treated water surface. The modification of the coalescence properties of water by very small quantities of surfactant has been known for a very long time (see, for example, Rayleigh 1879 [51], 1890 [52]). This research gave quantitative data for the probabilities of drops of a specific size containing surfactant residing on a similar plane surface having been dropped from a range of heights.

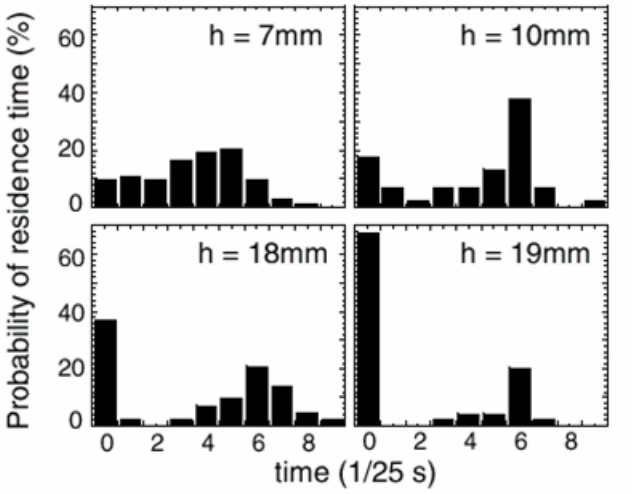

Figure 2.6. Probability distributions of lifetimes of drops released from different heights, *h*, on to a liquid surface for 1mM AOT solution. *(* From *Amarouchene et al, 2001 [50]).*

The results displayed in Figure 2.6 are for drops and a bulk surface of 1mM AOT *(bis-ethylhexylsulfosuccinate)* solution, an ionic surfactant, and show that for all values of dropping height, *h*, there is a tendency to a resident lifetime of *circa* 6/25 second, but that as heights increase so does the possibility of zero lifetime, i.e. immediate coalescence. The authors ascribe the period before coalescence in surfactant-containing systems to the retardation of airflow from the trapped interstitial barrier layer due to the presence of active superficial surfactant molecules, compared with the comparative freedom with which air moves over a pure water surface.

2.3.4 Electrostatic and Electrohydrodynamic Developments.

Comparatively speaking far more research effort has been undertaken into the hydro- and thermohydrodynamic aspects of floating drops and boules than into the effects of electric charge and electric fields in determining their existence and demise, and the previous section has traced the development of research interests in these respects. However, over approximately the last half-century a growing body of evidence has emerged that points to the considerable influence of electrical forces, both within and outside of liquid systems, in controlling the phenomena under consideration.

Allan and Mason in 1961 reported [53] on the effects of both direct and induction charging on the coalescence times of liquid (water) drops settling on a water surface surmounted with a layer of *n*-heptane. In the case of directly charged drops (with the bulk liquids grounded) increasing the drop potential was found to decrease the dwell-time before coalescence occurred. Partial coalescence was frequently observed, with production of secondary and tertiary drops. If the dwell-times be designated τ_1, τ_2, and τ_3 for primary, secondary and tertiary drops respectively, then under conditions of zero potential it was found that,

$$\tau_1 < \tau_2 > \tau_3 \text{ for } V = 0 \qquad (2.8.)$$

A carbon tetrachloride/water system was found to behave similarly, but a benzene/water system gave rise to successive diminutions in dwell time, such that,

$$\tau_1 > \tau_2 > \tau_3 \text{ for } V = 0 \qquad (2.9.)$$

Increasing the potential from zero to about 360 volts, brought little change in the mean values of τ_2 and τ_3 but above this potential these values decreased until coalescence was a single-staged process. The potential value at which this disappearance of secondary and tertiary coalescence processes began was found to decrease with reduction of the distance between the dispensing needle and the water/heptane interface.

In the case of induced charging of the drops both the conducting plane connected to the lower cell and the dispensing needle tip were grounded, and a field established by means of a charged plate. As previously, τ_1 was found to decrease with increasing field strength, but the diminution of τ_2 and τ_3 was far more pronounced, i.e.

$$\tau_1 >> \tau_2 >> \tau_3 \text{ as } V \uparrow \qquad (2.10.)$$

Some additional work was performed to evaluate the modifying effects of certain emulsifying agents in the system, concluding that the accelerated coalescence reported could be accounted for by both the increased rate of approach of the drop to the interface, due to electrostatic forces, and to field enhancement of the heptane layer by image charges.

A paper of some importance was presented in 1964 [54] by Jayaratne and Mason[1]. In this, the authors presented a detailed study of the conditions under which small uncharged water drops, of radii in the range 60 - 200μm, either coalesce or rebound at a water/air interface. This work built on that previously undertaken by Schotland [39] demonstrating that for uncharged drops to coalesce they needed to fall from a greater height at low angles of incidence, and that increasing the density of the surrounding gas produced a similar effect.

[1] **Note**: the second author of this paper was B.J. Mason, then at Imperial College, London, and not S.G. Mason of Mc. Gill University, Montreal, the second author of the previous paper.

The authors' method is interesting in that it made use of a vibrating capillary device, previously described by them in the literature [55], that made possible the delivery of streams of small droplets of consistent size and trajectory, thus eliminating some dynamic errors. During the majority of the experimental trials, which were concerned with uncharged drops, the stream of droplets was aimed on a given trajectory at a bulk water target through a slit in a grounded plate held at a convenient angle, in order to remove any random charge that they might have acquired. Jayaratne and Mason made the important statement that drops naturally develop a charge during their formation, and they measured the average charge for a 130μm drop as -2×10^{-6}esu, equivalent to 6.7×10^{-16}C, or just over 4000 elementary charges.

In their investigations of uncharged drops the authors found that, in the course of near-normal impact, the drops behaved as inelastic bodies with an effective coefficient of restitution of approximately 0.22. Reference to Figure 2.7 shows the geometry of the situation.

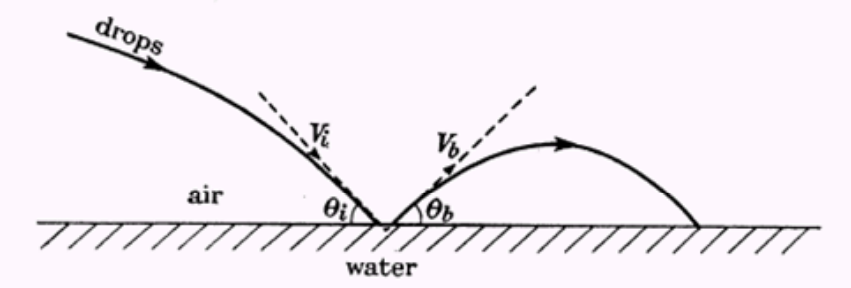

Figure 2.7. Incidence and rebound geometry. *(From Jayaratne & Mason. [54])*

The results obtained indicated a frictional energy loss of 0.95 for drops of any size in the range studied. This gave,

$$\left|V_b^2 / V_i^2\right|_{\theta \to 90^\circ} = 0.05 \qquad (2.11)$$

and $V_b/V_i = 0.22$. (*Vi* and *Vb* being the velocities of incidence and rebound respectively, and θ the angle of impact). The contact times were calculated by photographic interpretation of the data in terms of the expression,

$$t = T\left[1 - \left(x/a - y/b\right)\right] \qquad (2.12)$$

where t is the contact time, T the period of vibration of the drop-generating needle, and x, y, a and b are the distances as shown in Figure 2.8.

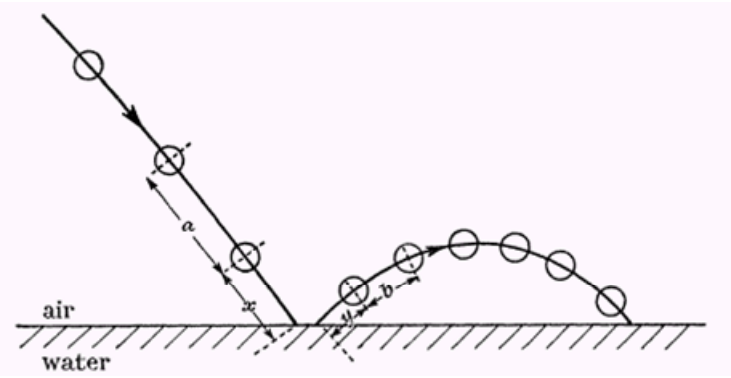

Figure 2.8. Geometry for time, t, calculation. *[From Jayaratne & Mason. [54])*

Measurements, confirmed by spark photographs, gave values for the contact time of the drops in the order of 1ms.

It was also demonstrated that the outcome in terms of bouncing or coalescence depended critically upon the angle of incidence, θ_i, with several zonal ranges for θ_i being identified. This behaviour is schematically represented in Figure 2.9, taken from the paper.

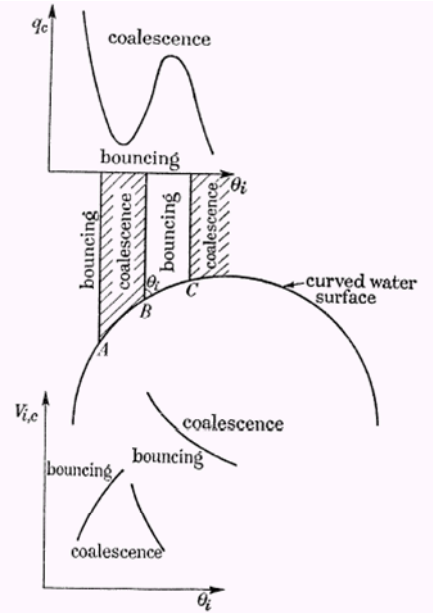

Figure 2.9. Schematic diagram showing that bouncing and coalescence occur in well-defined zones for drops contacting a convex water surface at an angle θ_i. *[From Jayaratne & Mason. [54])*

Jayaratne and Mason pointed out that whilst the downwards part of the colliding drop's motion, upon interacting with the surface, may be considered to be simple harmonic, its upward motion cannot, in view of the fact that only about 5% of the energy of the crater formed is communicated back to the drop. This observation was employed by J.T. Bartlett in an appendix to the paper in a determination of the geometry of the deformation of the surface, and hence of residency times and maximum surface depressions for drops of a given size and trajectory.

The part of Jayaratne and Mason's paper most pertinent to the present investigation is their consideration of either the bouncing or coalescence of charged drops. Extending Allan and Mason's work with heptane/water interfaces [53], experiments were carried out with a stream of droplets, of known charge, impinging, as before, at various angles upon a grounded bulk water surface. Charge species was found to influence the outcome only to the small extent of offsetting the small negative charges that the drops had acquired during their formation.

The technique used in these investigations was to establish initially a stable stream of uncharged droplets of the required velocity, impinging on the water surface at the angle of incidence under investigation. The potential on the needle voltage was then increased steadily until bouncing of the stream was replaced by coalescence. The stream was then photographed to record the geometry. It was observed that, just prior to complete coalescence, and while the potential was still being increased, a period of partial coalescence was apparent, during which the rebounding stream flickered and the rebounding drops were of much smaller size than the incident ones. High-speed photography showed that in these cases coalescence of the incident drop was occurring, followed by the ejection of a smaller drop, these latter forming the rebounding stream.

From this data, calculations were made of the critical charge, q_c, necessary to ensure coalescence, and correlations made between these values and corresponding values both of the incident velocity and the angle of incidence for drops of a range of sizes. These results gave values of q_c in the range $1.6 \times 10^{-14} - 7.7 \times 10^{-14}$ C (stated in the paper as 0.5×10^{-4} to 2.3×10^{-4} esu.), for drops in the range 139 – 182μm radius.

Further experiments were performed with the drops polarized by an electric field, established by an insulated charged disc above the water surface. Here it was found that fields in the order of 10kV/m induced coalescence.

In respect of the mechanism of the rupture of the intervening air-film at coalescence Jayaratne and Mason contribute little that is new, reiterating Rayleigh's comments on the possibility either of micro-discharge or of the presence of random particulates, but they concede that there will be drop distortion in the case of charged droplets due to the high field-strengths produced by small charges over distances equivalent to the draining air-film (say, 0.1 to 1μm).

The principal advances resulting from Jayaratne and Mason's work are therefore;

- Their extension of Allan and Mason's work to include situations in air,
- Demonstrating that the angle of impact is of importance, and that rebounding occurs periodically with increasing angle, even for uncharged drops,
- Their measurements of the charge necessary to inhibit bouncing,
- The experimental methodology used.

Treating this review chronologically, we now need to return to Hickman's work referred to in the previous section. In his paper of 1964 [40] reference was made to the impossibility of reliably forming large boules with his reflux apparatus unless the boule, bulk liquid and the drip-rod from which the boule-forming condensate dropped were all grounded. During the course of this phase of investigations, Hickman experimented with possible combinations of the grounding wires from the boule and the bulk liquid. Shorting them through the medium (~100kΩ) resistance of an observer ensured boule flotation, whilst the use of a resistor above about 5MΩ did not. Applying a voltage differential between the two connexions led to variable results, regardless of polarity. At about 5V, boules of only about 15 to 16 drops in volume could be produced, compared with the 24 to 26 being produced in the absence of a potential difference. At 10.5V boule production could not be achieved. He commented that *"at 10 volts drops would sometimes float, at 10.7 volts, never."* Further investigations involving increasing the

conductivity of the water by the addition of sodium chloride, ammonia solution or acetic acid had no effect on these findings.

Considerations of the interaction between falling droplets is of importance to meteorologists and cloud physicists, and in 1971 Brazier-Smith, Jennings and Latham [56] reported on a series of coalescence experiments that included some investigations into the behaviour of falling charged droplets. Much of this work is irrelevant to the present research, except inasmuch as it extended understanding of the conventional dynamics of droplet collisions by the formulation of an expression for droplet collision efficiency, ε, of,

$$\varepsilon = 2.40\left(\frac{\sigma}{U^2 r\rho}\right) f\left(R/r\right) \qquad (2.13)$$

where R and r are radii of two falling drops $(R>r)$, σ and ρ are respectively the surface tension and the density of the water, U the relative velocity and $f(R/r)$ a dimensionless function ranging from 1.3 for $R/r = 1$ to 3.8 for $R/r = 3$.

During these experiments two droplet streams were projected from needles at angles downwards such that they collided and coalesced, the ensuing stream falling vertically into a reservoir. Conditions of bounce or coalescence were studied for a variety of drop sizes and velocities. In the case of charged drops, the charging was accomplished by applying known potentials to the needles, and the drop charge calculated by collecting a known number of drops for each needle in turn and measuring the total charge collected. The experiments found that bouncing was completely inhibited if the drops, which had radii in the range 420 to 640μm, carried opposite charges of the order of 2 x 10^{-11}C, these figures being some three orders of magnitude greater than those reported by Jayaratne and Mason [54].

One of the most interesting, and stimulating, papers in the general field of boules was a semi-popular publication by Stong in the "*Scientific American*" magazine in August 1973 [57]. In this Stong reported on experiments performed by a Dutch schoolmaster, Gerard Schol, into the production of water boules and of their extinction by means of an

electric field. Whilst it might be argued that this article contributed little that was not present in the literature, either actually reported or by inference, its importance was considerable in that it served both as an accessible summary of much of the existing understanding of the phenomenon as well as a focus of interest. The citation of this piece in a number of subsequent publications is testimony to its effect!

Stong (who referred to water *globules* throughout the article) described Schol's method for producing boules on the brim-full surface of an insulated, elevated container by directing a fine upward water-jet from a constant-head source, such that it broke into droplets just before the top of its trajectory. The receiving surface was placed just lower than the zenith and a little aside from it, so that the droplets fell with relatively low kinetic energy on the water surface (see Figure 2.10)

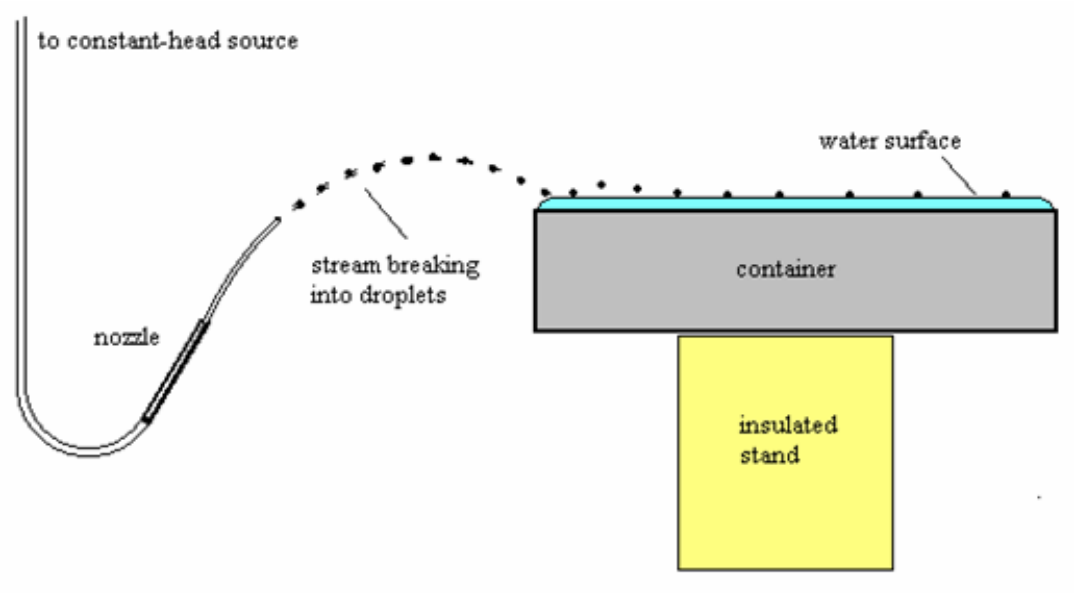

Figure 2.10. Schol's apparatus, as described by Stong *[57]*.

Stong's report of Schol's experiments stated that the extinction effect of an electric field had been found accidentally, when a piece of charged PVC tubing had been brought close to the operational apparatus, and that subsequent experiments with a piece of charged glass rod confirmed that the polarity of the field was immaterial in determining coalescence.

Subsequent experiments involved the use of a charged metal plate, held above the surface of the container and parallel with it. Schol found that a field of some 450V/cm

sufficient to cause complete extinction of the boules. This may be compared with the figure of 10kV/m reported by Jayaratne and Mason [54]. However, the very different geometries involved would play an important rôle in explaining the discrepancy, with Schol's apparatus providing a different field-intensity pattern to that of Jayaratne and Mason.

Stong also reported that Schol had attempted a measurement of the air-film thickness, using refracted sodium light and the pattern of Newton's rings from the diffraction involved. By this method Schol had estimated the air-film thickness to be less than one wavelength, i.e. well under 1μm.

Finally, it was observed that the addition of sodium chloride to the water increased the necessary field strength for extinction. This is in interesting comparison to the comment of Hickman, cited above, that increasing the conductivity of the liquid used in the production of his large boules had no influence on their response to an electric field.

A further article in 1978 by Stong in the same publication has already been noted [42], and the interest of the "*Scientific American*" in the matter of water boules continued in 1978 when Walker published an account of further experiments [58]. The extension of boule lifetimes by the addition of small quantities of surfactant was noted, together with the observation that lifetimes are dramatically extended by vibrating the bulk liquid surface.

A loudspeaker cone, set vertically and fed by a variable audio oscillator, formed the transducer upon which was set a shallow circular tray of water. The oscillator was adjusted to produce visible standing waves on the liquid surface, and drops lowered gently to the surface remained uncoalesced for periods of several minutes, with many tending to settle at nodes in the wave pattern. Larger drops caused too much dimpling of the surface for the nodes to be very apparent, and the behaviour of some of the smaller drops was likened to the frenzied on-the-spot activity observed with Leidenfrost drops. Walker did not state whether or not the same type of biaxial oscillation leading to an apparent epitrochoidal shape was observable, as is the case with Leidenfrost drops. The

question of boule maintenance on a vibrating substrate will be discussed in greater detail in Chapter 3.

In reviewing the possible electrical influences in the drops' suspension on the bulk surface, Walker considered the possibility of mutual repulsion between a negatively charged outer surface of the drop and a similar negatively charged plane liquid surface, but favoured the more conventional air-film interpretation, relying on the high pressure of the air-film to provide a dimple in the underside of the drop, and hence an air reservoir, from which, because of the extreme thinness of the remaining film air could only slowly bleed to the outside atmosphere. Figure 2.11 shows a simple interpretation of this situation.

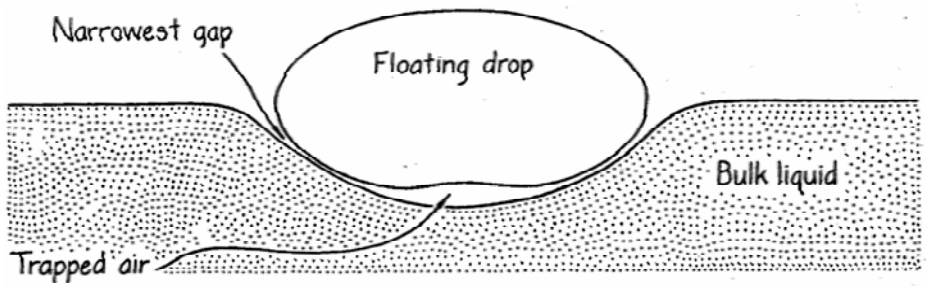

Figure 2.11. Trapped-air explanation of a floating drop. *(From Walker [58]).*

Whist partly peripheral to the present research, a paper of some relevance was published by Ochs and Czys in 1987 [59] concerning the effect of charge on the coalescence of drops in free-fall. This work proceeded from meteorological interests, but considered for the first time charged drops approaching at very small grazing angles, typical of precipitation drops falling freely under gravity. Charge magnitudes imposed on the experimental drops were of the range 10^{-16} to 10^{-12}C, with drop radii between 190 and 340μm, these quantities being chosen to best simulate precipitation parameters from both cumulus clouds and thunderstorms. The geometry of the apparatus was such that drops of the magnitude used had reached their terminal velocities.

Streak photography was employed to observe the droplet interactions, and the following effects were recorded;

1. that there is a unique impact angle separating the coalescence region from the non-coalescence region that is independent of charge,
2. the charge-difference range of the interacting drops separating conditions of rebound from certainty of coalescence is some two orders of magnitude,
3. temporary coalescences at higher charge levels, often accompanied by the ejection of a secondary or satellite droplet.

In the discussion of their results the authors made two statements pertinent to the present interest. First, for drops approaching at an angle of less than 43° bouncing was the inevitable result, *regardless of charge* (italics mine, JCA). For approaches greater than 43° the outcome of collision was charge dependent when the relative charge between the drops exceeded some 1.9×10^{-14}C, from which point the likelihood of coalescence increased until at a relative charge of 3×10^{-13}C bouncing was completely suppressed.

The second comment of interest in this paper is the evidence presented that coalescence is promoted by charge on the two drops concerned, even if these individual charges are of the same species (positive in the case of these particular experiments), if there be a magnitude difference between the charges involved, the larger charge inducing an equal opposite one on the drop carrying the lesser charge.

Both these observations have some relevance to the issue of floating drops. The first is to be borne in mind when the conditions under which boules will actually be formed is discussed, the latter when relative charges between drops and substrate are considered.

Further literature concerning the electrohydroynamics of boules of more recent date is small. A 1997 review paper by Orme [60] on the general topic of droplet collision, bounce, coalescence and disruption included some reference to papers cited in this review, but the author's particular interest was more directed to the specific behaviour of hydrocarbon droplets rather than droplets of water or polar liquids.

A paper by Ahern and Balachandran, 2000 [61], reviewed some of the literature of the topic and presented experimental results of field magnitude for boule extinction. Evidence was also presented that dynamic boules traversing a water surface acquire

additional charge, and that the growth of that charge may limit their range of movement by contributing to the rupture of the interstitial air-film. This work is discussed in greater detail in Chapter 5.

2.4 Summary.

This review, as stated at the beginning of the chapter, has been necessarily cast over a long period of time – some four centuries – and a wide range of scientific interests. The threads contributing to the present understanding of the phenomenon of water boules are diverse, and sometimes tenuous. The range of published work spans the period from the first stirrings of experimental science to the present, with its disciplinary strictures that mean that two men may sometimes pursue parallel paths in ignorance of one another. One is reminded of the words of D'Arcy Wentworth Thompson on a similar matter:

> *"We need not wonder if the way be hard to follow, and if these wayfarers have yet gathered little. A harvest has been reaped by others, and the gleaning of the grapes is slow."*
>
> D'Arcy Wentworth Thompson, "On Growth and Form" Cambridge, 1961, Chap. 1.

The development of present knowledge of the phenomena concerning water boules has been traced from its first known reference to include the most relevant aspects of our present understanding in terms both of the general dynamics and the electro-hydrodynamics of the topic. Some references are too specific to the understanding of particular processes and too silent in their reference to floating drops to warrant inclusion here, and these are quoted in subsequent chapters in the context of particular issues.

In order to offer a succinct summary two tables have been drawn up. Table 2.1 is a chronology of the more important references bearing on the topic, as here reviewed. Table 2.2 partly cross-refers with this and sets out the key points of knowledge concerning boules and floating drops prior to the present research.

Author	Date	Contribution	Ref.
Gilbert	1600	Charged amber draws a water drop into a cone.	1
Browne	1646	Above observation extended to oils.	2
Hauksbee	1710/12	First recorded quantitative experiments on capillary rise using wedge made of glass plates.	19, 20
Jurin	1717/19	Experiments on rise in capillary tubes. Relationship suggested that rise is proportional to tube radius.	21, 22
Gray	1731/2	First observation of fineness of spray, and of visible corona.	5
Nollet	1748	Charging a stream of water causes it to diverge in smaller streams.	6
Ellicott	1748	Attempts (unsuccessfully) to measure change in capillary rise on charging water.	7
Henly	1774	First qualitative measurements of conductivities of dry and moist air.	8
Young	1805	Essay on the cohesion of fluids. First comprehensive mathematical treatment of surface tension	23
Laplace	1806	Develops theory of surface tension in supplement to 'Mechanique Celeste'.	24
Bizio	1818	First record of water boules seen on the runoff of oars. First laboratory experiments with alcohol, ammonia & mercury.	11
Gauss	1830	Development of mathematical understanding of surface tension in 'Principia Generalia Theoriae Fluidorum in Statu Aequilibrii.'	25
Meunier	1863	Observation of boules of water, alcohol & acetic acid. 'Careful placement' technique developed.	13
Tomlinson	1863	Boules of essential oils. Noted streaming currents, and suppression by high humidity.	15
Rayleigh	1879	Coalescence of neighbouring drops by electric field.	9
Reynolds	1882	Considered surface cleanliness the only criterion needed for boules to form.	17
Rayleigh	1899	Speculation on causes of coalescence - dust motes. Possible local high fields, promoting instability and rupture.	10
Mahajan	1930	Two papers including work on film-drainage and the observation of ease of boule formation at high altitude	32,33
Prokhorov	1954	Practical and theoretical work on air-film. Measured effect of humidity on coalescence. 100%RH stated to guarantee coalescence.	35
Schotland	1960	Conditions for coalescence for drops rendered electrically neutral.	39
Allan & Mason	1961	Experiments with water/heptane interfaces. Conditions for bounce.	53
Jayaratne & Mason	1964	Work on angle of incidence for bounce/coalescence in charged and uncharged drops. Calculation of critical charge for coalescence.	54
Hickman et al	1964-67	Production of large boules. Need for electric neutrality noted. Measurements of extinction potentials for large boules made	40, 41
Dell'Aversana et al.	1964-95	Marangoni effects studied. Thermal difference experiments and cases of isothermal shear.	43-46
Brazier-Smith et al	1971	Limiting values of charge for bouncing drops investigated	56
Stong	1973	Popular article describing Schol's work on boules. Coalescence in electric field described	57
Walker	1978	Maintenance of boules by vibration of substrate described.	58
Ochs & Czys	1987	Collision of drops in free fall at small angles. Limiting angle of incidence for rebound. Charge measurements for coalescence	59
Tephany & Nehmias	1997-9	Extension of Dell'Aversana's work. Experiments under reduced pressure.	47, 48

Table 2.1. Chronological table of some key developments relating to the present research.

Development	Date	Ref.
First known recorded observation by Bizio. Experimental work on boules of water, alcohol, ammonia and mercury.	1818	11
Sire records the extended duration of ether boules, attributing this to their volatility.	1853	12
Meunier describes a technique for making boules, and works with water, alcohol and acetic acid.	1863	14
Tomlinson works with essential oils. Notes suppression of boules by high humidity.	1863	15
Reynolds considers surface cleanliness the only environmental criterion in boule production.	1882	17
Mahajan considers film drainage rate the criterion for boule longevity. Comments on ease of formation at high altitude compared with sea level.	1930	32,33
Benedicks and Sederholm remark on impossibility of forming boules in vacuo.	1944	34
Prokhorov states unsaturated conditions necessary for boule formation	1954	35
Allan and Mason investigate conditions for bounce rather than coalescence for water/heptane.	1961	53
Jayaratne and Mason investigate critical angle for coalescence for charged/uncharged systems.	1964	54
Hickman et al. work on large boules over superheated liquids. Electrical grounding is shown to be necessary.	1964-67	40,41
Stong describes Schol's work on boules. Extinction by electric field described.	1973	57
Walker describes long-lived boules maintained on vibrating substrate of water.	1978	58
Ahern and Balachandran report charging of boules traversing a water surface	2000	61

Table 2.2. Landmark events in the literature of boules and their dynamics.

3 METHODS OF EXPERIMENTAL BOULE PRODUCTION AND INITIAL INVESTIGATIONS.

3.1 Boule generation techniques.

For experimental purposes it was necessary to have available a reliable and consistent source of water boules, and attention was therefore given to satisfactory methods for their production. Five methods of forming boules have been identified, namely:

1. Random drops and splashes falling into water or on a wet surface. Whilst this represents the source of the majority of boules encountered in the natural environment it is the least satisfactory experimental source. The random nature of the process leads to a lack of control of such basic parameters as drop size, height, velocity and trajectory. In addition, the surface disturbances associated with such interactions can often be too disruptive for any significant dynamic or electrical measurements to be made.

2. The boule 'launcher'. In effect this involves the use of a fine water-jet, arranged so that the jet is breaking into discrete droplets just before the zenith of its trajectory, and allowing the stream of droplets to encounter a water surface just below this point. A method of this type was reported by Stong, 1973, [57] as being used by Schol in his experiments on boule extinction in an electric field.

3. The vibrating-needle source. This method allows for fine control of both the size and trajectory of the droplets produced, and was developed by Mason, Jayaratne and Woods, 1963 [55], and used in their 1964 bounce/coalescence experiments described in the previous chapter [54].

4. The 'gentle placement' technique. Originally devised by Meunier in 1863 [13], this relies on drops falling through heights of only a few millimetres, with

consequently low kinetic energy, on to a water surface. The method was extensively used by Tomlinson [15].

5. Methods involving a thermal difference between the two liquid components. These have had two principal exponents. Hickman and his co-workers [40, 41] used a super-heated substrate liquid for condensed drops to fall upon, again from a small height, whilst Dell'Aversana's school [43, 46] used oil drops on the adjacent extremities of two opposing rods of different temperature to produce their non-coalescing silicone oil drops.

In the present research boule production has been mainly by methods 2-4 above, or by developments of them, and a description now follows of the forms of apparatus used.

3.1.1 The Boule 'Launcher'.

Schol's original apparatus made use of a short length of glass tubing drawn to a capillary at one end to provide the water-jet for the formation of droplets. This is a perfectly satisfactory solution except that it makes it difficult to impose an electric charge by contact. An assembly made from the barrel of a 2ml (plastic) hypodermic syringe was therefore substituted for the glass tube. This enabled a range of different sized needles, to which electrical contact was easily made, to be affixed via the Luer fitting. A small rubber bung carrying a short length of 5mm glass tubing closed the other end of the barrel. This assembly was mounted on a small trunnion plate that could be clamped to a stand and adjusted to allow the stream of water to be projected at any required angle.

Feed-water to this assembly was from a constant-head apparatus fed by a pump, with the constant-head overflow being returned to source. The pump was capable of delivering 110ml/min, ample capacity for the task, thus ensuring that the constant-head chamber was full at all times.

Electrical contact could be made directly to the needle, and an insulating collar was fitted to the syringe barrel with a standoff carrying a 25mm length of 12.5mm diameter brass tube, coaxial with the needle. This could be used either to induction-charge the droplets or to neutralize any charge that they might carry as a result of their formation. A diagram of the complete nozzle assembly is shown in Figure 3.1.

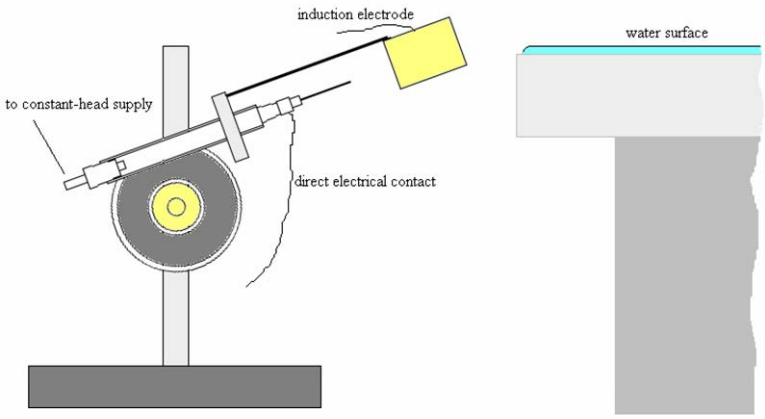

Figure 3.1. Boule Launcher.

This apparatus was found efficient and reliable in producing ‘dynamic’ boules for a number of the experiments detailed in this research. Droplet size could be controlled to a satisfactory extent in the diameter range of approximately 2 – 4mm.

3.1.2 Portable demonstration version.

An adaptation of the technique described above was used in a portable demonstration version of the apparatus used in the course of a demonstration of aspects of boule phenomena at the ESA Annual Meeting at Stanford University in 1998. A similar launcher was employed, but with a smaller needle diameter (200µm bore) fed from a reservoir by hand-pressure. The apparatus, affectionately dubbed ‘the flea circus’ contained a small variable high-voltage supply connected to an adjustable plate held parallel to the water surface to demonstrate extinction by an electric field. The water dish was driven by a built in oscillator to enable the effect of vibrating the bulk water surface to be demonstrated also. Figure 3.2. shows a photograph of the apparatus.

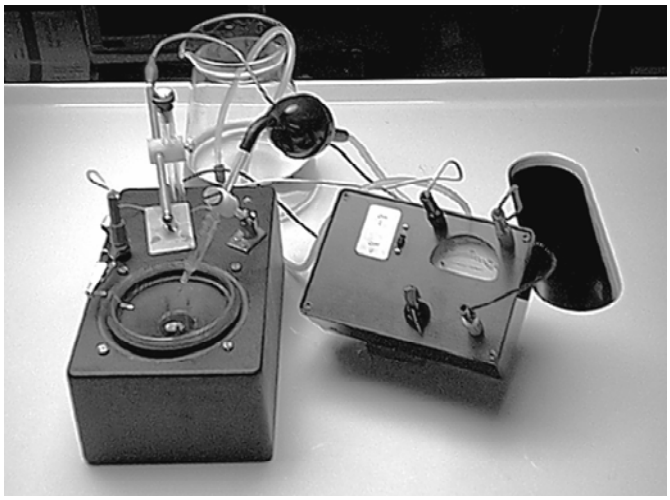

Figure 3.2. Portable demonstration apparatus.

The apparatus was housed in a small plastic box 21cm. x 13 cm. x 8 cm., containing a battery powered oscillator providing a variable frequency square-wave output within the range 5 - 120 Hz, and feeding a 10 cm. diameter loudspeaker horizontally mounted as a transducer. On this the bottom half of a 9 cm. glass Petri dish fitted conveniently, serving as a container for the bulk water. A rubber ring was fitted circumferentially around the Petri dish to increase the quality of coupling with the transducer, and to lodge it more securely in position.

Boules were produced by a squeeze-bulb, fed from a supply via a non-return valve, with the outlet of the bulb supplying a 0.3 mm outer diameter squared hypodermic needle mounted in a short length of glass capillary tube via a suitable plastic pipe. A small adjacent insulated pillar received the brass electrode to demonstrate boule extinction. A miniature DC supply, with a variable output from 300v to 1.8kV of either polarity supplied the electric field. During operation the bulk water and the needle were grounded with respect to the electrode.

3.1.3. Vibrating Needle Sources.

Some use was made during the course of experimental work of a source employing an electromagnetically-driven vibrating needle. This apparatus was a direct adaptation of the method described by Mason, Jayaratne and Woods [55], and used a Post Office-type

earpiece as a transducer, driving resonant lengths of hypodermic needle tubing. This apparatus produced drops of consistent size following a very precise trajectory, and was useful in stroboscopic observations of droplet interactions with a surface.

3.1.4. A 'Gentle Placement' Source.

Reference has been made previously to the method used both by Meunier and Tomlinson for placing droplets on a surface, and a very simple apparatus was devised to allow multiple drops to be thus positioned. It was found that by using a 0.9mm OD needle with a carefully squared and polished end in a 10ml 'Rocket' glass gas-syringe, and setting the assembly vertically above a water trough, boules could be reliably dispensed. The feed-pressure was supplied simply by the weight of the syringe piston.

During operation, this apparatus took some time before floating drops could be produced. It was thought initially that this might be a parameter of the water purity, but subsequent experiments showed that it would function as well with tap-water as with deionized or distilled water. Two factors were found to be important for boule production.

1) The surface needed to be clean and newly-formed. Dispensing a number of drops and allowing them to coalesce produced a suitable surface, after which water might be recycled from the trough back to the syringe without diminishing the formation of boules.

2) The height from which the drops fell appeared fairly critical. If drops were dispensed from too great or too small a height, then no boules formed, but setting the needle tip about 8mm above the water surface would produce a copious supply of them. This setting is discussed later in the chapter when the effects of surface vibration are under consideration.

The apparatus itself, which has proved to be a useful experimental tool, is illustrated in the Frontispiece to the thesis.

This simple type of apparatus was later developed into a form which allowed for the dispensing of a large number of drops by displacement from a small (20ml) glass container by air pressure from a 1ml syringe, connected via 1mm bore flexible capillary tubing. This development is described and illustrated in Section 3.2.3 and Figure 3.5.

3.2. Confirmatory Work on some earlier Investigations.

Initial investigations were directed to confirming those qualitative results arising from some of the earliest experiments recorded, together with the work of Schol, as reported by Stong [57] on the promotion of coalescence by an electric field, and that undertaken by Walker [58] concerning the use of vibrated water surfaces as a means of prolonging the lifetime of boules. In all cases, some adaptation of the original experimenters' methods was made, whilst keeping within the constraints of their original work.

3.2.1. Concerning the existence of the Air-Film Interface.

The first experiment in this category was of an extremely simple nature, and aimed at confirming the observations of Meunier [13] and Tomlinson [15], that there is no liquid-to-liquid contact as a boule traverses a surface. To do this a flat brass plate about 150mm square was prepared with a sheet of absorbent chromatography paper fixed firmly to its surface. The plate was set horizontally and its entire surface carefully flooded to a depth of some 3mm, with the resulting pool remaining in place due to the surface tension forces at the perimeter. The surface was first scavenged by sending a stream of plain water droplets from the boule launcher (Section 3.1.1 above) across it until boules were forming readily.

A solution of methylene blue dye in water was then used in the boule launcher and the droplets allowed to impinge on the nearest edge of the water surface. Some coalesced

immediately, resulting in a blue slick which remained as a stain on the paper, but others bounced, forming boules which traversed the surface and only left a tell-tale record of their progress at the actual point of coalescence. In many cases this was some considerable distance across the surface of the plate, and several boules were noticed shooting off the remote end of the plate, having successfully crossed its entire width. Careful observation coupled with a photographic record showed that under these conditions after an initial bounce the boules were crossing the surface horizontally, apparently smoothly, and without oscillating in the vertical plane.

Figure 3.3 shows a plan-view photograph of boules crossing the surface, together with the dye slicks indicative of coalescences.

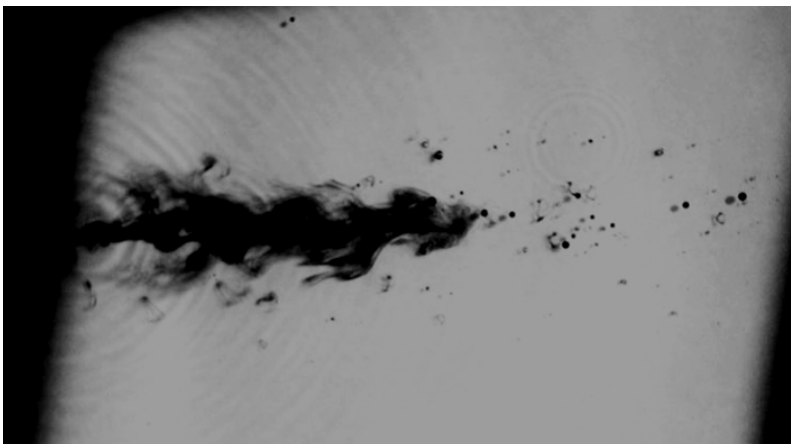

Figure 3.3. Water boules containing dye traversing a water surface. The surface width was about 150mm. The water depth may be inferred from the shadows cast on the bottom of the pool. In the upper right quarter of the picture ripples caused by boule coalescence may be seen.

3.2.2. Initial Investigation in Boule Extinction in an Electric Field.

In order to confirm Schol's findings concerning the extinction of boules in an electric field, and to make an independent measurement of the necessary field strength, the boule launcher was employed in the configuration shown in Figure 3.1. Droplets from this were arranged to fall at a small (10 - 20°) angle on the surface of water in a shallow stainless-steel dish, filled so that the meniscus was above the dish rim. Initially some difficulty was experienced in forming boules, due to problems of surface cleanliness of

the bulk water. Three solutions to this were tried, each being effective under different circumstances:

i) adding copious clean water until the overflow had effectively scavenged the surface;

ii) scraping the water surface with a clean metal edge (Pockels and Rayleigh's method);

iii) adding a minute speck of detergent solution. This immediately lowered the surface tension, causing the meniscus to break down, and water to spill radially from the edge. The new surface exposed supported boules well, and the effective removal of the surfactant was demonstrated by the subsequent build-up of the meniscus to its original height.

Method *(i)* was eventually selected as that most unlikely to add any surface contaminant to the water. In all the succeeding experiments, therefore, the bulk liquid surface was first flooded to achieve surface cleanliness, then grounded to dispel any random charge accumulating from the process.

Confirmation of Schol's findings of boule extinction by an applied electric field was made by arranging an insulated metal plate some 10 cm. x 4 cm. horizontally and symmetrically above the dish. The corners were radiused and the edges rounded to help reduce field irregularities at these places. The plate was connected to a variable high-voltage supply (Avo model RM215), and the launcher needle, its coaxial electrode and the stainless-steel dish grounded. Arrangements were made so that the plate might be positioned either 1 cm or 10 cm above the water surface.

A series of measurements was then made to determine the potential on the plate for boule extinction. Schol had reported that lower potentials extinguished smaller boules, but that larger ones required a higher potential. The apparatus described produced boules of reasonably uniform size, and the absence of any effective boundary wall to the dish (the water meniscus being above rim-level) meant that there were relatively few

larger boules forming as a result of rebounds and collisions. The droplet stream being continuous, it was decided to take the extinction point as having occurred when no boule was present under the electrode over a period of more than ten seconds. A series of ten measurements for the potential for boule extinction was then made with the electrode being positive with respect to ground, and then ten measurements with the electrode negative. This was done first with a 0.01m electrode height, and then at 0.1m. Schol's reported work was undertaken in an open environment, and it was thought valuable to obtain one set of measurements in this manner, with a second series being then undertaken with the apparatus shielded inside a Faraday cage. Table 3.1 records the data, which are displayed graphically in Figures 3.4, *a)* and *b),* overleaf.

Result no.	**1**	**2**	**3**	**4**	**5**	**6**	**7**	**8**	**9**	**10**	**Mean**
Open Environment											
0.01m, +ve	**32**	**37**	**38**	**36**	**40**	**31**	**33**	**38**	**37**	**37**	**35.9**
0.01m -ve	**30**	**35**	**36**	**37**	**36**	**38**	**33**	**35**	**34**	**31**	**34.5**
0.1m, +ve	**33**	**32**	**35**	**36**	**39**	**36**	**40**	**38**	**33**	**32**	**35.4**
0.1m,-ve	**34**	**34**	**37**	**36**	**33**	**34**	**33**	**35**	**40**	**35**	**35.1**
Inside Faraday Cage											
0.01m,+ve	***33***	***34***	***31***	***32***	***35***	***35***	***32***	***34***	***32***	***33***	***33.1***
0.01m, -ve	***32***	***31***	***34***	***34***	***32***	***34***	***33***	***33***	***31***	***32***	***32.6***
0.1m,+ve	***34***	***32***	***33***	***31***	***34***	***31***	***31***	***35***	***33***	***33***	***32.7***
0.1m, -ve	***33***	***33***	***33***	***34***	***31***	***33***	***32***	***34***	***33***	***30***	***32.6***

Table 3.1 Extinction field-strength data in kV m^{-1}. (Data inside Faraday cage italicized).

These data interpret in broad general agreement with Schol's figure of a field strength of <45kV m^{-1} for complete suppression of boule formation. The set of data from within the Faraday cage showed less range and slightly lower mean values than those obtained in an open environment, raising the question as to the cause. The field strengths employed, however, were high in relation to possible aberrations attributable to random ionization effects or to any influence by the earth's natural field gradient. In addition, the findings of Tomlinson [15] and Prokhorov [35] previously referred to that humidity plays a significant rôle in boule coalescence require consideration, especially in the light of

effects to be discussed later in the chapter, and the shielding effect of the Faraday cage may well have operated simply to reduce local air-currents, with a consequent increase of humidity within the experimental area.

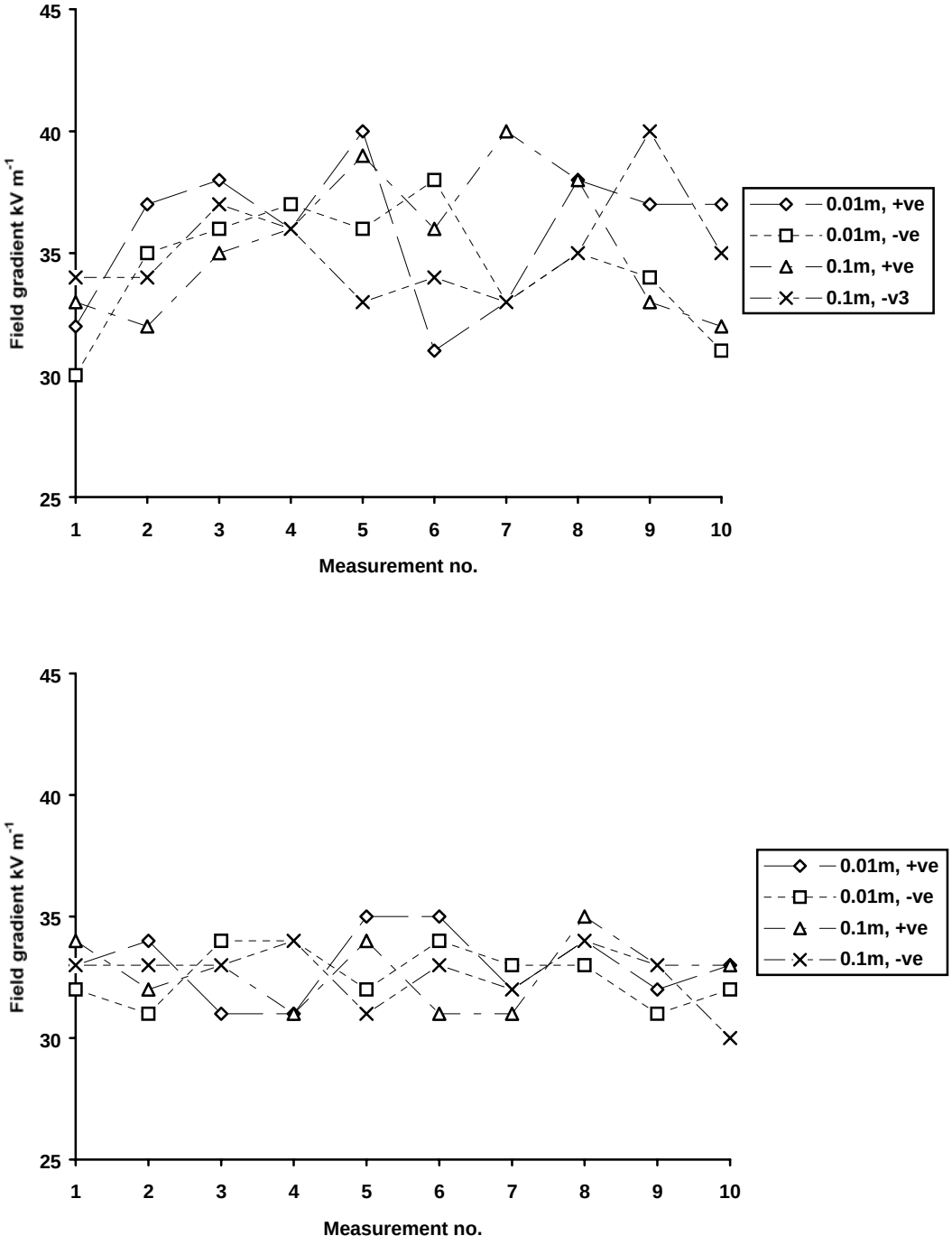

Figure 3.4. Field strengths for boule extinction for positive and negative fields and with the field electrode 1 and 10 cm above the water surface. *a) (above)* in open environment, and, *b) (below)* within a Faraday Cage.

It is recognized that the field produced by a flat plate of the type employed in these experiments does not produce a uniform field, although distortions are largely confined to its perimeter. Coalescences were, however, generally being observed in the central region of the field, where reasonable field uniformity could be assumed.

3.2.3. Extinction Field for Boules produced by 'Gentle Placement'.

Boules produced by the above method are essentially dynamic, i.e. they have a significant velocity across the surface. It was therefore considered worthwhile, for comparison's sake, to attempt a measurement of the extinction field strength for more quiescent boules.

The method employed in this investigation involved an apparatus derived from that described in section 3.1.4 above. As it was important to place drops carrying a charge on to a nearby surface a simple dispenser was devised whereby a small difference in air pressure provided by a syringe would cause the formation of a drop, thus allowing sensitivity of control to be combined with isolation from possible extraneous charging and leakage effects. Figure 3.5 illustrates the dispenser.

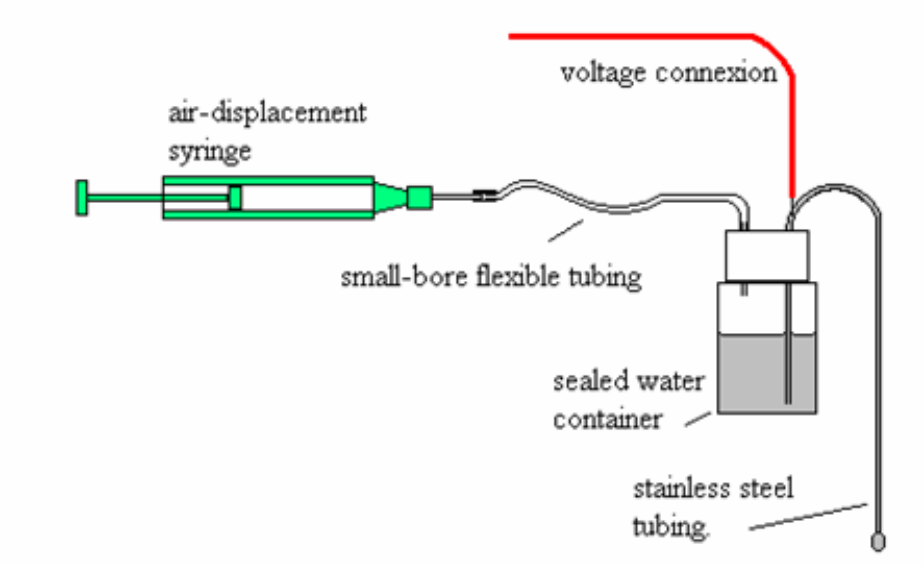

Figure 3.5. Drop displacement apparatus for 'gentle placement' technique.

The dispenser was held in a translation table, allowing for careful positioning over the water surface. The bulk water was contained in a stainless-steel dish some 12 by 10cm and approximately 2cm deep, with a raised rim that allowed a meniscus to form easily when the dish was slightly over-filled. Having the water surface proud of the top of the dish allowed easy sighting of the surface through a vernier microscope for level measurement purposes. Mean drop diameters were measured by dispensing a number of drops into a previously weighed container, and their diameters calculated. The dispenser container was then refilled and an electrical connexion to a variable voltage supply made to the needle. The large surface area of the water allowed for many coalescences with negligible variation in level height.

The filled dish was set horizontally on a lab-jack, to allow height adjustment, and electrically grounded. The dispenser needle was then set a few millimetres above the water surface, and, with the needle temporarily grounded, drops dispensed. During this process the height above the water surface was adjusted until boules were forming readily.

Drops falling from the needle were elongated into a prolate form, and it was then necessary to measure the distance from the base of a fully-formed drop with a vernier microscope, just prior to its parting from the needle, so that the true effective field-length might be found. Figure 3.6 shows a photograph of the apparatus during setup. All the components, with the exception of the dispenser syringe and the voltage supply, were contained within a Faraday cage, here shown open to allow access for the setup microscope.

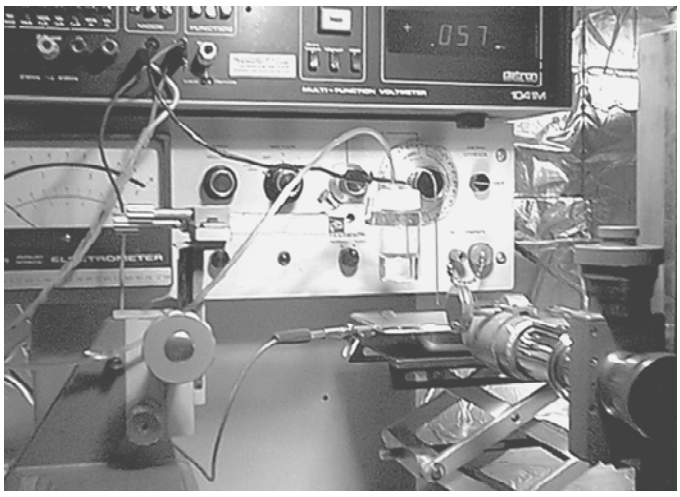

Figure 3.6. Photographic view of apparatus during setup (Faraday cage open).

A variable potential could be applied between the needle and ground derived from a 270 volt battery with a potentiometer across it, the output voltage being monitored by a digital voltmeter (Datron 1040M).

Results of the experiment were thus:

Diameter Calculation.

50 drops were found to have a mass of 1.021g, giving the mass of 1 drop as 20.42mg. Taking the density of water at 20ºC as 0.998g/cm³, this gave a drop volume of 0.0204cm³, whence the radius was found as 0.169cm – a 3.38mm drop diameter.

Measurement of the pendent height of the drop was 4.42mm, showing an elongation of 1.04mm.

It was not possible to arrange for droplets to fall through a variety of heights, as the drop-height for this method is fairly critical. Boules from uncharged drops were found to form most effectively when the lowest part of the fully-formed drop was 2.88mm above the water surface, and this setting was adopted for the extinction-field measurements.

The potential on the needle was increased gradually until boules ceased to form at all. A transitional phase was observed in this process. With a needle potential in the approximate range 45-60V, boule formation became increasingly erratic, and at this upper limit coalescences were starting to appear that produced obvious secondary droplets. These were considerably smaller than the 'parent' drops, the average diameter being estimated at about 1mm. The frequency of these diminished as the needle potential was taken above some 60V, until at a mean potential of 88V all drops coalesced immediately, with no secondaries being formed. Partial reduction of the potential immediately allowed the secondaries to appear, and when the potential was further reduced below about 60V normal boules again formed on the surface.

The field pattern for this geometry is substantially different to that produced by parallel plates as used in Section 3.2.2, but it is interesting to note that a (simplistic) calculation of the extinction field-strength yields a peak value equivalent to 386V/cm, or 38.6kV/m, which is in fairly good agreement with the mean value of some 34kV/m for dynamic boules as previously measured (Section 3.2.2). Both of these figures are somewhat lower than that of Schol (see Stong [57]), although it has to be borne in mind that this was quoted as <45kV/m: certainly at this value extinction would be very complete.

With respect to the production of secondaries it is relevant to note the observations of Allan and Mason [53], and Jayaratne and Mason [54]. As stated in Chapter 2, Section 2.3.4, both groups remarked upon the production of these at a point when charge levels had increased to a certain point. Allan and Mason reported on the dwell-times observed prior to coalescence, with secondary droplets being produced, these finally disappearing at a certain critical potential and being replaced by immediate coalescence of the parent drop. Jayaratne and Mason had found, in the case of a stream of monosized water droplets, that their apparently elastic rebounding from a water surface was modified with increasing charge, the main stream of rebounding droplets being replaced by a more erratic one of smaller droplets. High-speed photography had shown that at this intermediate stage the main drop was coalescing, but with the ejection of a smaller secondary droplet. This observation appears entirely compatible with that found in the present instance.

The measurements reported here were made with the dispenser needle positive with respect to ground, and the battery polarity was therefore reversed to investigate whether charge sign exercised any influence over the extinction potential. Despite a number of trials, no difference could be discerned.

3.2.4 Experimental Verifications of Duration Time Extension by Vibration.

Reference has already been made to Walker's paper [58], that the lifetime of boules might be considerably extended by vibrating the water surface on which they fell,

establishing standing waves that, it was hypothesized, replenished the entrained air in the interface. Some confirmatory work on this was therefore undertaken.

The first practical investigation into this used the ‘boule launcher’ as described above, (Section 3.1.1), with the addition of an electro-magnetic valve in the water feed line from the constant-head supply to the launcher. This addition allowed short burst rather than a continuous stream of droplets to be fired, and with practice ‘single-shots’ could be achieved, allowing for the placement of single boules on the apparatus.

A nylon moulding, adapted from the transit cover of a toner cartridge, was employed as the vibrating table. This had originally been slid over the cartridge and had a lip on three of its sides, with one end plain. Inverted, therefore, it provided a shallow trough, open at one end, with internal dimensions of approximately 28 x 5 x 0.3cm. This trough was mounted on two tubular aluminium pillars, 2.5cm. in diameter, and 3.5cm. long, which in turn rested upon the cones of two Mylar-coned loudspeakers, used as convenient transducers. These were driven by a variable-frequency oscillator, with a 180° phase relationship between them. It was found by this method that a fine adjustment of the standing-wave pattern on the water surface could be achieved through the altering of the respective oscillator phase amplitudes, and that the pattern of waves could be varied so as to retard the passage of boules across the surface and bring them to a standstill. Figure 3.7 shows the schematic arrangement of the vibrating table.

A series of measurements of boule duration was then undertaken. Frequency was found to exert more influence over this than amplitude, although very low amplitudes were ineffective, whilst very high ones led to chaotic disturbance of the water surface.

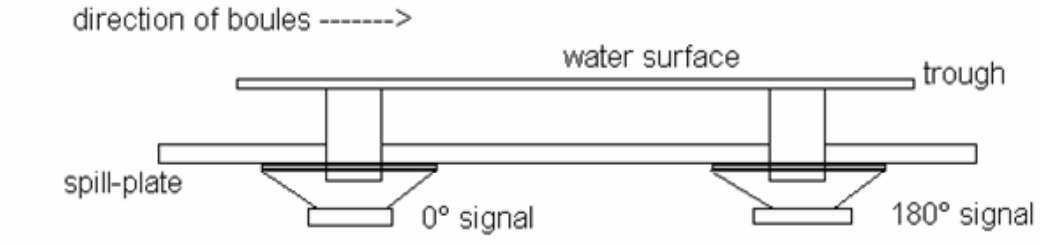

Figure 3.7. Schematic arrangement of vibrating table.

During trial runs little difference was perceptible between measurements of boule duration taken with the apparatus out in the room rather than screened in a Faraday cage, and screening was dispensed with (as in Walker's trials), to allow for the easier use of a stroboscopic lamp to view the boules. Figure 3.8. shows a view of the general experimental arrangement.

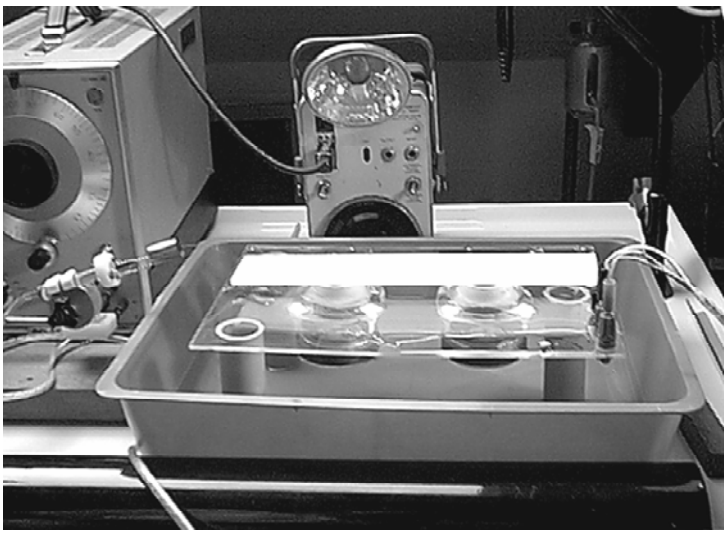

Figure 3.8. General view of vibration table.

The boules produced averaged 4.2mm. in diameter, this measurement being reached by firing boules into a weighing bottle, and using a light gate and counter to determine the number of boules producing a measured total mass. After initial trials of oscillator amplitude settings, this parameter was maintained constant, and data taken of the best-of-six duration times for a range of frequency settings. These results are displayed in Figure 3.9.

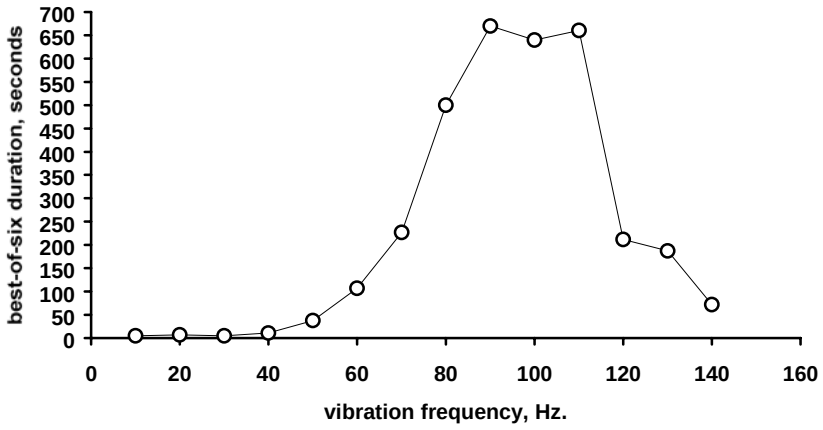

Figure 3.9. Boule duration shown against vibration frequency.

It may be seen from Figure 9 that the frequency of vibration determines boule longevity, the peak coming somewhere between 80 and 110 Hz. This value, however, is more related to the resonant frequency, or frequencies of the table. As this was open at one end, so that water might spill from it, there would have been different values for the damping effect of the water burden during the course of the experiments, and these uncertainties alone are sufficient to explain the relatively broad spectrum of frequencies over which boules might be sustained for long periods.

An example of the controllability of a drop on the table is given in Figure 3.10, which shows a boule that has been positioned almost centrally in the circular shadow of one of the transducer tubes, visible through the white nylon table.

Figure 3.10. Boule positioned inside a circular shadow, 11 minutes after formation. (Approx. 1½ times full size).

Under these conditions the drops appeared uncannily robust, and on such occasions as two collided the result seemed to be inevitable rebound rather than disruption of either. On rare occasions two colliding boules coalesced to form one larger one.

A stroboscopic lamp (General Radio Co. ‘Strobotac’ 1538-A) synchronized with the vibrator oscillator was used to view the boules, and by careful temporary off-setting this

allowed any part of a boule's vertical oscillatory motion to be viewed. It was not possible at the time to photograph these events satisfactorily in magnified detail, but a gas (NeHe) laser beam aimed at the interfacial area passed in part undeviated, suggesting an air film significantly greater than the light wavelength (633nm).

The portable demonstration apparatus previously described (Section 3.1.2 and Figure 3.2) also had the means to impart oscillations to the water surface. This particular apparatus did not give such extended longevity to boules, but comprised only a single oscillator and transducer. (In this respect it was more akin to Walker's apparatus). The needle used in the launcher gave smaller droplets – in the region of 2mm diameter – and these could be maintained for about 3 minutes at a frequency of 55Hz.

In addition it was found that boules might be sustained for long periods on a vibrating water surface if drops were dispensed by from 'gentle placement' source as previously described. The only reasonably critical factor here in determining complete success in producing the boule in the first place appeared to be the height through which the drop fell prior to arriving at the water surface. Drops of some 4mm diameter needed to fall from a needle whose orifice was between 7 and 8mm above the water surface. the explanation of this 'critical height' would appear to be that drops falling from a lesser height entrain insufficient air to generate an adequate air-film, whilst those falling from greater heights had sufficient kinetic energy to squeeze the air-film to too great a thinness to guarantee success.

3.2.5. The Influence of Relative Humidity on Normal Boule Formation.

Tomlinson [15] had observed boule suppression in conditions of high humidity, and Prokhorov [35] considered that coalescence could only be certain in a saturated atmosphere. These statements, combined with Mahajan's suggestion [32] that boules would form more readily at high altitudes than at sea-level, a difference involving pressure and humidity, were deemed sufficiently significant to merit possible confirmation.

This was confined to a series of simple experiments carried out in an enclosed environment where the relative humidity might be controlled within reasonable limits. To provide such an environment a fibreboard box measuring some 70 x 60 x 60cm was constructed, having a well-fitting but removable perspex front to provide access and observation. A vertical 70mm diameter DC circulating fan was installed a few centimetres from the floor at the back of the box to assist in the rapid establishment of a uniform humidity level.

A range of humidities was provided within the chamber by the following techniques:

i) an open container holding solid calcium chloride lumps in a saturated calcium chloride solution was used to establish a relative humidity of approximately 26%. The RH level achieved was higher than the theoretical value of 17 – 19% usually quoted for this material. (see International Critical Tables, [62]). This discrepancy was attributed to the small but significant amount of evaporation from the bulk water surface necessary for the experiment, and to the possible leaching of the moisture content of the chamber materials into the chamber atmosphere.

ii) Ambient humidity, obtained by simply removing the chamber front and allowing the atmosphere within to equilibrate with the environmental humidity of the room, was used to provide a mid-range humidity of 57%

iii) Humidities above ambient were established by the use of a damp filter paper placed inside the chamber below the circulating fan, such that the air-current assisted in the evaporation process. By careful control of both the initial wetness of the paper and the amount of its surface exposed fairly steady humidities of 78% and 92% were achieved without significant drop in the chamber temperature.

iv) Saturation was achieved by a more robust application of the previous technique, combined with an initial ‘injection’ of steam into the chamber just prior to sealing it. (This situation caused severe fogging of the observation

window, which was therefore treated inside with a thin film of silicone oil to discourage the formation of fine condensate. The large droplets of condensation resulting from this were not a serious obstacle to observation).

Boules were generated by the 'gentle placement' technique, as this allowed for a far smaller container to be used in the receiving vessel, with a consequent reduction of the evaporative surface and interference with humidity stability in the lower measurement ranges. A cylindrical stainless-steel trough 4cm in diameter and 2cm deep was used to hold the substrate water, and this was fitted with a drain-tube halfway up to allow significant drop numbers to be used without the necessity for opening the chamber. The dropping apparatus was essentially as described in Section 3.1.4 above, except that a larger reservoir was employed to allow for greater drop numbers to be produced. The needle was found to form drops of 24mg mass, giving them an equivalent diameter of 3.58mm.

Attention was paid to achieving and maintaining cleanliness during the experiment. Good quality deionized water was used, and prior to starting the water systems were well flushed with the same water stock. In addition, the stainless steel needle and trough were cleansed of surface oxide by immersion in chromic oxide solution, followed by thorough rinsing in deionized water. The completed apparatus is shown diagrammatically in Figure 3.11.

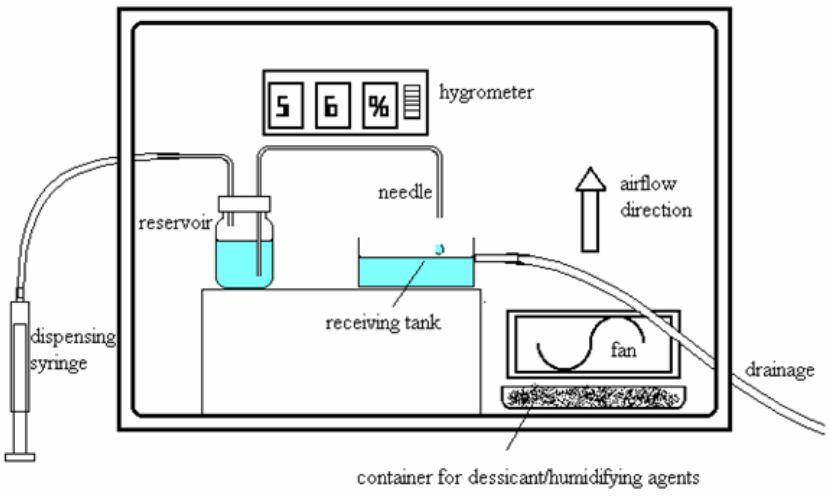

Figure 3.11. Schematic diagram of test chamber for humidity effect.

Finally, the needle was positioned so that boules were forming readily under ambient conditions. The self-draining facility in the receiving tank meant that its level could be kept within that required for the effective formation of boules.

For each of the humidity settings employed a total of 500 drops was slowly released. It was noted whether or not coalescence was immediate, or delayed with the formation of a boule. The number of boules formed throughout the run being noted, the 'formation efficiency' could be calculated. Note was also taken on an arbitary scale of whether the duration of the boule was long, say 1-2 seconds, or less so. 'Short' duration was taken to imply a time in the order of 100-150-ms – long enough for the eye to register but still an apparently short event.

Table 3.2. records the results.

RH%	No. of boules per 500 drops	Formation efficiency %	Duration (See caption)	Additional observations
26	254	51	L/M	Boules formed easily, some with durations in excess of 2 seconds.
57	263	53	M/L	Boules formed easily, but with fewer noticeably long durations. Some had duration times <1 second.
78	219	44	M/S	Formation still good, but with generally shorter durations. Some immediate coalescences produced secondary droplets, some of which became boules.
92	83	17	S	Far fewer boules formed, and those that did were of short duration. Some of these produced secondaries, as did many direct coalescences.
100	0	0	(n/a)	No boules observed. 2 cases of secondaries forming during coalescence, but both immediately re-coalesced on contacting the surface.

Table 3.2. Variations in boule coalescence rates with humidity. (Long duration was taken as >1second, Medium as between ~ 100ms and 1s, and Short as <~100ms).

The implications of these results are more fully discussed in Chapter 7 in the course of consideration of the influence of humidity on coalescence potential. They do, however, comprise an interesting reinforcement of the observations of previous workers that ambient humidity can have a profound effect on the ease, or even the possibility, of producing boules.

3.3 Summary of Confirmatory Experiments.

The experimental work detailed in this chapter was largely undertaken in confirmation of results and phenomena previously recorded. Such an undertaking might perhaps be viewed as surperfluous, or at the least indulgent. Justification for this effort, however, came from the following considerations.

i) Although floating drops are a common enough occurrence in nature, as has been reported in Chapter 2 they have produced a scant literature. Direct investigation was deemed to give a worthwhile insight into the overall behaviour of such drops.

ii) Some of the work previously reported has been in a popular science format from amateur sources, and not had the scrutiny that reviewed publications would receive. (This statement is in no way disparaging to the work of amateurs, and a moment's reflection brings home the enormous debt to such dedicated workers).

iii) Reported work has been qualitative and observational. There is relatively little by way of repeated and confirmed measurement, and explanations of aspects of the phenomenon have often been speculative.

As a result of the preliminary investigations reported in this chapter the following findings appear confirmed and relevant to the topic.

i) During the lifetime of a boule there is no matter exchange between it and the liquid substrate below.

ii) In the absence of any significant electric field, surface contamination appears to be the primary arbiter of whether boules will form or not.

iii) A boule ‘rides’ the liquid surface on a film of entrained air, and the eventual thinning of this is a factor in the boule’s demise.

iv) Vibration of the surface causes more air to be ‘pumped’ into the film, resulting in a longer-lived boule.

v) Coalescence with the liquid below is enhanced by the presence of an electric field, whether this be from charge imparted directly to the boule or present from a separate field-source.

vi) Ambient humidity appears to exercise considerable influence over the formation of boules in the first place. Under conditions of high humidity it is difficult to form boules, at saturation (i.e. 100% RH) they do not form at all.

With these findings in place a series of experimental investigations was undertaken in an attempt to determine the following specific questions;

How do electric forces interact in the final collapse of the supporting air-film?

How are these interactions different from those of ‘normal’ coalescence?

In the absence of any deliberately established field, what is the origin of such electric forces?

What is the rôle of humidity in the formation and demise of boules? Does this affect i) the hydrodynamics of the processes, or ii) the electrohydrodynamics?

Investigations of these questions, together with the interpretation and discussion of the results obtained, form the remaining chapters of this thesis.

4 WATER MOLECULES, THE ELECTRICAL DOUBLE LAYER AND DROP CHARGING MECHANISMS.

4.1. The structure of water molecules.

The chemical composition of water was established in the 1780s as a result of the experiments of Cavendish and Lavosier. The former of these investigators derived sufficiently accurate data for the composition volume ratio of two to one for hydrogen and oxygen to be deduced, but this finding went unpublished. Gay-Lussac and Humboldt re-made the discovery in 1805, and Dumas extended their work in 1842, showing that the weights of hydrogen and oxygen combining in water are almost exactly in the ratio of 2 to 16.

The subsequent discovery of two additional stable isotopes of oxygen (1929) and of deuterium as a stable isotope of hydrogen (1932), together with that of tritrium, an unstable radioactive isotope of hydrogen two years later, has meant that water cannot be considered as a simple molecule of the form H_2O. The relative abundancies of some contributory isotopes are small, but some of the possible species are found to an extent in most water samples. Table 4.1, quoted by Franks [63], lists relative abundancies of the four major species.

Species ⟶	$^{1}H_2{}^{16}O$	$^{1}H_2{}^{18}O$	$^{1}H_2{}^{17}O$	$^{1}H^{2}H^{16}O$
Natural abundance, (ppm)	**997 280**	**2000**	**400**	**320**

Table 4.1. Relative abundance of major isotopes in water *(after Franks [63]).*

In addition to these water species there exist low concentrations of H_3O^+ and OH^- ions, adding complexity to the structure as a result of their free charge.

In a water molecule the orbitals of two hydrogen atoms overlap the outer *2p* orbital of an oxygen atom, giving a valence bond length of 0.99Å, and an orbital structure enclosing the nuclei. The positive nucleus of the oxygen atom, containing 8 protons, attracts the negative charges of the hydrogen atoms forming a dipole with its positive bias in the region of the hydrogen nuclei and its negative one at the filled oxygen orbitals. Figure 4.4, adapted from Taylor [64], details the spatial relationship (in Å) between molecular orbitals in water molecules.

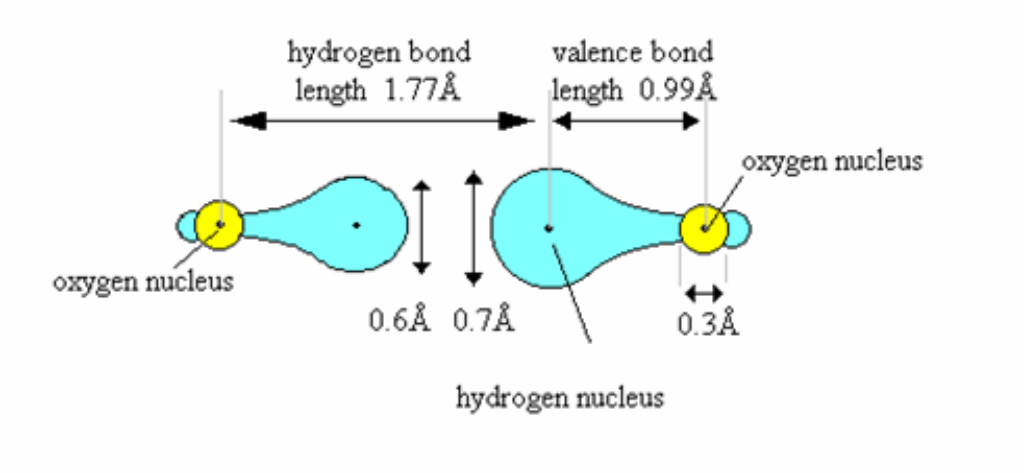

Figure 4.1. Spatial relationships between molecular orbitals in water. (Single hydrogen orbitals only shown). *(After Taylor [64])*

Resulting electrostatic attractions cause these molecules to form into tetrahedral structures, with three nuclei of a H_2O molecule forming an equilateral triangle with the oxygen nucleus at the apex and the two protons on the baseline. (Bjerrum, [65]). This structure is detailed in Bjerrum's diagram, reproduced in Figure 4.2.

As previously stated, all water, unless prepared with exceptional care, contains both a mixture of species and a number of polarized ions. The ion concentration of water is taken as 10^{-7} moles/litre, with a consequent pH of 7, but this is only based on a consideration of H+ ions. In reality these are most likely to be found in the hydronium ion form (H_3^+O), which was found by Eigen and de Maeyer [66] to have a mobility of $3.62 \times 10^{-7} cm^2 v^{-1} s^{-1}$, approximately twice that of the hydroxyl (OH^-) ion.

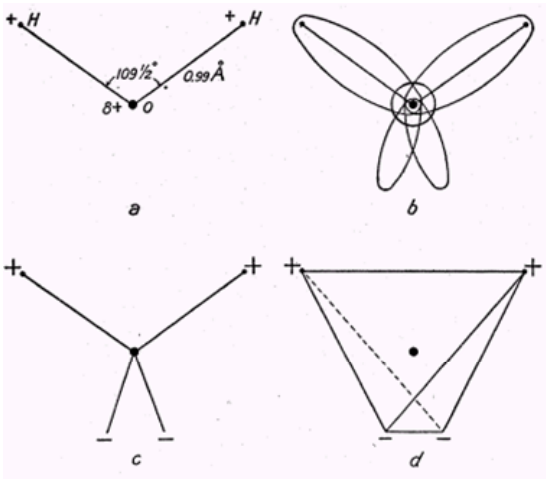

Figure 4.2. Electrostatic model of a water molecule. *From Bjerrum [65]*.

4.2 . The electrical double layer.

Water is an example of a liquid with a high dielectric constant (ε_r = 80, approx), and when in contact with a surface which tends to produce a solution, however weak, such as a metal, a charged double layer results. Image forces between ions in the metal and ions in the liquid result in charge separation at the interface, with one polarity being more tightly bound because it is smaller. In the case of a liquid and an insulating solid, dissociation processes within the insulator can also give rise to a charge imbalance, and consequent formation of a double layer.

The concept of double layers was first investigated by Helmholtz [67], and the investigations extended considerably by Gouy [68] and Chapman [69] and by Stern [70]. The development of the double layer concept resulting from these various studies is illustrated in Figure 4.3.

Helmholtz' initial theory [67] assumed that the counter-ions formed arranged themselves parallel to the charged surface in what was effectively a monomolecular layer. This would give a double layer in the form of a parallel-plate capacitor, and lead

to the rapid falling off of potential, as shown in Figure 4.3 *(A)*. Consideration of this model caused it to be seen as only an approximate description of the situation, as ions in solution would be subject to diffusion in the liquid as a result of thermal Brownian agitation, and the Gouy-Chapman model (Gouy [68] and Chapman [69]) incorporated this refinement as shown in Figure 4.3 *(B)*. This model, however, considered ions to be

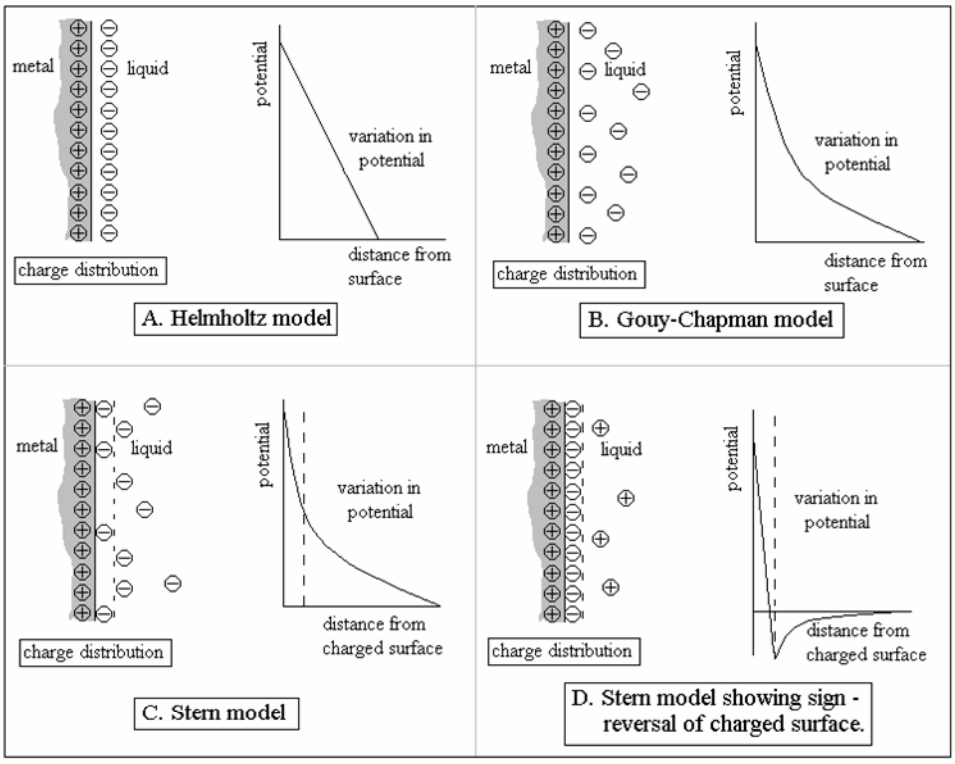

Figure 4.3. Development of the double-layer theory. *(adapted from Butler [71])*

point charges, neglecting their diameters, and gave an inadequate explanation of events close to the surface where charges were high and distances small. Gouy introduced the concept of a diffuse layer just within the surface as an explanation of the necessary balance between electrical and osmotic forces in the region. This dispensed with Helmholtz' initial concept of a simple capacitor, and allowed for a gradual increase in numbers of ions of one sign and decrease of the opposite sign on approaching the surface. Chapman developed Gouy's hypothesis, using Poisson's equation to find the equilibrium distribution of ions in the diffuse layer. This, however, gave rise to excessively large theoretical capacities (~240μF/cm²) for small potential differences. Stern [70] modified this theory to give a model in which the double layer had two parts.

One part comprised a single layer of counter ions held close to the bound surface charge – effectively the Helmholtz layer – the other a more diffuse (Gouy-Chapman) layer of the same polarity extending into the body of the liquid. This is illustrated in Figure 4.3 *(C)*. In this case the potential falls of rapidly and approximately linearly for short distances from the surface changing to a more gradual and exponential reduction on moving further into this diffuse layer. Stern also identified sign reversal as shown in Figure 4.3 *(D)*, leading to regions of net potential sign change.

The diffuse layer cannot approach the actual interface more closely than a few molecular diameters, and its actual thickness is dependent on the conductivity of the liquid. In the case of liquids of low conductivity, less than some $10^{-11}S/m$, say, the diffuse layer has significant thickness, and may extend across the whole cross-section of a liquid held in a small diameter tube, giving a uniform charge density across the section. Water and aqueous solutions, on the other hand, with conductivities greater than about $10^{-4}S/m$ have diffuse layers only a few molecular diameters thick. Polar molecules such as these are attracted to the free charges and orient themselves accordingly, therefore modifying the charge distribution in the liquid. This is illustrated in Figure 4.4.

A liquid flowing in a pipe carries charge from the diffuse layer, and currents in the range 10^{-9} – 10^{-14}A have been shown to result from this (see Cross [72]), this current appearing with both laminar and turbulent flow. Turbulent flow and rough surfaces both contribute to greater charging levels. Liquids with high conductivities and short charge relaxation times rapidly dissipate this charge to any pipe or tube containing them, whilst those with high resistivities, and consequent long relaxation times, carry charge with them. The charge relaxation time, τ, is given by,

$$\tau = \varepsilon\varepsilon_0 / \sigma \qquad (4.1)$$

where ε is the relative permittivity of the liquid, ε_0 the permittivity of free space, and σ is the liquid conductivity.

Thus it may be seen that any charge produced in a conductive liquid such as water ($\sigma >$ ~10^4 S/m) by dispensing drops through a needle, as in the present experiments, cannot remain bound to the liquid, and that the charge found upon the resulting free drops must originate from some mechanism other than that of fluid flow in the needle.

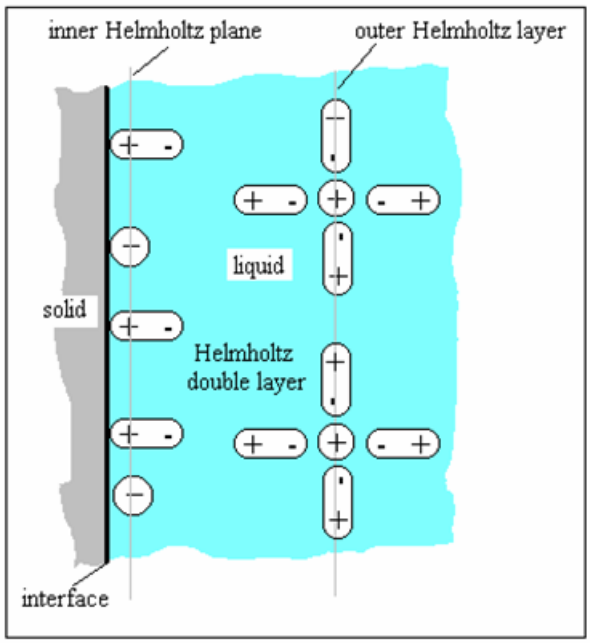

Figure 4.4. Double layer at interface of a solid with a polar liquid.

4.2.1. The double layer at a gas/liquid interface.

The early interpretation of the electrical double layer at a gas/liquid interface has been extensively reviewed by Loeb [73]. These early studies, originating from J.J. Thompson's laboratory, principally concerned cataphoretic effects on small gas bubbles in a liquid medium. McTaggart [74] suspended small bubbles of various gases in a water-filled cylindrical glass cell, spun on its horizontal axis so as to maintain a steady bubble position. This method allowed bubbles to become centralized within the liquid, remote from the cell walls and therefore eliminated the practical problems of bubble adhesion that had been a factor in the earlier electrophoretic work of Quincke [75]. A variable electric field could be established along the cell axis. From his measurements of v_x, the surface drift velocity, McTaggart was able to establish a value for ζ, the double layer potential, of,

$$\varsigma = 4\pi\, q_s d / \varepsilon_r = 55\text{mV} \qquad (4.2)$$

where q_s is the surface charge density, d the double layer thickness and ε_r the relative permittivity of the liquid medium.

McTaggart's work was extended by Alty [76] who found the charge on a bubble constant above a certain diameter limit (~ 0.33mm), but decreased for diameters lower than this. Improved measurement techniques led to a revised ζ value of 64mV. Alty explained the negative polarity of the water surface as resulting from the orientation of the O- end of dipoles towards the surface. This structure (*O*- end towards the surface and *H*+ end inwards), would allow free negative ions in the liquid bulk to attach themselves to the positive ends of dipoles, resulting in a tightly bound negative outer layer with a corresponding number of free positive ions within the liquid. Any removal of the outer surface would take negative ions away, leaving a bulk of positively charged ions in the water.

Consideration of the value of ζ was further continued by Chalmers and Pasquill [77], who established the higher value of ζ = 0.26V. Their experimental method attempted to eliminate as far as possible the effects of the inevitable use of metallic contacts, with their accompanying contact potentials. Drops were produced from a grounded metallic needle, falling on to a horizontal wet filter-paper. This was considered to be in effective contact with the *inside* of drops that formed beneath it, and therefore to be at the potential of the interior of the drop. These secondary drops then fell into a copper Faraday cup, where their charge was measured. A potentiometric measurement of the necessary potential between the filter-paper and the needle to neutralize the charge on the drops allowed the potential existing between the drop and the filter-paper to be established. Neutrality of the drops was checked by substituting a zinc cup for the copper one, there being different contact potentials between water/copper and water/zinc.

The results of this experiment led Chalmers and Pasquill to a measurement of –0.26V for the potential across the water drop, (the outer surface being negative). This figure

was found to be independent of both drop size and the material interposed between the needle and the Faraday cup. A variety of wetted intermediate materials was tested, including silk, cotton, glass wool, asbestos, wool and barium sulphate, all leading to the same result and thereby confirming that this material made no contribution to the chain of potentials involved.

Calculations based on this figure suggested that some 1 in 30 of the dipoles of the outermost molecular layer of the water is oriented normally with the surface, with their negative charges closest to the surface [1]. These calculations showed that the potential difference across the water surface, i.e. the double layer potential, is independent of the drop area and therefore of the drop diameter.

The origin of the charge on free drops is therefore a consequence of the double layer formed at their surfaces. For many practical purposes we may therefore consider a simple model of a water drop as having a net negative charge at its surface, this being balanced by the Helmholtz plane (i.e. close to surface charges) and the diffuse layer within, remembering that for polar molecules such as water this diffuse layer will be at most a few molecular diameters thick. Figure 4.5 presents such a simplified model.

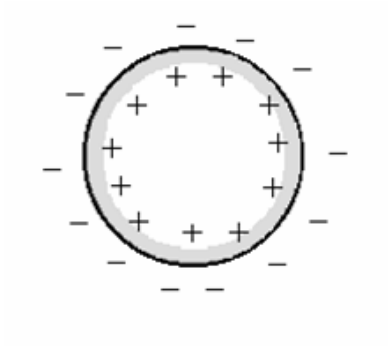

Figure 4.5. Simplified polarized water droplet.

[1] [Chalmers & Pasquill's calculation, in its original units, was thus: Consider the surface as a plane capacitor, of capacity C. $C=A/4\pi d$, where A is the area and d the dipole moment. If σ, the charge density, is qA, for A=1cm², $q=\sigma$. The potential, V, is therefore given by $V=q/C$, i.e. $V=4\pi\sigma d$ = 0.26/300, giving σd = 6.9 x 10^{-5} esu/cm. For water, d = 1.9 x 10^{-19}esu/cm giving 3.6 x 10^{13} dipoles per cm². Taking the surface area occupied by a water molecules as about 9 x 10-16cm² this produces a number of surface water molecules of 1.1 x 10^{15}/cm². From this it is seen that about 1 in 30 (i.e. 3.6 x 10^{13} / 1.1 x 10^{15}) dipoles is 'active' and therefore normal to the surface.]

4.3. Charging mechanisms.

The term ‘charging mechanism’ is taken to mean any action that brings about the redistribution of electrons in materials, thereby being the origin of the charge that appears in a process.

A total of five different mechanisms has been identified that can be responsible for charge on liquid drops (Cross [72, pp. 81-85]), these being;

i) disruption of the double layer at a liquid/air interface,
ii) similar disruption at a solid/liquid interface, as, for example, in an orifice,
iii) charge transfer arising from contact potentials at the liquid/solid interface during drop formation,
iv) charge separation within the bulk liquid in the presence of an electric field,
v) charge due to some rearrangement of the random distribution of ions within the liquid.

Of these five possible mechanisms the first three have most direct relevance to the current situations, and these are briefly considered.

4.3.1. Disruption of the double layer.

Most investigative work involving double layer disruption has concentrated on more dynamic and violent circumstances. Lenard, following his early observation that the mist above waterfalls carried a negative charge [78], extended his investigations to a consideration of the charge separation resulting from the disruptive break up of the double layer at air/water interfaces by splashing [79]. The magnitude of this charge was found to be of the order of 2×10^{-12} C per cm^2 of new surface thus produced. An extensive review of the process was given by Loeb [73] in the course of his consideration of spray electrification. He considered the values obtained by Lenard to

be of dubious accuracy in the light of those derived by Alty [76] from his studies of the cataphoresis of gas bubbles in pure water, which suggested a figure perhaps 50 times less than Lenard's.

Levin and Hobbs [80] made an extensive study of the charge separation taking place during splashing on solid and wetted surfaces, showing that the charge resulting from the formation of fragments thrown out by the crown of the splash are generally negatively charged, and that such a disruptive process generated charges of pico-coulomb order, most of this being transferred by droplets less than about 20μm in diameter. Their calculations of theoretical charge magnitude were based on Chalmers and Pasquill's experimental determination reviewed above to produce a potential of 0.26V across the water-air interface.

Levin and Hobbs considered other possible contributory charging mechanisms on disruptive splashing, including the random distribution of the ions within the liquid on break-up. This, however, was deemed to represent a statistically insignificant chance of any noticeable charge being produced. Induction due to the influence of external fields in the vicinity of the breakup was also identified as being a possible charging process. Finally, in the context of their particular research, contact charging from ice was also considered.

4.3.2. Disruption at an orifice, contact and induction charging.

These may be considered partly as an extension of the previous process. Suppose a drop be formed at the orifice of a grounded metal capillary such as a needle, with a coaxial electrode surrounding it. At the point of rupture from the column of liquid within the needle, the drop will acquire a small charge from the rearrangement of the constituent molecules within it, and the consequent formation of a new double layer. However, there is likely to be a far larger charge imparted as a result of the contact potential between the drop and the needle. In an interesting experimental study by Wang and Bailey [81] it was shown that, even in the field-free condition obtained by grounding the coaxial electrode, a drop thus leaving a grounded needle will acquire a charge by

induction, the magnitude of the charge being attributed to the contact potential between the liquid and the needle. Wang and Bailey used a variety of needles with varying outer diameters, and found for deionized water passing through stainless-steel needles an approximately linear relationship between the needle diameter (and hence drop diameter) and the charge appearing on the drops[2]. Their results are reproduced in Figure 4.6.

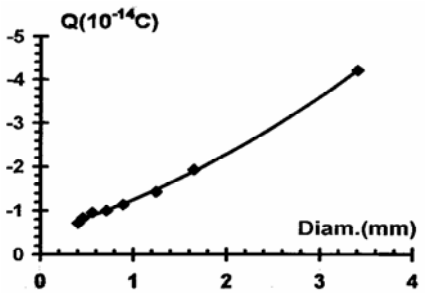

Figure 4.6. Charge on deionized water drops against needle outer diameter. *from Wang and Bailey [81].*

4.4. The effect of charge on surface tension.

It is known that an electric field modifies the surface tension of a liquid. This effect was investigated by Efimov, Zvonov and Efinova in 1979 [82] for benzene, where the reduction in surface tension of drops with a range of voltages applied to them showed an almost linear reduction in surface tension with voltage. Table 4.2. gives their results in terms of the ratio γ_f / γ_0, where γ_0 is the surface tension in zero field and γ_f the surface tension in a field, f, against applied potential, together with the equivalent charge to radius cubed ratios q/R^3, where q is the drop charge and R the drop radius.

A similar investigation into surface tension reduction for water by an applied electric field was carried out in 1998 by Sato, Kudo and Saito [83]. Distilled water was

[2] [This relationship between drop charge and capillary diameter may be interpreted in the light of Rayleigh's investigations [10] into the sizes of drops produced from different orifices. Rayleigh concluded *(i)* that the outer rather than the inner diameter of the tube exercised the greater influence over the size of drop produced, with the effect of wall thickness being only slight, and *(ii)* that all other things being equal the mass of the drop (and hence its volume) was a linear function of the outer diameter of the tube. With this in mind, it may be seen that the results obtained by Wang and Bailey effectively relate to a constant charge to mass ratio.]

subjected to charging potentials between zero and –8kV. Their results are shown in Figure 4.7.

Voltage, kV	γ_t/γ_0	q/R^3 mC/m^{-3}
0	1	0
1	0.811	5.87 – 6.33
2	0.681	13.50 – 13.98
2.5	0.523	20.20 – 20.60
4	0.293	32.4 – 32.9

Table 4.2. Variation of surface tension of benzene with applied voltage. *(From Efimov, Zvonov and Efimova.[82]).*

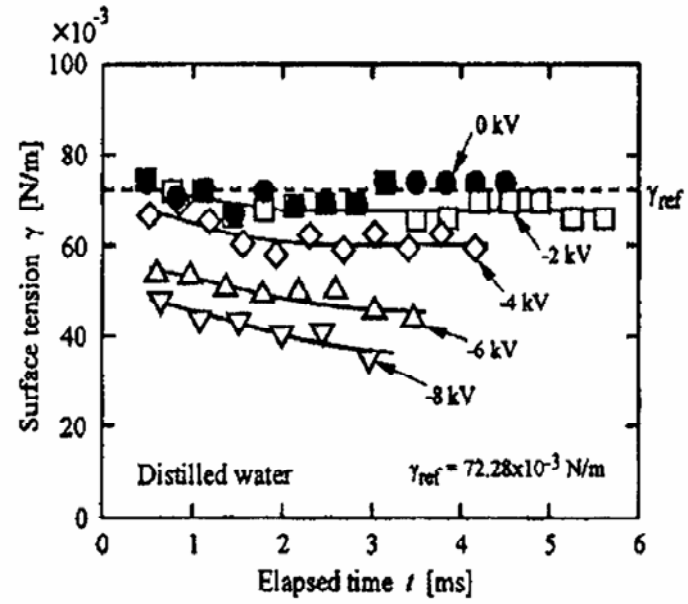

Figure 4.7. Variation of surface tension of distilled water with applied potentials between 0 and –8kV. *(From Sato, Kudo and Saito [83]).*

This reduction in surface tension is attributed to increased alignment of the dipoles in the surface layer of the water – the charge being only present at the surface – resulting in increased repulsion between these dipoles. This leads to a lower net surface energy and a consequent reduction in the surface tension. A previous investigation by Schmidt, Hurd and Snavley [84] using a surface balance had involved potentials up to 10kV of both polarities. Whilst both polarities showed a reduction in surface tension, this was found to be slightly greater for negative potentials, and attributed to the normal

preferential alignment of water molecules at the surface, with more constituent hydrogen atoms outward-facing.

It is important for the purpose of the present research that this reduction of surface tension is properly contextualized. A consideration of the equivalent charge necessary to achieve any perceptible deviation in surface tension value from that of uncharged conditions shows that charge to radius cubed ratios need to be in the order of $>5mC/m^3$, a figure well in excess of those encountered in water boule systems.

4.5. Conclusions

From the foregoing we may conclude that;

i. Water drops can carry a small but significant charge, even if formed in the absence of an external field or of any deliberate charging process. This may be attributed to all or any of *(i)*, the existence of a double layer at the interface between the drop and the air, giving a net negative charge, *(ii)*, a contact potential between the drop and a metal surface such as a dispensing needle, and, *(iii)*, an induction charging process in a field-free situation, whereby a small potential on the forming drop from either or both of *(i)* and *(ii)* imposes a charge on the drop as it leaves the needle.

ii. The magnitude of this charge, for drops of a few millimetres diameter is generally in the order of a few tens of femtocoulombs.

iii. It is established that a potential exists across the double layer forming the liquid surface of a drop, and that this is independent of the drop diameter.

iv. Surface tension is reduced by surface charge. This effect only begins to take on any significance when charges exceed those encountered in boule systems by some two to three orders of magnitude.

5 CHARGE TRANSFERRED BY WATER BOULES AND BY FALLING AND DISRUPTED DROPS.

5.1 . The charge transferred by boules traversing a surface.

It has been shown in the Chapter 3 that boules may be caused to traverse a surface for some considerable distance, sometimes even completely crossing short to medium length surfaces and projecting off a far edge. This observation was exploited in a series of experimental investigations to measure the charge level associated with water boules, as it suggested a relatively straightforward method of measuring any charge that they might have, simply by allowing them to fall, from as short a height as practicable, into a Faraday cup. For this purpose apparatus used in the initial experiments on boule extinction in an electric field (Chapter 3, section 3.2.2) and after removal of the field electrode was modified in the following manner;

i) the stainless-steel dish was replaced by a carefully polished brass plate, 15 cm. square by 16 s.w.g, set horizontally. This allowed easy access to the surface, and entailed using only a relatively small volume of water to cover it;

ii) a Faraday cup was constructed in stainless steel, with a short length of screened cable terminating in a Teflon-insulated BNC plug. The capacity of this system in picofarads was measured using a recently calibrated Wayne-Kerr Capacitance Bridge, type CT492. The dry mass of the removable inner container was measured;

iii) control of boules from the 'launcher' was assisted by use of the electrically operated solenoid valve (Section 3.2.4) in the supply line from the constant-head apparatus, permitting either a 'single-shot' or a continuous flow.

At the time of this experiment an electrometer was not available, and charge measurements were therefore made by transferring the accumulated charge in the

Faraday cup to a 1nF high-quality polystyrene capacitor, (approximately 100 times the capacity of the collection system), and measuring the capacitor potential by means of a high impedance voltmeter (Hewlett Packard type 425A).

The fundamental relationship between charge, *Q*, capacity, *C* and potential, *V* is,

$$Q = C \times V \tag{5.1}$$

and if C and V are measured in Farads and Volts respectively, then Q will be in Coulombs, thus allowing for charge to be measured directly as a potential difference produced across a known capacity[1].

This technique and choice of transfer capacitor value ensured a minimum of 99% charge-transfer. During the experiment the needle, its coaxial electrode, the brass plate and the outer casing of the Faraday cup were all connected to a common ground, and the whole apparatus, except for the constant-head system, operated within a Faraday cage. Figure 5.1. shows a general view of the setup.

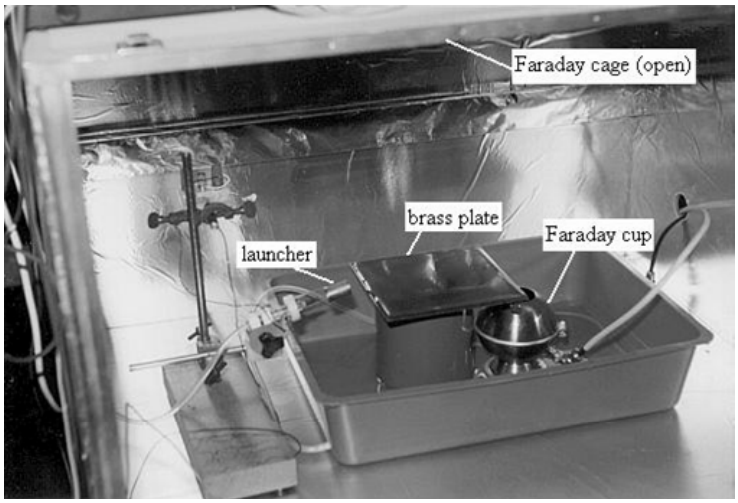

Figure 5.1. Experimental arrangements for measuring charge transfer.

[1] Following the subsequent acquisition of a Keithley 610C Electrometer these measurements were repeated with directly comparable results.

Prior to actual charge measurements it was necessary to establish the mean boule size, and this was done by counting boules falling off the far edge using a light-gate and counter, measuring the mass of water collected in the Faraday cup, and calculating mean drop size as before. This preliminary allowed for boule numbers during the experiment to be directly inferred from the masses of water collected. (This determination was performed first rather than have the light-gate in position during actual charge measurement to avoid the effects of any stray fields emanating from the counting electronics). Results of a total of 6 tests for mean diameter are shown in Table 5.1.

Mass (g)	8.63	6.55	6.87	5.68	8.09	6.30	**Total**	42.12
No. of Boules	157	119	124	100	145	117	**Total**	762

Table 5.1. Data for boule numbers compared with water masses collected.

From this it was calculated that the average mass per boule was 0.055g, and hence the average diameter was 4.7mm.

A series of cumulative measurements was taken recording the total charge transferred by successively greater numbers of boules, and these are recorded in Table 5.2, and displayed graphically in Figure 5.2.

Collected mass (g)	3.52	3.93	4.52	4.88	4.91	5.14
Transferred charge (x 10^{-10} C)	1.03	1.14	1.3	1.4	1.45	1.5

Table 5.2. Transferred charge for different masses of boules collected.

For drops of uniform size the charge transferred may reasonably be assumed proportional to the mass of the collected water, and a linear regression of these data showed that the magnitude of the total transferred charge in terms of the total mass of boule-water collected could be expressed in the form of the equation,

$$q_t = 0.2909m - 0.001 \qquad (5.2)$$

where q_t is the transferred charge in Coulombs x 10^{-10}, and m the mass of collected water in grams. The constant, 0.001, may realistically be explained in terms of the

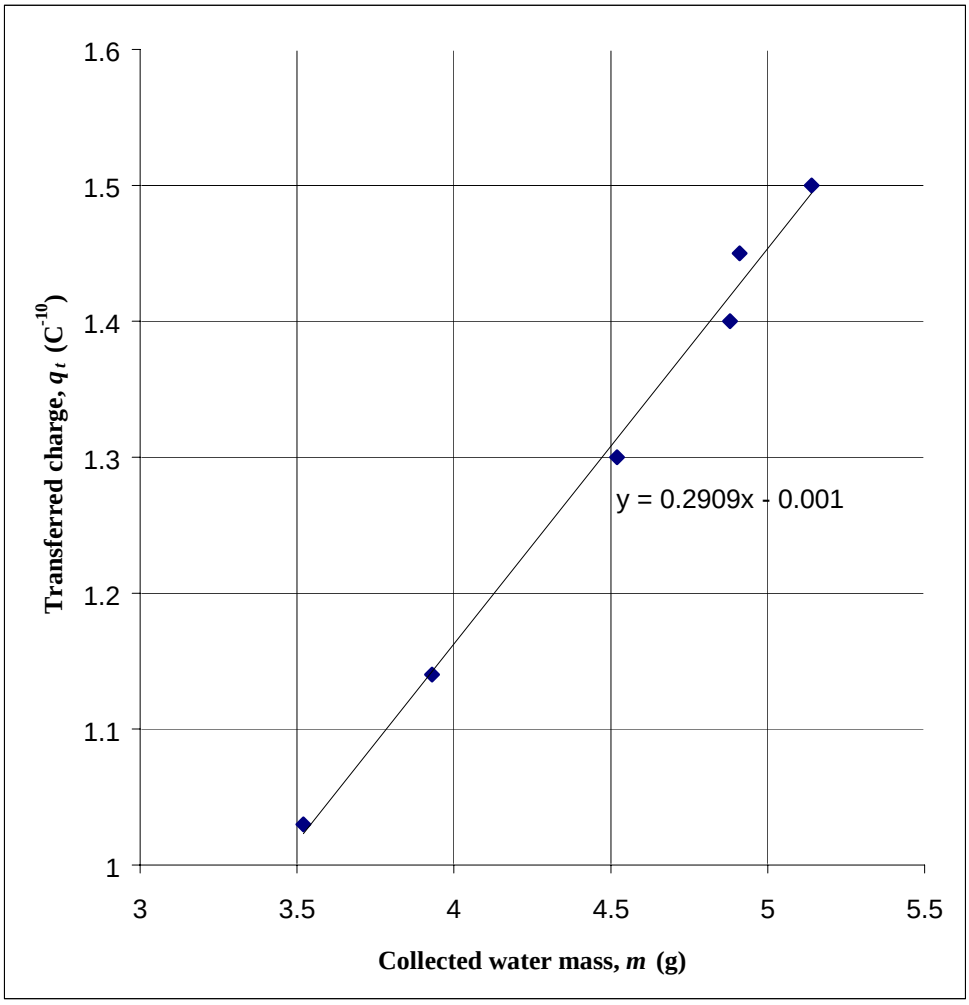

Figure 5.2. Plot of total boule mass collected against transferred charge.

imperfection of the regressional analysis fit, brought about by some inevitable experimental error, and discounted. Charge transfer for the geometry and drop sizes used is therefore closely described by,

$$q_t = 0.29m \tag{5.3}$$

A single boule of average mass 0.055g, was therefore transferring a charge of,

$$0.29 \times (0.055 \times 10^{-10}) = 1.6 \times 10^{-12}\text{C}. \quad (5.4)$$

this quantity being equivalent to 10^7 elementary charges.

5.2. Experimental consideration of initial drop charge just prior to landing.

The average charge on 0.055g dynamic boules calculated above (Equation 5.4) is sufficiently large to warrant an investigation into its origin. This must be from one of two possible sources: either the charge is resident on the future boule when it is an airborne droplet, and derives from its initial formation or from its trajectory through the air, or else the charge must be imparted to the boule as it traverses a surface. If the first case proves true, then it is necessary to explain the formation of the charge; if the latter case, then the charging mechanism must be explained. It must also be considered that both cases might be cumulative contributory factors.

Investigations were therefore undertaken to gather information on these possible origins of the final charge.

5.2.1. Charge transferred by drops from a grounded source: Method 1.

In this instance the apparatus used was as just described (5.1), except that the brass plate was removed and the Faraday cup repositioned so that its opening coincided with the trajectory of the droplet stream from the launcher. The launcher, its shielding electrode and the outer shield of the Faraday cup were grounded as before.

The stream was allowed to play into the Faraday cup, and the total transferred charge, q_t, measured. This showed that the charge to mass (q_t/m) ratio of the liquid collected was some 3.64×10^{-13} C/g, so that individual 0.055g drops were therefore transferring a mean charge of the order of 2×10^{-14} C.

During these investigations it was observed that, if the solenoid valve were used to send only individual or small groups of droplets into the Faraday cup, then there was a very occasional reversal of charge sign to positive from the more common negative. This observation was in accord with occurrences previously noted in certain other circumstances, and occasionally commented upon in the literature, where a sudden short-lived reversal of charge is found. The explanation of this effect is obscure, and warrants further investigation, but serves to counsel caution in interpreting cumulative charge data too rigidly!

5.2.2. Charge transferred by drops from a grounded source: Method 2.

A second investigation into the charge on droplets from a grounded source took place in order to compare the charge found on such droplets that were falling vertically simply under the force of gravity, rather than being first projected upward as was the case in the previous experiment. By this it was hoped to determine whether trajectory time through the air had any bearing on the final charge transferred.

The apparatus used in the 'gentle placement' method for boule production was employed as the droplet source, allowing the dispensing of individual drops in vertical fall. Following Rayleigh's investigations into the sizes of drops, and his methods developed for producing drops of different diameters [10], the needle had two metal collars of different outer diameters made to be a push-fit on its end, so that a total of three different drop sizes might be produced.

For this application a Faraday cup was constructed with particular care being given both to achieving very good insulation of the interior cup and to the elimination of charge leakage through the aperture in the shielding case. The cup was set well down in the outer shield, and the top opening made slightly smaller than the cup diameter. An additional screen was made to close most of the main aperture during use. This took the form of a concave stainless steel dish with a 3mm diameter opening at its lowest point through which the dispensing needle might pass, and which sat in the principal aperture of the apparatus.

A PTFE-insulated BNC connector was used both to make the electrical contact to the inner cup and to provide its physical support, resulting in a substantially air-insulated suspension of the cup and a minimal PTFE surface. (It had been found during previous experiments that residual charge on PTFE is sometimes a source of measurement error).

The complete apparatus had an electrical capacity, including its direct connector to the electrometer, of 16pF. Figure 5.3 shows dismantled and assembled views.

Figure 5.3. Faraday Cup, dismantled *(left)* and assembled *(right).*

Drop sizes being ascertained, the dispensing needle was inserted through the small hole in the assembled top shield. The inner cup was connected to the measuring electrometer (Keithley Model 610CR), and the needle, Faraday cup shield, electrometer ground and the Faraday cage in which all the apparatus was set all grounded to a good earth point.

Drops were dispensed into the cup, and the cumulative charge noted. The cup was removed and weighed to determine the number of drops contained. This process was twice repeated to find charge data three different drop sizes. Results are shown in Table 5.3.

Mean drop mass (g)	**Mean drop dia. (mm)**	**Collected water mass (g)**	**No. of drops collected**	**Total charge (x 10^{-12} C)**	**Mean drop charge (x 10^{-14} C)**	**Charge/mass ratio (C/g)**
0.020	2.120	0.941	47	5.0	10.61	5.31 x 10^{-12}
0.052	4.630	2.845	55	3.2	5.82	1.12 x 10^{-12}
0.093	5.616	4.995	54	4.0	7.40	7.96 x 10^{-13}

Table 5.3. Charge transferred by grounded drops of different diameters.

It was noted that the medium drops (0.052g mass) recorded a proportionally smaller charge. This may possibly have arisen as a result of a slight variation in the conductivity of the deionized water during the course of the experimental measurements.

These results compare favourably with those found by the previous method (Section 5.2.1), and all lie within an order of magnitude of one another. It will be recalled that the results obtained from charge measurements on boules indicate that a boule may gather a charge some two orders of magnitude greater than this initial drop charge in the course of traversing a surface (Section 5.1.)

5.3. Measurement of charge resident on freely-falling drops.

An investigation was undertaken to determine compare the charge transferred by the methods previously described (Sections 5.2.1. and 5.2.2.) with measurement by induction of the charge on freely-falling drops. This experiment therefore sought to determine the magnitude of charge that might be found on free-falling drops of the diameters previously measured, dispensed vertically downwards from a needle. Two important conditions needed to be met. First, the stock water and the dispensing system should be at ground potential, and shielded from the influence of any extraneous fields, and second, the charge measurement should not involve contact with a solid material so that possible contact potentials might both be avoided.

The first experimental requirement was met by using the dispensing apparatus already described in the last determination of grounded drop charge measurements (Section 5.2.2 above). This needle assembly, together with its two collars, allowed for the production of drops of 2.12, 4.63 and 5.62mm diameters. The second criterion, inductive measurement, was addressed by the use of a shielded induction tube 15mm in diameter and 30mm long. Figure 5.4 shows a diagrammatic representation of the experimental arrangement.

The needle orifice was positioned so as to be just above the top of the induction tube through which the drops fell, this position maximizing as far as possible the effective transfer of charge by induction to the tube rather than the outer screen. Drops fell through the apparatus on to a pad of grounded wire-wool in a container about 20cm below the measurement area. This served to retard the drops less violently than splashing on a surface, and to assist in dissipating any charge to ground rather than to the air above.

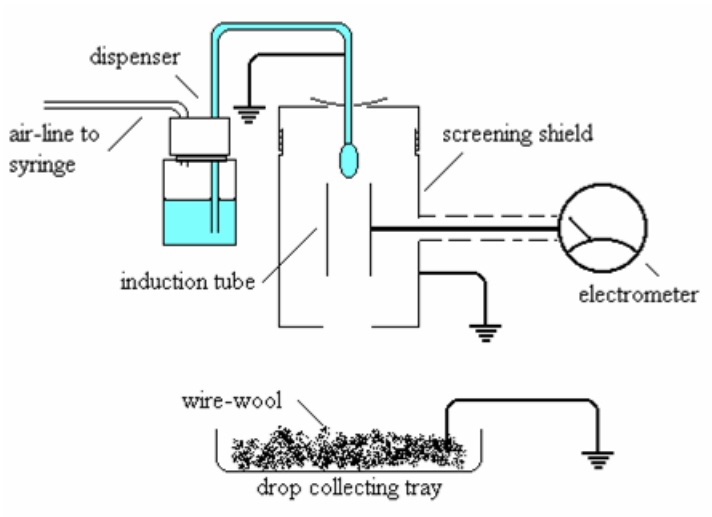

Figure 5.4. Experimental arrangements for measuring charge on freely-falling drops.

Drops could be dispensed slowly, and each one produced a sufficiently long pulse from its passage through the induction tube to allow an accurate reading of the electrometer scale. After each pulse the induction tube was fully discharged before allowing the next drop through. Each of the three series showed little variation in the individual charge measurements within it. Results of the measurements of 50 drops of each size are tabulated in Table 5.4.

Drop diameter, mm	**Mean charge/drop x 10^{-14} C**	Charge sign.
2.12	2.3	Always negative
4.63	3.0	Always negative
5.62	3.1	One positive, all others negative.

Table 5.4. Mean drop charges and charge sign for freely-falling drops.

It has been shown previously (Section 5.2.2) that comparable drops, similarly produced but falling into a Faraday cup, yield charge levels some two to four times greater than these (Table 5.5), and some explanation of this difference is required.

Drop diameter, mm	**Faraday cup method Charge x 10^{-14} C**	**Free-fall method Charge x 10^{-14} C**	**Difference in charge measurement (x10^{-14} C)**
2.12	10.61	2.3	8.31
4.63	5.82	3.0	2.82
5.62	7.40	3.1	4.3

Table 5.5. Charge comparisons, Faraday cup and free-fall methods.

Assuming consistency in drop-formation between the experiments, there remain three factors to consider in comparing these results. These are,

i) possible variations in height fallen and interaction with extraneous fields during fall,
ii) variation in conductivity of the water sample used,
iii) inaccuracy of induced charge measurement.

Examining these possibilities in turn, there seems little likelihood that the first explanation is of significance. In both cases the drops were dispensed *within* the shielding of the measuring device, and fell comparable small heights before the measurement point was reached. Additionally, the outer screening provided by the environment of the Faraday cage would have removed the effect of small external fields arising naturally in the environment.

The same stock water was used in all experiments, and in the latter two the measurements were carried out within two hours of one another. It is possible that contamination of the water due to either leached alkalis from the glass container or from the formation of weak ionic solutions forming within the hollow dispensing needle was sufficient to contribute to the difference in charge values obtained.

Drops were dispensed approximately 3mm above the top of the induction tube. Their velocity on entering the tube was therefore 0.243m/s, and on leaving it 0.80m/s. the residence time within the induction tube therefore being approximately 57msec. Whilst this was within the response time of the measuring instrument used (50msec) the possibility has to be considered that the induced charge measured was incomplete.

The results achieved in this series of experiments lead to the conclusion that drops produced from grounded sources carry a charge whose existence may be explained in terms of double layer theory, and whose magnitude, for drops of a very few millimetres diameter, is in the general order of 10^{-14}C.

There remains to consider what part is played in coalescence by both the net surface charge on a free drop and by the potential existing across the electrical double layer, and aspects of these issues are addressed in Chapter 6.

5.4. Additional charge gathered by boules traversing a water surface.

A consideration of Sections 5.2.1 to 5.3 above established that a droplet landing on a water surface brings with it a charge, and the experimental work reported has ascertained the approximate size of that charge. It remains, however, to consider the ‘charge amplification’ demonstrated by a boule that has traversed a water surface, survived intact, and been measured after leaving the surface.

There is clearly a charging mechanism or mechanisms at work but the exact nature of these is not obvious. It is perhaps helpful to review the available options as a prelude to investigating this issue.

An early, but useful, review of charging types was given by Loeb [85]. In this he identifies the following principal charging mechanisms.

i) Electrolytic effects.

ii) Contact electrification between metallic surfaces or metallic/semi-conducting surfaces.

iii) Spray electrification, involving the mechanical disruption of the surfaces of liquids and films, such as atomizing, bubbling and impact.

iv) Frictional (tribo-) electrification by impacts, friction, mechanical separations &c.

v) Ionic/electronic effects as in flames, produced by mass-movement of gases or solids.

Whilst some of these descriptions might be revised in the light of more recent knowledge they nonetheless remain a concise summary of many principal sources of charge. To Leob's list, however, should be added, *vi)* induction in an electric field.

Perusal of the categories listed above give some immediate disqualifications in the case of dynamic boules. There is no major disruption of surfaces in the sense of splashing and fragmenting, only the impact and surface deformation effects as the boule traverses the flat water surface. Whilst these cannot be discounted, the surface deformation is small when compared with surface destruction and reforming. Likewise the surface materials involved are liquid/liquid ones, and contact electrification in a simple sense as defined above is obscure.

The issue of electrolytic effects may also reasonably be discounted by a consideration of the interfacial systems involved in the experimental process. If the drop was induction charged as a result of an original contact potential between it and the needle, then this is manifest as part of the drop's charge *prior to its arrival* at the water surface, that is, as the whole or part of the small charge that the drop was bringing with it. As the plane upon which the bulk water surface lay was grounded, any charge resulting from electrolytic processes between the plate and its water film would be conducted away. It must be recalled that the drop is not in direct contact with the bulk water surface – such a situation would cause immediate coalescence – and therefore effectively it is in a capacitive relationship with the water surface, with an intervening dielectric layer of

vapour-laden air. This capacitive consideration of the boule/liquid system and its possible implications are introduced in (5.5), following, and developed in (8.3).

Whilst the exact mechanism by which the boule gathers additional charge is obscure, a consideration of the mechanisms summarized above suggests some initial lines of development. First, it is apparent that whilst the liquid surfaces of boule and bulk water are not disrupted, they *are* deformed. This deformation results in a constantly changing local curvature, particularly for the lower water film, as the boule passes across. It seems plausible that this deformation might result in transient local charging, passing to the boule as an image.

Additionally, whilst there is no direct liquid/liquid or liquid/solid contact, the existence of net movement within the system means that there exists the opportunity for charge separation between the different interfacial components. In the early stages of a dynamic boule's career the air-film will have a thickness sufficient for the entrained air to exercise a viscous drag on the boule surface. It is currently unclear whether the process is cumulative, i.e. the charge increases with distance travelled, or whether the additional charge is simply generated as a by-product of the drop's initial deformation of the surface. It has been historically demonstrated by Meunier [13] and again in the present series of investigations (Section 3.2.1) that there is no appreciable bulk transfer of matter across the interface in a boule system. It should, however, be considered that the highly active interfacial area might possibly give rise to small but significant matter-transfer arising from evaporation/condensation processes, and that this, together with the surface deformation previously noted could be sufficient to transfer charge of the magnitude encountered.

Several parameters require consideration in attempting to model such a charging process, amongst which the following might be suggested as being of potential significance.

i) The high humidity within the interfacial air film produces an atmosphere conducive to vapour-condensation, resulting in small, free and mobile droplets.

ii) It has been demonstrated by Prokhorov [35] that under conditions below saturation the vapour-pressure imbalance between the ambient atmosphere and the interfacial air film results in a net pumping of air into the interface. Pressure variation between the inner air-film and the ambient air may be sufficient to produce local condesation leading to a mechanism for the tansfer of matter from one liquid component of the system to the other.

iii) The forward motion of a dynamic boule creates air-flow both around the boule itself and into the interstitial air-film. The form and direction of the resulting viscous drag would be of importance in determining the paths taken by small condensed particles.

iv) The small interfacial separation results in relatively large field gradients being produced from modest charge differences between the boule and the bulk surface.

v) Free-running boules on a bulk surface may be seen by casual observation to decelerate prior to their coalescence, and their loss of kinetic energy must therefore contribute to the dynamics of the situation. Whilst this might be thought conventionally to be manifested in thermal energy changes, the availability of energy to the system must be carefully considered.

Environmental conditions are therefore in place that might realistically lead to an interchange of material between the contiguous surfaces that, whilst too small to manifest itself as an obvious matter-transfer on the macroscale, is adequate to result in a charge-producing mechanism. Such a mechanism is apparently distinct from tribo-charging, as it does not involve solid/solid contact, but operate rather across a vapour-phase interface. It is suggested that, pending further investigation, the term *trans-phase charging* might be applied as an identifier. This appears an appropriate term in view of the possible transfer of charge from one liquid phase to another, via an intermediate gas phase. In order to determine the detail of such a mechanism considerable further

investigation is required, and suggested initial lines for such research are detailed in Chapter 9.

5.5. A conceptual model – the boule system as a capacitor.

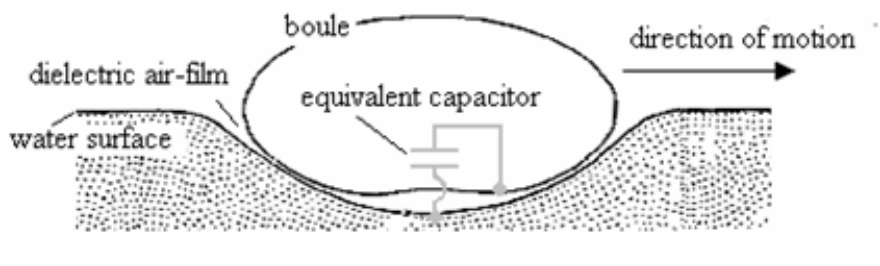

Figure 5.5. Moving boule in capacitive relationship to a bulk surface.

The situation is illustrated in Figure 5.5. A potential difference between the water surface and the underside of the boule will therefore result in a stress in the dielectric air-film, although the geometry of the interfacial region is such that the system is complex. This issue is considered in greater detail in Chapter 8, where a capacitive model descriptive of the system is developed, and consideration is given both to the interfacial geometry and the dielectric nature of the air-film at the interface.

5.6. Summary.

It has been shown that all drops, even if originating from a grounded source, have an inherent charge in the general order of a few tens of femtocoulombs.

When boules are formed from drops originating from a grounded source they therefore arrive at the plane water surface with a small charge. It has been demonstrated experimentally (5.1) that if such boules traverse a surface and leave it without coalescing, then they carry a charge enhanced by some two orders of magnitude. The mechanism of such charging is unclear (5.4), although a consideration of the interfacial

environment and the dynamics pertaining to it suggest that there is possible scope for matter-exchange between the respective liquids of the system, and that such an exchange might feasibly result in charge separation. The term ‘trans-phase charging is tentatively ascribed to the mechanism.

Attention has been drawn (5.5) to the capacitive nature of the boule system, resulting in dielectric strain within the interfacial air-film, and this topic is discussed in greater detail in Chapter 8.

6 A CONSIDERATION OF SOME ELECTRICAL POTENTIAL EVENTS AT COALESCENCE.

6.1. Introduction.

Consideration of the earlier work of Chalmers and Pasquill [77] concerning the potential considered to be resident on the outermost molecular layer of a drop prompted an investigation of the rôle that this might play in the coalescence process in water/water systems, and experimental work was undertaken to investigate this.

Most of the practical investigations reported thus far in this research have been concerned with the determination of charge-magnitudes as a means of measuring the transfer of electricity. Whilst these are convenient, and often relatively straightforward in terms of experimental technique, the very concept of charge implies a *quantity* of electricity that has somehow *accumulated*. Charge measurement does not, in this sense, give any record of time-dependency, being effectively the integral of current with respect to time. In order to observe time-variable flows of electricity some other parameter needs to be employed in measurement. Conventionally this might well be a current measurement, but if a measurement system with a fixed ohmic input is employed, then voltage variation, which is often an easier parameter to monitor, answers the same purpose. In the context of the present research potential measurement is also easier to relate to criteria established by previous workers.

With this in mind, a series of experimental investigations was undertaken in order that changes of *potential* with respect to time during coalescence events might be measured. It was recognised early in this work that it might be possible to combine the electrical potential record with a visual one, thus providing another data channel.

The first investigations were aimed at establishing the approximate magnitudes of such potential variations, if any, and the following sections trace the development of this approach.

6.2. Initial experiments.

Apparatus was constructed in the form of a 'drop-chamber'. This comprised an insulated needle assembly, held in a vertical plane with a micrometer screw to allow for its precise positioning over a surface. Thermal control of the environment was provided, although this was not actually used during the experiments. A horizontal, electrically insulated copper plate provided the surface upon which a small stainless-steel well for the bulk liquid might rest. The copper plate was well coupled thermally to a Peltier array, allowing temperature control in the approximate range of -5 to 65°C.

A small metering pump, initially hand-powered and subsequently motorized, supplied water to the needle through a flexible capillary pipe of 13 x 10^{-8} m^3 per unit length, the pump delivering a maximum of 0.015 l hr^{-1}.

Electrical integrity was maintained by ensuring that all relevant parts of the apparatus were screened within a Faraday cage. This entailed placing the water supply and the pump (but *not* its low-voltage DC motor) inside the cage, and making the signal leads to the oscilloscope short, (<0.4 m.), well screened, and of a low capacity (~ 12 pF). Figure 6.1 shows a schematic representation of the apparatus.

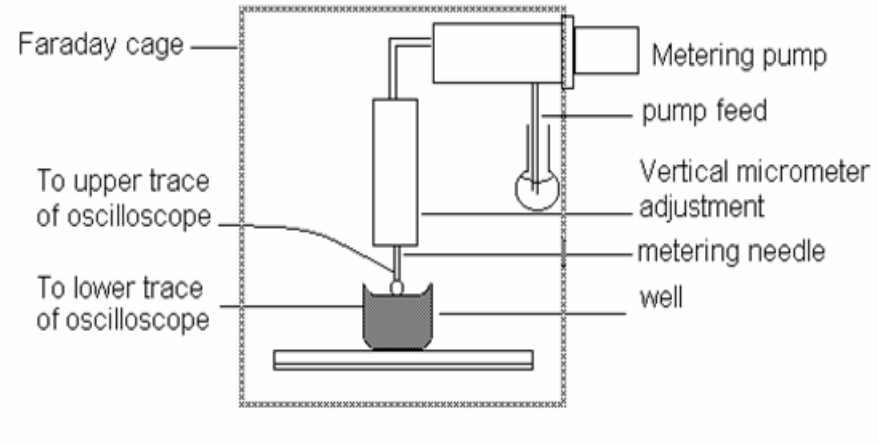

Figure 6.1. Schematic diagram of drop-chamber.

Visual access to the drop-chamber was by means of a 10 cm. square window in the removable front panel. To maintain electrical screening this was coated with a thin layer of Wimshurst's conductive varnish.

A small CCD-camera mounted within the apparatus allowed monitoring of drop production at the needle. Figure 6.2 shows a general view of the drop-chamber with its front cover removed.

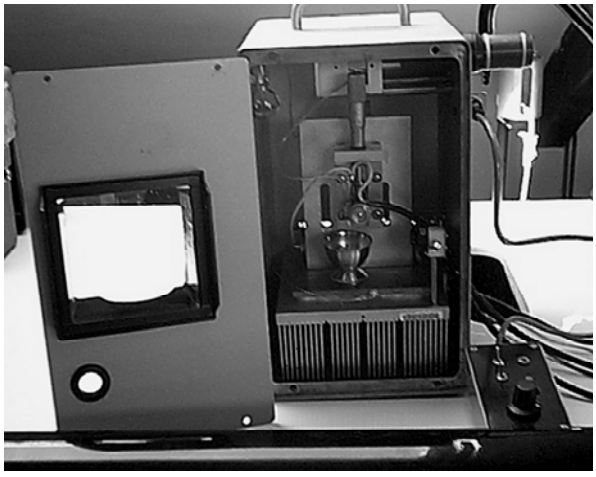

Figure 6.2 General view of drop-chamber (open).

Initial experiments considered only the signal from the well when the needle was positioned a small distance above the water surface, and a drop allowed to form and coalesce with the surface. This produced a signal with the general form shown below in Figure 6.3. It was apparent from simple video recordings of the CCD camera images that, as expected, the event duration of the signal corresponded with the period of the coalescence event.

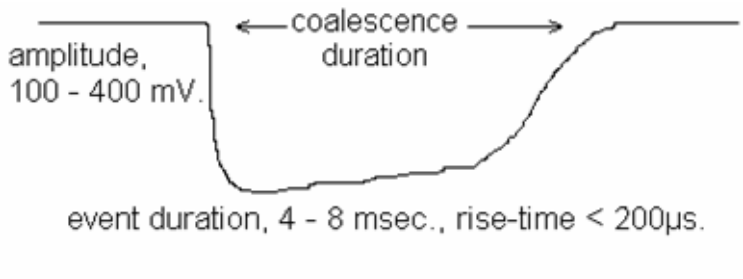

Figure 6.3. General form of well signal at coalescence.

The size and nature of this event, which proved very repeatable, suggested that investigating also the signal from the needle might be advantageous. The fast rise-time, together with the magnitude of the signal and its duration strongly suggested that an electrical potential event of some size was occurring during the process of normal drop/surface coalescence. A perfectly audible signal was detected by connecting a crystal earpiece to the well and ground and initiating a coalescence event. It was decided to correlate the electrical events with a visual record of the process, using high-speed video techniques, in an attempt to ascertain whether the magnitude of the signal and its persistence at this amplitude for a significant time was accompanied by any observable occurrences during coalescence.

6.2.1. Experimental investigation using high-speed video.

An experiment was therefore set up with two electrical recording channels, one from the needle and one from the well, and synchronized with a video recording made at 500 frames per second. Video was obtained using a NAC Memrecam C^3 instrument, and the electrical events recorded by a two-channel digital storage oscilloscope (Thurlby DSA524). The experimental set-up is illustrated schematically in Figure 6.4, with a photographic view of the arrangements in Figure 6.5.

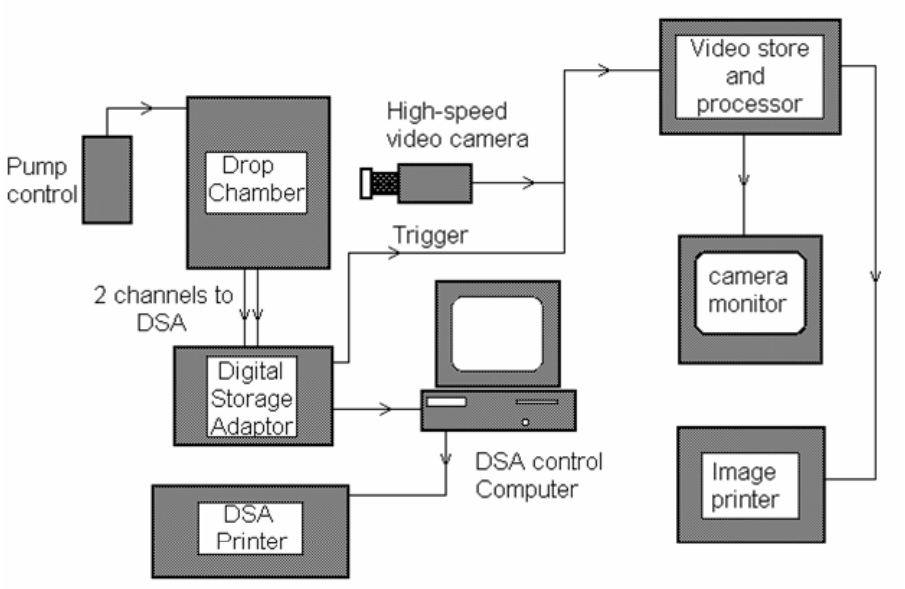

Figure 6.4 Schematic diagram of video and electrical event recording.

Figure 6.5. General experimental view.

The experimental conditions were as follows.

The needle height was set so that drop sphericity was good, i.e. coalescence occurred through surface contact before the drop had reached the stage of becoming excessively prolate. For the needle geometry used this gave the needle a height above the water surface of 4.5 mm., and hence a drop effectively of this diameter at the coalescence point. The volume of the well was large in comparison with drop volume, so a number of drops might be released with an insignificant rise in the well water-level.

Deionized water was used throughout, with a conductivity of 1.05×10^{-6} S/m, measured just prior to the experiment. The ambient temperature was 22°C, and the relative humidity 46%.

A preliminary series of 50 coalescence events was made so that the repeatability of electrical waveforms might be checked. These were divided into distribution bands, according to their duration and the recorded peak voltages of needle and well. The results are summarized in Table 6.1.

Event Duration		**Peak Needle Volts**		**Peak Well Volts**	
<8 msec	**>8msec**	**<300 mV**	**>300 mV**	**<400 mV**	**>400 mV**
12	38	16	34	19	31

Table 6.1. Repeatability data.

A sequence of 23 coalescence events was then performed, and the electrical and video data obtained. These showed a considerable degree of consistency, with a waveform of the type shown representatively in Figure 6.6.

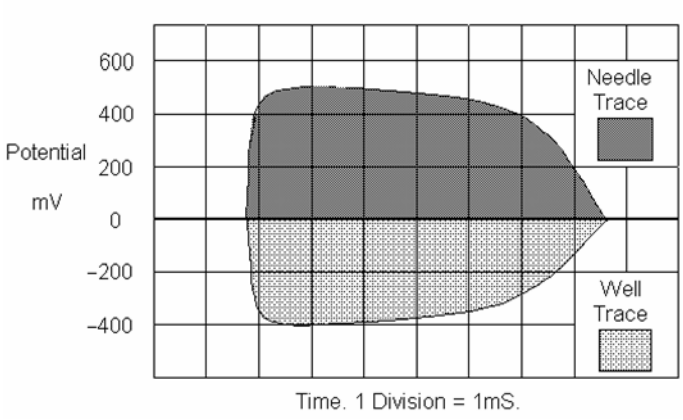

Figure 6.6. Typical coalescence waveform.

The waveform always exhibited a fast rise-time, typically <200μsec to 90% of peak amplitude, the peak value persisting for half the event time or longer, and then decaying slowly to zero. The shaded areas of the waveforms shown in Figure 6.6 represent the total charge associated with the event, and despite the high level of symmetry between the needle and well traces, it was noticeable that there was a difference of charge between them, amounting to some 10-15%.

This discrepancy was first investigated by attempting to detect whether there was any charge transfer to the surrounding air. An annular electrode, connected to an electrometer, was suspended coaxially with the needle about 2mm above the water surface, such that its plane was approximately at the equator of fully-formed drops. This failed to detect any significant charging of the air in the vicinity.

[This failure to detect the 'missing' charge led to an investigation of possible light emission during the event as a possible explanation of the apparently incomplete charge transfer. This exercise, whose details are recorded in Appendix 2, also gave negative results.]

The difficulty was eventually resolved by a careful balancing of the capacities of the two input systems, using the circuit shown in Figure 6.7. *VC1* and *VC2* were small variable air-spaced trimmer capacitors connected in parallel with the needle and well outputs respectively. These were sited at the ends of the signal cables remote from the measurement points, so that adjustments might be made without introducing temporary fields in the measurement vicinity. This allowed for the balancing of the two channels. The existence of a capacitance between the drop and the water surface *(C_{DS})* should be noted. This will vary in value, as was shown in Chapter 5, (5.5), but its symmetrical arrangement across the channels does not cause imbalance in the total channel capacities, merely altering their global values slightly. The overall effect of any variation in C_{DS} is to raise or lower the potentials on the channels by proportionate amounts.

A drop was dispensed such that it was almost in contact with the water surface and the resulting system capacity was as close as could be obtained statically to that pertaining at coalescence. The line capacities were then adjusted by means of these variable capacitors to be equal and to give the lowest possible identical value to each.

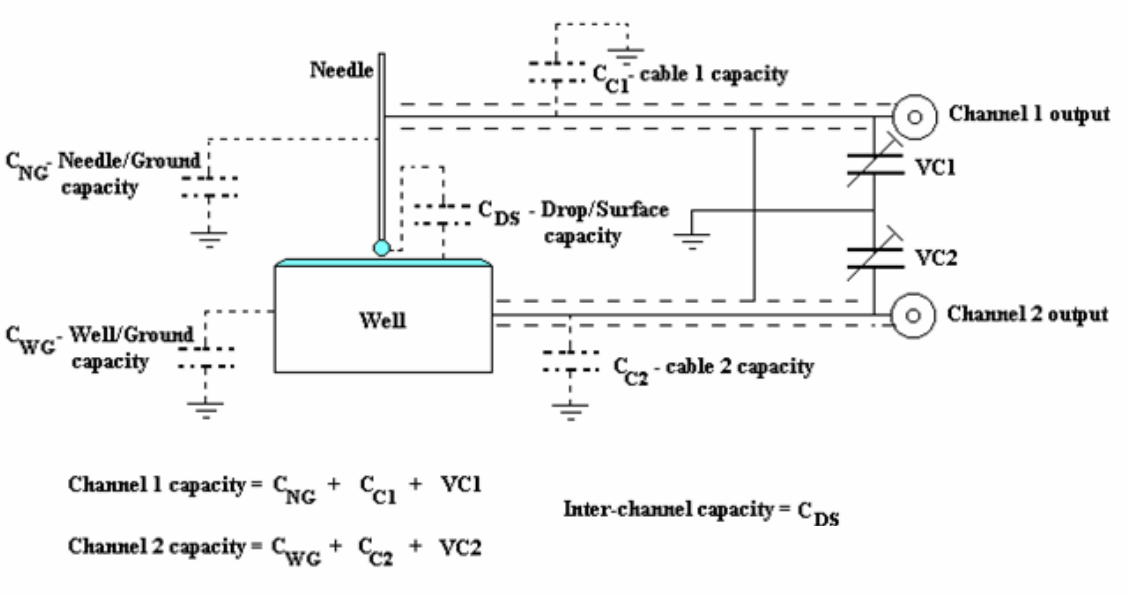

Figure 6.7. Capacity correction circuit, showing the contributory equivalent capacities for each recording channel.

Correlation between the oscillographic and the video records being made through the use of a common trigger signal derived from the needle, it was possible to compare pictures of coalescences with their simultaneous electrical record. Figure 6.8 shows a sequence of images at 2 ms intervals, with their corresponding needle and well voltages.

The sizes of the potential recorded in these events gave rise to some surprise. Simple voltaic effects were initially suspected, although the symmetry of the results about the x-axis would have been difficult to explain in view of the materials employed as electrodes. Both needle and well were made from similar formulations of non-magnetic stainless steel conforming to BSS-EN58J. A very simple test of voltaic potential differences was made by lowering the needle into the water in the well and monitoring the potential difference produced. This showed only a few millivolts – perhaps one eightieth of the P.D. measured during the recorded coalescence events. Further investigations were therefore undertaken with two objectives: *i)* to attempt a more detailed visual analysis of the coalescence process, and *ii)* to attempt to ascertain the exact source of the potentials appearing on the water surfaces.

6.2.2. Experimental extensions using higher framing rates.

A Kodak 4050 high-speed video camera, capable of framing speeds up to 40,500 fps became available for a short period, and this was employed to increase the time resolution of coalescence images.

The experimental arrangements were as before, with the exception of a modification to the electrode system to reduce electrolytic potentials to a minimum. The stainless-steel well was replaced by a well-leached glass vessel, thoroughly cleaned before use. The stainless-steel needle was replaced by a fine-drawn glass capillary.

Platinum electrodes were employed throughout, having been prepared with due consideration to surface cleanliness and to the elimination as far as practicable of adsorbed gases.

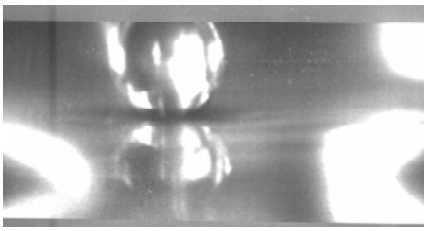

1. Time: 0.000 sec. Needle: 0.00V. Well: 0.00V

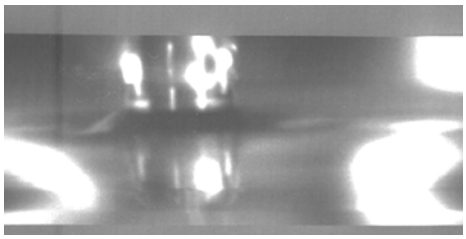

2. Time: 0.002 sec. Needle: 0.54V. Well: -0.52V

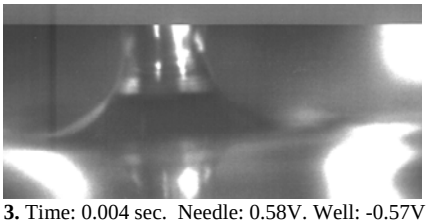

3. Time: 0.004 sec. Needle: 0.58V. Well: -0.57V

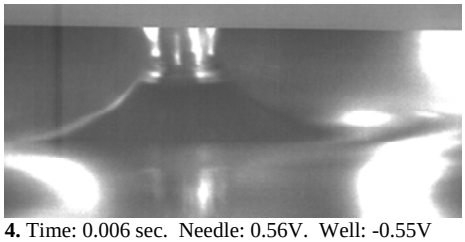

4. Time: 0.006 sec. Needle: 0.56V. Well: -0.55V

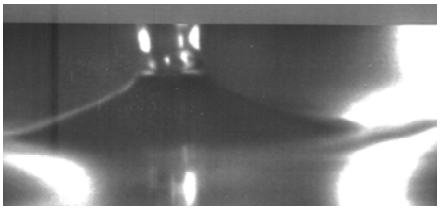

5. Time: 0.008 sec. Needle: 0.53V. Well: -0.50V

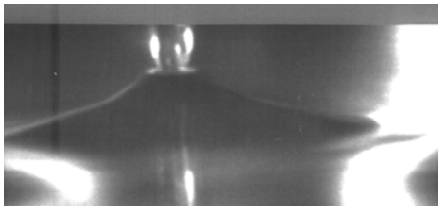

6. Time: 0.010 sec. Needle: 0.49V. Well: -0.47V

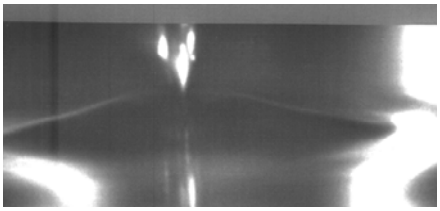

7. Time 0.012 sec. Needle: 0.43V. Well: -0.40V

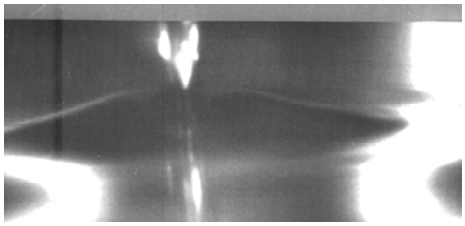

8. Time: 0.014 sec. Needle: 0.11V. Well: -0.10V

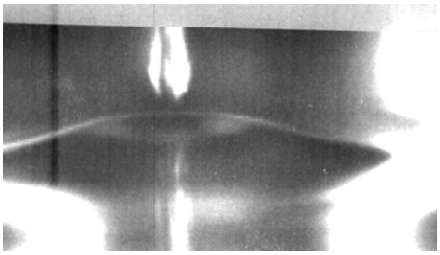

9. Time: 0.016 sec. Needle: 0.00V: Well: 0.00V

Figure 6.8. Video record of coalescence at 2 msec. intervals. The corresponding needle and well potentials (corrected for capacity) are shown below each frame.

Platinum has been shown by Elton [87] to adsorb oxygen and hydrogen at its surface which can lead to the production of spurious potentials, and an out-gassing process was employed aimed at reducing these unwanted potentials to a minimum.

A length of 0.8mm diameter platinum wire was heated to redness, and cleaned of surface deposit by quenching in nitric acid. The wire then had electrical contacts made to it and was placed in the bell-jar of a high-vacuum system. The wire was then electrically heated to redness in vacuo, out-gassed, and allowed to cool. After this it was only subject to forceps handling.

Screened leads were attached to each end of the wire, which was then cut centrally in two, one part being used for a contact electrode to the water in the well, the other for use at the capillary.

The capillary electrode was prepared as shown in Figure 6.9.

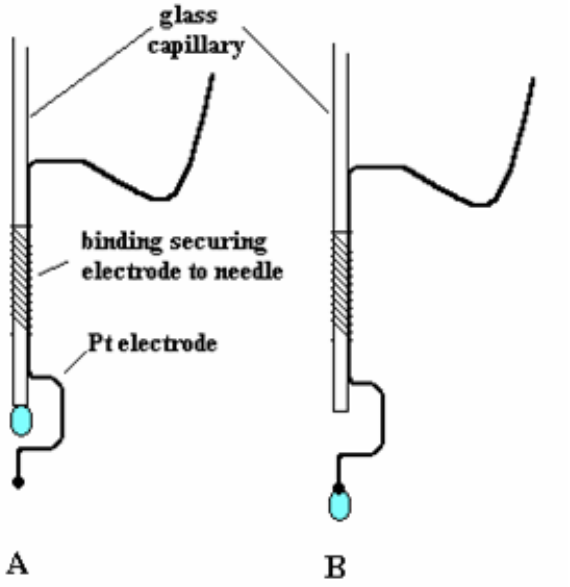

Figure 6.9. Dropping needle detail, showing method of securing electrode to needle and dropping sequence. ***A***, drop forming at capillary orifice, and, ***B***, drop transferred to platinum electrode.

At one end the wire was swaged into a small ball, after which the whole wire was formed into the shape shown in Figure 6.9, and carefully bound to the glass capillary. A wire soldered to the other end of the electrode allowed for electrical contact to be made. The offset at the lower end of the electrode allowed a drop to fall on to the platinum from the glass capillary, after which it quickly slid down the electrode wire, to fall as a drop from the swaged tip. This process allowed a drop to be dispensed in a controlled manner, but with its only metallic contact being to the platinum.

During operation the needle and well electrodes were connected via short screened cables to channels 1 & 2 respectively of the digital oscilloscope, the signal lead screens and the instrument both being grounded. DC coupling was used on both channels so that each electrode was in effect grounded via the 1MΩ input impedance of the oscilloscope. Any pre-existing charge would therefore leak to earth. The trigger signal was taken from the well, set to fire on a rising negative wavefront. The trigger-level was set to as low a level as possible without leading to false triggerings from very small transients from the environment.

The immediate effect of the modification to the electrode system was to reduce significantly the potential levels recorded, thus indicating that electropotential between the water and the stainless-steel had been responsible in part at least for the high potentials previously recorded. Similar curves were obtained as before, with a potential event averaging some ± 35mV, whose duration equated with the coalescence event time.

By using the Kodak 4050 video camera it was possible to take images at approximately 25μs intervals with rather low resolution (64 x 64 pixel imaging). The camera system stores images in a ‘revolving carousel’ form. When operating, images are constantly stored and over-written when the frame-store is filled. When an event is triggered, therefore, it is often possible to view immediately pre-trigger events.

Several sequences obtained showed a small asperity arise on the bulk (well) water surface, just preceding the trigger point. Copies of the image files obtained were turned into difference files, these showing the data areas that changed between successive

image files of a sequence. From these it was possible to confirm that the asperity seen rising on the bulk water surface immediately prior to the main coalescence event was not an artifact of the recording process. This asperity may be seen briefly (<40μs) rising, apparently from the plane surface, although it is not possible from the image quality obtained to make any accurate direct measurement of the interfacial distance.

An example of one set of the results obtained from this investigation is given in Figures 6.10 to 6.12. Figure 6.10 shows a composite image compiled from a video sequence originally taken at 40,500 fps, but with every third image shown. The twenty frames therefore represent a total time of just under 1.5ms.

During the first 4 frames a small protuberance appears to rise on the plane surface, contacting the drop. [This is more obvious when seen in a video sequence, and the eye is presented with successive images more quickly]. Successive frames then show this asperity modifying in form. Frame 09 of Figure 6.10 contains the trigger point somewhere in its duration, and is therefore designated as zero time. After this point the remaining frames of the sequence shown represent the development of the coalescence process.

Figure 6.11 shows a series of drawings made from the events in Figure 6.10, showing the apparent change in the major surface profiles recorded in the sequence.

Inspection of the accompanying electrical record from the oscilloscope (Figure 6.12) reveals an interesting electrical event parallel with the production of the ‘asperity’. A small signal is recorded on both channels, having an amplitude in the range 1 - 5mV. The sign of this was always *opposite* to the channel sign for the main coalescence event. Thus the needle gave a negative pre-trigger signal and a positive main event one, and the well vice versa.

Care has been taken in the foregoing description to sound a note of caution in terms of interpreting these events at face value. It is necessary to consider the observations in the light of known events at and just preceding coalescence.

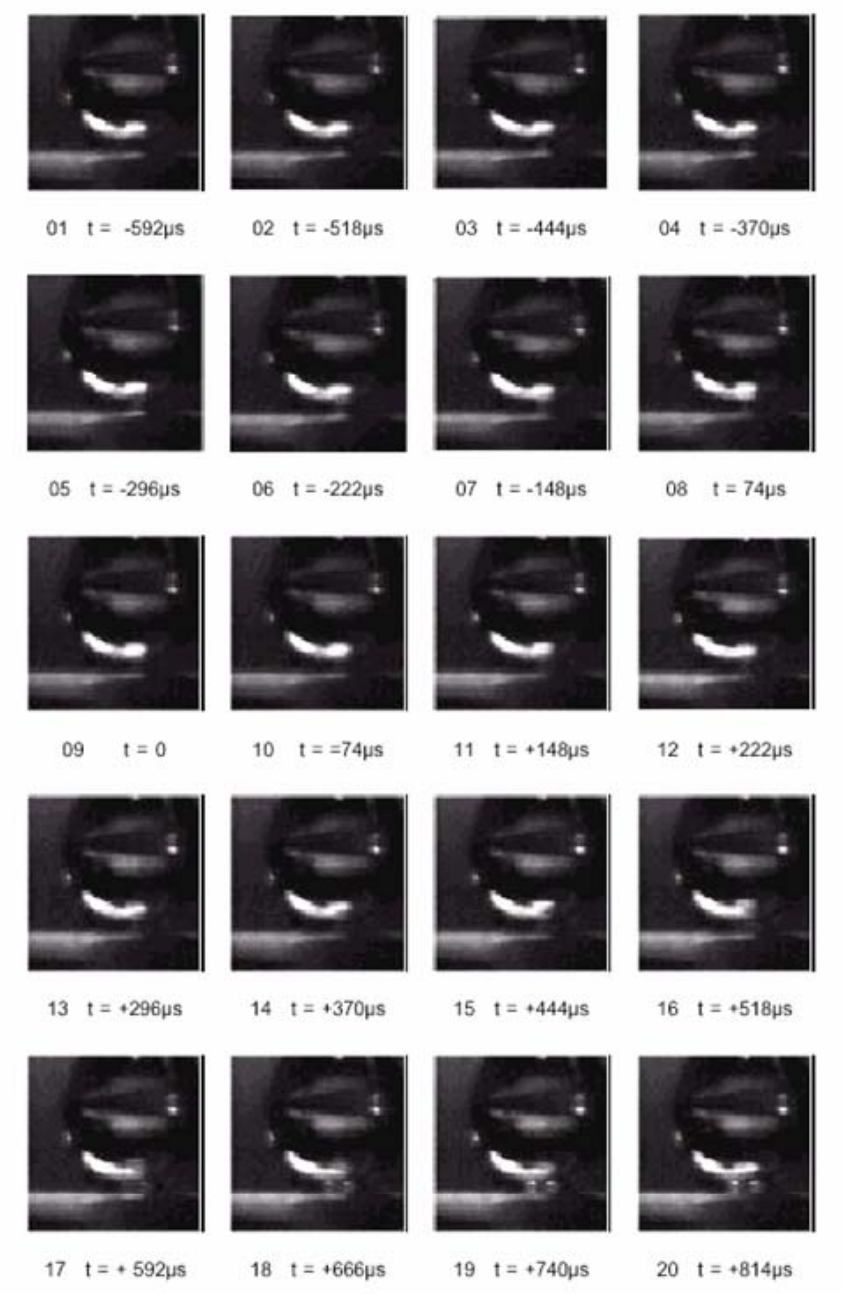

Figure 6.10. Image sequence of the coalescence of a drop with a plane water surface. Originally recorded at 40,500fps, this composite illustration shows every third frame in the sequence, thus giving an elapsed time of almost exactly 74µs between frames. Original image resolution, 64 x 64 pixels.

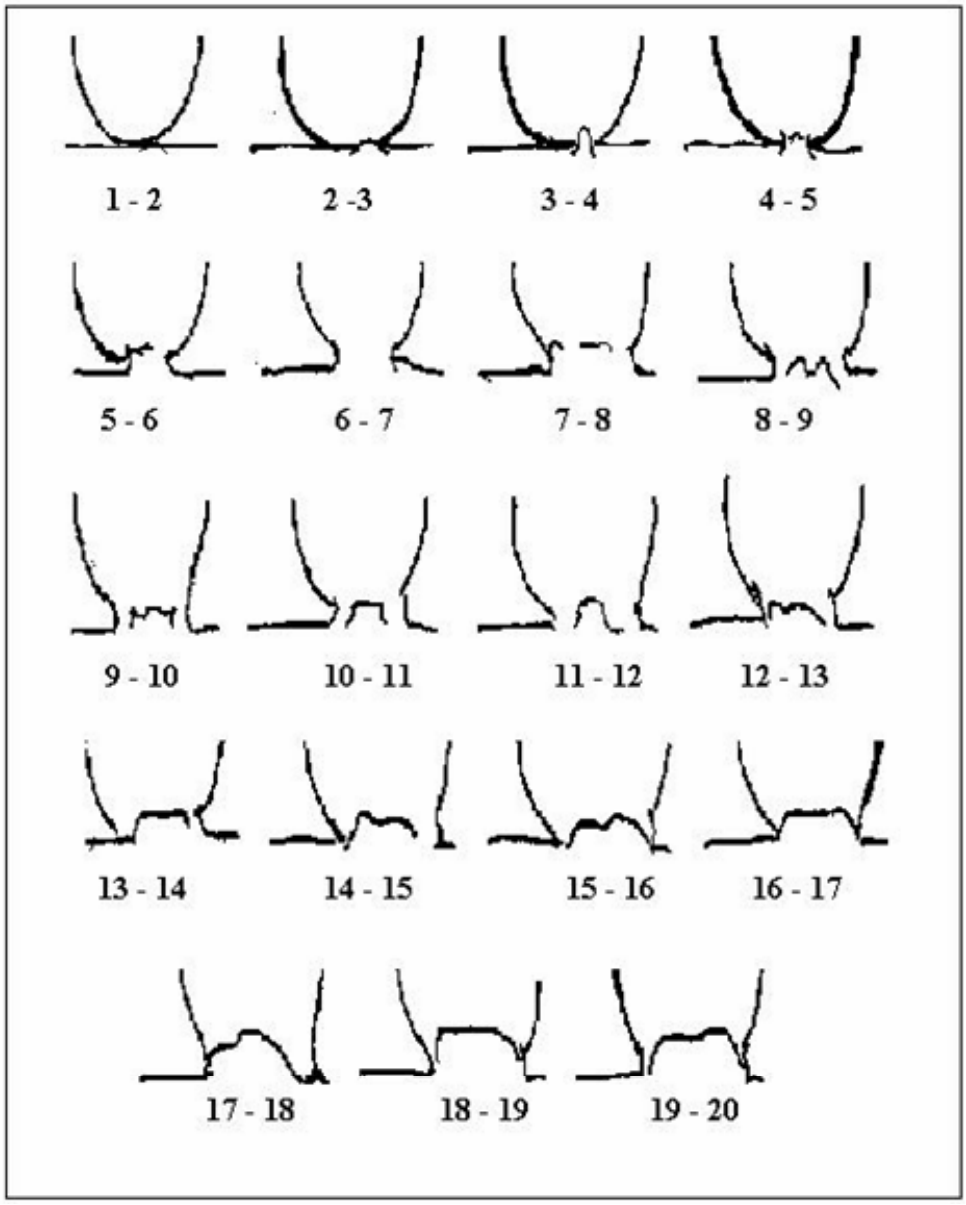

Figure 6.11. Major surface profiles in Fig. 6.11, drawn from generated difference files between frames.

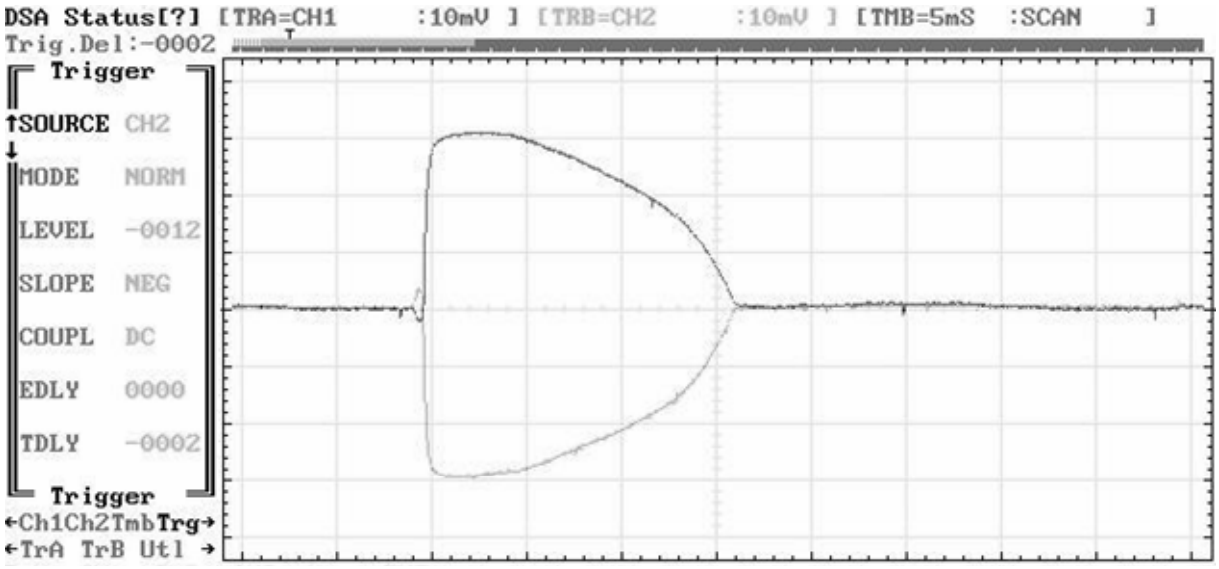

Figure 6.12. Electrical record of coalescence shown in Fig. 6.10. Timebase is 5ms/divn., amplitude on both channels is 10mV/divn. The darker (upper) trace is the needle, the lower the well.

The pre-trigger event shown in Figure 6.12 shows the following characteristics;

i) Event duration (to crossover point), 0.7ms.
ii) Peak positive (well) signal, 2.7mV.
iii) Peak negative (needle) signal, 2.2mV.
iv) Rise-time to peak signal, ~500μs.

For the particular experiment recorded here the temperature was 23.7°C, and the ambient relative humidity 52%.

As the measurement was made via resistive input ($10^6\Omega$) the equivalent current flowing may be readily found. Converting the y-axis therefore to current units, and applying a Simpson's rule analysis to the trace obtained, charge transfer values for the pre-trigger and main events for this example were found to be;

- Pre-trigger event: 1.75×10^{-12}C. [*Event range for all measured cases,* 1.2×10^{-12}C to 4.8×10^{-12}C.]
- Main event: 3.8×10^{-10}C. [*Event range for all measured cases,* 3.4×10^{-10}C to 4.5×10^{-10}C.]

Oscillograms relating both to this series and to a subsequent series of experiments are displayed in Appendix 4. It is important to remember that the terms ‘pre-trigger event’ and ‘main event’ have been used in an arbitary, if literal, sense so far. The configuration of the apparatus used made it possible to view and record events just prior to the trigger signal reaching a certain critical pre-set value, and the terminology has been convenient so far in that it allows events to be related to a threshold appearing at the recording instruments. It should not, however, be implied that triggering is co-terminous with the onset of coalescence, but simply as reaching the trigger threshold voltage.

The pre-trigger charge value is in good agreement with those figures obtained for the charge on grounded drops contacting a surface disruptively (see Chapter 5, Table 5.3), and suggest strongly that this ‘initiating’ phase of the coalescence process is driven by the disruption of the inherent electric charge on the surface.

Consideration of double layer theory (Chapter 4, Section 4.2.1) indicates that the outer surface of the drop will carry net negative charge, and this is shown in the sign of the needle trace in the pre-trigger process. The sign-reversal during the main event is less easily explained in view of the comparatively large charge transferred, and needs to be the subject of further research.

The visual and electrical events described must be placed in the context of present knowledge of the interfacial geometry of approaching liquid surfaces, together with current understanding of their associated electrohydrodynamics. It is therefore appropriate briefly to review these topics prior to attempting to interpret the results obtained.

6.3. Geometry and film drainage of approaching liquid surfaces.

The dimpling of a liquid surface as it approaches either a solid or a liquid surface has been noted and investigated by several workers. [35, 87- 92]. Prokhorov [35] considered an essentially static system, similar to that used by Elton [87] in his early studies in

electroviscosity. Aspects of the work of Prokhorov are discussed in more detail in the following chapter (Section 7.2).

In each of these instances a cell of some sort was employed where the liquid/liquid or liquid/solid surfaces were brought slowly into contact by the gradual displacement of one of them by carefully controlled air pressure. Using a similar type of configuration Frankel and Mysels [88] established a purely hydrodynamic interpretation of the dimpling effect, and demonstrated that whilst double layer and eventually van der Waals forces might have a modifying effect on the geometry as the film drained to very small thickness, they were not essential to explain the formation of the interfacial dimple. An approximate expression for the thickness of the dimpled film at the centre and rim as a function of time was developed for a bubble or drop approaching a solid plane surface.

Figure 6.13 shows the relevant geometry.

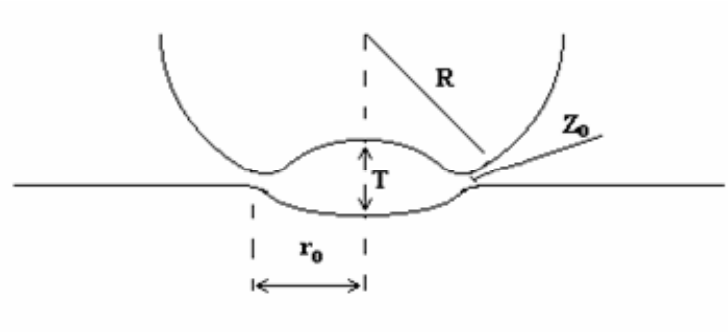

Figure 6.13. Geometry for Frankel and Mysel's consideration of bubble dimpling [88].

For a bubble of radius, R, the thickness T at the middle of the dimple was calculated as,

$$T = (0.0096 r_0^6 \eta n^2 / \gamma R t)^{1/4} \qquad (6.1)$$

where r_0 is the radius of the barrier ring (i.e. the "contact" radius), η the viscosity, γ the surface tension and t the time. n is a factor of either 1 or 2 depending on the number of non-dilating surfaces involved (i.e. surfaces not expanding radially outwards).

The minimum (peripheral) thickness, Z_0, of the barrier ring was found to be,

$$Z_0 = 3.05RT^2 / r_0^2 \qquad (6.2.)$$

whence, by substitution from (6.1),

$$Z_0 = (0.060n^2R^5\rho g\eta / \gamma 2t)^{1/2} \qquad (6.3.)$$

Frankel and Mysel's expressions represent thinning of the interfacial rim and the central dimple as functions of time, and in this respect are particularly applicable in the present research, and will be drawn upon in a later discussion of the development of a model for the capacitive changes in a boule system with respect to time.

Chen [89], again considering a liquid/solid interface, considerably extended this work to take account of the effect of van der Walls and double layer forces as well as adsorption and structural forces on the thinning of the dimpled region. The former of these pairs is effective over distances in the order of 100nm, whilst adsorption and structural forces, which are less understood, are effective over shorter ranges (~10nm). Chen found that in the presence of van der Waals or electric (double layer) forces the pressure arising from these caused either a flattening or a rupture of the rim of the barrier ring.

The comparative effect of change in the electrical double layer was investigated experimentally by Schulze [90] using different concentrations of KCl. Low concentrations (0.0001*N*), giving a strongly negative disjoining pressure, produced rupture in films greater than 100nm in thickness, whilst increasing the concentration to 0.01 – 1.0*N*, sufficient to suppress the double layer pressure and leave only van der Walls forces acting, reduced the rupture thickness to between 32.5 and 50nm.

Further developments of a purely hydrodynamic nature were made by Yiantsios and Davis [91, 92], considering the problem from the viewpoint of lubrication theory to describe the flow in the interface between the drop and surface. they demonstrated [91] that the formation of the dimple is independent of viscosity ratios, and that the rate of long-term thinning is always of the form,

$$-d\delta/dt \propto t^{-n} \qquad (6.4)$$

where δ is the interfacial thickness, and $-n$ some simple inverse fractional power of time, t. An extension of this work [92] gave consideration to the effect of the London-van der Waals type forces, but ignores the effects of double layer charging.

Thus we have a fairly well-developed knowledge of the geometry of the dimpled interfacial area and hydrodynamic descriptions of the film draining forces, but less information on the interfacial modifications that may occur in the presence of charged surfaces on either or both of the liquid entities.

6.4. Interpretation of video evidence.

In the light of the preceding section it is necessary to interpret the experimental video record obtained cautiously. There have been many studies of drop disruption and coalescence processes employing high speed photography extending over many years [30, 95-98]. These all lead to a similar overall picture of the total coalescence process, with which the sequences under consideration agree. A careful scrutiny of the available published records, however, gives little insight into the very primary stages of the process. Most published records were obtained either at framing rates significantly lower than those employed in the present research, or as discrete, isolated images such as those of Edgerton and Killiam [95]. It is therefore difficult to make comparisons between those images obtained and the results of other workers.

The principal difficulty with these images is that they appear to show an initial *upward* movement of material from the surface to the drop. The drop has excess pressure with respect to the surface, and this apparent direction of flow appears contrary to basic laws of capillarity. Therefore at coalescence there is an excess pressure within the drop compared with the plane surface, and matter-flow should therefore be from the drop to the bulk liquid. The visual impression from these images is of a very short (~200μs) initial upthrust, stemming from an asperity which may or may not be in immediate

contact with the drop, followed by conventional streaming of the drop contents downwards as coalescence proceeds over the next thirty or so milliseconds.

The explanation of such an asperity appears far from straightforward. The visual record suggests that it may originate from the region of the rim of the interfacial dimple described above. This appears realistic in view of this region representing the closest point of contact between the two liquid systems, and the one therefore most likely to experience the greater electrical stress.

6.5. Summary.

This chapter has described patterns of potential events recorded at coalescence. By measuring potential rather than total charge transfer it has been possible to produce time-dependent data for the coalescence process. From this the observation has been made that there is an initial electrical phase in the process, whereby charge transfer equivalent to that expected from a disrupted uncharged drop occurs. This process, involving charges in the pico-coulomb range and a potential in the order of a very few millivolts, takes place in time-spans of normally <1msec. The main coalescence process follows this, and occupies several tens of milliseconds for drops of negligible approach velocity.

7 THE INFLUENCE OF HUMIDITY ON THE COALESCENCE POTENTIAL BETWEEN TWO CLOSELY SPACED DROPS.

7.1. Introduction.

Frequent reference has been made to humidity as a modifying parameter both in the coalescence process and to the relative ease with which floating drops may be produced, and it is now necessary to focus more closely on the rôle played by variations in humidity in both normal and anomalous, or delayed, coalescence.

The effect of humidity on coalescence has received sporadic attention over the past seventy-odd years, with considerable discrepancies between observed results and subsequent conclusions. There are several possible reasons for this, the prime candidates being the different regimes studied and the attention or otherwise given to the effects of charge on the process.

Some investigators working in the general field of cloud physics have been more concerned with precipitation-sized drops in free fall whilst others approaching the problem from a different standpoint have investigated sessile drops of a range of radii. The work of Ochs' group at the Office of Cloud Precipitation Research of the Illinois State Water Survey [59, 99, 100] is typical of the cloud physics approach, whilst that of Jayaratne and Mason [54], whilst deriving from cloud physics interests, is more concerned with the dynamics of drops moving horizontally across a bulk liquid surface, and with sessile drops.

The rôle of film-drainage in the coalescence process, and the modifying effects of charge upon this, has also been the subject of investigation by various researchers [100-103], and there have been attempts to formulate direct relationships between the coalescence process and the conditions of charge and drop geometry as well as physical parameters such as surface tension.

In examining and evaluating this body of investigative work it is necessary to adopt a structure, and the background to the problem is therefore considered under the following headings.

i) A general review of the scope and findings in the area, presented in approximate chronological order, considering first the effects of humidity on coalescence, and then of electric charge.
ii) Experimental work carried out as part of the present research.
iii) A discussion of the experimental results obtained in the light of previous work by other researchers, and an evaluation of the applicability of this past work.
iv) Noting suggestions for further research and developments in the topic.

The first significant research into the influence of humidity on the coalescence process was carried out by Prokhorov [35] in 1954. This treatment was a purely hydrodynamic, rather than an electrohydrodynamic one, leading to some important conclusions. These may be summarized thus:

1. Failure for a coalescence to occur is attributable to the presence of an air gap between the drops.
2. It is impossible to prevent coalescence on contact between drops in an atmosphere saturated with the liquid vapour.
3. Drop coalescence in unsaturated atmospheres may be inhibited by the surplus pressure in the inter-drop air-vapour gap, brought about by external air being drawn into the gap by diffusion.

7.2. The work of Prokhorov and Lindblad.

Prokhorov's practical work principally utilized hexane and hexane vapour, and the applicability of his findings to water needs to be evaluated in the context of the higher vapour-pressure of hexane, its lower surface tension and non-polar nature, compared with the high surface tension of water and its dipole moment of 1.85 debye.

Prokhorov termed any situation less than saturation of the surrounding air the with liquid vapour as a ‘humidity deficit’. It was necessary to consider the pressure balance in a system consisting of two opposing drops with a small intervening air gap. His approach was first to investigate the pressure arising from vapours diffusing through a narrow gap, analagous to an inter-drop air-gap. A simple but effective practical method consisted of making a manometric pressure measurement with respect to the ambient air pressure, using an arrangement as shown in Figure 7.1.

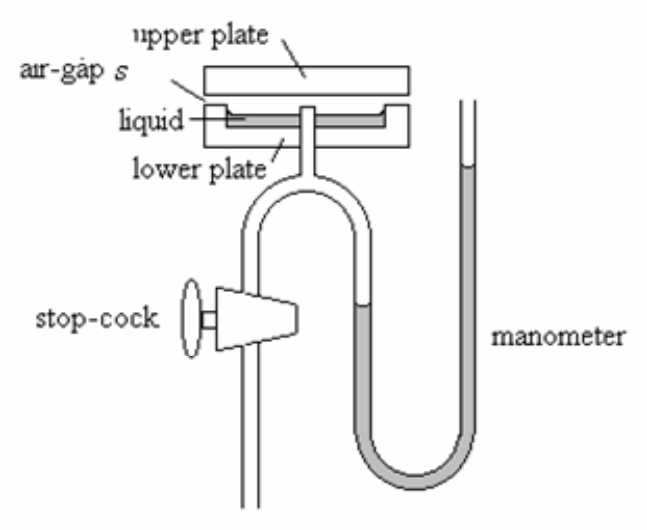

Figure 7.1. Diffusion-pressure measurement *(after Prokhorov [35])*.

Two plates were set with a small air-gap, *s*, between them, and some of the liquid under test dispensed into a recess in the lower plate. The stop-cock, initially open to equalize pressures, was closed, and after a few minutes the manometer recorded a pressure differential, ΔP, which proved to be always the same for a given setting of *s*, regardless of whether or not there was initial excess pressure in the system.

The treatment of these results was considered for two extreme cases, *i)*, $\lambda.\lambda_1 >> s$, and *ii)*, $\lambda.\lambda_1 << s$, where λ and λ_1 are the respective mean free paths of the air and the vapour molecules. Case *i)* resolved simply to the partial pressures inside and outside the chamber being the same, meaning that, if p is the saturated vapour pressure inside the chamber and p_0 is the vapour pressure of the surrounding atmosphere, then,

$$\Delta P = p - p_0. \tag{7.1}$$

For case *ii)*, however, the motions of each fraction of the molecules are mutually related, and Prokhorov uses a first approximation of Pascal's hydrostatic law to derive the following approximate expression for ΔP,

$$\Delta P = \frac{12\eta D_{va}}{H^2}.\frac{\Delta P}{P_0} \qquad (7.2)$$

where η is the liquid viscosity, D_{va} the diffusion coefficient for the vapour/air mixture, and P_0 is the atmospheric pressure.

Pressures computed from this formula were shown to be adequate to balance the capillary pressure of $2\gamma/r$, γ being the surface tension and r the capillary radius, with the result that coalescence does not occur. The implication of the theory is that if the vapour pressure around the drop increases, then ΔP decreases, unless balanced by a reduction in the air-gap, s, a situation confirmed by experiment. In the case, therefore, of static drops in contact, failure to coalesce over an extended period may be attributed to surplus pressure in the air gap between the drops due to the suction of air into the gap from the exterior by liquid vapours diffusing out of the gap. Experimental extensions were performed to dynamic situations where drops fell through heights of up to 4mm (*cf.* 'gentle placement' method) under different conditions of relative humidity, that is different concentrations of the liquid vapour in the surrounding air, and the trend from non-coalescence at low RH values to invariable coalescence at saturation were recorded.

Whilst Prokhorov went on to develop an application of his basic theory to the coalescence conditions pertaining to water droplets in a rising fog, his primary results came from the consideration of a small range of organic liquids. As has been previously noted, these have very different physical properties of conductivity, dielectric constant and polarity and consequent dipole moment from those of water, and the application of results obtained from their use should be extended to water with some caution. To this should be added the lack of consideration of evaporative effects from the drops in the case of high humidity defecits – i.e. low relative humidities.

This situation was, in part at least, addressed by Lindblad in 1964 [104]. His investigations were confined to water, and centred around measurements of the

coalescence times for water drops, in both semi-static and dynamic regimes, as functions of relative humidity.

Lindblad's technique was to make high-speed photographic sequences of the interface between two opposing drops – in this case represented by menisci at the ends of closely spaced opposing capillaries – illuminated by a monochromatic light source, and to use the resulting interference patterns to determine the proximity of the opposing surfaces. A thinning process taking place in discrete steps was described, illustrated in Figure 7.2.

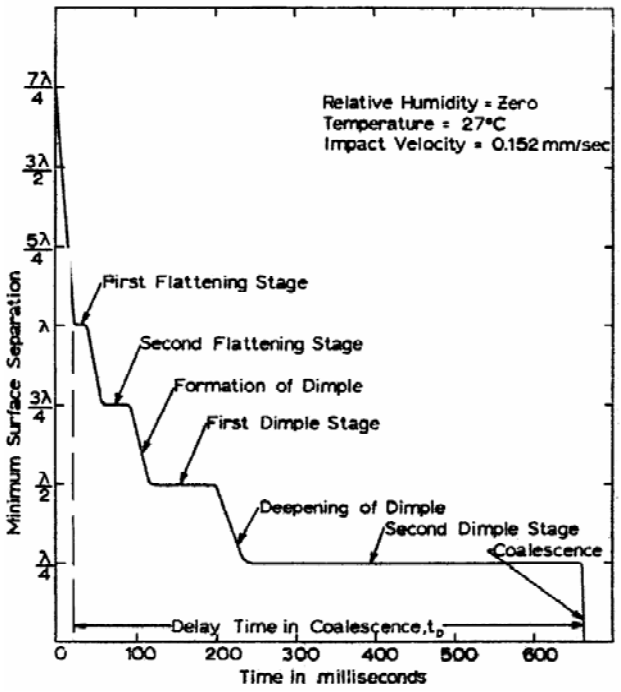

Figure 7.2. Surface deformation against time *(from Lindblad, [104]).*

This result, apparently showing distinct time lapses between air-gap thinning stages, raises the issue of whether actual events are being recorded, or whether the steps are merely artifacts of the optical observational procedure. The illuminating wavelength was quoted as λ = 580nm, meaning that the events to coalescence in the graph of Figure 7.2 span one and a half wavelengths, (0.87μm). The precise observation of the peaks of interference fringes by the method used is non-trivial, a fact that Lindblad acknowledges, and it may well be that the process described is in fact a continuous one, and a relatively smooth graph may be drawn to describe it. Indeed, it seems unlikely

that the formation of the flattened areas should coincide so exactly with simple sub-multiples of the wavelength used.

As well as describing the flattening of the dimpled areas of opposing drop surfaces, adding confirmation to Prokhorov's findings, Lindblad also investigated the effects of small potential differences on the coalescence of opposing drops. The potential differences applied were relatively small in magnitude (typically about 0.6 volt), but gave rise to field intensities of high orders as a result of the small separations between the drops. Thus for quarter-wave separations in Lindblad's experiments (145nm) a P.D. of 0.6v gives an equivalent peak field gradient of 4.138MV/m.

This figure is substantially greater than that normally associated with the breakdown potential (~3MV/m), but needs to be considered in terms of the modification in breakdown potentials in the case of small gaps as described by Paschen's Law. A practical expression of this is,

$$E_B = 10^8\, p(365)/\left[1.18 + \ln\left(p.d/100\right)\right] \qquad (7.3)$$

Where p is the pressure in Torr, d the gap distance in m, and E_B the breakdown field in MV/m. (The factor 365 is a unit-conversion ratio). For a standard atmospheric pressure of 750 Torr, this gives an implied breakdown field of some 8.2MV/m. Paschen's Law, however, has a singularity at a gap distance of about 4μm, and the application of this law to very small gaps is a complex consideration, being more pertinent to spark gaps between solid conductors than liquid interfaces. In the latter case, when breakdown occurs it will most likely be as a result of electro-hydrodynamic instability rather than the breakdown of the intervening air (8.4). Lindblad further investigated the onset of this instability in the case of liquid drops with a potential difference between them, and observed the formation of surface asperities just prior to coalescence which manifested themselves as bright spots in the dark interference arising from λ/4 separation between the opposing surfaces. The production of such surface aspereties would form an inter-droplet bridge, allowing coalescence to proceed.

The question of such asperities has already been raised in Chapter 6, in discussing the results obtained from high speed video recording of coalescence events. As concluded

there, the physical size, form and mechanism of such asperities, if they occur, is far from clear, and only extensive further investigation of the topic will resolve this issue and lead to their satisfactory explanation. Lindblad's observations, however, add additional weight to the hypothesis that such surface irregularities are indeed the initiators of the coalescence process.

Prokhorov and Lindblad's conclusions differ from one another in part, although both researchers contributed usefully to the establishment of ideas of the effects of humidity on the coalescence process during 1950s and 1960s. Table 7.1 shows a comparative summary of their investigative conditions and principal findings.

Prokhorov	**Lindblad**
Situations examined: • Quasi-static and dynamic. **Conditions for coalescence:** • Existence of entrained air between opposing droplets. • Coalescence inevitable only in the presence of saturated or supersaturated vapour. • In cases of non-coalescence the air-gap is maintained not by the viscosity of air but by a pressure due to inward diffusion of air molecules. **Humidities measured:** • 20, 75 & 100% (of saturation with the relevant vapour). **Temperature:** • constant 20°C. **Liquids considered:** • hexane, pentane, ether, water.	**Situations examined:** • Quasi-static and dynamic. **Conditions for coalescence:** • Existence of entrained air between opposing droplets. • Coalescence delayed by high humidity (contrary to Prokhorov). • Thinning of air-gap (i.e. flattening of the interfacial regions) proceeds step-wise. **EHD effects:** Coalescence accelerated by presence of electric field. **Humidities measured:** • 0 (*sic*), 50 & 97%. **Temperature:** • approx. 27°C **Liquids considered:** • water.

Table 7.1. Comparative Summary of Prokhorov's and Lindblad's Investigations.

The results of the researches described above made it desirable to have a more detailed knowledge of the extent, if any, to which relative humidity might affect the electric field strength necessary to promote instability, and hence the coalescence of two closely-spaced water drops. A consideration of Taylor's paper of 1968 [105] on the topic, discussed in detail later in the chapter, makes no mention of humidity as an influencing parameter, and a series of experiments was therefore undertaken to investigate the situation. In these experiments opposing drops were dispensed at the ends of needles, with a known air gap between them, and the electric field strength necessary to promote instability and coalescence measured for a range of relative humidities.

This information was thought applicable to any consideration of the charge that a boule might have before its supporting air-film is inevitably ruptured by the onset of instability.

7.3 Development of Experimental Apparatus.

7.3.1. The Experimental Chamber and Environment.

In order to give validity to these experiments certain environmental parameters required strict control. These were principally; humidity, temperature, conductivity of the water, air cleanliness and the absence of stray electric fields.

An environmentally controlled chamber was established, consisting of a heavy die-cast aluminium box measuring some 28 x 22 x 11cm externally was mounted on a granite slab to minimize transmitted vibrations. The box front incorporated a hermetic seal. A 6cm square viewing window of thin (1mm) glass was incorporated in a sliding viewing hood in the box front to allow a horizontal microscope to observe the working area. A similar window in the back of the box allowed for external illumination. Both windows were treated with Wimshurst's conductive varnish to maintain integrity of electrical screening. (This useful varnish is made by steeping copper filings in clear shellac varnish for two or three weeks, until the varnish has taken on a light green colour due to the formation of a copper complex with the alcohol. It is then filtered off, and applied in

a thin layer on the glass, leaving it electrically conducting whilst maintaining high optical transparency).

In order to prevent fogging of the windows at high humidity levels, the glass was then treated with ‘Rain-ex’ a proprietary anti-misting formulation for vehicle windscreens, which deposits a fine silicone layer on the glass preventing the formation of very small droplets but causing them to coalesce into a smaller number of larger ones with less overall interruption of the optical pathway.

The box was fitted with spring connector strips to ensure continuous electrical conductivity between the box and front, and was finished inside and out with a gloss white enamel paint to minimize the absorption of radiant heat.

40mm diameter ports were made in opposite sides of the box for communication with an adjacent solid-state dehumidifying system, and these ports were fitted with viral-grade filters to prevent the ingress of airborne particulates.

Two fans were situated within the box, one adjustable in position from outside and acting as a circulating fan for the air inside the box, the other within the outlet port either to purge the air within the box or to circulate it in a closed-cycle mode when connected to the dehumidifier.

An active humidifier/heater was incorporated in the box, consisting of a circular plastic box, 6cm in diameter and 3cm deep packed with clean sand, in which a 12Ω wire-wound resistor was buried. The top of the box was covered with fabric under an aluminium gauze. In use, the sand was damped and a current of up to 1A passed through the resistor, thereby producing warm, humid air in the vicinity, which was then circulated by the internal fan. A lid could seal this unit when not required in use.

Humidity and temperature sensors were mounted on a sliding mechanism in the apparatus front, controllable for position from outside, so that measurements could be taken close (< 2cm) to the working area.

The approach to humidity and temperature control was centered around variations above or below the ambient conditions of the time of experiment. If a humidity greater than ambient were required then the internal humidifier was used; if less, then the external de-humidifier. Temperature control was concerned with maintaining approximately the ambient laboratory temperature. In practice the chamber temperature was found to vary very little – i.e. within ±0.3°C – for extended periods.

7.3.2. Solid-State Dehumidifier.

The dehumidifier system is illustrated schematically in Figure 7.3. It was based around a pair of Peltier elements, of 30W maximum dissipation, in contact on their 'cold' side with a copper block carrying a finned aluminium extrusion. The 'hot' side of the Peltier elements was in good thermal contact with a heavy fan-cooled heatsink, providing a temperature characteristic of 0.2°C/W. A 40mm diameter plastic pipe was shaped to seal over the finned aluminium section, and air from the experimental chamber was circulated through the dehumidifier by the purge fan, where cooling causes the condensation of airborne water vapour on the fins.

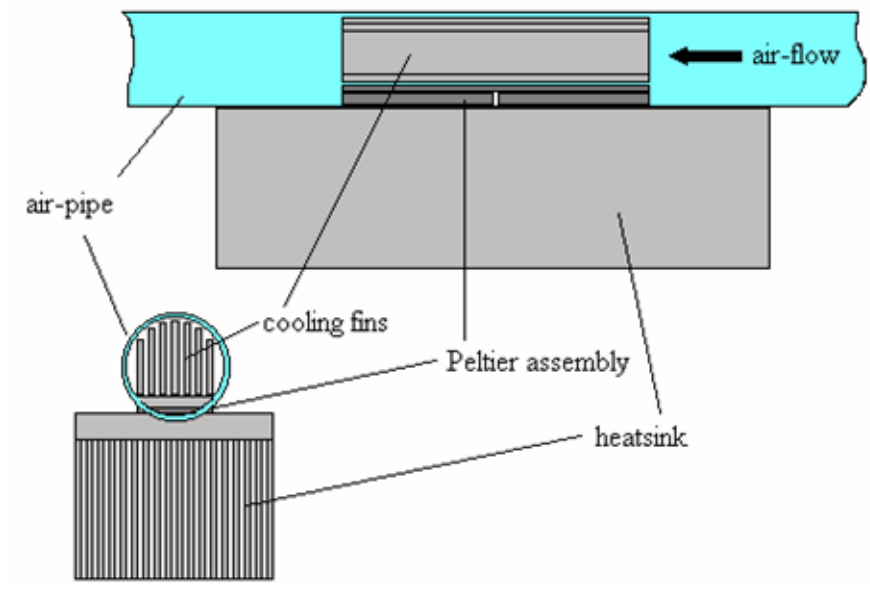

Figure 7.3. Section (upper) and end elevation (lower) of de-humidifier.

In operation the unit proved effective in lowering the relative humidity to about 50% below ambient. The total swept volume of the system (including the experimental chamber) was approximately 6 litres, and Figure 7.4 shows the rate of reduction of chamber humidity starting at a RH value of 70%.

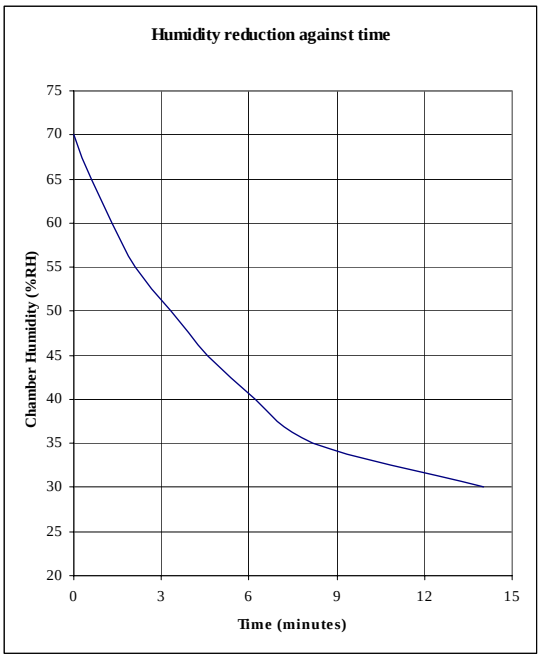

Figure 7.4. Rate of Humidity Reduction.

The non-linear nature of this graph reflects more than merely the reduction of water molecules per unit volume of air in a given time. The heat exchanger fins are cooling at the same time that water vapour from the airflow is being deposited on them, resulting eventually in less efficient thermal contact with the airflow. In conditions of high initial humidity ice begins to appear on the fins, and the rate of humidity drop lessens. When it was required to make a large change in relative humidity quickly, it was found easier to do this in two stages. The dehumidifier would be operated for four or five minutes, the chamber ports then temporarily plugged to prevent rapid re-humidification, and the dehumidifier allowed to acclimatize to room conditions for two or three minutes. It was then re-started and a second dehumidification process done, which resulted in a total drop of some 70 percent of the initial humidity in about ten minutes.

7.3.3. The Experimental Working Area

The experimental area of the apparatus consisted of two opposed lengths of 1mm OD hypodermic needle tubing held rigidly in a brass framework, and electrically insulated from it. This framework was in turn held by four anti-vibration mounts in the centre of a 125 x 125 x 12mm aluminium plate, having a central hole of 75mm diameter for illumination purposes. The plate was mounted vertically on a heavy machined aluminium block, rigidly fixed to the chamber, and could be oriented so that the needles were either vertical or horizontal as required. Electrical connexions to each needle were taken to insulated stand-offs, and the water-feed delivered to each via 1mm ID PVC tubing. The details of the needle assembly are shown in Figure 7.5.

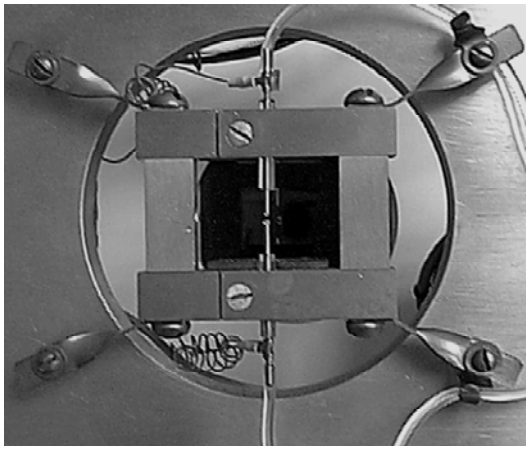

Figure 7.5. Needle Assembly.

Feed water was supplied to the needles by a twin-channel precision metering pump. Two 1ml glass syringes, with integral needles, formed the reservoirs. Both pump and reservoirs were inside the chamber to provide screening from stray electric fields. The pump was hand-operated from outside via a reduction gearbox, and the pump peristaltic tubing was of 250µm bore, allowing for very precise dispensing.

7.3.4. The Optical System

The optical system comprised two main elements, illuminator and microscope. Illumination through the rear port was provided by an Oriel monochromator, operating

at a wavelength of 470nm, this having been found by trial to be the optimum for reducing to a minimum unwanted optical fringing on closely-spaced drop images. A condenser lens situated 1.5cm behind the needles provided a flat plane of illumination.

Optical imaging was achieved by using a high-power vernier microscope, set for horizontal measurement, just outside the viewing window, and equipped with a calibrated micrometer eyepiece with a purpose-made CCD camera attached, leading to a video card and a personal computer. The optical working distance was approximately eight millimetres. Real-time image acquisition software was employed to display the microscope image on a screen, minimizing operator fatigue during long periods of observation. It also added a significantly useful level of extra magnification; when the eyepiece parallels were adjusted to 40µm they appeared on the monitor screen some 2.8cm apart – and implied magnification of 700 diameters.

7.3.5. Potential supplies to the needles and Chamber Electrical Supplies.

The variable potential difference to the needles was derived from a 240 volt dry battery via a potentiometer as a potential divider. This potentiometer was controlled by a slow-motion dial, allowing for fine incremental adjustment of potential, and with a quick-return mechanism for rapid zeroing. The potential applied between the needles was measured with a Datron 1040M fast-sampling digital voltmeter, with an input resistance of 10MΩ. All other aspects of the apparatus that required external electrical power were operated at 12v D.C., supplied from storage batteries. By avoiding connexion to the electrical mains of any system in physical contact with the experimental chamber any possible risk of exposure to mains-borne transients was removed. The chamber itself was connected to earth via the main laboratory earth, which is a substantial buried copper rod.

Figure 7.6. shows a schematic arrangement of dispensing and measurement system and photographs of the apparatus with the front cover removed appear in Figure 7.7.

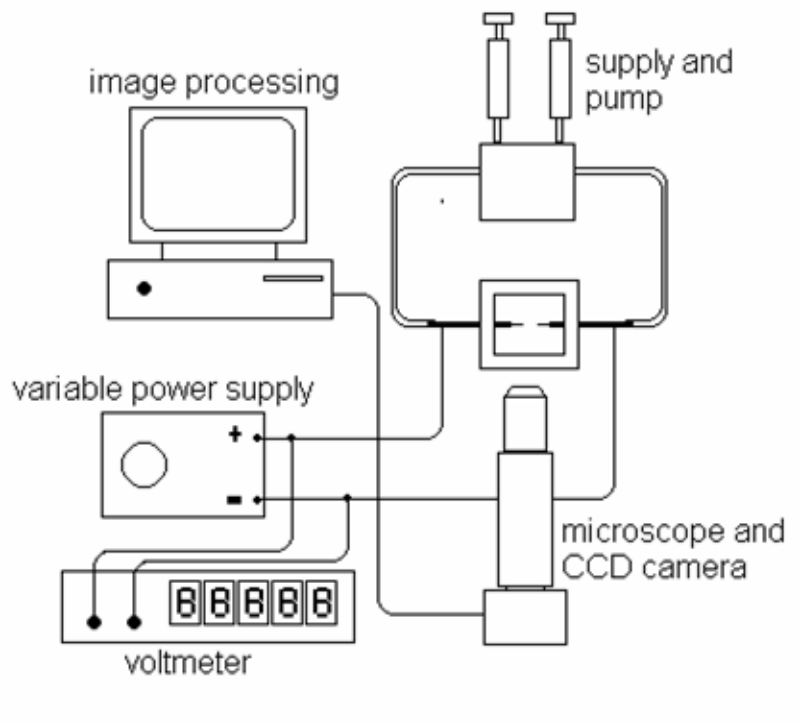

Figure 7.6. Schematic of experimental arrangement.

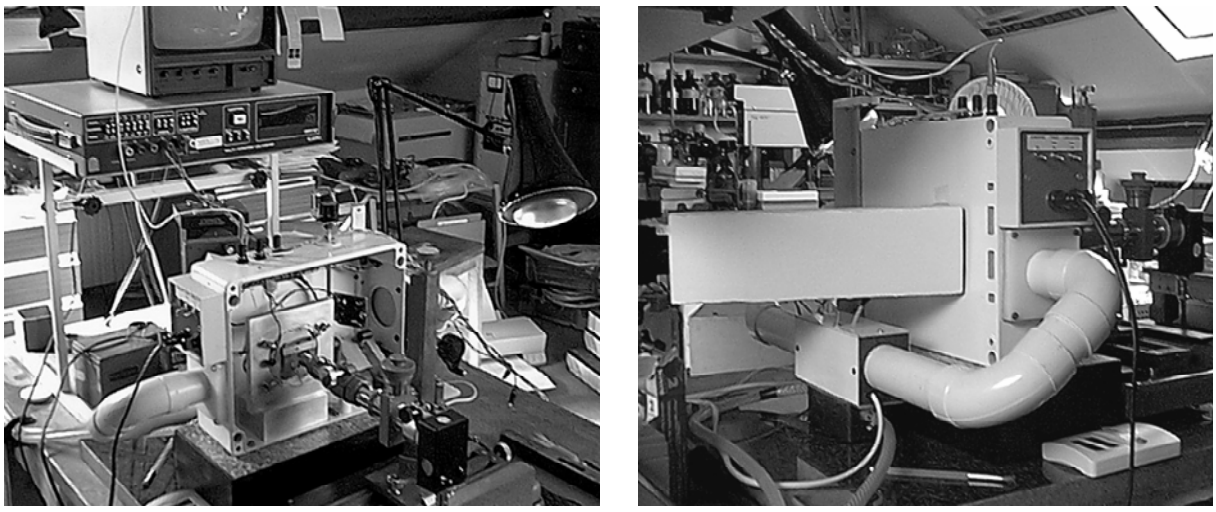

Figure 7.7. Experimental apparatus. *a)* view with chamber cover removed; *b)* side view showing dehumidifier.

7.4. Experimental Method.

As previously noted, the needles could be used in either a horizontal or a vertical position, and the choice was a matter of convenience or of appropriateness to the particular investigation being undertaken. A vertical orientation could be used when droplets greater than hemispherical were required, as this prevented asymmetry of drop profile caused by gravitational forces. Vertically dispensed pendent and sessile drops were very little distorted provided their radius was less than twice the needle radius, and the small tendency of a pendent drop to elongate or of a sessile drop to be depressed was found by measurement to be insignificant on the scale of the measurements used. This distortion is discussed in several textbooks, see, for example, Newton and Searle [106].

It was found experimentally that clean hypodermic needle tubing, with the end squared and polished, and given a light internal chamfer, would reliably dispense a hemispherical drop of radius equal to the outside radius of the tubing. By restricting the drop profile to a hemisphere when the needles were used horizontally the gravitational distortion of the meniscus was found to be negligible. This meant that the inter-needle gap could be set to $2r + h$ where r is the needle radius and h the required inter-drop spacing. It was further found in preliminary trials that dispensing drop pairs with the needles set as described, forcing the drops to coalescence by over-pumping and then retracting them by reversing the pump, led to high reproducibility of both drop size and position. With 40µm parallels set on the micrometer eyepiece each successive pair of drops would be positioned well within a micrometre of its predecessor.

The technique of taking a coalescence potential reading was thus: a pair of hemispherical drops was dispensed and the inter-drop spacing required checked against previously set micrometer parallels. The potential difference between the needles was then increased by means of the potentiometer until instability and coalescence occurred. This resulted in a brief current flow, so the pump was immediately backed off, pulling the drops apart. The voltmeter was read at this stage. Prior to taking a subsequent reading the potentiometer was reset to zero and the small internal circulating fan operated for a few seconds to homogenize the air in the vicinity of the needles and

disperse any possible build-up of a local humidity gradient. Humidity and temperature readings were then checked before taking the next reading.

7.5. Experimental Results.

Two series of experiments were undertaken. The first of these was concerned with finding the coalescence potentials for different inter-drop spacings at a number of humidity marker points. The second series concentrated on a single inter-drop spacing with series of measurements taken at much closer intervals of relative humidity.

7.5.1 Results, Series I – Coalescence Potentials.

This sequence of measurements was made with the needles vertical. The inter-needle gap was adjusted using a standard gauge, and drops dispensed. Figure 7.8 shows a screen-capture at the stage of preliminary vertical alignment, with the opposing surfaces of both drops separated by a gap of 40μm, indicated by the visible parallels.

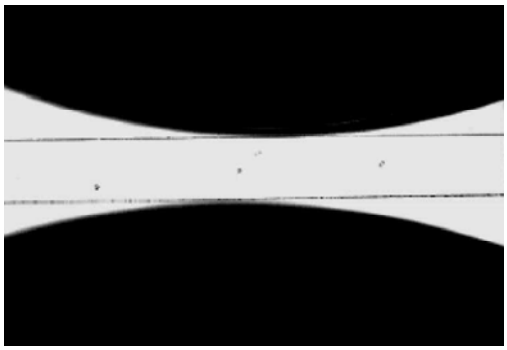

Figure 7.8. Detail of opposing drops, taken during alignment.

- The temperature during the experimental series was 25.4±0.3°C.
- The conductivity of the stock water was 3.3 x 10^{-5}S/m at the beginning of the series, and had risen to 4.2 x 10^{-5}S/m ten days later at the end.

- The surface tension of a water sample from the decanted stock was measured by Du Nüoy's method [107], using a platinum-iridium ring and a Pye tensiometer. This gave a value of 72 x 10^{-3} N/m at 25.4°C.
- The barometric pressure during the series ranged between 998 and 1007mb.

Five approximately equispaced relative humidity points were chosen; 21, 43, 61, 83, and 100% R.H. Four needle separation distances were used; 2.50, 2.00, 1.50 and 1.00mm, with needles of outer diameter 1.05mm being used in all cases. Prior to each sequence the needles were set to the required spacing, aligned coaxially, checked with a gauge and secured with pinch-screws. This setting determined the maximum drop diameter for the sequence. The case was then sealed, the air purged to ensure a clean working environment, and the instrument stabilized to the temperature and humidity settings required.

A total of ten readings for each setting was taken, and their means found. These are recorded in Table 7.2 below. (The complete data are to be found in Appendix 3).

Needle sepn.			**2.50mm**					**2.00mm**		
RH,%	**21**	**43**	**61**	**83**	**100**	**21**	**43**	**61**	**83**	**100**
Gap,µm										
40	76.5	77	72.9	72.7	64.2	83.1	87.6	80.2	79.1	76.2
30	55.8	56.8	59.1	54.1	52.3	67	65.1	65.3	57.6	54.7
20	38.8	42.2	39.7	39.7	35.8	44.7	47.1	45.7	37.3	38
10	22.3	24.8	24.6	21.1	20.6	25	30.2	26.9	20.1	22.1
5	14.2	16.7	16.6	12.5	9.7	19.1	21.7	18.1	14.2	11.9
Needle sepn.			**1.50mm**					**1.00mm**		
RH,%	**21**	**43**	**61**	**83**	**100**	**21**	**43**	**61**	**83**	**100**
Gap,µm										
40	92.9	115.1	94.3	88.2	85.1	132	145	125.8	87.9	98.1
30	72.9	92	73.8	65.8	64	103.6	108	105.6	76.3	72.6
20	47.2	67.8	50.4	47	41.6	72.5	79.1	68.7	47	50.2
10	24.6	40..8	31.3	25.8	25	43.5	47	38.9	28.4	28.3
5	19.5	28.6	20.1	16.2	17.8	24	24.1	21.4	15.9	20.4

Table 7.2. Summary of mean coalescence potentials in Volts for a sequence of humidities, inter-drop gaps and needle separations – Series I.

7.5.2. Calculation of drop radii.

It was necessary to know the radii of the drops at any given needle setting. The most direct way of determining these is by measurement, using the travelling microscope, but this course was not followed as it would have required a much larger field of view than the apparatus was set up to provide. Direct calculation was therefore used, as follows;

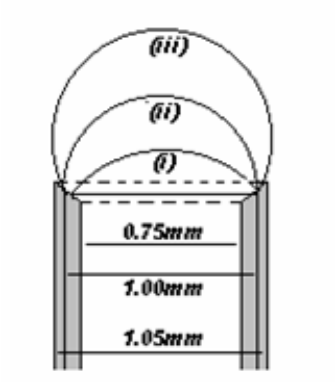

Figure 7.9.

Figure 7.9 shows the orifice of a needle. An exaggerated internal chamfer is shown for clarity, and the 1mm diameter *effective* diameter of the bore is indicated. Arcs *(i), (ii)* and *(iii)* represent possible drop configurations over the range of needle separations used, signifying minor, semicircular and major arcs respectively.

In each case,

let h be the drop height above the orifice,
r be the drop radius, and,
x be the effective orifice radius.

Considering case *(i)*, the arc being minor, i.e. $r > h$ (Figure 7.10).

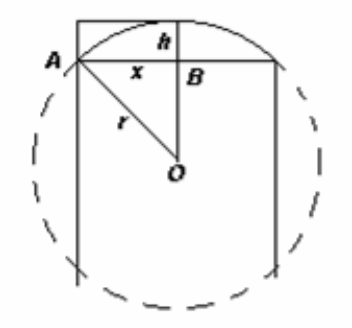

Figure 7.10.

In Figure 7.10, $AO^2 = AB^2 + OB^2$

i.e. $r^2 = x^2 + (r - h)^2$

$= x^2 + (r^2 + h^2 - 2rh)$

whence $\underline{\boldsymbol{r = (x^2 + h^2) / 2h}}$ (7.4)

Case *(ii)*, the arc being a semicircle. In this situation it is self-evident that $r = h$

Case *(iii)*, the arc being major, i.e. $r < h$. (Figure 7.11)

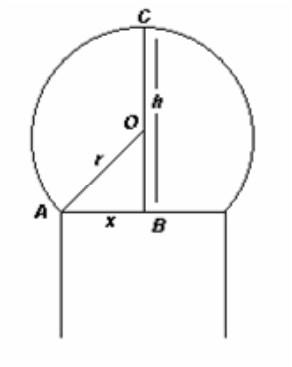

Figure 7.11.

Now, $OB = (h - r)$, and the equation again reduces to;

$$\boldsymbol{r = (x^2 + h^2)/2h} \quad (7.4)$$

In practice it must be remembered that h is not exactly equal to half the separation s, as there is a gap, g, between the drops. The value of h is therefore $(s - g) / 2$. (See Figure 7.12). Table 7.3, below, gives the effective values of h for each setting of separation and gap over the experimental range.

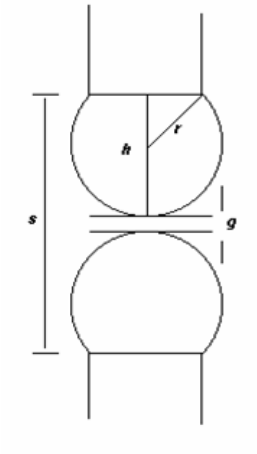

Figure 7.12.

	g =40µm	g = 30µm	g = 20µm	g = 10µm	g = 5µm
s = 2.5mm	1.23	1.235	1.24	1.245	1.248
s = 2.0mm	0.98	0.985	0.99	0.995	0.998
s = 1.5mm	0.73	0.735	0.74	0.745	0.748
s = 1.0mm	0.48	0.485	0.49	0.495	0.498

Table 7.3. Values of *h* (mm) for different values of *s* and *g*.

Using the above values for *h*, and $x = 0.5$, and inserting them in the formula

$$r = (h^2 + x^2) / 2h$$

we arrive at the effective values of drop radii in Table 7.4 below;

	g = 40µm	g = 30µm	g = 20µm	g = 10µm	g = 5µm
s = 2.5mm	0.716	0.719	0.720	0.723	0.724
s = 2.0mm	0.616	0.619	0.621	0.623	0.624
s = 1.5mm	0.536	0.538	0.539	0.540	0.541
s = 1.0mm	0.500	0.500	0.500	0.500	0.500

Table 7.4. Values of *r* (mm) for different values of *s* and *g*.

The results of this first series of experiments may conveniently be displayed graphically, showing the entire envelope representing the range of measured values for each setting of the needle separation. These are shown in composite form in Figure 7.13, followed by the individual needle separation envelopes (Figure 7.14) exhibiting between them the total range of potentials encountered for all conditions of humidity and separation.

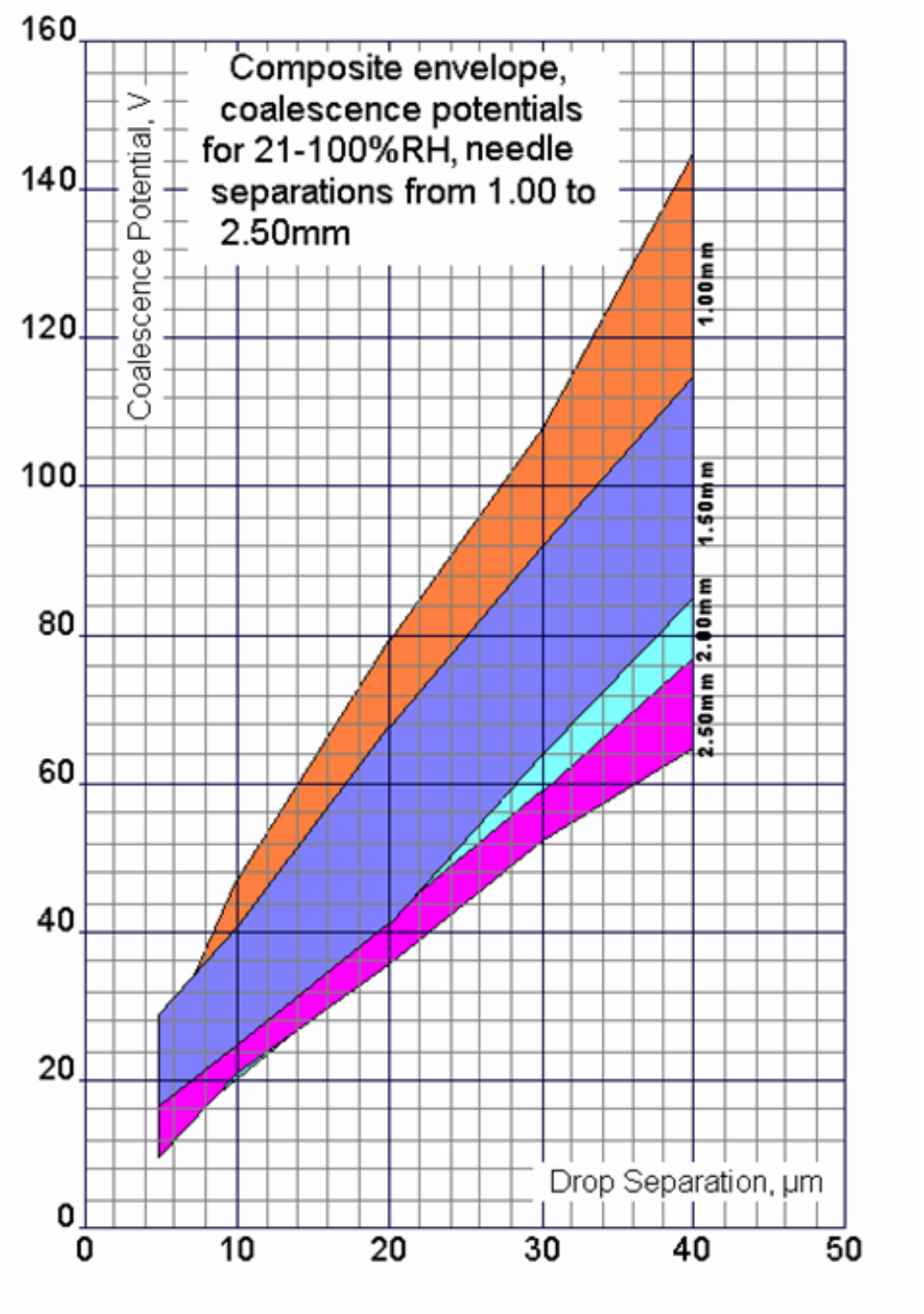

Figure 7.13. Composite coalescence potentials envelopes – Series I.

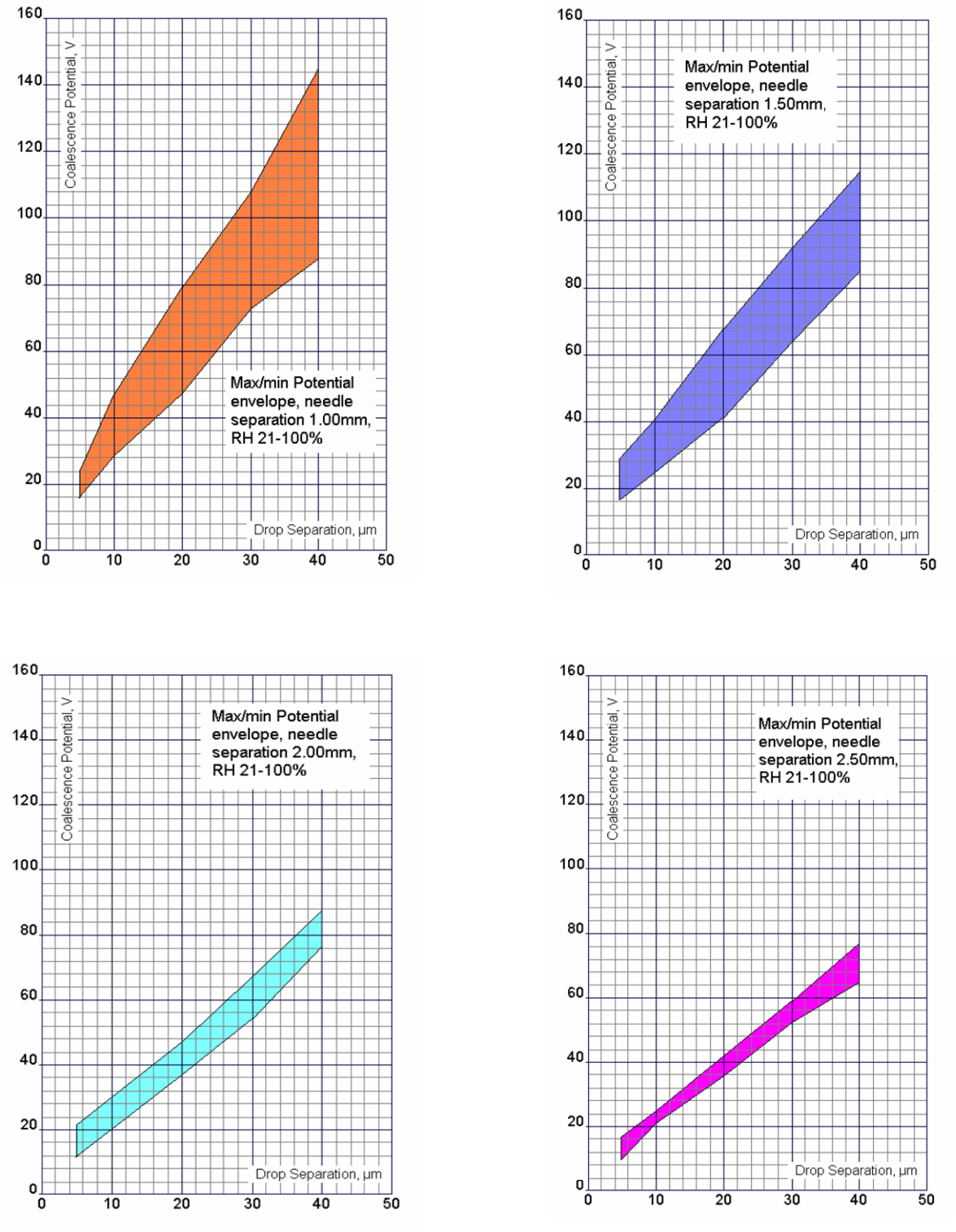

Figure 7.14. Coalescence potential envelopes for needle separations 1.00 to 2.50mm.

7.5.3. Results, Series II – Coalescence Potentials.

The vertical range of the individual envelopes of the Series I results strongly suggested that for all needle and drop separations the prevailing relative humidity exercised an influence on the onset of instability and hence the coalescence potential. A second series of experiments was undertaken to ascertain how this critical potential varied with humidity for a specific geometry. As a subsidiary to this, an experimental investigation was also made into the rôle of evaporation in affecting the experimental results.

Experimental Arrangements.

The same apparatus was used as previously described, with certain minor changes. The needles were re-oriented in a horizontal position, as drops of hemispherical form only were to be used, and, as previously noted, these might be reliably dispensed providing the needles had been internally profiled at the orifice as described earlier.

1mm OD needle tubing was used, and the inter-needle gap set to 1.04mm, thus allowing for two hemispherical drops of 0.5mm radius to be dispensed with a 40µm gap between them. This value of 40µm was selected to reduce the tendency of reflections in the drops leading to undesirable interference fringing, whilst keeping a sufficiently small gap to require only a potential in the order of one to two hundred volts for coalescence. The first Series had experienced some problems with evaporation when operating at low humidities, causing slight radial shrinkage in the drops. By using hemispherical drops there was less exposed surface than in the former Series, and by setting a gap at the larger end of the previous range, the proportional enlargement due to any evaporation was reduced significantly.

- The temperature during the experimental series was 21.5±0.5°C.
- The conductivity of the stock water was 4.6×10^{-5}S/m.
- The surface tension of a water sample (Du Nüoy ring method) was 71.9×10^{-3}N/m at 21.5°C.
- The average barometric pressure during the experiments was 1001.5mb.

Measurements of V_c, the critical coalescence potential, were taken at 20 approximately equi-spaced intervals between 41% and 100% RH. In each case ten readings were taken, and the means calculated. The full data are to be found in Appendix 3, and the summary data are reproduced in Table 7.5.

RH%	**41**	**43**	**45**	**46**	**47**	**48**	**49**	**50**	**51**	**53**
***Vc* (v)**	145.6	145.5	141.8	141.2	139.6	133.1	139.3	131.8	129.1	125
***Xc* (kV/m)**	3640	3638	3545	3530	3490	3328	3483	3295	3228	3125
RH%	**56**	**61**	**65**	**69**	**71**	**75**	**81**	**83**	**89**	**100**
***Vc* (v)**	120.2	114.7	107.9	103.9	102.3	98.0	91.3	89.9	85.1	77.8
***Xc* (kV/m)**	3005	2868	2698	2598	2558	2450	2283	2248	2128	1945

Table 7.5. Summary data for coalescence potentials (V_c, volts) and equivalent field-strengths (X_c, kV/m) for humidities between 41% and 100% RH.

These data were initially plotted as a simple graph of coalescence potential against humidity. For humidities above 50% an arbitary line of best fit was added, but for the more anomalous results in the range 41 – 50% were joined point to point. The result is displayed in Figure 7.15.

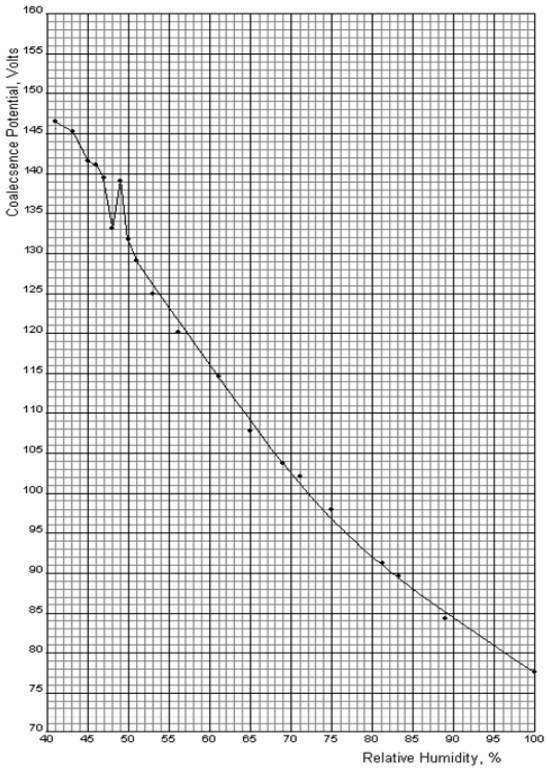

Figure 7.15. Mean coalescence potential plotted against relative humidity.

7.5.4. Experimental Extension – Mid-Range Humidities.

Both Series I and Series II experiments had highlighted some potential anomalies in the results obtained between approximately 40 and 50% RH, and a short pair of experiments was undertaken to investigate this a little further. In the first of these readings were repeated for four gap settings between 10µm and 40µm at closer humidity intervals between 35 and 55%RH using 1.25mm diameter needles. The results are displayed in Figure 7.16.

RH%	40µ	30µ	20µ	10µ
35	97.2	79.2	60.5	50.4
40	93.3	74	59.8	49.3
42	91.8	75.1	58.2	41.7
44	88.8	76.7	60.8	44.5
46	91.9	74.3	62.4	43.8
48	92.4	78.6	61.0	47.5
50	81.0	67.0	53.7	36.8
55	90.6	73.3	58.6	42.1

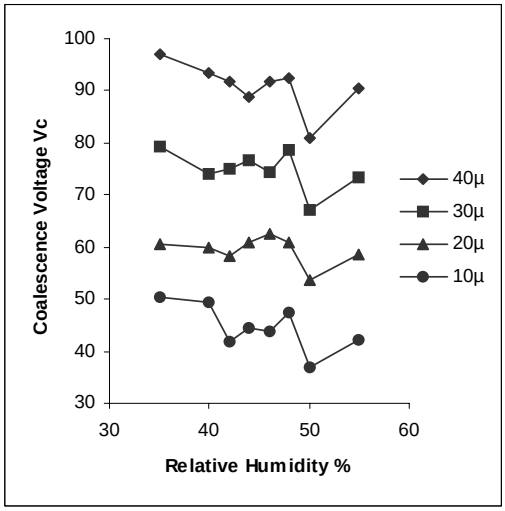

Figure 7.16. Close-range humidity results - I.

In the second experiment 1.00mm diameter needles were used at a separation of 40µm, reflecting the conditions of the second main experimental Series. Ten readings at each of four RH points between 47 and 50% was taken, and the mean values plotted. Figure 7.17 shows these results.

DATA NO.	RH 47	RH 48	RH 49	RH 50
	Vc	Vc	Vc	Vc
1	132.7	131.8	130.5	139.3
2	152.2	135.1	136.2	133.2
3	146.8	131.7	141.8	127.5
4	136.1	129.6	141	136.7
5	140.1	132.8	139.6	126.5
6	141.2	136.1	134.4	125.7
7	137.6	132.2	144.3	130.2
8	138.3	134.8	137.8	129.8
9	139	131.9	143.9	127.4
10	132	140.3	142.2	135.3
MEAN	**139.6**	**133.6**	**139.2**	**131.2**
Xc (kV/m)	**3490**	**3340**	**3480**	**3280**

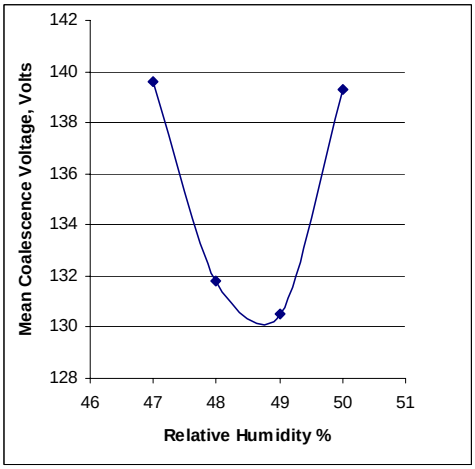

Figure 7.17. Close-range humidity results - II.

7.6. Experimental Extension – Determination of Evaporation Rates.

The experimental work undertaken to this stage had raised some questions concerning the extent to which evaporation might be an influence by causing dimensional loss of the droplets during the experimental procedure. The issue of evaporation of small spherical forms was first addressed by Langmuir in 1916 [108], and subsequently by several authors [109-111]. Experimental verification was sought for the evaporative rates for small droplets *i)* dispensed vertically upwards from a needle, and *ii)* sessile. Taylor [105] had made the suggestion that a dispensing system might be subject to viscous flow, thus altering the volume of liquid dispensed, and the two droplet types were investigated to see if there was any discrepancy between them.

The same drop-chamber was used as before, with the following modification to the dispensing arrangements. The needles were set vertically, and for Case *i)*, the upper needle and supply was simply removed. A drop was dispensed at the top of the lower needle of 1mm diameter, and allowed to shrink back to a predetermined height above the needle orifice. At this point its further evaporation to specific height intervals was timed. This process was repeated three times for each of the five humidity settings used in Series I of the main experimental series.

In the second case, sessile drops of the same initial volume were produced thus: the lower needle was replaced by a piece of steel rod of 1mm diameter whose end had be accurately squared and polished. The upper needle was now replaced, and set a convenient height above the rod, and coaxial with it. If a drop was dispensed from this upper needle it contacted the end of the rod and coalesced with it, forming a liquid bridge. Reversing the pump ruptured this bridge, leaving a droplet *in situ* on the end of the rod. Careful setting of the gap between rod and needle resulted in the formation of a droplet of approximately the same height as the dispensed drop in Case *i)*. This was then allowed to evaporate back to the same predetermined height as before, and the evaporation date measured as previously.

For both configurations relative humidities of 21, 43, 61, 83 and 100% were used. Initial values of h (see Figure 7.18) of 0.3, 0.5 and 0.7mm were used, corresponding to

drop-radii of 0.566, 0.500 and 0.528mm respectively, as derived from Equation 7.18. The times for *h* to decrease by 10, 30, 50, 70, 90, 110 and 130μm were measured.

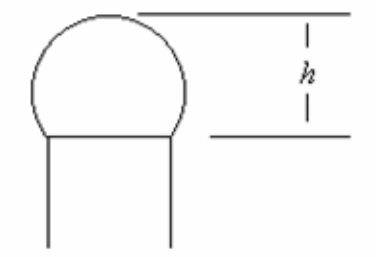

Figure 7.18. Measured height, *h*, of drop above orifice.

7.6.1. Experimental Results – Evaporation.

The experimental results are tabulated in Table 7.6, and shown graphically in Figure 7.19.

Time in seconds for drop height decrement by evaporation for different drop heights and humidities

A. Evaporation from drop on needle connected to dispensing system

	Series 1. RH = 21%			Series 2. RH = 43%			Series 3. RH = 61%			Series 4. RH = 83%			Series 5. RH = 100%		
h (mm)	**0.3**	**0.5**	**0.7**	**0.3**	**0.5**	**0.7**	**0.3**	**0.5**	**0.7**	**0.3**	**0.5**	**0.7**	**0.3**	**0.5**	**0.7**
Decrement															
μ															
10	4	7	8	8	12	18	12	13	16	20	23	44			
30	13	17	21	20	29	33	30	36	47	59	71	120			
50	24	29	35	33	46	75	49	58	75	100	110	193			
70	33	41	50	48	63	82	67	80	107	136	152	261			
90	41	52	63	61	80	101	84	102	137	174	192	326			
110	49	62	77	75	96	124	102	122	163	211	228	388			
130	58	72	93	88	112	144	119	141	194	244	266	449			
150	66	82	105	104	128	165	137	164	221	279	302	503			

No significant evaporation in 300s (5mins)

Data not taken

B. Evaporation from drop deposited on 1mm diameter metal surface

h (mm)	**0.3**	**0.5**	**0.7**	**0.3**	**0.5**	**0.7**	**0.3**	**0.5**	**0.7**	**0.3**	**0.5**	**0.7**	**0.3**	**0.5**	**0.7**
Decrement															
μ															
10	4	8	9	9	13	17	12	15	19	22	27	40			
30	12	19	22	18	30	38	33	37	54	61	78	130			
50	21	30	39	33	48	59	52	59	88	106	130	204			
70	30	41	52	46	63	80	66	88	115	140	178	278			
90	38	53	66	59	78	100	86	115	142	181	215	352			
110	47	63	83	71	94	122	101	141	172	219	240	396			
130	56	74	100	83	110	142	117	167	202	258	278	460			
150	63	85	113	96	122	162	132	193	228	290	318	535			

No significant evaporation in 300s (5mins)

Data not taken

Table 7.6 . Evaporation rates, **A,** for drop at needle orifice, and, **B,** for isolated drop.

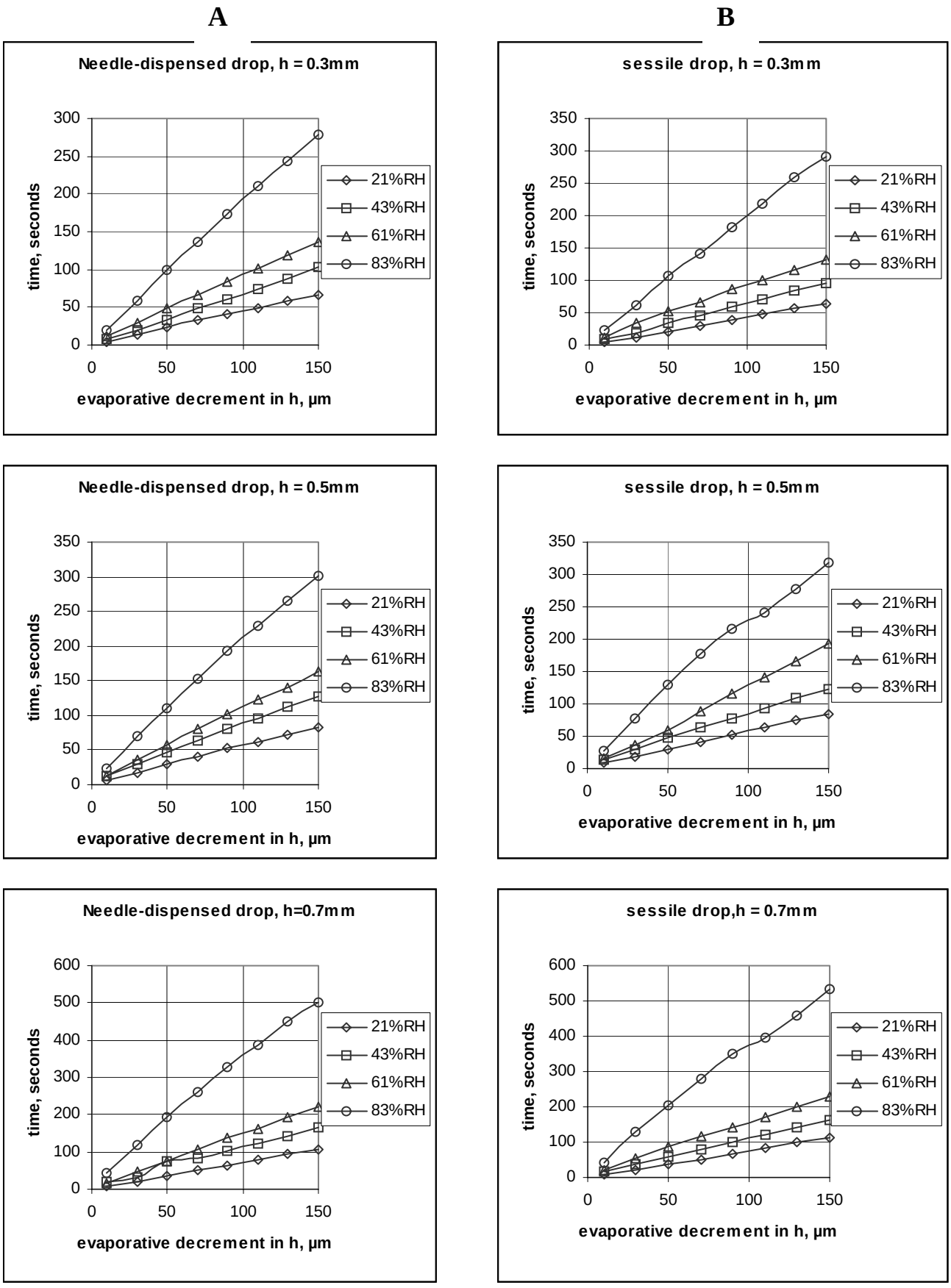

Figure 7.19. Evaporation-rate data for, *left*, needle-dispensed drops *(A)*, and, *right*, sessile drops *(B)* under equivalent conditions.

7.7. Discussion of Experimental Results.

7.7.1. Evaporation Data.

These results are discussed first, having possible implications for the interpretation of the principal results of Series I and Series II of the main experiments.

The correlation between the A (dispensed) and B (sessile) groups is very high, implying that there is little difference in practice between a droplet formed at the end of a needle and an isolated one with an equivalent chordal base area.

In the case of the sessile drop, formed atop the 1mm diameter steel rod, the contact area of the drop was found to be the entire end-surface of the rod, i.e. the drop completely wetted the end of the rod. As evaporation proceeded this contact area was undiminished, providing an exact parallel with the dispensed drop evaporating at the end of the needle. Both drops were, therefore, dimensionally comparable. Figure 7.20 shows sections through both the sessile and the dispensed drop for situations comparable with the start and end of the evaporative experiments.

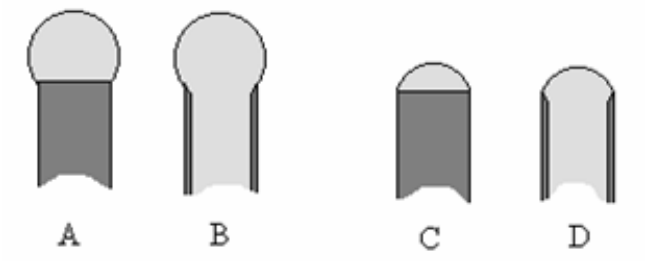

Figure 7.20. Sections through sessile (*A,C*) and dispensed (*B,D*) drops. *A* and *B* represent the start of the evaporation experiments, *C* and *D* the end.

The sphericity of the drops in each case had been determined by comparing three diametral measurements, as detailed in Figure 7.21.

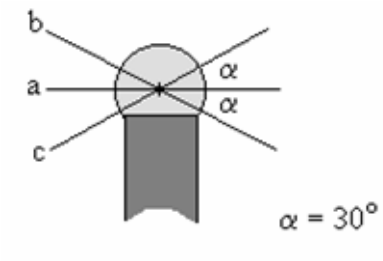

Figure 7.21. Diametral measurements.

Whilst the geometry of the setup precluded measurements at right-angles, the three diameters indicated were identical within the limits of accuracy (1.0μm) of the vernier microscope used, indicating that sphericity was also well within the limits of experimental accuracy.

The rate of loss of mass from a drop by evaporation has been addressed by many workers. Langmuir, 1918 [108], developed an expression of;

$$-\frac{dm}{dt} = \frac{4\pi rDMp}{RT} \qquad (7.5)$$

where,

- dm/dt is the rate of loss of mass, r is the radius of the evaporating sphere, D is the diffusion coefficient, M is the molecular weight, R is the gas constant, and T is the absolute temperature.

The immediate implication of this is that the loss of mass is proportional to the radius – an initially counter-intuitive concept, as one might reasonably consider evaporation to be a function of surface area, and hence of r^2. It was shown by Birdi *et al*, 1989 [112], that in the case of a sessile drop, i.e. one deposited on a solid surface that it does not wet, the radius r_b of the circle of contact remains constant, with the angle of contact, θ, varying as evaporation proceeds. The rate of loss of mass was shown to relate to the drop radius across the spherical interface, r, as;

$$-dm/dt = -4\pi r^2(dc/dr)D \qquad (7.6)$$

where c is the vapour concentration and D its diffusion coefficient, as before. If c_0 is the saturation vapour at the drop temperature, and r_d the drop radius, then the boundary conditions for this equation are;

$$c = c_\infty \text{ when } r = \infty, \text{ and } c = c_0 \text{ when } r = r_d \qquad (7.7)$$

leading to the conclusion that,

$$-dm/dt = 4\pi r_d D(c_0 - c_\infty) \qquad (7.8)$$

From a consideration of Figure 7.10 and Equation 7.4 it is seen that the drop radius, *r*, is proportional to *h*, i.e. decreases in *h* are reflected in directly proportional variations in *r*, and the linear evaporation rates recorded in the graphs of Figure 7.19 are as expected. In the case of dispensed drops it should be noticed that the radius of the interfacial liquid circle with the needle orifice cannot change. Any variation of the evaporation rates between the sessile and dispensed drops for a given initial diameter, and hence area of spherical sector exposed, must therefore be due to one or more of three causes;

1. Viscous flow through the needle,
2. Local convection variations,
3. Pressure changes within the drop as evaporation proceeds.

These issues may be addressed by a consideration of the experimental arrangements.

In the case of a drop dispensed from a needle, any viscous flow through the needle (or associated tubing, including the pump) would be brought about by a pressure gradient within these components. The actual experimental method involves a time interval whilst the initially oversized drop is evaporating back to its starting size, thus allowing sufficient time for pressure balance within the system to be achieved.

Thermal convection variations have two possible origins. The first of these is due to any temperature variation within the liquid system, the second to local temperature variations in the air around the outside of the drop brought about by the absorption of heat during evaporation.

The entire system was contained within a thermally stabilized environment, and the possibility of thermal gradients within the enclosure sufficient to give rise to any perceptible fluid flow within the system is very small, especially considering the homogenization of the chamber air by means of the circulating fan between measurements. Thermal gradients due to evaporation certainly do exist, but the mobility

of vapour molecules from the surface of an isolated drop is sufficient to render the temperature differential between the dispensed drop and the liquid column feeding it very small.

Pressure changes within the drop would only have an effect in the case of the dispensed drop, where it is conceivable that a variation in 'back-pressure' in the liquid system might result. This system, however, is limited in the way in which any volume change might occur. The pump was, as previously described, peristaltic, meaning that when the pump is at rest a finite volume of liquid is 'pinched off' within the tube feeding the needle. The wall of the feed-tube from pump to needle was thick relative to the bore, and small pressure variations would have an insignificant effect upon the volume of the liquid it contained, with any consequent variation of the droplet radius at the end of the needle.

There is a high correlation between the evaporation rates of the dispensed and sessile drops for any given value of *h*, and the liquid column in the former case may therefore be treated as a rigid body during the evaporation stage of the experiment. The evidence for the comparative equality between the two systems is most manifest under conditions of high humidity, where the rates of mass loss are at their lowest, and high correlation is still maintained.

A consideration of the results of the evaporation experiments led to the conclusion that, within the framework of the main investigation to determine coalescence potentials, high confidence might be placed in measurements at higher rates of relative humidity. At lower rates, however, evaporation is more significant, and shrinkage of the drops due to evaporation more likely to introduce error in the inter-drop gap, and hence the potential for instability and coalescence. The time taken to increase the potential between the drops in a controlled manner was up to some 5 seconds, depending on gap, and it was therefore decided on the grounds of caution to discount results for relative humidities below 50%. (The apparently anomalous but repeatable results for RH values between 40 and 50% need to be the subject of further investigation).

7.7.2. Coalescence Potential Data.

The experimental data obtained from both Series I and Series II of the main coalescence potential investigations suggest strongly that Relative Humidity is a parameter exercising significant influence on the potential difference between closely spaced drops necessary for the onset of instability and coalescence.

The theoretical conditions governing the potential difference necessary for instability and coalescence were examined by Nolan, 1926 [113] and Macky, 1931 [114] and extended by Latham and Roxburgh, 1966 [115]. This latter work was subsequently further extended by Taylor, 1968 [105], who examined the conditions for instability in pairs of soap bubbles and liquid droplets.

Latham and Roxburgh began with the results derived from Nolan and Macky's respective papers that had led to the establishment of the empirical equation,

$$F(R_0/\gamma)^{\frac{1}{2}} = K \qquad (7.9)$$

where F is the field strength (esu), R_0 the original (i.e. undistorted) drop radius, γ the surface tension, and K a numerical constant. The value of this latter constant was calculated by Wilson & Taylor, 1925 [116] as 1.61±0.4 for spheres significantly separated (i.e. separation >>radius), and for water drops by Macky [114] as 1.51.

Latham & Roxburgh computed values for K, applying Davis' work of 1964 [117] on field enhancement between more closely-spaced pairs of rigid spheres, deriving values of $F(R_o/\gamma)^{½}$ as shown in Table 7.7 below.

Separation (radii)	10	1	0.1	0.01	0.001
$F(R_o/\gamma)^{½}$	1.555	9.889E-1	7.887E-2	3.910E-3	1.898E-4

Table 7.7. Latham & Roxburgh's computed values of $F(R_o/\gamma)^{½}$

These computed results were the subject of experimental investigation, and their results are reproduced in Figure 7.22, which shows the experimental values of $F(R_o/\gamma)^{½}$ plotted against X_0/R_0, X_0 being the initial inter-drop separation. The continuous curve shows the predicted theoretical relationship, and the discrete data points the corresponding experimental values obtained. Numerical data were not published, and a grid was therefore superimposed on the original graph to allow for the extraction of approximate values, shown in Table 7.8, below.

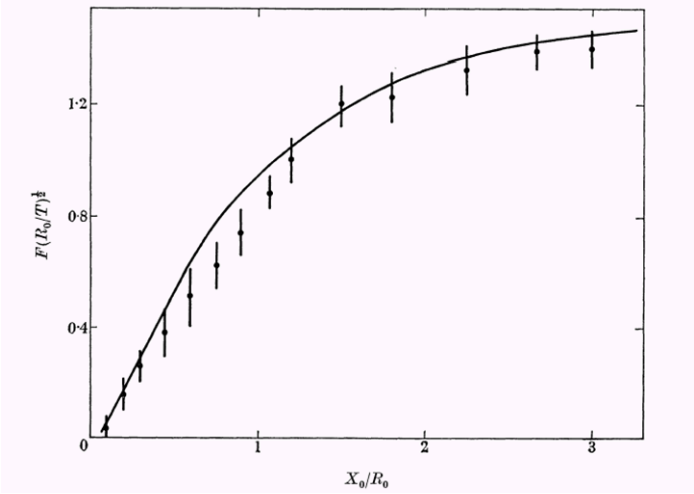

Figure 7.22. Values of $F(R_o/T)^{½}$ plotted against X_0/R_0. (From *Latham & Roxburgh, [115]*. *Note*: *T* is used for surface tension in the paper from which this facsimile diagram is taken, rather than the more conventional modern symbol γ, used in the text.)

X_0/R_0	$F(R_o/\gamma)^{½}$ - experimental	$F(R_o/\gamma)^{½}$ - theoretical
0.1	0.03	0.04
0.2	0.15	0.16
0.3	0.26	0.27
0.45	0.38	0.46
0.60	0.51	0.64
0.75	0.62	0.78
0.90	0.74	0.88
1.05	0.88	0.92
1.20	1.00	1.04
1.50	1.20	1.16
1.80	1.22	1.28
2.25	1.32	1.38
2.65	1.395	1.42
3.00	1.40	1.44

Table 7.8. Derived data from *Latham and Roxburgh [115]*

These data show a fairly consistent shortfall of some 10% between the experimental results achieved and the theoretical ones predicted. It is possible to argue that this discrepancy is due to evaporation having occurred in the time elapsing between drop dispensing and disintegration in the increasing electric field. Evaporation would cause an increase in X_o (the inter-drop spacing), and a decrease in R_o (the drop radius). The ratio X_o/ R_o would therefore increase in value, with a (smaller) decrease in the value of $F(R_o/\gamma)^{½}$. This would result in the curve of Figure 7.23 being depressed slightly downwards and moved to the right, resulting in a much better correlation with theoretically predicted values.

The next major investigation in the area was that made by Taylor, 1966 [105], which utilized in part the work of Latham and Roxburgh, but which merits a far closer examination in the context of the present research.

In this investigation an axisymmetric arrangement was considered, in the first instance of opposed soap-bubbles and extended to opposed liquid drops, separated by a small initial gap. Figure 7.23 shows Taylor's geometry, and his original nomenclature has been retained in the subsequent discussion, with the exception of the use of γ rather than T to denote surface tension.

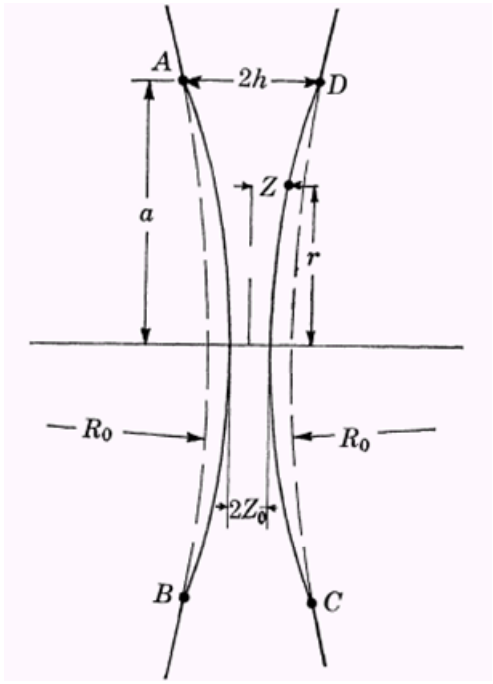

Figure 7.23. Geometry and nomenclature used by Taylor [105].

Drops of radius R_o were produced at the ends of needles of diameter *a*, these needles being separated by a distance *2h*, such that the drop menisci were separated by a distance $2Z_o$. Potentials of $+V$ and $-V$ were imposed on the needles *AB* and *CD* respectively, resulting in a potential difference of *2V* between the drops. The value of *2V* to produce instability, and then coalescence, was calculated from a consideration of the physical forces opposing instability and the effect of an increasing electrical force normal to the drop surfaces in producing instability.

Taylor's derived equation for small inter-drop gaps (i.e. where $Z_o << h$) is;

$$V = 0.38 \frac{Z_0}{R_0} \left(\frac{\gamma R_0}{\varepsilon_0} \right)^{1/2} \tag{7.10}$$

Writing V_c for the total coalescence potential, and remembering that $V_c = 2V$ we may re-write this expression as,

$$V_c = 0.76 \frac{Z_0}{R_0} \left[\frac{\gamma R_0}{\varepsilon_0} \right]^{\frac{1}{2}} \tag{7.11}$$

Substitution into this expression of the values of *Zo,* R_o and γ used in the practical investigation leads to a predicted value of V_c of 61.3 volts, compared with the measured value at 100%RH of 77.8 volts, where there has been demonstrated to be no evaporation consideration. (See *Experimental Results – Evaporation*, 7.6.1, above).

7.7.3. Consideration of Experimental Error and Evaporation Effects.

In considering the rôle of experimental errors in the measured results it should be noted that the principal sensitivity to error in Taylor's expression lies in the ratio Z_o/R_o. These two quantities are dependent on the setting of the initial capillary spacing, *2h*, and their relationship is such that small deviations in *2h* lead to larger errors in Z_o/R_o. The ratio is

also affected by errors in the measurement of Z_o. The experimental arrangements were such that *2h* could be determined to within ±5μm, and $2Z_o$ (the total inter-drop gap) to within ±2μm. This leads to boundary values of Z_o/R_o in the practical investigation of,

$$0.0433 > Z_o / R_o > 0.0377 \qquad (7.12)$$

Substitution of these maximum and minimum values in Equation 7.11 leads to a deviation from the predicted value of Vc of only ± 5.4%, compared with the 27% higher than predicted value actually measured.

Measurements made at relative humidities below 100% require a consideration of the possible gap geometry variations due to evaporation. These have been shown to be linear (i.e. $\propto R_o$) with respect to time, and an extrapolation of the data of Table 7.6 (for dispensed drops, h = 0.5mm) allows the maximum deviations for Z_o/R_o within the experimental time-frame to be calculated.

These are given in Table 7.9 which shows the values of Z_o/R_o at relative humidities of 43, 61, 83 and 100%, corrected for evaporative loss based on a mean experimental time of 5 seconds per measurement, together with the consequent coalescence potentials $({}^pV_c)$ predicted by Taylor's equation, the actual potentials measured at that humidity $({}^pV_c)$, and the ratios of the predicted to measured values, $({}^pV_c/{}^mV_c)$.

R.H.%	**43**	**61**	**83**	**100**
Z_o/R_o	0.0514	0.0503	0.0456	0.0400
$({}^pV_c)$	78.4	76.8	68.3	61.3
$({}^pV_c)$	145.5	114.7	89.9	77.8
$({}^pV_c/{}^mV_c)$	0.53	0.67	0.76	0.79

Table 7.9. Evaporation correction data.

From this it may be seen that whilst surface evaporation within the experimental time-frame can have an effect on the value of coalescence potential predicted, it is insufficient to account for the values obtained by experimental measurement.

There now remains to be considered the ratio ($^pV_c/^mV_c$) obtained at saturation, where the predicted value of V_c at 100%RH is some 79% of that actually measured.

Consider the constant, 0.38 in Equation 7.10. Taylor derived the expression,

$$\frac{d^2y}{dx^2} + \frac{1}{x}\frac{dy}{dx} = \alpha + \frac{\beta}{y^2} \tag{7.13}$$

to describe the equilibrium for the surface, where α and β are the parameters $2a^2/hR_0$ and $V^2\varepsilon_0\alpha^2/2h^3\gamma$ respectively. The boundary conditions for Equation 7.13 are $y = 1$ at $x = 1$, and $dy/dx = 0$ at $x = 0$. When $\beta = 0$ the solution satisfying the boundary conditions is,

$$y = 1 + \tfrac{1}{4}\alpha\left(x^2 - 1\right) \tag{7.14}$$

To calculate the stability limits it is therefore necessary to find the greatest value of β to satisfy the boundary conditions for all values of α in the range $0 < \alpha < 4$. These were computed by Ackerberg (quoted in Taylor [105, Table 1]), and allowing for negligible error in the case of $\alpha = 3.995$ leads to a result of $\sqrt{\beta} = 0.38\ Z_0/h$, the coefficient of $\sqrt{\beta}/Z_0/h$ giving rise to the constant of 0.38 in Equation 7.10. However, an examination of Taylor's derivation of α shows that ascribing a value of 3.98 to α satisfies other criteria almost as exactly, and it may be seen from Taylor's table that this produces a value for $\sqrt{\beta}$ of $0.498\ Z_0/h$, and if we place this new value in Equation 7.10 we arrive at,

$$V = 0.498\frac{Z_0}{R_0}\left[\frac{\gamma R_0}{\varepsilon_0}\right]^{\frac{1}{2}} \tag{7.15}$$

Substitution of the experimental values obtained at 100% RH into Equation 7.15 yield a result of V_c = 80.3 volts, a figure within 3% of the measured value.

7.8. Correction Factor for Humidity.

Regressional analysis of the results of Table 7.5 show that they are very closely described by the equation,

$$^{H}V_c = 2450H^{-3/4} \tag{7.16}$$

where $^{H}V_c$ is the coalescence potential and H is the relative humidity. This suggests that a correction or scaling factor may be quite simply derived. At 100% RH, Equation 7.16 becomes,

$$^{100}V_c = 2450 * 100^{-3/4} = 77.5 \tag{7.17}$$

and a scaling factor for a relative humidity, H, in the range $50\% < H < 100\%$ is therefore of the form, $^{H}V_c / {}^{100}V_c$, i.e.

$$\frac{2450H^{-3/4}}{77.5} = 31.61H^{-3/4} \tag{7.18}$$

Combining this with a corrected Taylor's expression (Equation 7.15), we arrive at,

$$^{H50-100}V_c = 31.48H^{-3/4}\frac{Z_0}{R_0}\left[\frac{\gamma R_0}{\varepsilon_0}\right]^{1/2} \tag{7.19}$$

as a descriptor of the coalescence potentials between two drops for a range of relative humidities between 50 and 100% for the geometry described.

Equation 7.19 is therefore specific to a particular experiment. In seeking to establish the modifying effect that humidity plays on coalescence potentials over small distances generally, it is helpful to reconsider Equations 7.16 and 7.11. The former of these gives

the experimentally derived relationship between coalescence potential and humidity, which we may re-write in general form,

$$^{H}V_c = kH^{-3/4} \qquad (7.20)$$

k being a constant whose numerical value is dependent on the system geometry. Application of this generalized form to the results obtained in experimental Series I (Table 7.2), shows that the same negative three-quarters power relationship will describe them also, with only the value of *k* different. Let us hypothesize for the moment, then, that the critical coalescence potential is proportional to the negative three-quarters power of the relative humidity – for RH values above a certain limit, say 45%. It is now necessary to attempt some consideration of *why* this should be so.

The second of the referred equations, 7.11, is simply Taylor's expression re-written so that the total potential difference between the drops is considered. Perusal of this equation shows it to be dependent on;

1. Linear measurements (Z_0, R_0), assumed fixed.
2. Surface tension, γ.
3. Permittivity (free space), ε_0.

The linear measurements are subject only to accuracy of experimental measurement, although it may be necessary to consider possible evaporative effects at lower humidities (see 7.7.1).

Surface tension is temperature, but not humidity dependent. (Temperature variation is therefore indirectly incorporated in the expression). Whilst it has been demonstrated [82-84] that charge influences surface tension the potentials involved in this investigation are too small for any significant variation to apply.

The incorporation of ε_0 into Equation 7.11 arises from Taylor's analysis of the forces acting on a drop in an axial electric field [105, *page 424*]. The electrical stress acting

normally to the drop surface (using the nomenclature of Figure 7.23) was approximated to $V^2\varepsilon_0 / 2Z^2$, on the condition that h/a was very small.

In the case of medium-sized separations, say Z having a value of several micrometres, this is a valid assumption, as the gap $2Z_0$ is of sufficient size to be treated as homogenous air, and the assumption that $\varepsilon_r = \varepsilon_0 = 8.854 \times 10^{-12}$ F/m is a fair one. As the gap reduces, however, the question of the true permittivity of the interface becomes significant. This assumption, however, assumes an isotropic dielectric – actually a vacuum. The reality of the interface, however, is of a region populated with both non-polar gas molecules – nitrogen, oxygen and to a lesser extent carbon dioxide – together with polar water molecules whose numbers increase with increasing relative humidity. We may imagine a simple representation of this in the form of a dielectric between two polarized parallel plates (Figure 7.24).

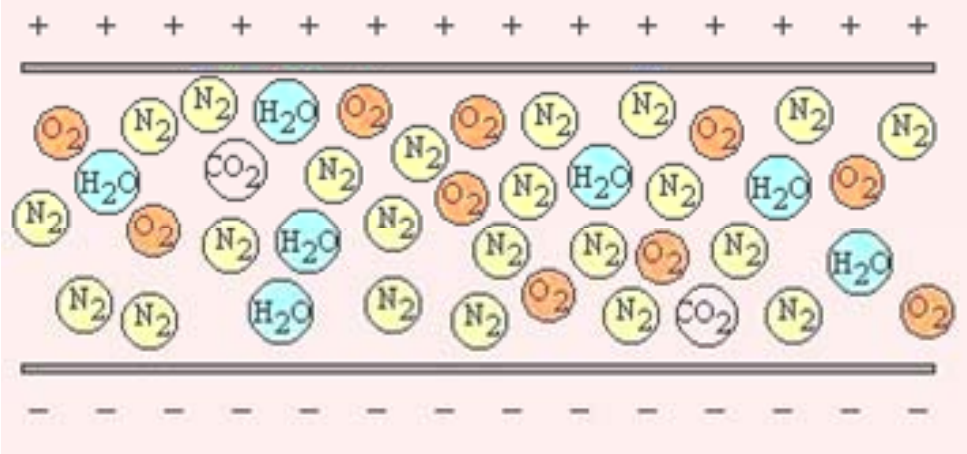

Figure 7.24. Polar and non-polar constituents of humid air as a dielectric.

The behaviour of such a dielectric is complex, and in the presence of a vertical field the arrangement of molecules at any given instant will be the product of both diffusion and electric forces. Current values of ε_r for air of increasing humidity are the result of measurements made either at high radio or optical frequencies. These show only very small variations of relative permittivity with increasing humidity, i.e. 1.00045 at 0% RH, rising to 1.00067 at 100% RH. There is a lack of data concerning the static, or DC, permittivity of moist air, a measurement complicated by drift of polar molecules within

the dielectric. In the case of free air, where normal diffusion processes can assist in the repopulation of the medium as water molecules are deposited, such a measurement should be feasible, and a suggested approach for future work in the area is made in Chapter 9. In particular data for the relative permittivity of small air-gaps containing moist air would assist considerably in the explanation of the trend towards the lowering of critical coalescence potentials with increasing humidity. Examination of Equation 7.10 shows that such an increase in the value of ε_r has the effect of reducing the quantity $(\gamma R_0 / \varepsilon_0)^{½}$, with an ultimate reduction in the value of V_c, which may be expressed as,

$$V_c = k\,(s / \sqrt{\varepsilon_0}), \quad \text{where } k = 0.76 Z_0 / R_0, \text{ and } s = \sqrt{\gamma R_0}. \qquad (7.21)$$

Substitution of a number of hypothetical relative permittivity values, ($\varepsilon_r = 1,2,3,4\ldots$), such that the absolute permittivity, $\varepsilon_0\varepsilon_r$, has values 8.854×10^{-12} $(1,2,3,4\ldots)$ F/m, yields a range of predicted values of V_c when substituted in Equation 7.11. Figure 7.24. shows clearly the predicted reduction in V_c with increasing permittivity, for the experimental geometry used above.

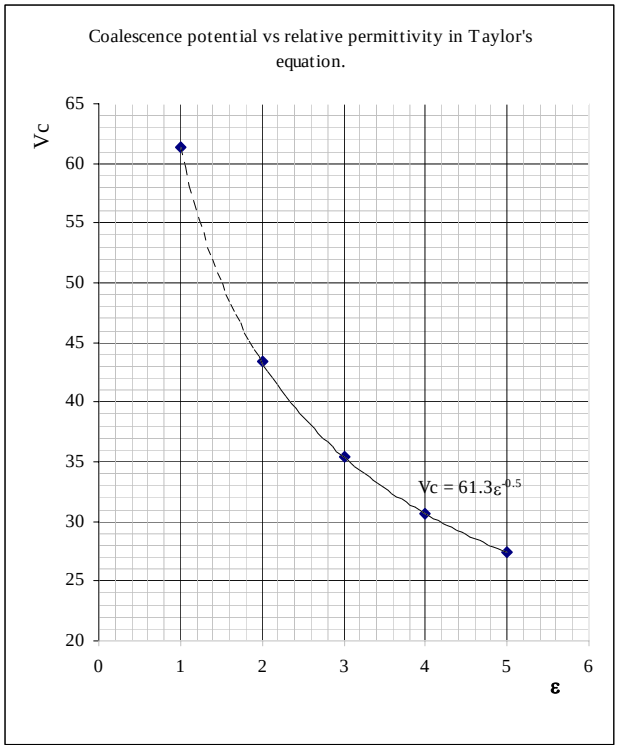

Figure 7.24. Hypothetical permittivity variation vs. critical coalescence potential, V_c, computed for an inter-drop gap of 40µm between 0.5mm radius drops.

Examination of Figure 7.24 indicates that the variation range in V_c found experimentally would be partially explained by an approximately threefold variation in the relative permittivity of vapour-laden air in a small gap for the range of humidities studied.

Assuming that evaporative considerations have been corrected for, V_c is proportional to the negative one-half power of the relative permittivity. It has been demonstrated that V_c is also proportional to the negative three-quarters power of the relative humidity. This suggests, therefore, that the permittivity of a small vapour-laden air gap varies as the three-halves power of the relative humidity. Progress in the development of an appropriate relationship is dependent upon the acquisition of permittivity data for a range of humidities.

7.9. Summary.

This chapter has demonstrated that previous considerations of the potentials necessary to promote instability between closely-spaced liquid surfaces must be reconsidered to include the effects of ambient relative humidity. Apparatus and experimental procedure to measure the critical coalescence potentials between two closely-spaced drops has been described (7.3). It has been demonstrated experimentally that the value of this potential for a given small gap can drop by about a factor of two as relative humidity rises from 40% to 100%, and that whilst variations in the geometry arising from evaporation can be significant, they do not account for the variation in the critical coalescence potential.

It has been shown that a significant weakness in G I Taylor's calculation of the forces acting normally to a drop surface is the assumption that in small interfaces the permittivity is that of either free space or dry air (7.8). Whilst it has been demonstrated that it is relatively straightforward to develop a correction factor to Taylor's expression for specific geometries, a more radical reconsideration is necessary in order to make a general correction.

The anisotropic dielectric nature of humid air has been considered, and the effect of a proportional increase in the number of polar water molecules discussed. It has been pointed out that the available data for the relative permittivity of humid air is the result of measurements made at either high radio frequencies or optically, both of these being situations which would minimize the effects of polar water molecules, and that there is a real need for accurate determinations of the permittivity of the complex interphase conditions to be found in small humid air-gaps.

8 COALESCENCE DYNAMICS AND BOULE SYSTEM MODEL

8.1. Introduction.

All coalescence processes occupy some finite time. Those events which we consider as 'normal' take short periods; photographic and electrical observations have shown them typically to be complete in periods of milliseconds. Water boules may be viewed as a form of delayed coalescence – delayed because external conditions are such that the initiation of the coalescence is for various reasons deferred. Drops forming boules under natural conditions generally demonstrate a delay of between a few hundreds of milliseconds to perhaps a second or two, although it has been demonstrated in Chapter 3 (3.2.4) that the delay in the onset of coalescence may be artificially extended to several minutes by surface vibration of the underlying bulk liquid, due to the replenishment of the entrained air forming the interfacial film.

Boule-formation is also known to depend on low levels of electric fields, with complete failure to form in the presence of fields of greater strength than some 30kV/m (Section 3.2.2).

In this chapter a model by which the electric forces acting on boules may be described will be developed, and experimental results obtained will be evaluated to help to establish the electrical boundary conditions that either allow for the continuance of uncoalesced drops as water boules or lead to their extinction.

Two distinct contributory factors have been identified in the process of boule maintenance and extinction. These are the entrainment of air, to provide the air-cushion support for the drop, and the action of electric charge in promoting instability between the two liquid surfaces. As a precursor to this the question of impact velocity, and hence the kinetic energy of the incident drop, must be considered. Experimental investigations have all pointed to the necessity of minimizing the energy of the drop on impact, to reduce or remove the chance of disruptive splashing.

8.2. Considerations of air entrainment and impact.

A body of previous work has been presented demonstrating the rôle played by air entrainment in the delaying of coalescence (Sections 2.3.2, 3.2.4 and 7.2).

Practical methods of consistent boule-production (3.1) all involve some impact with the bulk liquid surface. It is not feasible to generate boules by dispensing drops directly on the water surface as done, for instance, in the cases of opposing drops of a variety of liquids by Prokhorov [35] and of silicone oils by Dell'Aversana [45]. The plano-convex geometry of a boule system involves the approach of surfaces of different energies, and unless air is entrained as part of a dynamic approach then coalescence will ensue. In the case of a 'boule launcher' technique the drop arrives obliquely at the surface at significant velocity. 'Gentle placement' causes drops to approach the surface normally, but at much lower velocity. In each case, however, sufficient air entrained is to allow the establishment of an interfacial film.

Drops arriving obliquely at a surface initially bounce. The dynamics of this interaction were extensively studied by Jayaratne and Mason [54], together with the necessary charge to inhibit rebounding for a range of velocities and incidence angles. For the velocity range 0.6 to 1.2m/s bouncing of small (0.28 – 0.36mm diameter) drops was inhibited by fields of the order of 10kV/m, although it must be emphasized that range represents a limiting field value for droplet rebound from the surface, and *not* for boule-production. Higher velocities resulted in a reduced charge threshold for coalescence, although the graphs are non-linear, having two points of inflexion. A similar format was found for the curves relating to impact angle for drop streams of different charge. (Figure 8.1)

Under such conditions the geometry of the interfacial air-gap is essentially both dynamic and evolving, and the format significantly different to that below a boule that has slowed almost to rest. It is questionable whether or not the dimpled interface is present at this stage. Direct observation is technically difficult, but visual indications from photography suggests that the moving boule flattens into an oblate sphere and

forms a depression in the bulk water surface whose profile matches that of the boule itself.

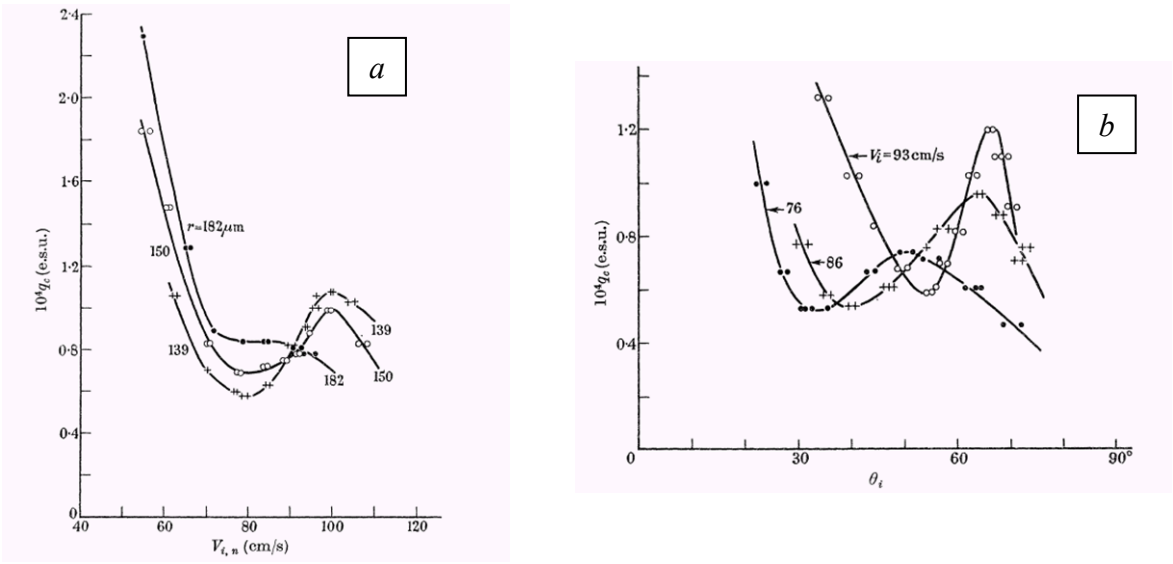

Figure 8.1. Jayaratne and Mason's results for the drop charge necessary to inhibit bouncing compared with *(a),* impact velocity, and *(b),* angle of incidence. *(Jayaratne & Mason [54])*.

It has been implied (Stong, [57] and Section 3.2.4) that under these conditions the air film has a thickness around a micrometre. As the boule slows, interfacial air is squeezed slowly out, but, as shown by Prokhorov (7.2) for ambient air conditions other than saturation, diffusive pumping both assists in maintaining the interface and also in providing excess pressure, thus forming the dimpled region.

In the case of drops arriving at a surface with higher kinetic energy consideration must be given to the question of whether this energy, together with the angle of incidence, is sufficient to cause disruptive splashing, or whether bouncing will occur. The work of Jayaratne and Mason in this connexion has already been largely reviewed previously (3.2.4), and the tendency to bounce over specific ranges of the incidence angle noted. After initial surface bounce it has been shown by several studies, including those of Jayaratne and Mason and the present research, that droplets traverse the surface almost completely horizontally. It has been further demonstrated during the present research that the drops thus traversing the surface attain additional charge in the region of 10^{-12}C. Under these conditions, therefore, the interfacial profile is the result of forces other than purely hydrodynamic ones, and a consideration of these forms the main part of this chapter. Section 5.4 has examined some of the possible charging methods, and a charge-

separation mechanism arising from the interchange of material in the highly active interfacial region has been postulated, temporarily referred to as 'trans-phase' charging.

Drops contacting the surface more gently, as, for example those from the 'gentle placement' sources used, are relatively free from the effects of disruptive splashing. In the case of drops approaching the surface normally with low velocity (0.28m/s for drops falling through a height of 8mm), the kinetic energy transferred to the surface at impact is low (4.3×10^{-6}J for drops of the size studied). Air entrainment is sufficient to allow for the establishment of an initial interfacial film, and for damped oscillation of the liquid systems without coalescence, the interface developing into a dimpled geometry as diffusion forces and the partial pressures of the liquid surfaces build up.

It is appropriate at this point to gather together the principal experimental findings relating to drops and water boules thus far, together with relevant data from other sources. This summary is given in Table 8.1.

No.	Observation/Data	Reference
1	Boules will not form in electric fields greater than about 33kV/m.	Chapter 3 3.2.2.
2	Boules will not form in conditions of high humidity.	Chapter 3 3.2.5.
3	Drops from a grounded source carry a charge in the region of 10^{-14}C, developed during their formation. Smaller drops carry proportionally greater charge.	Chapter 5 5.2.1.
4	Boules gain charge by traversing a surface. The mechanism is unclear, but may be connected with matter interchange between the two liquid surfaces across the intervening gas boundary. They have been shown to gain charge some two orders of magnitude greater than that possessed by the initial drop.	Chapter 5 5.1.
5	Coalescence is shown to be accompanied by two electrical events. The first of these is small and fast, typically involving the transfer of some 10^{-12}C in ~1ms, followed by a larger and longer event extending over tens of milliseconds, in which potentials of tens of millivolts are reached. This may be explained as arising from the collapse of the double layer.	Chapter 6 6.2.2.
6	The critical coalescence potential between drops is shown to vary with humidity. Higher humidities result in lower coalescence potentials. This variation might be explained by a rise in the relative permittivity of vapour-laden air in small gaps, leading to proportionally lower instability potentials. The field-gradients for coalescence are shown to range from ~ 1945kV/m at 100%RH to > 3500 kV/m at 41%RH or lower.	Chapter 7 7.5.3.

Table 8.1. Summary table of principal observations and data on boules and drops.

8.3 A capacitive model of the boule system.

This section develops the capacitive model of the boule system introduced earlier (5.5), and is divided into a sequence of arguments. These may be summarized thus;

i) Initial consideration of a simplistic model (8.3.1).
ii) Development of this initial model to consider the interfacial profile (8.3.2).
iii) Investigation of a parallel-plate determination of the interface (8.3.4).
iv) Development of the capacitive system by sectioning the interface into a number of concentric ring capacitors, connected in parallel (8.3.5).
v) The application of calculated potential and interfacial field-strength data to this model (8.3.6).
vi) Consideration of instability potentials at an air/water interface from previous work (8.4).
vii) A consideration of instability potentials produced by various charge magnitudes (8.5).
viii) Interpretation and conclusions (8.6).

8.3.1 Preliminary consideration.

In Chapter 5, Section 5.5, reference was made to the capacity extant between a floating boule and the underlying bulk surface. This will now be examined more closely in an attempt to build a model descriptive of the electrical boundary conditions pertaining to such a system. As a first approximation a simplistic geometry taking no account of the interfacial profile is illustrated in Figure 8.2.

Provided that the separation distance, δ, is small in relation to the radius, then a good approximation to the capacity of the system may be had by treating it as a parallel-plate capacitor. If we assume that the 'contact' area is approximately one-third of the surface area of the sphere, then the effective area becomes $4/3\pi r^2$.

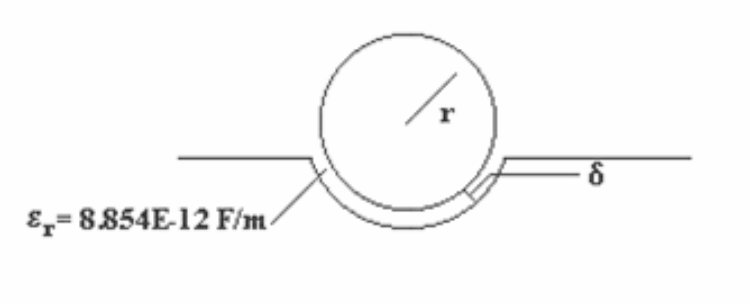

Figure 8.2. Simplest capacitor model of system.

Taking the sphere radius as 2.35mm, equivalent to the boules experimented on in Section 5.1, and the permittivity of air as 8.854 x 10^{-12}F/m, a separation of 1µm gives a capacity (ignoring any fringing effects) of;

$$C = \frac{8.854 \text{ x } 10^{-12}\left[4/3\pi(0.00235)^2\right]}{10^{-6}} = 205\text{pF} \qquad (8.1)$$

This capacitance is substantially large, and the model is manifestly an inadequate representation of the real state of affairs, and must be refined in order to develop a more realistic description of the actual situation.

8.3.2 Development of model considering interfacial profile.

Figure 6.13 described the approximate interfacial profile as used by Frankel and Mysels [88] in their derivation of time-dependent expressions for the maximum (central) dimple thickness, *T*, and the air-film thickness at the boundary rim, Z_0. For convenience an enlarged radial profile of this area is given in Figure 8.3.

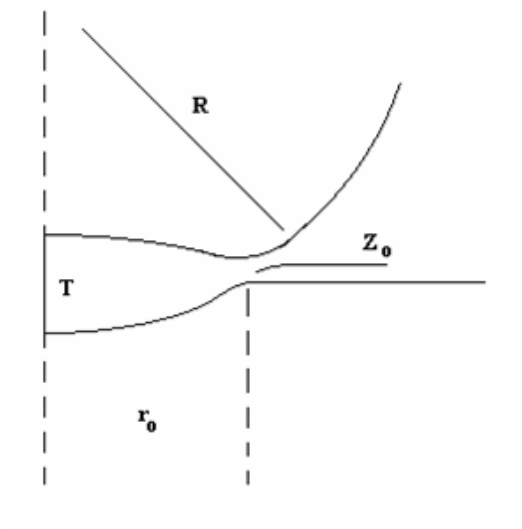

Figure 8.3. Boule system – interfacial geometry.

Here, R is the mean drop radius, r_0 the radius of the boundary ring or rim, and T and Z_0 as defined above. The relevant equations for the calculation of time-dependent values of r_0, T, and Z_0 are:

$$r_0 = R^2(2\rho g/3\gamma)^{1/2} \tag{8.2}$$

$$T = (0.0096 r_0^6 \eta n^2 / \gamma R t)^{1/4} \tag{6.1}$$

$$Z_0 = 3.05 R T^2 / r_0^2 \tag{6.2}$$

where ρ is the effective density difference, g gravitational acceleration, γ the interfacial tension, η the viscosity and n the number of deformable surfaces. For the drop size under consideration the values are taken;

$$\begin{aligned} R &= 0.00235\text{m} \\ \rho &= 988\text{kg/m}^3 \\ \gamma &= 0.073\text{N/m} \\ g &= 9.8\text{m/s} \\ \eta &= 0.001\text{N/s/m}^{-2} \\ n &= 2 \end{aligned}$$

Substitution of these values into Equation (8.2) gives a value of r_0 of 5.22×10^{-4}m.

From Equations (6.1) and (6.2) a series of values for T and Z_0 respectively was calculated for time periods up to t = 10 seconds, the first few calculations giving values over short intervals. These were plotted on a common time-axis, and are displayed in Figure 8.4.

It may be seen from these graphs that the most rapid changes in the values of both T and Z_0 take place in the earlier stages of the system, showing that the change in capacity throughout the system lifetime is non-linear.

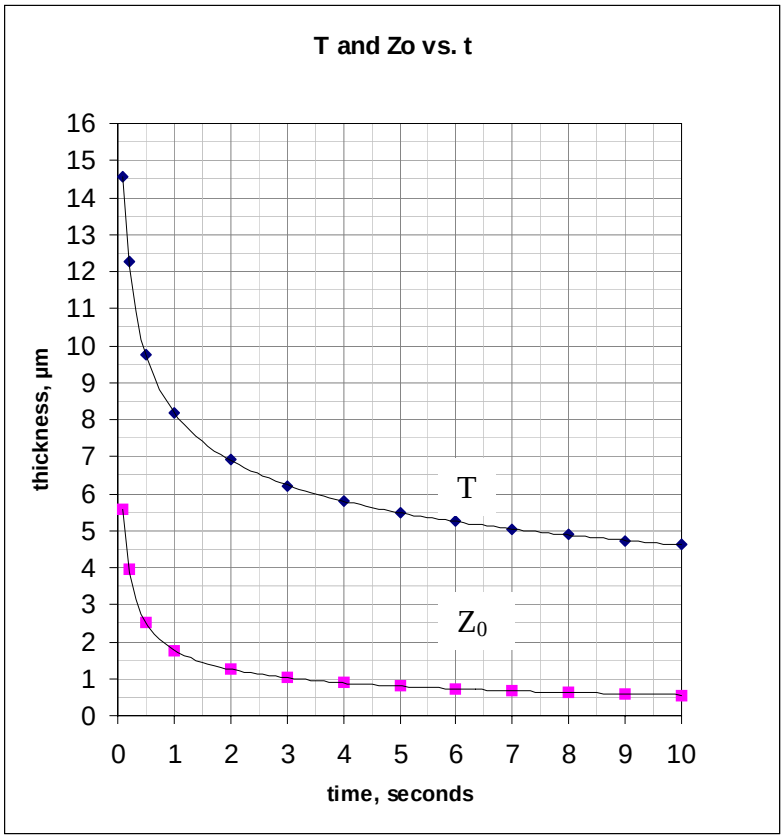

Figure 8.4. Changes in T (dimple thickness) and Zo (rim film thickness) with respect to time.

8.3.3. Capacitance modelling.

The capacity, C, of a parallel-plate system is given by;

$$C = \varepsilon_0 \varepsilon_r A/d \tag{8.3}$$

where ε_0 is the permittivity of free space, ε_r the relative permittivity of the dielectric medium, A the effective plate area and d the plate separation. In the present case the complex profile of the interface adds difficulty to the determination of both A and d.

To arrive at satisfactory values for both A and d, involves a knowledge of the equations governing the profiles of both opposing surfaces. Direct calculation from the profiles at different time intervals is an exceptionally complex task. It has been shown by Yiantsios and Davis [91] that there is a large series of inter-related equations describing

the gap profile at different times, and the practical difficulty of implementing a calculation of the time-related effective areas and separations based upon these is prodigious. There are therefore two possible recourses to obtaining realistic data for the two variables under consideration; *i)*, the calculation of mean values, equivalent to parallel plates, and *ii)*, attempting a more refined model by considering the system as a number of concentric annular ring capacitors at different separations. Both of these approaches have been used in the present investigation.

8.3.4. Parallel plate model results.

For this first evaluation an equivalent capacitor was considered in the form of opposed circular discs, of radius r_0. (Figure 8.5). This made the following assumptions:

- The interfacial surfaces were symmetric,
- No fringing effects applied,
- The effective plate-spacing is T/2.

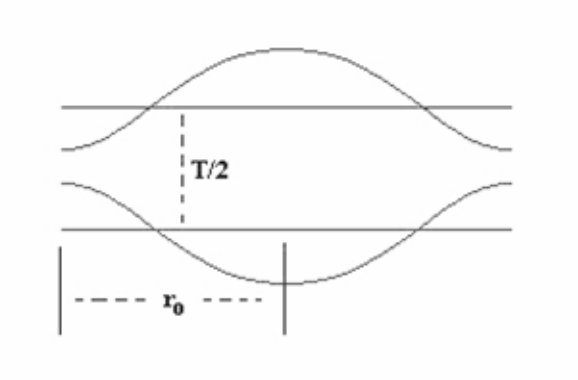

Figure 8.5. Initial parallel-plate model.

Results for this model for time values, *t*, from 0.1 to 10 seconds are shown. (Table 8.2).

t, sec	0.1	0.2	0.5	1	2	3	4	5	6	7	8	9	10
C (pF)	1.07	1.27	1.59	1.90	2.26	2.50	2.68	2.78	2.97	3.08	3.19	3.29	3.37

Table 8.2. Capacity variation with time, parallel-plate model.

Although useful as a guideline to the expected capacity variation, this initial model has serious shortcomings. First, curvature is not uniform from centre to edge, but possesses a complex geometry. Second, this model assumes that the capacitive effect ‘stops’ at a

distance r_0 from the centre, whilst in fact the opposed interfaces have their greatest capacity in that region, being at their closest, and the edge-effect due to this must form a significant part of the total capacity.

8.3.5. Model based on capacitive sectioning.

Failing the data necessary to define the surfaces accurately, a second model was developed which treated the total surface as made up from a number of annular concentric rings, each pair having a specific separation. As such a system is effectively a number of such capacitors in parallel, the total capacitance is simply the sum of the individual components.

Using the calculated data for r_0, T and Z_0 a series of curves was therefore produced to give the closest replication of the interfacial surfaces possible without precise determination by calculation. Sections of the upper and lower surfaces were taken, starting with a central disc 0.05mm in radius, and working outwards from the central vertical axis to produce successive annuli with 0.05mm radial increments. For each pair, the mean value of Z_0 was obtained from scale measurements, and the equivalent capacity obtained.

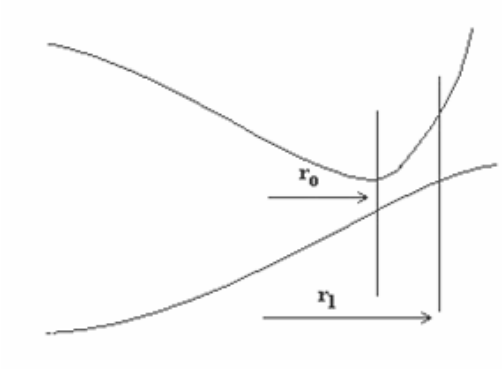

Figure 8.6. Illustrating fringing area.

The problem of the extremity capacitance at distance r_0 was addressed by taking radius r_1 as the limiting radius instead, where $r_1 = r_0 + 0.05$mm, this extra distance being

reckoned to represent the limit of where the upper surface's proximity to the lower one added significant capacitance[1].

Figure 8.7 shows a diagrammatic representation of the dissection of the opposed faces into capacitive annuli.

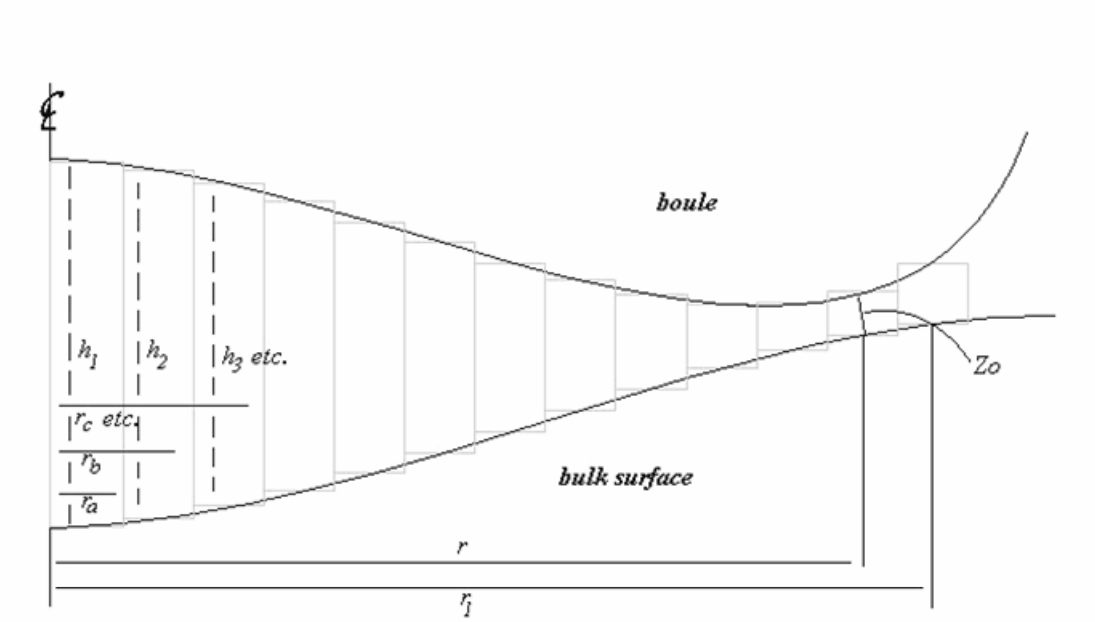

Figure 8.7. Radial section of boule system divided into approximately equivalent annular sections for capacitance measurement.

Consider the section of radius r_a nearest the central vertical axis of the system, the interfacial spacing being, h_1, say. The area/separation ratio is therefore $\pi . r_a^2/h_1$. For the next section, of radius r_b and separation h_2, the ratio becomes $\pi . (r_b^2 - r_a^2)/h_2$, etc. The total capacity is therefore,

$$C_{total} = \varepsilon_0 . \varepsilon_r . \pi \left[\sum \frac{r_a^2}{h_1} + \frac{(r_b^2 - r_a^2)}{h_2} + \frac{(r_c^2 - r_b^2)}{h_3} \text{ etc.} \right] \qquad (8.4)$$

[1] It was noted that at the greatest value of t analyzed, i.e. when Z_0 had its least value, this additional sector added approximately 10% to the total calculated capacitance. Extending beyond r_1, however, added little further significant capacity.

Analysis in this way was made for a total of 4 time measurements, at t = 0.1, 0.5, 4.0 and 10 seconds, and the resulting graph is shown in Figure 8.7.

Regresional analysis of the data obtained shows the variation of capacitance with time very closely follows the equation,

$$C = 2.3265t^{3/8} \tag{8.5}$$

This graph was then used to obtain the capacitance values for other time values by interpolation (Table 8.3).

t, sec	0.1	0.2	0.5	1	2	3	4	5	6	7	8	9	10
C (pF)	0.95	1.2	1.79	2.4	2.97	3.46	3.84	4.2	4.5	4.75	5.0	5.22	5.4

Table 8.3. System capacitance for time, t, = 0.1sec to t = 10sec, by interpolation from Fig.8.7.

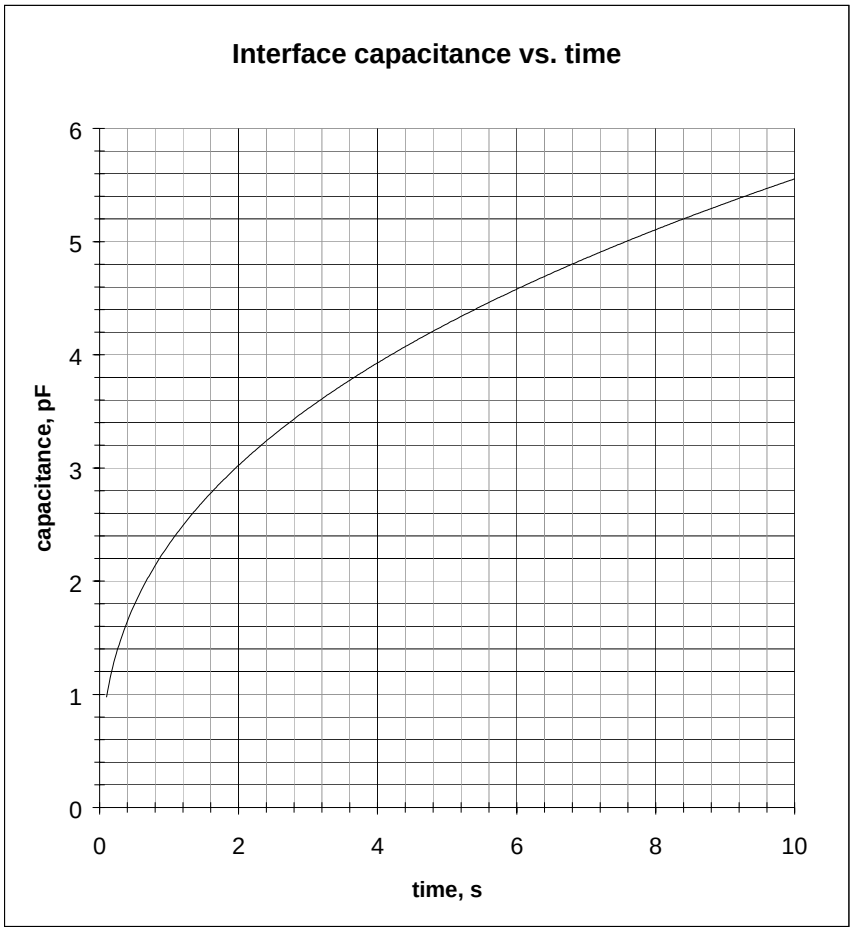

Figure 8.7. Interfacial capacitance, C, against time, t.

8.3.6. Potential and interfacial field-strength data.

As the magnitude of the charge on the drop is known, knowledge of the probable capacitance of the system at a given time makes it possible to determine the likely potential difference appearing across the interface. Table 8.4 shows the calculated time-dependent interfacial PDs, V_1 and V_2 arising from 4.7mm diameter drops carrying charges of *i)* 3 x 10^{-14}C and, *ii)* 1.6 x 10^{-12}C. These charges are equivalent to those found, *i)* on drops of this size produced from a grounded source, *ii)* on boules that have traversed a water surface, left it, and been collected.

***t*, sec**	**0.1**	**0.2**	**0.5**	**1**	**2**	**3**	**4**	**5**	**7**	**6**	**8**	**9**	**10**
V_1, **V**	0.0320	0.0260	0.0170	0.0130	0.0100	0.0087	0.0078	0.0071	0.0063	0.0066	0.0060	0.0057	0.0056
V_2, **V**	1.68	1.33	0.89	0.66	0.54	0.46	0.42	0.38	0.34	0.36	0.32	0.31	0.30

Table 8.4. Potential differences arising from, *i)* a drop charge of 3 x 10^{-14}C (V1), and, *ii)* a drop charge of 1.6 x 10^{-12}C (V2) at different times, *t*.

Interpretation of the field-strengths produced by these potential differences is complex in view of the interfacial geometry. Greatest curvature is to be found in the immediate vicinity of the boundary rim, where the surfaces are also closest. If, therefore, the field-strength is taken in those regions as V/Z_0, then the greatest interfacial fields V_1/Z_0, V_2/Z_0 with respect to time are (Table 8.5);

***t*, sec**	**0.1**	**0.2**	**0.5**	**1**	**2**	**3**	**4**	**5**	**6**	**7**	**8**	**9**	**10**
V_1/Z_0 **kV/m**	5.75	6.56	6.8	7.3	8.0	8.51	8.81	8.96	9.14	9.40	9.58	9.66	10.0
V_2/Z_0 **kV/m**	301	336	356	373	432	450	475	480	499	507	511	526	536

Table 8.5. Field strength in kV/m at closest interfacial region for, *i)* a drop charge of 1.6 x 10^{-12}C (V_1/Z_0), and, *ii)* a drop charge of 3 x 10^{-14}C (V_2/Z_0) at different times, *t*.

To understand the effect of these fields it is necessary to consider the onset of instability for water drops and surfaces in an electric field.

8.4. Instability at air/water interfaces.

Early accounts of instability at water/air interfaces are recalled in the opening pages of Chapter 2 of this thesis, where the observations of Gilbert [1], Gray [5] and Tyndall [3]

were recounted. The first systematic study of instability was that of Rayleigh [121], who investigated the instability conditions for a charged drop.

A drop tends to have a spherical shape because of the surface tension of the liquid (γ). If the drop is electrically charged, the electrostatic repulsion between ions, if sufficiently great, can overcome the surface tension, leading to the drop's breakup into smaller droplets. An upper value for the charge, q_R, in a drop of radius r is given by the Rayleigh limit:

$$q_R = [64\pi^2 \varepsilon_0 r^3 \gamma]^{1/2} \tag{8.6}$$

Rayleigh's work was extended by that of Zeleny [122] who considered the potential rather than the charge for instability. Cases of both oblate elliptical and spherical drops were investigated leading to relationships for instability potential, V, in the first case of,

$$V = 2\sqrt{\pi a\gamma \frac{\sqrt{1-e^2}\log^3\frac{1+e}{1-e}}{\left(1+e^2\right)\log\frac{1+e}{1-e}-2e}} \tag{8.7}$$

a being the transverse minor radius and γ the surface tension, and in the second (spherical) case of,

$$V = \sqrt{12\pi a\gamma} \tag{8.8}$$

a being the drop radius.

Considerable advances in the understanding of liquid surface instability in an electric field were made by Taylor. In a series of papers [105 and 123-125] over a five year period during the 1960s he examined many aspects of the problem, much of the work involving instability leading to electrohydrodynamic atomization from the surface asperities thus formed, now known as Taylor cones.

Taylor's work on the instability arising between two drops at different potentials [105] has already been extensively referred to in Chapter 7 in the course of considering humidity effects. Attention is now turned to instabilities arising on a horizontal liquid plane in the presence of an electric field. Taylor, 1964 [124] considered the situation in which a vertical field was established to a water surface, with either air or oil above it. (Oil was employed in many of the investigations partly to reduce the chance of sparkover, and partly to damp violent surface motions at the onset of instability). Figure 8.8 shows the experimental arrangement.

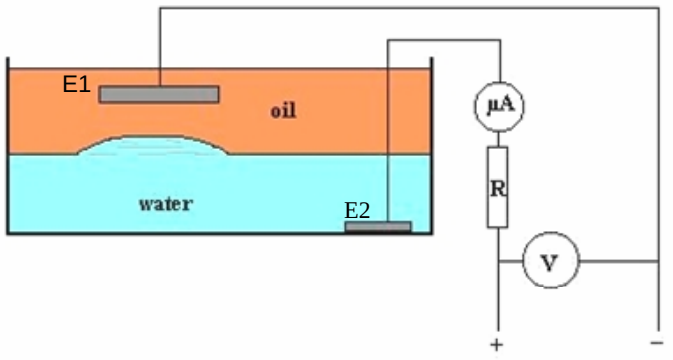

Figure 8.8. Arrangements for measuring instability of a liquid surface *(after Taylor [124])*

A small circular metal electrode, *E1*, was suspended a known height, h_0, above the water/oil interface, with a second electrode, *E2*, submerged in the water. The potential, measured by voltmeter *V*, was increased until interfacial disturbance and instability was observed. Surface corruscations appeared as illustrated in Figure 8.9.

In the case of a water/air interface, without the damping effect of the oil, the aspereties were far more turbulent but of the same general form, resulting in ligaments of water rising to the electrode and forming short-lived direct contact. This contact time was measured with an oscilloscope and found to represent an extremely small fraction of the time between successive emission events.

Taylor calculated the limiting field gradient, V/h_0, for instability for a water/air interface to be,

$$V/h_0 = 0.3\{g\gamma(\rho_1 - \rho_2)\}^{1/4} \ (8\pi/\varepsilon_r)^{1/2} \qquad (8.9)$$

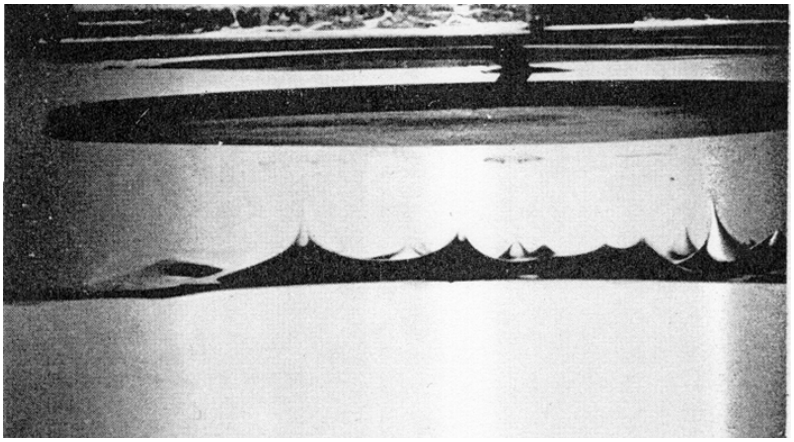

Figure 8.9. Surface instability at a water/oil interface. V = 17.7kV, h_0 = 2.62cm.
(From Taylor [124])

where (ρ_1 - ρ_2) is the interfacial density difference, γ the surface tension and ε_r the relative permittivity of the medium.

For a water/air interface this gives a limiting gradient, V/h_0, of

$$V/h_0 = 2610\text{kV/m.}, \tag{8.10}$$

This result means that under most circumstances the onset of surface instability will be before the sparking potential in air, but this limiting gradient is presented as being true only for values of $h_0 > 1$cm and its applicability in the case of small gaps is questionable in view of the mixed dielectric nature of the interface.

The question of interfacial instability in different liquid/liquid systems has been very recently investigated by Eow and Ghadiri [126], and by Eow, Ghadiri and Sharif [127]. Both of these investigations, like Taylor's, have considered primarily water/oil and water/organic systems, and have led to suggested field strengths of 350 – 380kV/m for instability of small (1.2mm diameter) water drops in contact with such second liquids. For curved surfaces the expression derived by Taylor in 1968 [105], and already considered in terms of humidity influence, offers a route to the calculation of the onset of instability. It will be recalled that this derived from an axis-symmetric consideration of two opposed drops of equal radius, with a small intervening air-gap. In this case the

point of closest approach of the drops was considered as being small in relation to the drop radius and the fixed boundaries of the field, allowing approximations to be made that led to the derivation of a critical potential as shown in Equation 7.10. In the case of opposed drops with a potential difference between them the field intensity will be greater than that between a drop and a plane surface.

Experimental work undertaken during the course of this research has suggested that the figure for the critical potential from this expression may be lower than that encountered experimentally, and also that that the relative humidity of the surrounding air exercises a significant influence in determining the field strength for the onset of instability. Experimental figures obtained (Chapter 7, Table 7.5) show, for a particular geometry, field-strengths ranging from 3640kV/m at 41%RH to 1945kV/m at 100%RH. Larger diameter drops require a proportionally lower field gradient for the onset of instability. If this finding is correct, then the instability potential for a plane water surface will be correspondingly smaller. In the case of spherical drops the electrical force normal to the surface is opposed by the surface tension force, $2\gamma/r$. In the case of a plane surface, however, $r = \infty$, and there is no normally acting surface force other than a gravitational one opposing the electrical force.

In considering a boule suspended over a surface a complex geometry is involved, the two components being neither in straightforward plano-convex nor convex-convex opposition to one another. Whilst direct application of the work of Taylor to this situation is therefore not possible, it yields useful guidelines to the magnitudes of the potentials necessary to produce instability on both water surfaces.

A figure of ≤ 2500kV/m is therefore hypothesized as being that which will promote instability in a small interface of the type found in a boule system.

8.5. Application of derived data to the model.

Calculations were performed to determine the effective range of V/Z_0 values produced when drops carrying specific charges became part of a boule system. From these V/Z_0

values the limiting charge values for falling drops to establish interfacial fields of different magnitudes over a period up to ten seconds were established, these determining, within the constraints of the system geometry, the likely longevity of the boule.

It has been argued that some uncertainty attends the actual value of the limiting interfacial field to produce instability and coalescence. Results are therefore given for a range of instability values between 1500kV/m and 3500kV/m (Table 8.6). These are expressed in terms of the maximum duration time that a boule might have after forming from a drop carrying a specific charge.

Instability limit 1500 kV/m		**Instability limit 2000 kV/m**		**Instability limit 2500 kV/m**	
Drop charge	Max duration	Drop charge	Max duration	Drop charge	Max duration
x E-12C	sec.	x E-12C	sec.	x E-12C	sec.
8	0.1	10	0.1	12	0.1
7	0.2	8	1	10	1
6	1	7	3	8	6
5	5	6	10	7	>10
	Instability limit 3000 kV/m		**Instability limit 3500 kV/m**		
	Drop charge	Max duration	Drop charge	Max duration	
	x E-12C	sec.	x E-12C	sec.	
	15	0.1	20	<0.1	
	12	1	15	0.5	
	10	3	12	3	
	8	>10	10	>10	

Table 8.6. Duration times for boules forming in a range of external fields, shown for limiting instability field-strengths between 1500kV/m and 3500kV/m.

8.6. Interpretation and Conclusions.

The full calculated data are presented in Appendix 5, and from these it may be seen that the model suggests that for boules forming, however briefly, and carrying a charge greater than that inherent to drop-formation, the limiting drop charge for a boule duration of 0.1 second is of the order of 1.2×10^{-11}C. This assumes that the field for instability of the boule system is 2500kV/m. Instability limits below this figure depress

the value of maximum charge for boule formation, whilst values above 2500kV/m for the instability limit result in a higher level of limiting drop charge to prevent brief boule formation. More detailed effects of variation of the interfacial instability potential may be found from perusal of the full data in Appendix 5. These figures are subject to an important caveat, as the model has assumed the interfacial field to be uniform. Inspection of the geometry, however, shows that a measure of field-enhancement will occur in the region of the interfacial rim, i.e. in the area most likely to see the onset of interfacial instability. Quantitative computation of the degree of such enhancement requires a knowledge of the precise geometry of the interfacial surfaces, but it is reasonable to assume that as a result of charge redistribution on the interfacial surfaces the actual limiting drop-charge will be lower than that initially calculated.

In considering the conditions for boule formation and maintenance, then, two primary inter-related parameters are involved. These are;

i) The interfacial field limit for instability,

ii) The capacity of the boule system at any time.

i) Evidence from practical investigations (7.3.2) shows that small opposed convex surfaces have an instability limit of 1945kV/m to 3500kV/m as relative humidity falls from 100% to 41%. Taylor and McEwan [124], presented evidence that in the case of a vertical field interacting with a plane horizontal water surface the limit for instability is some 2600kV/m, but there is no available extension of this to consider the possible – indeed probable – effect of gap reduction to micrometre distances. The possible influence of humidity variation on the relative permittivity of small gaps filled with moist air cannot be ruled out. The data shown in Table 8.5 present options for a range of instability limits within the global compass of their probable range.

ii) The calculation of the boule system capacity for times up to 10 seconds has been made on the basis of the most likely interfacial geometry, failing a precise description of the surface profiles. The permittivity of the air-film has by default been taken as ε_0, the permittivity of free space. If the relative permittivity were

to be greater than that figure then the interfacial potential for a given charge would lessen. In order to reach sufficient potential for instability the gap, Z_0, would have to decrease. This would represent a longer duration time for the system before coalescence was promoted. It has already been demonstrated (7.5) that variation in environmental ambient humidity exercises a significant influence over the potential difference (and hence, effectively, the local field strength) for coalescence between closely-spaced drops. Furthermore, it has been argued (7.8) that the most realistic explanation of this effect is the modifying influence of humidity on the relative permittivity of small interfacial air-gaps, and the capacitance value of the system at a given time is therefore related to the relative humidity.

At first sight a raising of the capacity of the system as a result of increased relative permittivity might reasonably be seen as lowering the interfacial potential in a capacitive system produced from a given charge. In this context, however, it should be borne in mind that it has been demonstrated (Table 7.5) that the instability potential is also proportionally lowered.

Taking, therefore, an instability limit of *circa* 2500kV/m, and the relative permittivity of the interface as ε_0, the capacitive model developed shows that boules fail to form at all if the drop has an initial charge of $>1.2 \times 10^{-11}$C.

It should be considered, however, that were the interfacial capacitance to be increased either as a result of an increase in interfacial relative permittivity or of a modified geometry, then the interfacial potential arising from a given charge would decrease, lowering the tendency to interfacial instability.

The capacitive model, therefore, offers a realistic way forward to understanding the rôle of charge in determining whether or not boules will form, and if they do, then their maximum duration.

9 RESEARCH SUMMARY AND RECOMMENDATIONS FOR FURTHER STUDY.

9.1. General summary of the research.

This thesis has considered aspects of the conditions under which water boules may form, and those electrical influences which cause their coalescence. Whilst there is a body of literature relevant to aspects of these processes there is much that is qualitative or anecdotal. It has therefore been necessary to mount a number of practical investigations to determine more rigorously the conditions under which boule formation is or is not possible.

Initial work reported by Stong [57] has been extended to establish more accurately the limiting external field strength below which boules may be formed, and in the case of dynamic boules this figure has been experimentally set at approximately 33kV/m., irrespective of field polarity.

It has been demonstrated that boules traversing a plane water surface and falling from the further side carry a significantly larger charge than that found on the drops from which they are formed. The charging mechanism in this case is unclear. Stroboscopic investigation shows the drop stream to bounce on initial impact with the water surface, and the additional charge cannot therefore be due to drop disruption. Frictional contact with the air and small-particulate matter exchange within the dynamic interfacial region may contribute to a possible mechanism, which has been tentatively referred to as trans-phase charging. A practical and theoretical enquiry into such a possible mechanism needs to be the subject of further detailed investigation.

High humidity has been experimentally and theoretically connected with a failure to produce boules, being observed or discussed by Tomlinson [15], Mahajan [32], and Prokhorov [35]. It has been shown that the potential difference necessary to promote the coalescence of water drops, investigated by Latham and Roxburgh [115] and by Taylor

[123], is reduced with increasing humidity. This has been reported by Ahern and Balachandran [128], who have produced a correction factor to Taylor's expression for the coalescence potential for a specific geometry.

Prokhorov [35] had demonstrated that in the absence of saturation of the surrounding air the interfacial volume is maintained by diffusive ingress of air, this being in excess of the drainage until the air-film thickness at the interfacial rim had risen sufficiently to allow equilibration.

Electrical events accompanying conventional coalescence of drops with a bulk surface have been investigated from a new viewpoint, namely that of potential events rather than charge transfer ones. This approach has allowed a time-dependent investigation of the process rather than returning an overall integral result. These investigations were accompanied by a high-speed visual record, and have resulted in finding a short-lived initial charge-transfer event previously unrecorded. Correlation with the video record has shown this event to be accompanied by an apparent surface instability on the plane surface. Relatively poor resolution of the video record has made accurate interpretation of this event difficult, but its electrical record together with the fact that, between this preliminary occurrence and the coalescence of the bulk of the drop there is a charge sign reversal, render further investigation necessary.

Investigations have been undertaken to consider the influence that humidity might have on the potential difference between two drops necessary to promote their coalescence. The findings from this research show that the instability potential decreases with increasing humidity, and the theoretical work of G I Taylor [105, 123-125], which leaves humidity issues unaddressed, has been shown to require some correction. At present this extends to a correction factor applicable to a specific geometry, but it is demonstrated that a more general correction might be obtained from a re-evaluation of the DC permittivity of vapour-laden air. Measurements at radio and optical frequencies have hitherto shown only a very small change in permittivity with humidity, but a consideration of the mixed dielectric nature of moist air has shown that this situation may well be different at very low frequencies or under DC conditions. This topic is developed later in this chapter in the section of recommendations for further study.

The dimpled interfacial profile of the interstitial air-film between a drop and a bulk surface had been established by several authors [88, 90, 91]. In particular, the work of Frankel and Mysels [88], which allows for the computation of the central maximum and peripheral minimum values of the film thickness at a time, *t*, has been used to build up a realistic profile of the interface for a number of specific times between 0.1 and 10 seconds. From these a time-dependent capacitive model of the interface has been constructed. This has allowed calculation of the variation in potentials appearing across the capacitive interface and their comparison with the thinning of the extreme regions of the dielectric. By considering the potential at a given time and comparing it with that considered necessary for instability, calculations of the likely duration of boules formed from drops with a range of initial charges have become possible. This model demonstrates that the lowering of potential in the system resulting from capacity rise is always overtaken by the rate of thinning of the peripheral rim of the interface. This finding goes far to explain the observation that boules will not form under conditions of high humidity. It was shown by Prokhorov that high humidity led to a thinning and collapse of the interface, and the peripheral rim is always thinner than the central dimpled area. As humidity increases, therefore, the rim region collapses to a point where its instability potential is sufficiently low for the capacitive charge to promote coalescence. The tendency to boule formation is therefore suppressed as humidity increases, despite the evidence that a humidity increase also lowers the instability potential. It has been shown experimentally that this model conforms reasonably well with the chance of formation and duration time of boules from drops that have been subject to electric fields, or which carry electric charge for other reasons.

The observation of surface asperities on the plane (bulk) surface of a boule system, together with the evidence of concurrent electrical activity is of significance. Whilst imaging limitations have hitherto caused difficulty in determining the precise region of such instability within the interface, there is good circumstantial evidence that this correlates with the breakdown of the interfacial rim, and that the system is behaving in the manner predicted by the capacitive model.

As with the determination of humidity effects on coalescence potential, so this capacitive model is intrinsically dependent on the relative permittivity of the interfacial

gap. Were this figure to increase above unity the effect would be both to raise the overall instability potential and to lower the interfacial potential resulting from any specific charge. Both of these factors would raise the value of the external field necessary for boule suppression.

9.1.1. Thesis summary chart.

Topic	Principal findings	Chapter references
Inherent drop charge	Drops are shown to carry an inherent charge, resulting from their formation. This may be due to double-layer disruption during formation, disruption at an orifice, contact or induction charging.	4.3. 4.3.1. 4.3.2. 5.2, 5.3.
Dynamic boule charging.	Boules are shown to gather additional charge on traversing a water surface. The mechanism is as yet unclear, but 'charge amplification' of some two orders of magnitude occurs.	5.1. 5.4.
Humidity and boule formation.	Evidence from past work [15, 32, 35] has been quantified.	3.2.5.
Effect of humidity on the instability potential (critical coalescence potential).	Critical potential for instability and subsequent coalescence is shown to vary with ambient humidity – a rise in RH lowering the instability potential. Evaporation is shown to have only a modest influence at RH values > 50%.	7.5.1 - 7.5.3. 7.7.1.
Capacity of boule system.	A boule system demonstrated to act as a capacitor. Interfacial profile is demonstrated to lead to a variable capacitor whose drop in breakdown potential with time is greater than its capacitance rise, leading to eventual onset of instability for a given initial drop charge.	5.5. 8.3.5. 8.3.6. 8.5.
Interfacial permittivity.	It is shown that values of relative permittivity for the interface >1 would help to explain the variations of coalescence potential with humidity, also the failure of boules to form in humid conditions.	7.8. 8.6.
Electrical events at and during coalescence.	The coalescence process is demonstrated to have two distinct electrical events associated with it. The initial event occurs at the onset of instability and is accompanied by a charge transfer approximately equal to that attributable to double layer disruption. This is followed by a longer event, with sign reversal.	6.2.1. 6.2.2.
Formation of surface asperities at coalescence.	Video evidence strongly suggests that surface asperities form immediately prior to coalescence. In the case of plano/convex surfaces the asperity is on the plane surface. This is in good agreement with instability at the interfacial rim suggested by the capacitive model.	6.2.2. 6.4. 8.6. 9.1

Table 9.1. Summary table of the more important findings of the research, relating to the electrohydrodynamics of boule formation and coalescence.

The major findings of the research relating to the formation and coalescence of water boules are summarized in Table 9.1, and this part of the thesis concludes with a graphical representation of the interactions of the various contributory factors under consideration (Figure 9.1).

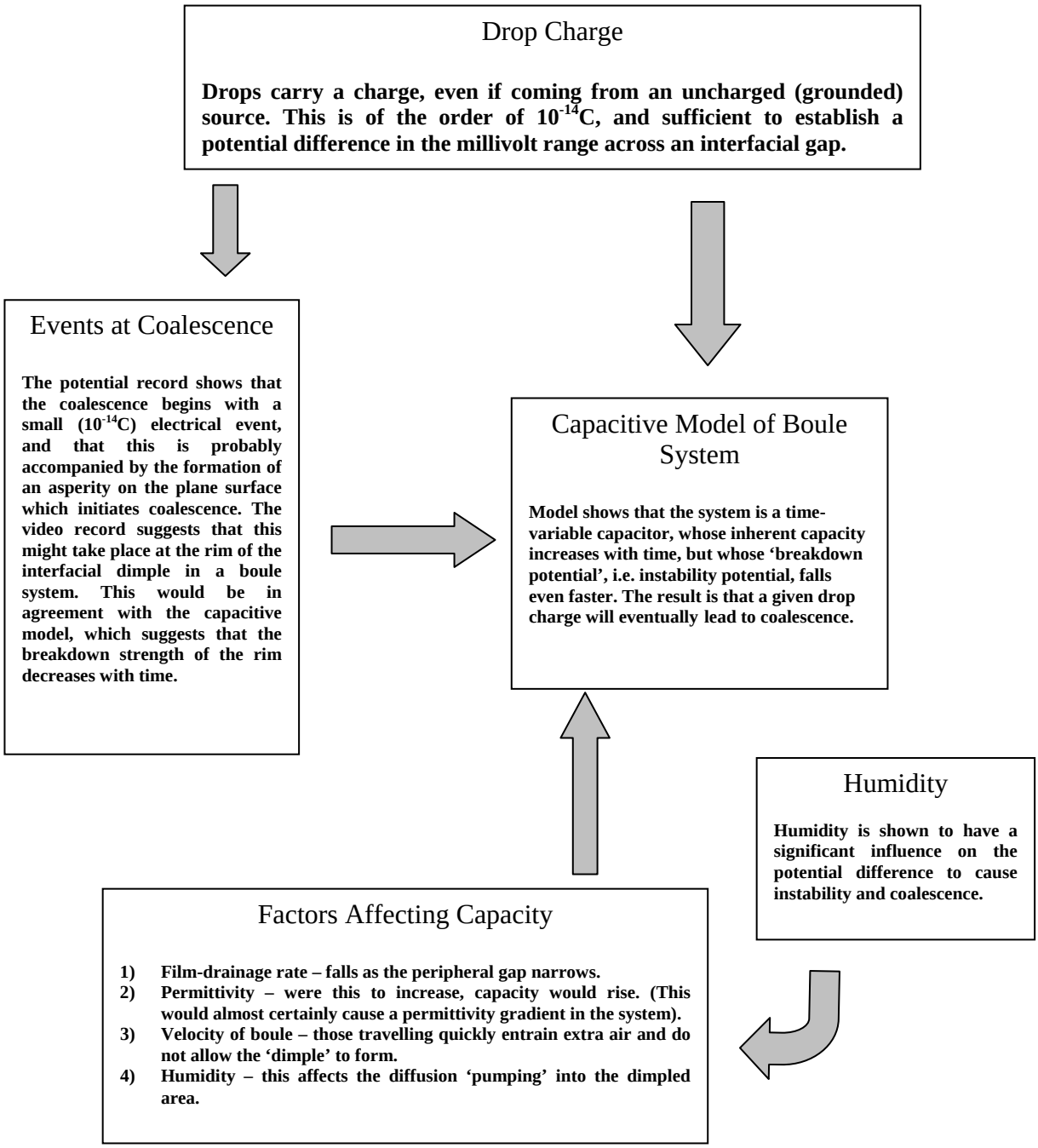

Figure 9.1. Schematic summary of major influences on the formation and coalescence of water boules.

9.2. Recommendations for further study.

This present research has served to highlight certain areas where a greater understanding would be most beneficial, and these have been from time to time noted. This final section focuses on five of these, making suggestions for possible ways forward.

9.2.1. The relative permittivity of moist air in small interfacial gaps.

The DC and low-frequency permittivity of moist air is normally assumed to be very close to that of dry air, and approximately equal to that of free space. Standard tables quote figures of ε_r = 1.00045 at 0%RH and 1.00067 at 100%RH. These figures, however, derive from measurements made either optically or at radio frequencies.

In a small interface, where the thickness of the dielectric layer is <10μm, say, the non-homogenous nature of the dielectric becomes increasingly important in terms of the interfacial capacitance. In the case of air-film interfaces in polar liquid systems the situation is further complicated by the activity of the conducting surfaces adjoining the dielectric. Under DC and low-frequency conditions such a system could conceivably exhibit a time-dependent capacitance, with deposition of water molecules on the conducting surfaces gradually serving to narrow the interfacial gap.

It is therefore suggested that an initial investigation be done to determine the relative permittivity of small gaps between metallic electrodes at different humidities. A brief preliminary investigation carried out during the course of the present research employed a small air-spaced variable capacitor of 20pF nominal maximum capacity. The average spacing of the capacitor vanes was 150μm. This was suspended in an environment of saturated air, and its capacity measured at 400Hz was found to double over a period of about five minutes. Upon removal from the saturated air the capacity returned to 20pF in a matter of seconds. Consideration was given to the possible lowering of the surface resistivity of the ceramic support framework of the capacitor. A screw-down type mica capacitor of similar value, mounted on a similar ceramic framework and whose design inhibited ingress of water into the dielectric region, was also tested. This showed a rise

in capacity of less than 1pF when left overnight in a saturated air environment, suggesting that change in surface resistivity was relatively unimportant. A proposed approach to the problem is as follows.

It may be desirable to measure capacitance by charging the system to a known potential and measuring the retained charge, rather than employing a bridge system. This enables a clearer picture of the possible rôle of any change in surface resistivity to be assessed. If, for example, the charge stored were to decrease with increasing humidity, then this might reasonably be attributed to leakage arising from lowered resistivity. If the charge increased then the cause must be a rise in the effective relative permittivity, whether caused by a modification of the dielectric itself or by the effective shortening of the inter-electrode spacing through deposition of layers of conducting water molecules.

The form of an experimental capacitor system requires some thought. The following appear the most important criteria.

- The capacitance should be considerably greater than that of any associated circuitry.
- Fine control of the inter-electrode spacing should be possible, in a range of perhaps 10 - 1μm.
- Steps should be taken to ensure that the dielectric layer is initially homogenous for any particular value of relative humidity.

The first two of these criteria might be addressed by the use of two coaxial tapered tubular electrodes of convenient size, one fitting within the other. This arrangement allows for fine control of the dielectric layer by slow advance of the inner electrode within the outer. Figure 9.2. shows a partly-sectioned diagram of a capacitor whose electrodes consist of a cylindrical metal stator having an internally tapering bore, in opposition to an adjustable cylindrical rotor with an external taper. The undercut, *U*, in the stator bore means that this electrode has a constant effective length of *l*. the arrangement does not, as shown, allow for end-effects at the capacitive interface. The incorporation of a guard-ring system, whilst constructionally challenging, is not impossible.

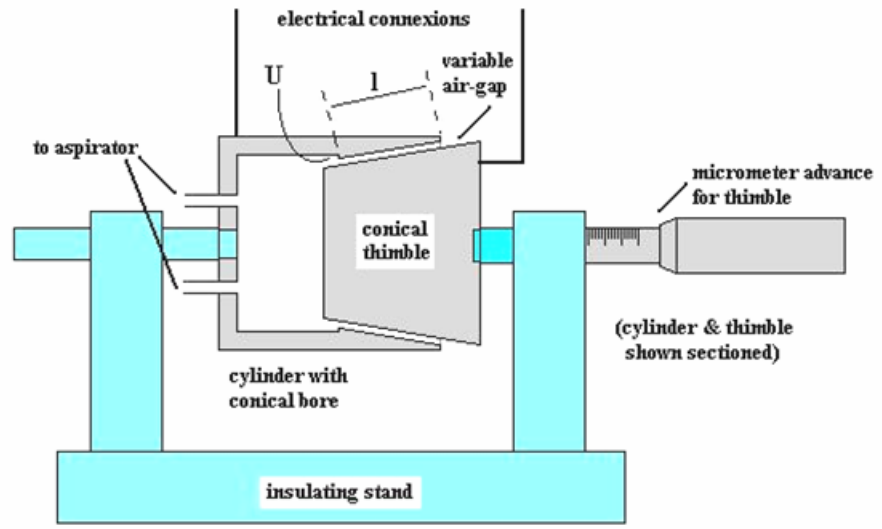

Figure 9.2. Variable capacitor for different humidities (partly sectioned).

With a taper of, say, 1 in 10, the air-gap would be readily controllable to a micrometre, given accurate alignment and a standard micrometer advance screw. With stator/rotor mean diameters of circa 5cm, and an effective length, *l*, of 2cm, the capacitance range in dry air for air gaps of 10 – 1μm would be approximately 3 – 30nF. This value is sufficiently high that stray capacitance in the apparatus becomes very small in comparison and also allows for the production of robust charges from low voltages. A 1-volt source, for example would produce charges in the range 3×10^{-9}C to 3×10^{-8}C, these being readily measured.

Figure 9.2. also suggests a possible way forward to ensure dielectric homogeneity. The stator is shown with inlets for conditioned humid air. This is provided at low positive pressure from an aspirator which feeds humid air derived from a known humidity source. Humid air therefore fills the stator chamber and vents to atmosphere through the capacitor, thus keeping a constant-humidity dielectric.

The advantage of this arrangement is that the main apparatus may be kept either in laboratory air or in dry air, this contributing significantly to the reduction of leakage paths arising from moisture deposition on the insulating framework of the apparatus. A circuit arrangement for charge measurement is given in Figure 9.3.

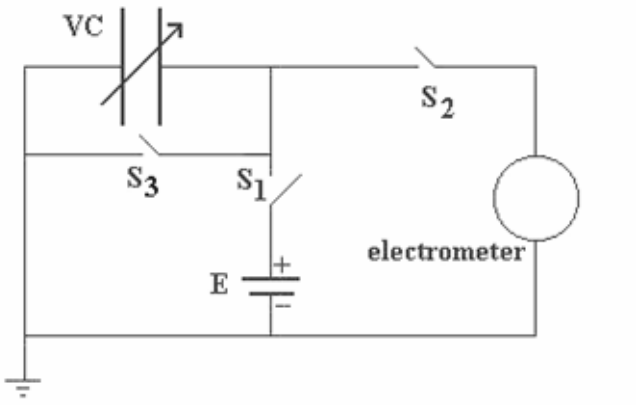

Figure 9.3. Circuit for capacitance measurement.

In use the test capacitor, *VC*, is charged from E by temporarily closing *S1*. After charging, the charge is transferred to the electrometer by closing *S2*. The capacitor may be discharged by temporarily closing *S3*. It is suggested that *S1, S2* and *S3* be reed switches. These have the advantage of low self-capacity, together with the facility to be remotely operated by a small magnet, thus helping to remove random operator capacity from the system.

Such a design offers a robust and stable investigative platform, which with relatively minor modifications could be adapted to the examination of other liquid-vapour systems.

It is considered that an investigation along the lines described would assist in resolving the issue of possible change in relative permittivity, especially as relative humidity approaches saturation.

9.2.2. Instability potential between a convex and a nearby plane or concave liquid surface.

In attempting to evolve a capacitive model for a boule system some frustration has arisen resulting from the lack of definitive information about instability potentials

between a convex water surface and a nearby plane or concave one. There is therefore a need to determine this practically, and to evolve a realistic theoretical model for this situation. The practical difficulties in such an investigation are considerable, as static conditions in such an interface are effectively unattainable. Past work on instability has been on a far larger scale than is applicable to the small interfacial gaps found in drop/drop, drop/plane and boule systems, and needs to be confined to dielectric gaps of below 10μm. It is suggested, therefore, that the work reported by Ahern and Balachandran [128] be extended initially to cover coalescence potentials between a pendent drop and both a plane water surface and a plane non-deformable conductor.

A practical investigation of these quantities involves some difficulties, the chief of them being the question of accurate measurement of interfacial distances. In the drop/drop measurements detailed in Chapter 7 and reported in [128], the optical arrangements were relatively easy, as visualization was restricted to the converging edges of two identically sized drops, allowing for considerable accuracy in measurement. Accurate determination of, say, a plano-convex interface is considerably more difficult, and direct observational measurement would almost certainly have to give way to interferometry.

Practical difficulties aside, a determination of instability potentials for such systems for a range of humidities would throw considerable light on the problem of establishing the boundary conditions for the electrostatically induced breakdown of such an interface.

9.2.3. Extension of investigations of electrical potential events at coalescence.

It has been shown in Chapter 6 of this thesis that the time-dependent consideration of electrical change at coalescence reveals a two-stage process that is masked by straightforward charge measurements. In particular there is a preliminary event of short duration, which appears to coincide with the onset of coalescence. This initial event is followed by sign-reversal and a much larger charge transfer attributable to the disruptive breakdown of the electrical double layer in the coalescing drop. Further investigation of these events, especially the former, would contribute considerably to our understanding

of the part played by electrostatic forces in coalescence, and to the mechanism of drop disruption.

One of the chief problems attending investigations of this nature is the acquisition of a good visual record. In the experimental work reported in Chapter 6 uncertainty concerning the production of apparent asperities was chiefly due to poor resolution of the video system when operating at very high speeds. Future work needs to address the issue of image resolution. More recent high-speed video systems than were available for this research may well answer the problem in part. The alternative is to use photographic film which is capable of fast exposure time and high resolution, but entails a drastic reduction in the lengths of time during which exposures may be made. Thought therefore needs to be given to experimental method in order to achieve good correlation between electrical and visual record and high image quality.

9.2.4. Interfacial modelling through molecular dynamics.

Over very short distances many of the quantities considered in various aspects of the thesis cease to have any significance. One cannot speak meaningfully of the surface tension, viscosity or permittivity of a *molecule*. These quantities are essentially bulk effects – statistical outcomes of a large number of events. At molecular distances these have been shown to become insignificant [129], and short-range forces, largely electrical forces, become dominant. A consideration of the changing and diminishing interface between two liquid systems eventually arrives at a scale where explanation of events through a mere scaling-down of bulk effects becomes nonsensical. Such a situation, for instance, arises when the permittivity of a small interface is being considered. At micrometre scale this may well be amenable to treatment with bulk quantities; at the nanoscale the relevance of these begins to disappear.

It is therefore thought that the synthetic approach of molecular dynamics might be profitably brought into use, building, as it were, from individual events up, rather than analyzing from the bulk down.

Molecular dynamics is a rapidly expanding field, that has proved its usefulness in a wide variety of applications. Some work has already been done in the field of coalescence. Koplik and Banavar [130] investigated the small-scale dynamics of interfacial rupture and re-formation for a system of about 10,000 Lenard-Jones particles, finding that thermal fluctuations produced strings of mutually attracting particles on the boundaries of two adjacent surfaces, forming a tendril that developed and bonded rather similarly to the action of a zip-fastener. To such a basis the perturbation of external electrical forces might well be added to determine the modifications to the process that would result.

9.2.5. Investigation of charging mechanism within a boule system.

The research has demonstrated that a water droplet skimming on an air cushion above a bulk water surface experiences a charging process, which in the case of drops of the size employed experimentally represented a charge augmentation of some two orders of magnitude. Consideration of the mechanism involved (Section 5.4) has shown that the currently accepted charge mechanisms are inadequate to explain the process. It has been suggested in the thesis that the dynamic conditions in the interfacial region may be sufficient to cause small-scale matter transfer from one liquid to the other, and that this might offer an opportunity for charge-transfer.

Further investigation of the observed phenomena might realistically be structured to incorporate the following aspects;

i) Dynamics of the mobile boule, in terms of , *a)* its velocity, and *b)* its deceleration.

ii) Boule electrohydrodynamics, taking account of, a) charge developed in relation to distance traversed, and b), the influence, if any, of charge species initially present on the boule-forming droplet.

iii) Evidence of matter interchange on the microscale between boule and bulk surface.

Treating these considerations in turn, it is suggested that the following approaches might be employed.

1) Dynamic aspects.

A modification of the apparatus described in Section 5.1 would allow for a boule's dynamics to be measured either via light-gates across its trajectory, or probably better by recording video sequences at a mediumly high framing rate – say 250fps – and deriving distances from scaling the enlarged images. As recorded in Section 5.4, deceleration is apparent by casual observation in the case of boules that have run a significant distance, and a measure of this deceleration is important in calculating the energy lost by frictional drag and viscous forces in the interface.

2) Electrohydrodynamic considerations.

An extension of the method of measuring boule charge described in Section 5.1 would permit the measurement of boule charge acquired after traversing different distances. Some care, however, is needed in the interpretation of such results, as it is apparent in practice that some boules are incapable of being sustained sufficiently long to allow them to travel significant distances. This could be from one of two causes. Either the dynamics of their 'collision' with the bulk surface has resulted in less than usual entrained air in the interface, with consequently faster drainage, or some variation in initial charge is quickly increased to the point of interfacial instability. The first of these possibilities might be monitored by the careful used of high-speed photography or video recording, allowing the impact geometry of successive boules to be compared. Variation in initial charge on the drops arriving at the surface might be observed by the careful use of an induction electrode in the area of the impact with the bulk surface. In the case of pre-charged drops this latter consideration is likely to be of less significance, but the geometry of the interface at its earliest formation is likely to be modified by comparison with that found from drops carrying only a minimal charge.

3) Matter interchange.

Elementary experiments to investigate matter exchange between the surfaces, such as detailed in Section 3.2.1 may be insensitive to low levels of material transfer. It is therefore suggested that the bulk surface be doped with an appropriate contaminant, and the water collected from boules that have successfully traversed the surface be examined chemically for evidence of its presence. This would give confirmation of matter transfer from bulk liquid to boule. The reverse arrangement of doping the liquid forming the boules and running it across a clean water surface would check for material transfer in the other direction, but is technically more difficult to achieve as any boule failing to traverse the surface, and coalescing with it, would cause contamination. (See Figure 3.3).

9.3. Summary of recommendations.

The five suggested lines of future study are closely inter-related. Knowledge of the *effective* relative permittivity of a vapour-laden interface has bearings on the theoretical understanding of the instability potentials for different geometries. Further understanding of the sequence and magnitude of electrical events immediately preceding, at the start of, and during coalescence would help to confirm the veracity of the first two investigations, as well as yielding important information concerning the coalescence process itself. Investigation into the charging mechanism by which boules augment their initial charge in the course of crossing a liquid surface would not only add to our fundamental knowledge of electrostatic processes, but also have possible significance for our understanding of a number of biological processes.

APPENDIX 1.

Translation of Meunier's Paper of 1863 (Reference 13)

De la Forme Globulaire que les Liquides et le Gaz peuvent prendre sur leur propre Surface.

M.S. Meunier.

COMPTES RENDUS v. 57, pp 401-403. 1863.

OF THE GLOBULAR FORM WHICH LIQUIDS AND VAPOURS MAY ASSUME UPON LIKE SURFACES.

One cannot filter certain liquids, such as alcohol or glacial acetic acid, without giving rise to the formation of small globules, which run in all directions upon the liquid surface, and which are soon absorbed into it. When I observed this for the first time I did not doubt that it was well known, but I have found no reference to it in any book, and M. Demain made no allusion to it in a recent communication on similar topics (C.R. LVI, p. 1103). I have therefore decided to pursue the matter, and in this Note I shall seek to give the most reasonable explanation for their formation.

For alcohol, acetic acid, ethers &c, one can drop the liquid on to a clean surface by means of a pipette. The globules are numerous, sometimes large, and present exactly the same spherical appearance that M. Boutigny found formed on an incandescent dish. That they are not in contact with the surface on which they are formed may be found by direct means. For instance, if I project a drop of colourless alcohol on to strongly red-coloured tincture of iodine, if there were any contact then the drop would become coloured, but it remains completely colourless. Moreover, when arranged conveniently in the daylight one notices a distinct depression under the drop, which could not be formed if there were contact. When a globule is absorbed in to the liquid it more often than not causes a multiple rather than a single event. After the drop is absorbed there is a vertical ejection of part of it, which on returning to the surface forms a tiny sphere.

Also, two colliding drops will coalesce, giving rise to the same ejection of material and tiny spherules.

Forming globules by means of a pipette is, however, unsuccessful with a number of liquids. In such cases it is usually better to proceed thus: a glass rod is introduced below the surface of the liquid, and a drop raised on it which one then places on the surface. The drop will become a globule and will run across the surface before being quickly absorbed. Using this method all the liquids that I have studied have produced globules with the greatest certainty, and with an ease similar to water.

All difficulty disappears if one places the experimental liquid thinly on a layer of another liquid with which it will not mix. The globule now loses part of its weight in the lower liquid, and this lightening permits both a lengthening of the globule's existence and an increase in its volume. In terms of duration, globules of carbon disulphide are in the first rank, and from the point of size, globules of water on benzene are the most remarkable. There is some evidence of how these latter are absorbed. The absorption occurs in five or six coalescences, each one producing a globule smaller than its predecessor. We can therefore say that when two liquids are superposed on one another, the lower liquid produces globules *above* the interface, and forces the upper liquid to produce globules *below* the same interface, so that one obtains at the same time two different species of globule.

The production of globules of a less dense liquid upon a denser one leads me to think that the *vapour* produces the globules in the liquids. Experiment confirms this conjecture. If some aerated water be moderately heated, bubbles of vapour are forced to the interfacial surface between the fluids, and show all the characteristics of *liquid* globules. For this reason I consider the mechanism maintaining the bubble of air in the water as pertaining to the vapour, and as operating in the plane of separation between itself and the liquid, denoted in the title of this Note by the word *surface*, applying it to the particular situation of two species of fluids.

To summarize, it follows from the preceding that the ability to produce globules must be considered as a general property of fluids, which was my intention to demonstrate.

APPENDIX 2.

An Investigation into possible Light Emission at Coalescence.

Introduction.

It has been noted in Chapter 6 (6.2.1) that during the initial investigations of electrical events at coalescence an imbalance in charge transfer from a drop to a bulk surface was observed. As explained in that chapter, this was eventually traced to a capacitive imbalance in the signal leads to the oscilloscope, but at the time the question arose as to whether or not there might be any possible optical emission from the event that might account for an energy loss.

Light emission from charged drops has been recorded several times before. Both anecdotally[1] and within the literature, many instances are recorded of light emission during liquid interactions as a result of corona discharge. In 1965 Miller, Shelden and Atkinson [131] investigated the luminosity accompanying the coalescence of oppositely charged water drops of about 1mm diameter and carrying charges in the region of 5 x 10^{-11}C, detecting light emissions in a wavelength spectrum between 330.5nm and 432.6nm. Subsequent to this, Phelps, Griffiths and Vonnegut [132] observed the corona produced by the disruptive splashing of water drops on to a water surface in a strong electric field. In their investigation drops falling from varied heights were induction charged by an electric field adjustable in the range 0 – ±25kV. It was found that the Worthington jets resulting from the splashing emitted light when they were formed from 3mm radius drops falling at terminal velocity through a field of 180kV/m. Each resulting splash liberated charge in the order of 10^{-7} to 10^{-6}C. It was observed that this critical field strength was independent of polarity, but inversely related to the drop momentum.

[1] Dr Colin Pounder reported a conversation to the writer that he had had some time ago with Professor Lundquist of Uppsala, in which the latter recalled his grandmother's memory of sometimes seeing flashes of blue light as heavy raindrops struck the cobblestones at night. The present writer recalls similar memories of a glow from heavy rain on the dark yard of a remote house over fifty years ago.

More recently Matsui et al [133] have observed light emission from water drops rolling down an inclined plane formed from a hydrophobic dielectric (PTFE). Drop charges in this instance were 9.6 x 10^{-10}C. This background gave cause for wondering if the events of normal coalescence might also lead to light emission, and apparatus was constructed to mount an investigation. In the event the experiment gave negative results for the coalescence of a drop with a nearby surface, but a brief description of the investigation is included here for the sake of completeness.

Some care was taken to produce a photomultiplier system of the greatest sensitivity. The tube used, a Hammamatsu type R1463, was a selected grade having both high gain and very low dark current. The optical window was transmissive down to 185nm. The power supply was designed to provide a stable voltage of 1kV across the dynode chain, with a tolerance of ±200mV. Figure 1 shows a block diagram of the circuit.

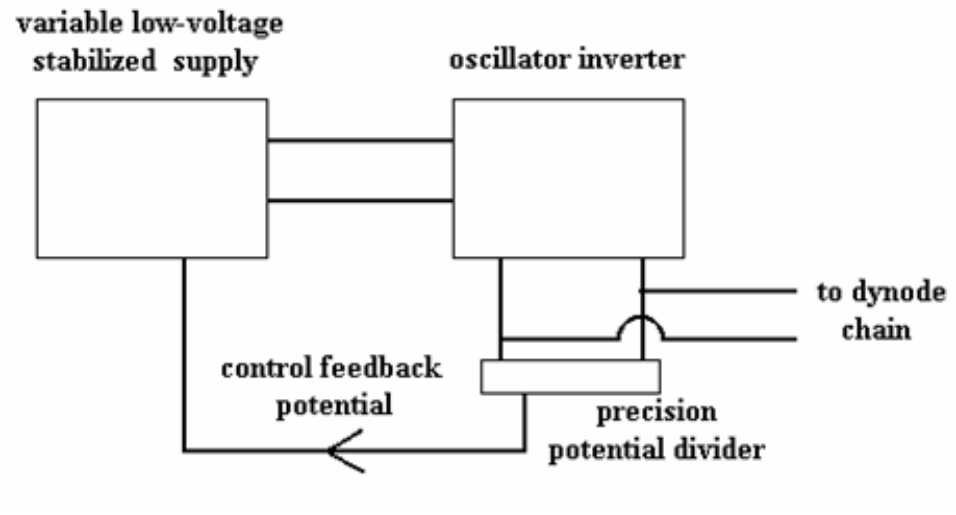

Photomultiplier power supply block diagram

In this an oscillator inverter was used to generate the high voltage, powered from a variable-voltage stabilized supply. A precision potential divider across the DC output of the inverter derived a voltage signal proportional to the inverter output. This signal was used as a feedback control to the low-voltage supply. The completed system was capable of providing currents up to 2mA with less than ±0.02% variation in output voltage.

The photomultiplier was housed in a screened case, and included a light-tight shutter that enabled handling of the equipment in daylight. Photon-counting configuration and current configuration were both possible, and current measurements were made with a Hewlett-Packard type 425A vacuum-tube microammeter, capable of resolving 10^{-14}A.

The drop cell was machined from an aluminium block, having an internal cavity 5cm in diameter by 5cm deep in it. Within this cavity was fitted a small circular brass table, with a needle for dispensing drops above it. In use, the table carried a shallow film of water, with which drops might coalesce. The photomultiplier assembly attached to this drop cell such that the photocathode was aligned with the liquid interface. Figure 2 shows views of the apparatus.

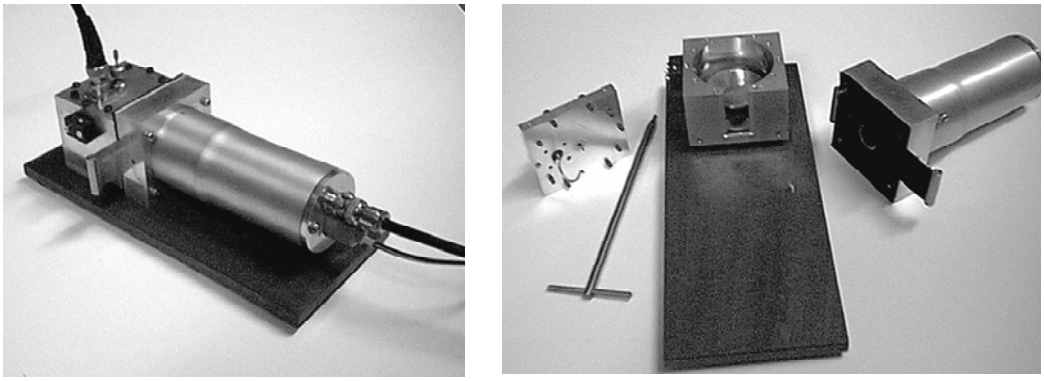

Drop cell and photomultiplier, *left*, assembled; *right*, dismantled.

No optical emission at coalescence was recorded with this apparatus for drops grounded with respect to the bulk surface. An adaptation was made to the experiment in the form of a light-tight tubular tower 80cm high to which the photodetector system would fit, and in which drops could fall freely on to a water surface. The drop source could either be grounded or charged. In the former case no photoemission was detected, but once drop charges exceeded about 10^{-8}C photoemission from the splashing was recorded (*cf.* reference 132 above)

APPENDIX 3

Dataset for critical coalescence potentials.

Overleaf are printed,

1. The complete dataset of the experimental results for measurement of critical coalescence potentials at a variety of initial needle settings, and covering 5 specific relative humidity points (*21, 41, 61,83 and 100%RH*). The potential measurements are accompanied by the individual temperature and humidity values at the time of measuring the potential. (Relevant to Series I, section 7.5.1)

2. The dataset for the measurement of critical coalescence potential for drops at a fixed gap of 40µm, for small variations in relative humidity between 41 % and 100%. (Relevant to Series II, section 7.5.3)

Dataset for coalescence potentials at 21, 43, 61% RH at needle spacings 2.5 to 1.0 mm.

MEASURED VALUES OF V_C FOR SERIES 1 (21%, 43% & 61%RH)

Critical Potentials for Coalescence, V_c

Relative Humidity for series = 21%

Needle Separation = 2.50mm

Data No.	Gap 40µ V_c	Gap 30µ V_c	Gap 20µ V_c	Gap 10µ V_c	Gap 5µ V_c
1	76.2	51.8	40.5	24.1	12.3
2	81.3	59.9	39.9	19.7	15.3
3	76.2	56.2	40.3	21	13.9
4	77.3	54.1	36	23.5	14.6
5	72	54.9	39.2	20.7	12.4
6	77.5	604	37.7	20.8	15
7	75.6	55.1	41	24.3	14.7
8	74	55.7	37.9	20.1	14.9
9	75.7	55.1	37.1	24.9	15.9
10	78.7	55.3	38.2	23.7	13.1
V_C Mean	76.5	55.8	38.8	22.3	14.2
Temp °C	25.4	25.4	25.4	25.4	25.4

Critical Potentials for Coalescence, V_c

Relative Humidity for series = 21%

Needle Separation = 2.00mm

Data No.	Gap 40µ V_c	Gap 30µ V_c	Gap 20µ V_c	Gap 10µ V_c	Gap 5µ V_c
1	92.2	61.9	43.6	24.6	19.4
2	82.9	64.3	50.2	26.3	19.7
3	86.8	66	43.9	25.4	18
4	81.1	72.4	44.9	23.8	19.5
5	79	68	44.9	20.6	19.7
6	84.1	65.6	44.2	24.8	18.5
7	78.2	67.3	42.6	26.4	19.1
8	74.8	64.8	45	25.7	19.4
9	84.7	69.6	47	26.5	18
10	87.2	70.4	41.1	26.3	19.7
V_C Mean	83.1	67	44.7	25	19.1
Temp °C	25.3	25.2	25.3	25.4	25.3

Critical Potentials for Coalescence, V_c

Relative Humidity for series = 21%

Needle Separation = 1.50mm

Data No.	Gap 40µ V_c	Gap 30µ V_c	Gap 20µ V_c	Gap 10µ V_c	Gap 5µ V_c
1	93.3	76.3	48	22	19.5
2	92.5	68.3	49.7	24.7	21.1
3	95.7	71.9	51.4	28.1	18.9
4	91.5	76.2	45.1	23.8	20.5
5	92.5	74.7	47	22.7	19.5
6	93.6	69	46.9	27.1	19.2
7	89.2	77.5	46.7	24	18.4
8	94.7	73.7	45.6	26	19
9	92	71.2	45	23.7	19.5
10	93.7	69.9	46.5	23.6	19
V_C Mean	92.9	72.9	47.2	24.6	19.5
Temp °C	25.2	25.3	25.4	25.4	25.3

Critical Potentials for Coalescence, V_c

Relative Humidity for series = 21%

Needle Separation = 1.00mm

Data No.	Gap 40µ V_c	Gap 30µ V_c	Gap 20µ V_c	Gap 10µ V_c	Gap 5µ V_c
1	125.1	109.4	76.6	45.3	24.8
2	139.8	107.7	73.4	42.8	23.8
3	132	107.3	73.3	45.1	24.2
4	131.9	95.3	69.5	43.4	19.1
5	135.8	100.7	76.7	48.3	23.5
6	132.4	100.5	64.2	40	23.8
7	138.7	104.7	71	45.7	24.2
8	126	113.6	66.6	42.1	28.8
9	131.9	99.6	78.7	41.9	27.8
10	126.1	97.5	74.7	40.1	24.1
V_C Mean	132	103.6	72.5	43.5	24.4
Temp °C	25.2	25.2	25.2	25.1	25.1

Critical Potentials for Coalescence, V_c

Relative Humidity for series = 43%

Needle Separation = 2.50mm

Data No.	Gap 40µ V_c	Gap 30µ V_c	Gap 20µ V_c	Gap 10µ V_c	Gap 5µ V_c
1	80	64.1	41.8	26.8	18.1
2	79.4	60	41.2	24.4	15
3	78.1	51.2	40.7	25.3	15.2
4	78	55.3	45.6	24.5	18.3
5	77.8	53.2	42.4	25.1	15.8
6	71.9	56.6	40.4	25.4	16.5
7	75.5	59	43.4	24.4	16
8	73.2	57.9	41.3	23.9	15.6
9	81.5	53.8	39.1	25.6	17.6
10	75	57.3	45.8	23	18.5
V_C Mean	77	56.8	42.2	24.8	16.7
Temp °C	25.4	25.4	25.3	25.3	25.3

Critical Potentials for Coalescence, V_c

Relative Humidity for series = 43%

Needle Separation = 2.00mm

Data No.	Gap 40µ V_c	Gap 30µ V_c	Gap 20µ V_c	Gap 10µ V_c	Gap 5µ V_c
1	89.3	63.6	46.1	30.6	24.7
2	86.5	64.5	44.3	30.2	19.8
3	89	70.3	46.5	29.9	21.2
4	84.4	64.3	48.9	29.5	22
5	89.3	65.7	49.5	31.8	22.9
6	88.8	65	45.1	28.9	20.9
7	92.3	68.2	47.5	28.4	21.1
8	83.8	62.4	48.6	30	21.3
9	85	64.1	44.1	32.5	20.3
10	87.4	63	50.5	29.7	22.3
V_C Mean	87.6	65.1	47.1	30.2	21.7
Temp °C	25.3	25.4	25.4	25.4	25.4

Critical Potentials for Coalescence, V_c

Relative Humidity for series = 43%

Needle Separation = 1.50mm

Data No.	Gap 40µ V_c	Gap 30µ V_c	Gap 20µ V_c	Gap 10µ V_c	Gap 5µ V_c
1	119.4	86.2	69.6	46	26.4
2	115.4	86.5	69.3	46.2	29
3	116.6	92.4	71.3	40.7	27
4	118.2	101.8	61.1	39.2	29.7
5	116.6	91.4	66.7	45.8	28.5
6	112.9	92.5	69.8	40.1	30.7
7	113.7	91.7	68.8	36.9	28.1
8	113.5	94.2	63.5	40.7	28.8
9	116.1	88.8	69.8	36.1	28.5
10	108.4	94.4	68.3	39.2	28.9
V_C Mean	115.1	92	67.8	40.8	28.6
Temp °C	24.4	25.4	25.3	25.3	25.3

Critical Potentials for Coalescence, V_c

Relative Humidity for series = 43%

Needle Separation = 1.00mm

Data No.	Gap 40µ V_c	Gap 30µ V_c	Gap 20µ V_c	Gap 10µ V_c	Gap 5µ V_c
1	142.7	107.6	80.8	49.4	27.1
2	144	109.8	78.7	50.8	25.1
3	153.8	107.8	85.5	46.4	26.7
4	159.5	110.9	79.7	45.3	25
5	139.4	115.9	74.3	51.6	24
6	140.9	110.7	78.1	43.2	27.6
7	137.9	99.3	76.1	43.6	20.1
8	154.1	103.6	83.4	46.5	22
9	136.9	99.7	77.5	45.4	21.4
10	140.7	114.8	77.1	47.4	21.6
V_C Mean	145	108	79	47	24.1
Temp °C	25.4	25.4	25.4	25.3	25.3

Critical Potentials for Coalescence, V_c

Relative Humidity for series = 61%

Needle Separation = 2.50mm

Data No.	Gap 40µ V_c	Gap 30µ V_c	Gap 20µ V_c	Gap 10µ V_c	Gap 5µ V_c
1	77.1	60.7	43.1	23.1	15.7
2	71.2	59.1	36.6	23.5	15
3	72.8	60	42.5	26.3	18.3
4	70.8	57	40.9	26.5	18.3
5	74.5	61.5	41.4	24.8	16.4
6	69.8	59.3	35.9	21.4	18.5
7	72.2	58.1	38	25	16.2
8	75	58.9	39.6	23.2	14.1
9	74.2	59.2	40	26	15.4
10	70.9	57.3	39.3	26.2	18.5
V_C Mean	72.9	59.1	39.7	24.6	16.6
Temp °C	25.2	25.2	25.3	25.4	25.5

Critical Potentials for Coalescence, V_c

Relative Humidity for series = 61%

Needle Separation = 2.00mm

Data No.	Gap 40µ V_c	Gap 30µ V_c	Gap 20µ V_c	Gap 10µ V_c	Gap 5µ V_c
1	81.7	65.5	44.1	27	18.7
2	80.6	67.8	49.4	26.5	16.9
3	80.3	66	45.9	28.1	19.2
4	81.7	65.3	48.7	27.8	17.3
5	80.7	64.5	49.7	30.2	18.5
6	76.8	67.9	45.3	26.1	18.4
7	79.7	62.3	40	25.4	19.3
8	79.6	63	48.2	24.7	17.5
9	80.7	63.4	45.4	28.1	16.2
10	79.8	67.2	40.6	24.9	18.8
V_C Mean	80.2	65.3	45.7	26.9	18.1
Temp °C	25.2	25.2	25.2	25.2	25.2

Critical Potentials for Coalescence, V_c

Relative Humidity for series = 61%

Needle Separation = 1.50mm

Data No.	Gap 40µ V_c	Gap 30µ V_c	Gap 20µ V_c	Gap 10µ V_c	Gap 5µ V_c
1	98.4	70.3	51.6	32.6	19
2	95.7	72.1	46.7	30.1	19.9
3	89.3	73.3	51	30.5	20
4	101.3	73.7	49.3	35.6	21.4
5	95.5	72.4	53.4	29.1	19.1
6	88.4	72	52.8	30.2	19.7
7	93.4	75.4	50	29.9	18.5
8	95.8	77.9	46	30.7	21.1
9	93.6	76	52.3	33.6	20.8
10	91.9	74.5	50.6	30.8	21.2
V_C Mean	94.3	73.8	50.4	31.3	20.1
Temp °C	25.4	25.4	25.4	25.3	25.3

Critical Potentials for Coalescence, V_c

Relative Humidity for series = 61%

Needle Separation = 1.00mm

Data No.	Gap 40µ V_c	Gap 30µ V_c	Gap 20µ V_c	Gap 10µ V_c	Gap 5µ V_c
1	129.1	107.8	74.1	45.1	20.6
2	128.3	112.5	71.4	41.9	23.6
3	127.2	103.9	65.6	34.7	19.4
4	122.1	106.8	66.9	39.5	22.3
5	119	105.4	69.7	41.7	19.3
6	122.8	97	69.3	35.2	20.5
7	125.1	105.6	69.5	35.1	23.7
8	126	110.3	74.4	38.2	23.2
9	128.6	110	59.8	41.4	19.5
10	130.2	96.8	66	41.9	22.1
V_C Mean	125.8	105.6	68.7	38.9	21.4
Temp °C	25.5	25.5	25.5	25.5	25.5

MEASURED VALUES OF V_C FOR SERIES 1 (83% AND 100% RH)

Critical Potentials for Coalescence, V_c

Relative Humidity for series = 83%
Needle Separation = 2.50mm

Data No.	Gap 40µ	Gap 30µ	Gap 20µ	Gap 10µ	Gap 5µ
	V_c	V_c	V_c	V_c	V_c
1	75.5	56.5	39.6	23.3	11.7
2	70	51.3	38.1	21.9	12.9
3	72.7	53.8	39.7	19.6	13.1
4	75.9	54.5	38.1	21.6	12.3
5	71.7	52.6	41.9	19.2	12.5
6	73.2	51.8	39.6	21.8	12.4
7	72.9	53.6	41.1	21	12.1
8	70.5	57	39.2	18.9	14
9	77.1	53.6	38.1	21.7	11.8
10	67.8	55.9	41.2	21.9	12.5
V_C Mean	72.7	54.1	39.7	21.1	12.5
Temp ºC	25.6	25.6	25.5	25.5	25.6

Critical Potentials for Coalescence, V_c

Relative Humidity for series = 83%
Needle Separation = 2.00mm

Data No.	Gap 40µ	Gap 30µ	Gap 20µ	Gap 10µ	Gap 5µ
	V_c	V_c	V_c	V_c	V_c
1	81.4	55.4	36.2	21.2	14.9
2	78.5	56.3	37.5	19.3	13.9
3	83	56.6	36.9	19.1	13.7
4	80.3	57.7	36.3	20	15.5
5	74.9	59.7	36	19.1	13
6	77.4	56.1	39.3	21.3	14.9
7	82.4	56.1	37.1	19.8	13.9
8	77.1	59.7	37.8	19.4	13.3
9	78	56.7	39.6	21.1	13.9
10	78.1	61.4	36.7	21.1	14.7
V_C Mean	79.1	57.6	37.3	20.1	14.2
Temp ºC	25.6	25.6	26.6	25.5	25.5

Critical Potentials for Coalescence, V_c

Relative Humidity for series = 83%
Needle Separation = 1.50mm

Data No.	Gap 40µ	Gap 30µ	Gap 20µ	Gap 10µ	Gap 5µ
	V_c	V_c	V_c	V_c	V_c
1	93.6	63.8	48.8	26.5	16.4
2	86.1	69.1	46.5	25.9	16.7
3	91.9	69.8	44.9	26.4	15
4	88.1	64.9	42.8	26.2	16
5	78.9	65.9	48.7	27.4	16.9
6	88.2	65.4	50.1	25.5	16.5
7	92.2	64.6	50.2	25.9	16.8
8	92.1	63.9	45.2	24.9	15.4
9	86.1	66.3	45.8	24.5	16.4
10	85.1	64.7	47.2	25	15.5
V_C Mean	88.2	65.8	47	25.8	16.2
Temp ºC	25.5	25.5	25.6	25.6	25.6

Critical Potentials for Coalescence, V_c

Relative Humidity for series = 83%
Needle Separation = 1.00mm

Data No.	Gap 40µ	Gap 30µ	Gap 20µ	Gap 10µ	Gap 5µ
	V_c	V_c	V_c	V_c	V_c
1	86.9	78.8	45.2	30.2	14.3
2	95.5	78.1	49.2	29.7	16.7
3	83.3	74.9	48.4	26.9	14.6
4	77.1	78.2	48.3	27.8	17
5	79.1	75.1	47.1	28.9	16.5
6	86.9	76.2	45.2	29.6	16.8
7	94.7	73.4	44.6	29.8	14.5
8	88.8	76.9	46.7	23.4	15.8
9	92.3	71.9	47.4	28.5	16.1
10	94.9	79.1	47.6	29.4	16.2
V_C Mean	87.9	76.3	47	28.4	15.9
Temp ºC	25.5	25.5	25.6	25.6	25.6

Critical Potentials for Coalescence, V_c

Relative Humidity for series = 100%
Needle Separation = 2.50mm

Data No.	Gap 40µ	Gap 30µ	Gap 20µ	Gap 10µ	Gap 5µ
	V_c	V_c	V_c	V_c	V_c
1	62.3	51	35.9	21.1	11
2	65	52.1	37.2	19.7	9.6
3	61.7	51.4	35.6	19.4	10.3
4	64.5	52.7	37	20.9	10
5	64	53.8	35.7	21.2	10.4
6	65	51.6	35	20.4	8.3
7	63.6	53.8	36.5	20.6	8.3
8	64.5	51.4	35	20.6	8.6
9	65.4	51.6	35.5	20.6	10.4
10	65.9	53.3	34.9	21.8	10.2
V_C Mean	64.2	52.3	35.8	20.6	9.7
Temp ºC	25.4	25.4	25.4	25.4	25.4

Critical Potentials for Coalescence, V_c

Relative Humidity for series = 100%
Needle Separation = 2.00mm

Data No.	Gap 40µ	Gap 30µ	Gap 20µ	Gap 10µ	Gap 5µ
	V_c	V_c	V_c	V_c	V_c
1	78.7	54.2	38.3	22.1	11.9
2	78.6	56.2	39.1	21.1	12.6
3	75.4	55.4	38	23.5	12.6
4	75.5	54.1	37.6	22.2	13.4
5	75.8	53.9	36.4	20.8	10.8
6	78.9	55.9	38.1	21.2	11.1
7	76.6	53.6	38.9	21.5	11.3
8	74.7	54.7	38.7	21.7	12.5
9	74	54.4	36.3	23.2	11.3
10	73.7	54.1	38.1	23.6	11.3
V_C Mean	76.2	54.7	38	22.1	11.9
Temp ºC	25.4	25.4	24.5	24.5	24.5

Critical Potentials for Coalescence, V_c

Relative Humidity for series = 100%
Needle Separation = 1.50mm

Data No.	Gap 40µ	Gap 30µ	Gap 20µ	Gap 10µ	Gap 5µ
	V_c	V_c	V_c	V_c	V_c
1	84.4	65.1	41.9	25.3	17.7
2	84.7	62.5	40.1	22	18.4
3	87.6	65.3	42	22.1	17.4
4	83.5	62.7	40.9	22.4	16.3
5	86.2	63.7	41.9	27	18.6
6	86.1	63.1	42.8	25.5	17.1
7	84.4	65.8	42	26.2	18.9
8	84.6	65.6	42.3	26.9	16.2
9	82.2	62.1	41.6	24.6	19
10	87.5	64	40.7	27.6	18
V_C Mean	85.1	64	41.6	25	17.8
Temp ºC	25.3	25.4	25.3	25.2	25.2

Critical Potentials for Coalescence, V_c

Relative Humidity for series = 100%
Needle Separation = 1.00mm

Data No.	Gap 40µ	Gap 30µ	Gap 20µ	Gap 10µ	Gap 5µ
	V_c	V_c	V_c	V_c	V_c
1	97.3	72	52.7	27.6	20.2
2	97.4	75.2	51.8	29.8	19.2
3	97	69.8	48.2	29.4	20
4	97	71	51.6	28.4	19.3
5	102.6	72.6	49.5	30.4	20.2
6	98.6	74.8	52.4	29.1	21.3
7	95.2	70.4	46.9	29.2	21
8	96.8	73	47.2	26.2	20.5
9	100.4	73.3	52.9	26.7	20.7
10	98.7	73.4	48.8	26.5	21.6
V_C Mean	98.1	72.6	50.2	28.3	20.4
Temp ºC	25.3	25.4	25.4	25.4	25.4

Dataset for coalescence potentials at 83 and 100% RH at needle spacings 2.5 to 1.0 mm.

	CLOSE-RANGE COLAESCENCE VOLTAGE DATASETS - all taken with drop diameter 1.00 mm and 40µm inter-drop gap. Temperature 21°± 0.3°C.									
DATA NO.	RH 41	RH 43	RH 45	RH 46	RH 47	RH 48	RH 49	RH 50	RH 51	RH 53
	Vc	Vc	Vc	Vc	Vc	Vc	Vc	Vc	Vc	Vc
1	147.0	150.6	130.2	147	138.3	133.2	136.3	138.8	121.8	129.4
2	147.5	142.7	151.5	140.7	142.8	133.4	139.7	125..7	127.9	130.6
3	154.9	141.7	146.8	140	132.9	126	133.7	125.4	133.7	129.1
4	142.0	135.8	133.9	143.3	155.1	129.4	141.7	133	138.5	120.5
5	145.3	154.9	134.3	134.4	145.1	134.6	146.1	137.3	137.2	132.5
6	138.7	141.3	155.5	143	130.6	133.3	144.5	134	120.1	112.8
7	154.9	142.7	147.9	143	136	137.4	131.7	121.9	125.1	124.5
8	139.3	158.2	149.1	138.9	131.9	138.2	136.2	130.6	125.7	123.5
9	140	133.2	137.5	140.4	141.6	128.4	141.8	133	134.4	122
10	146	154.1	130.8	141.7	142.1	137.4	141	139.3	126.5	125.1
MEAN	**145.6**	**145.5**	**141.8**	**141.2**	**139.6**	**133.1**	**139.3**	**131.8**	**129.1**	**125.0**
DATA NO.	RH 56	RH 61	RH 65	RH 69	RH 71	RH 75	RH 81	RH 83	RH 89	RH 100
	Vc	Vc	Vc	Vc	Vc	Vc	Vc	Vc	Vc	Vc
1	120.9	107.2	110.1	108	103.9	107.1	91.4	88.6	86.4	78.7
2	117.3	123.9	114.9	105.3	103.5	91.9	91.7	93.3	87.2	79.4
3	119.3	125.4	115.5	108.6	99.6	103.8	92.2	87.2	85.1	78.7
4	124.3	106.4	100.4	93.3	102.4	96.5	88.3	89.7	85.9	77.1
5	117.5	120.2	103.9	101.1	100.1	100.1	90.5	93.3	87.2	73.6
6	116.9	113.7	103.9	105.5	101.9	93.7	90	90.9	85.8	78.6
7	119.6	112.8	102.6	108.6	103.4	96.1	93.8	92.1	81.2	78.4
8	122	107	112.9	92.4	106.8	97	90.8	87	83.6	78.9
9	120.2	109.6	105.2	106.2	101	99.6	90.4	88.6	81.4	76
10	124.4	121.2	109.1	109.9	100.3	93.7	93.6	88	87.2	78.4
MEAN	**120.2**	**114.7**	**107.9**	**103.9**	**102.3**	**98.0**	**91.3**	**89.9**	**85.1**	**77.8**

Dataset for coalescence potentials at constant 40µm drop spacing for RH values 41-100%.

APPENDIX 4

Oscillograms of coalescence events.

A number of oscillograms of coalescence events is displayed below. Some were taken with a simultaneous video record in the course of the work described in Chapter 6 (Section 6.2.2), whilst others were recorded on subsequent occasions.

All traces show the two-part form described in Chapter 6. The first five (Figures 1 to 5) are of the same general form as that shown in the main thesis text (Section 6.2.2, Figure 6.12), and show a short initial potential event, followed by a larger one, accompanied by a sign reversal. Figures 1 to 3 are of traces taken during the sequence of experiments described in Section 6.2.2. Figures 4 and 5 relate to a subsequent experimental series for which there is no complementary high-speed video, the equipment for this being unavailable at the time.

Figures 6 to 10 show a sequence of traces made during another series of measurements and exhibit progressive extension of the initial event duration, and more significant modification of the envelope of the main event. These records were obtained in quick succession (approximately 30 seconds between measurements) and reflect a gradual scavenging of the bulk water by successive coalescences resulting in a sufficiently clean surface to allow the start of boule formation (see Section 3.2.2). By the time that the event recorded in Figure 10 was reached, it was just possible for the eye to notice the brief dwell-time of the drop on the bulk surface prior to its coalescence. The envelope of the main events in this latter sequence shows a sharper rise time to maximum, together with a more triangular form. The magnitude of this main event reduces somewhat, demonstrating a reduction in overall charge transfer. In Figure 10 it has a much attenuated form.

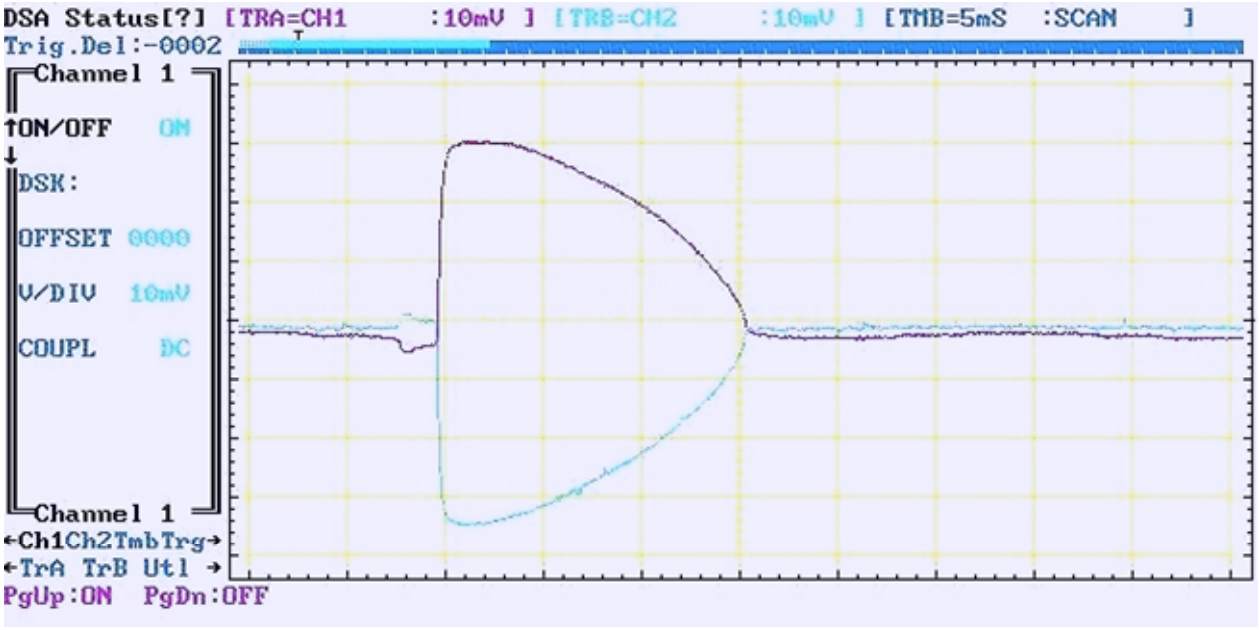

Figure 1.Initial event: peak voltages; drop -2.3mV; plane surface 2.3mV. Event duration, 2.4ms.

Figure 2. Initial event: peak voltages; drop –3.4mv; plane surface 2.7mV. Event duration, 1.7ms.

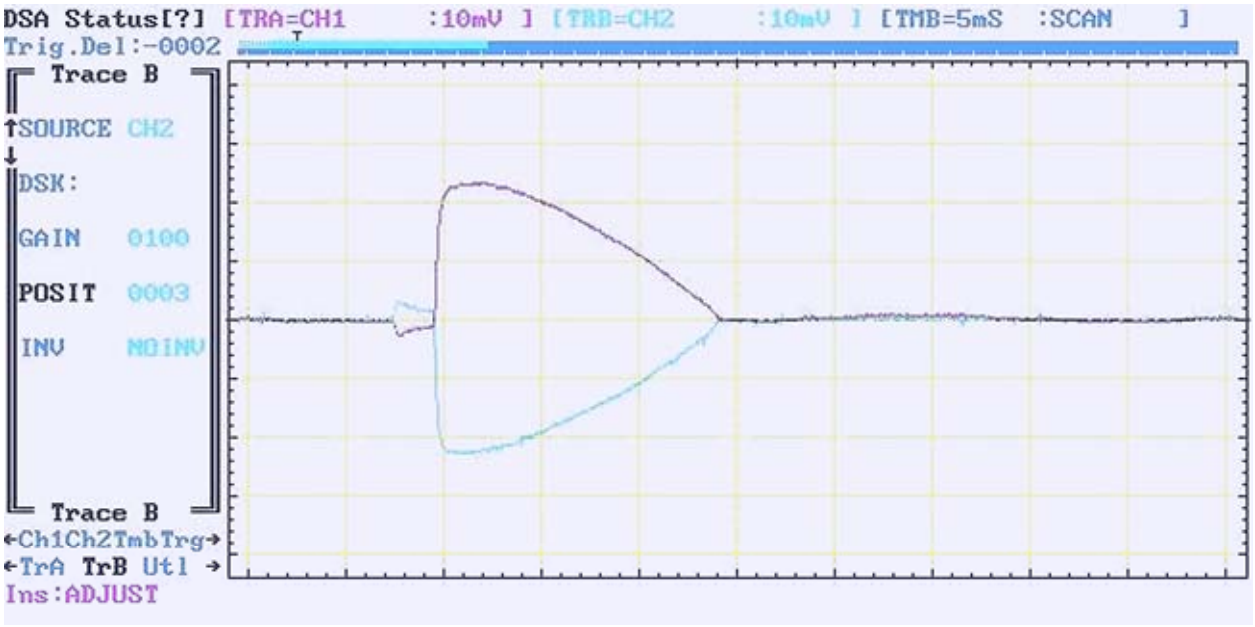

Figure 3. Initial event: peak voltages; drop –3.0mv; plane surface 3.0mV. Event duration, 2.3ms.

Figure 4. Initial event: peak voltages; drop –1.8mV; plane surface 2.2mV. Event duration, 1.9ms.

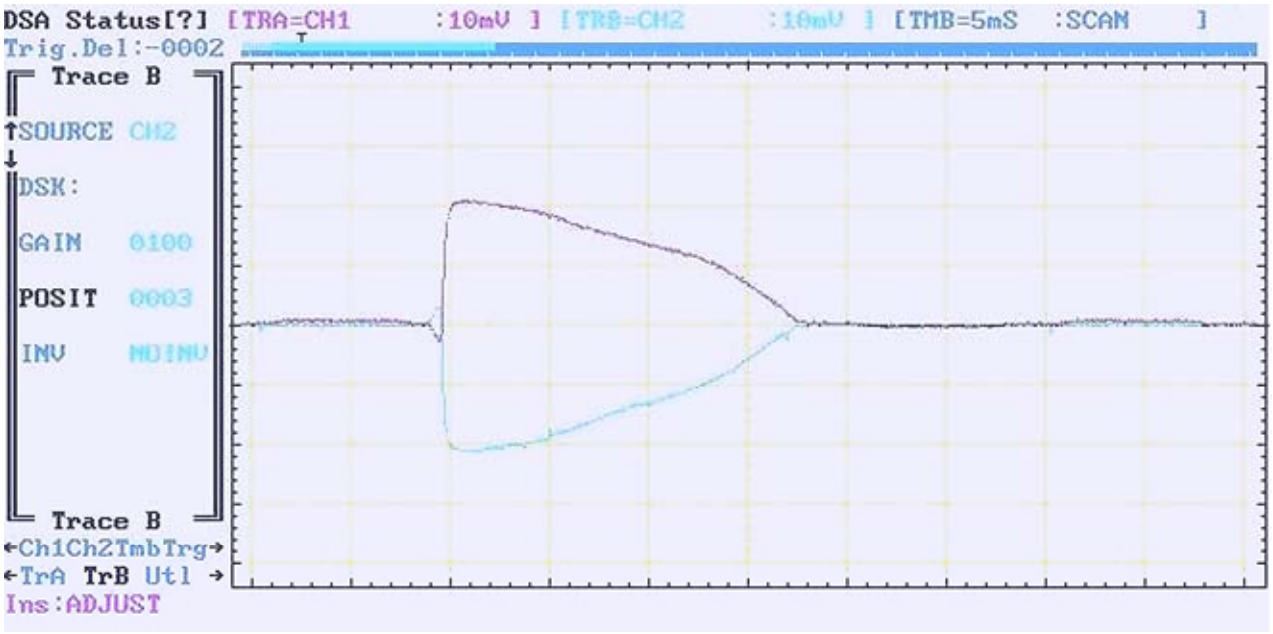

Figure 5. Initial event: peak voltages; drop –1.7mV; plane surface 1.9mV. Event duration, 0.9ms.

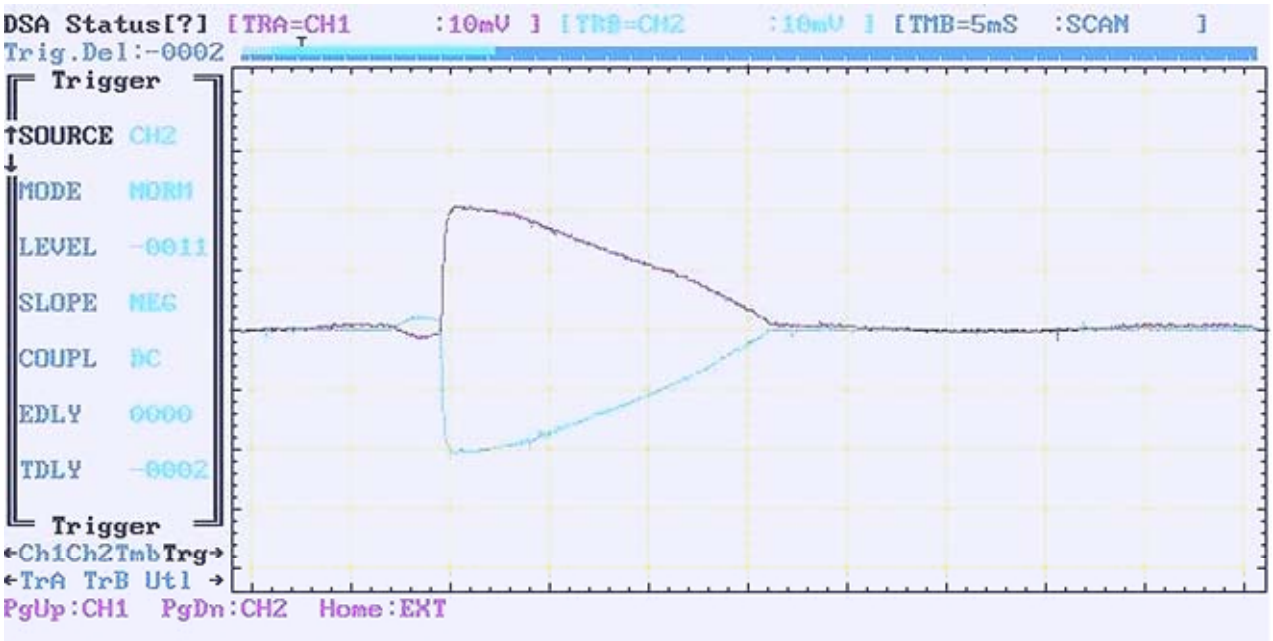

Figure 6. Event showing the onset of time-extension for the initial event. This is considered to be as a result of the gradual cleansing of the water surface in the well by repeated coalescences. Initial event: peak voltages; drop –1.2mV; plane surface 1.3mV. Event duration, 2.6ms.

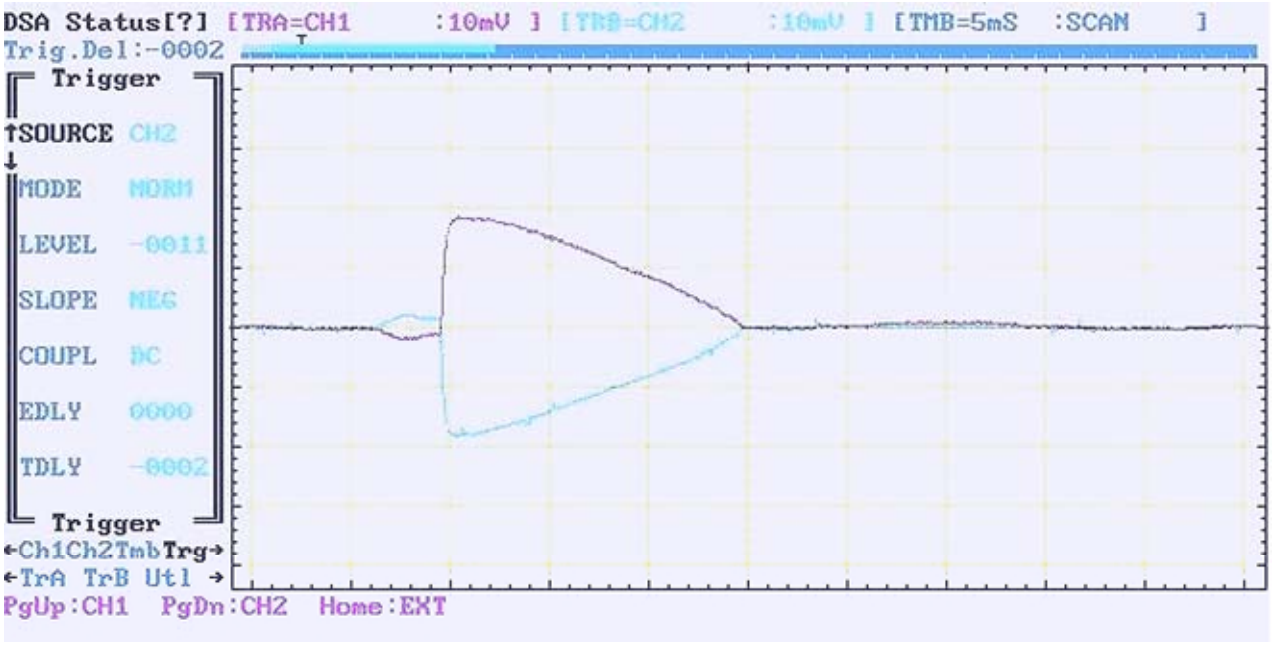

Figure 7. Initial event: peak voltages; drop –1.2mV; plane surface 1.2mV. Event duration, 3.7ms.

Figure 8. Initial event: peak voltages; drop –1.1mV; plane surface 1.2mV. Event duration, 3.9ms.

Figure 9. Initial event: peak voltages; drop –1.1mV; plane surface 1.2mV. Event duration, 4.9ms.

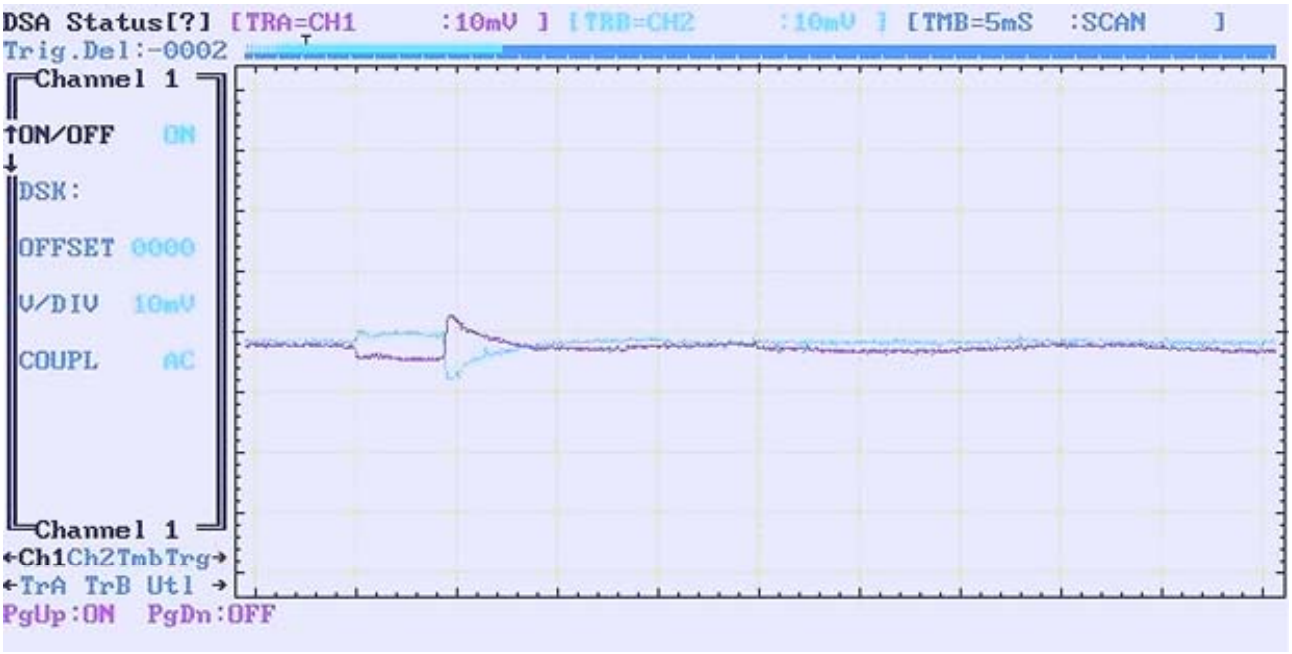

Figure 10. Initial event: peak voltages; drop –2.8mV; plane surface 2.5mV. Event duration, 4.6ms. Note the flatter form to the initial event traces, as well as the greatly attenuated main event. The drop in this case had a brief but perceptible dwell on the surface prior to coalescence.

APPENDIX 5

Dataset of interfacial fields within a boule system for different initial drop charges over a range of times.

Overleaf is printed the dataset arising from the theoretical calculation of the interfacial field-strengths produced on 4.7mm diameter drops forming a boule system. These cover a range of times between 0.1 and 10 seconds and initial drop charges between 1 x 10^{-12}C and 2 x 10^{-11}C.

The following nomenclature is used:

t is the time in seconds from the formation of the interface,

Z_0, the rim film-thickness in μm,

C, the system capacity in picofarads,

q, the drop charge in Coulombs.

V, the potential in Volts produced by the system capacity at the time, t,

V/Zo, is the resulting interfacial field-strength in kV/m at time t.

			q=1E-12C		q=2E-12C		q=3E-12C		q=4E-12C	
t	Zo	C	V1	V1/Zo	V2	V2/Zo	V3	V3/Zo	V4	V4/Zo
sec	μm	pF	(V)	(kV/m)	(V)	(kV/m)	(V)	(kV/m)	(V)	(kV/m)
0.1	5.59	0.95	1.0526	188.306	2.10526	376.612	3.15789	564.919	4.21053	753.225
0.2	3.96	1.2	0.8333	210.438	1.66667	420.875	2.500	631.313	3.33333	841.751
0.5	2.5	1.79	0.5587	223.464	1.11732	446.927	1.67598	670.391	2.23464	893.855
1	1.77	2.3	0.4348	245.64	0.86957	491.28	1.30435	736.92	1.73913	982.56
2	1.25	2.97	0.3367	269.36	0.6734	538.721	1.0101	808.081	1.3468	1077.44
3	1.022	3.46	0.289	282.796	0.57803	565.592	0.86705	848.387	1.15607	1131.18
4	0.885	3.84	0.2604	294.256	0.52083	588.512	0.78125	882.768	1.04167	1177.02
5	0.792	4.2	0.2381	300.625	0.47619	601.251	0.71429	901.876	0.95238	1202.5
6	0.722	4.5	0.2222	307.787	0.44444	615.574	0.66667	923.361	0.88889	1231.15
7	0.67	4.75	0.2105	314.218	0.42105	628.437	0.63158	942.655	0.84211	1256.87
8	0.626	5	0.200	319.489	0.400	638.978	0.600	958.466	0.800	1277.96
9	0.59	5.22	0.1916	324.696	0.38314	649.393	0.57471	974.089	0.76628	1298.79
10	0.56	5.4	0.1852	330.688	0.37037	661.376	0.55556	992.063	0.74074	1322.75
			q=5E-12C		q=6E-12C		q=7E-12C		q=8E-12C	
t	Zo	C	V5	V5/Zo	V6	V6/Zo	V7	V7/Zo	V8	V8/Zo
sec	μm	pF	(V)	(kV/m)	(V)	(kV/m)	(V)	(kV/m)	(V)	(kV/m)
0.1	5.59	0.95	5.2632	941.531	6.31579	1129.84	7.36842	1318.14	8.42105	1506.45
0.2	3.96	1.2	4.1667	1052.19	5.000	1262.63	5.83333	1473.06	6.66667	1683.5
0.5	2.5	1.79	2.7933	1117.32	3.35196	1340.78	3.91061	1564.25	4.46927	1787.71
1	1.77	2.3	2.1739	1228.2	2.6087	1473.84	3.04348	1719.48	3.47826	1965.12
2	1.25	2.97	1.6835	1346.8	2.0202	1616.16	2.3569	1885.52	2.6936	2154.88
3	1.022	3.46	1.4451	1413.98	1.7341	1696.77	2.02312	1979.57	2.31214	2262.37
4	0.885	3.84	1.3021	1471.28	1.5625	1765.54	1.82292	2059.79	2.08333	2354.05
5	0.792	4.2	1.1905	1503.13	1.42857	1803.75	1.66667	2104.38	1.90476	2405
6	0.722	4.5	1.1111	1538.94	1.33333	1846.72	1.55556	2154.51	1.77778	2462.3
7	0.67	4.75	1.0526	1571.09	1.26316	1885.31	1.47368	2199.53	1.68421	2513.75
8	0.626	5	1.000	1597.44	1.200	1916.93	1.400	2236.42	1.600	2555.91
9	0.59	5.22	0.9579	1623.48	1.14943	1948.18	1.341	2272.87	1.53257	2597.57
10	0.56	5.4	0.9259	1653.44	1.11111	1984.13	1.2963	2314.81	1.48148	2645.5
			q=1E-11C		q=1.2E-11C		q=1.5E-11C		q=2E-11C	
t	Zo	C	V10	V10/Zo	V12	V12/Zo	V15	V15/Zo	V20	V20/Zo
sec	μm	pF	(V)	(kV/m)	(V)	(kV/m)	(V)	(kV/m)	(V)	(kV/m)
0.1	5.59	0.95	10.526	1883.06	12.6316	2259.67	15.7895	2824.59	21.0526	3766.12
0.2	3.96	1.2	8.3333	2104.38	10.000	2525.25	12.500	3156.57	16.6667	4208.75
0.5	2.5	1.79	5.5866	2234.64	6.70391	2681.56	8.37989	3351.96	11.1732	4469.27
1	1.77	2.3	4.3478	2456.4	5.21739	2947.68	6.52174	3684.6	8.69565	4912.8
2	1.25	2.97	3.367	2693.6	4.0404	3232.32	5.05051	4040.4	6.73401	5387.21
3	1.022	3.46	2.8902	2827.96	3.46821	3393.55	4.33526	4241.94	5.78035	5655.92
4	0.885	3.84	2.6042	2942.56	3.125	3531.07	3.90625	4413.84	5.20833	5885.12
5	0.792	4.2	2.381	3006.25	2.85714	3607.5	3.57143	4509.38	4.7619	6012.51
6	0.722	4.5	2.2222	3077.87	2.66667	3693.44	3.33333	4616.81	4.44444	6155.74
7	0.67	4.75	2.1053	3142.18	2.52632	3770.62	3.15789	4713.28	4.21053	6284.37
8	0.626	5	2.000	3194.89	2.400	3833.87	3.000	4792.33	4.000	6389.78
9	0.59	5.22	1.9157	3246.96	2.29885	3896.36	2.87356	4870.45	3.83142	6493.93
10	0.56	5.4	1.8519	3306.88	2.22222	3968.25	2.77778	4960.32	3.7037	6613.76

Dataset of equivalent interfacial fields produced by a range of charges across a time-dependent capacitor.

BIBLIOGRAPHY AND LIST OF REFERENCES.

Reference Works and Cited References.

This Section contains, *i)* a list of the major works of reference consulted during the course of the present research*, together with cited references to specific publications by various researchers, followed by, *ii)* a list of the present author's publications.

*Where a published book has been used both for general and for topic-specific reference it appears in both sections.

Reference Works.

Adam, N.K. *The Physics and Chemistry of Surfaces.* Oxford University Press, 1941.

Bachelor, G.K.(Ed.) *The Scientific Papers of Sir Geoffrey Ingham Taylor. (Vol. IV)* Cambridge University Press, 1971.

Bleaney, B.I & Bleaney, B. *Electricity and Magnetism.* Oxford University Press, 1962.

Boutigny, P-H. *Etudes sur les Corps a l'Etat Spheroidale.* Paris, 1844.

Butler, J.A.V. (Ed.) *Electrical Phenomena at Interfaces.* Methuen, 1951.

Cross, J.A. *Electrostatics.* Adam Hilger, 1987.

Eisenberg, D & Kauzmann, W. *The Structure and Properties of Water.* Oxford, 1969.

Eyring, H & Jhon, M-S. *Significant Liquid Structures.* John Wiley & Sons, 1969.

Faraday, M. *Experimental Researches in Electricity.* Royal Society of London, 1832-1856.

Harper, W.R. *Contact and Frictional Electrification.* Oxford University Press, 1967.

Heilbron, J.L. *Electricity in the 17th and 18th Centuries – a Study in Early Modern Physics.* Dover Publications, New York, 1999.

Jeans, J.H. *The Mathematical Theory of Electricity and Magnetism.* Cambridge University Press, 1920.

Jenkins, F.A & White, H.E. *Fundamentals of Physical Optics.* McGraw-Hill, 1937.

Keithley Corp. *Low-Level Measurements.* Keithley Corporation, Cleveland Ohio, 5th Edn., 1998.

Le Cadet, G. *Etude de Champ Electrique de l'Atmosphere.* Libraire J.B. Bailliere et fils, Paris, 1898.

Leidenfrost, J.G. *De Aquæ Communis, nonnullis Qualitatibus, Tractatus.* University of Duisburg, 1756.

Loeb, L.B. *Static Electrification.* Springer Verlag, Berlin, 1958.

Loeb, L.B. *Electrical Coronas – their Basic Physical Mechanism.* University of California Press, 1965.
Moore, A.D. *Electrostatics.* Laplacian Press, California. 2nd Edn., 1997.
Plateau, J.A.F. *Statique Experiméntale et Théorique des Liquides soumis aux seules Forces Moléculaires*. Paris/Ghent, 1873.
Rayleigh, J.W. Strutt, Baron. *Scientific Papers.* Cambridge University Press, 1899-1900.
Temperley, H.N.V. *Properties of Matter.* University Tutorial Press, 1965.
Tolansky, S. *Multiple-beam Interferometry of Surfaces and Films.* Oxford University Press, 1948.
Worthington, A.M. *A Study of Splashes.* Longmans, Green, 1908.

Cited References.

1. Gilbert, W. *De Magnete, Magnetisque Corporibus, et de Magno Magnete Tellure.* London, (1600), English translation by P. Fleury Mottelay, (1893). Book II, Chap 2.
2. Browne, Sir Thomas. *Pseudodoxia Epidemica.* London, (1646). Book II, Chapter 4.
3. Tyndall, J. *Lessons in Electricity at the Royal Institution, 1875-6.* Longmans, 2nd. Edition, (1881). Section §5.
4. Gray, S. *A letter to Cromwell Mortimer containing several experiments in electricity.* Phil. Trans. 37, (1731-2) pp. 18-44.
5. Gray, S. *A letter concerning the electricity of water, from Mr. Stephen Gray to Cromwell Mortimer, M.D. Secr. R.S.* Phil. Trans. 37, (1731-2) pp. 227-30.
6. Nollet, The Abbè. *Part of a letter from Abbè Nollet, of the Royal Academy of Sciences at Paris, to Martin Folkes, concerning electricity.* Phil. Trans. 45, (1748), pp. 187-194.
7. Ellicott, J. *Several essays towards discovering the laws of electricity.* Phil. Trans. 45, (1748), pp. 195-202.
8. Henly, W. *An account of some new experiments in electricity.* Phil. Trans. 64, (1774), pp. 389-431.
9. Rayleigh (Lord). *The influence of electricity on colliding water drops.* Proc. Roy. Soc. 28, (1879), pp. 406-9.
10. Rayleigh (Lord) *Investigations in capillarity.* Phil. Mag. 48, (1899), pp. 321-337.
11. Bizio, B *Di un fenomeno ch' offrono in vari casi le gocciole cadenti sulla superfice di un liquido omologo.* Giornale di fisica, chimica e storia naturale. Brugnatelli, Pavia, 1, (1818), pp. 279-288.
12. Sire, G. *Phenomène des globules d'éther qui flottent sur un surface étherique.* Comptes Rendus, 37. (1853), p.657.
13. Meunier, S. *De la forme globulaire que les liquides et le gaz peuvent prendre sur leur propre surface.* Comptes Rendus, 57, (1863), pp. 401-403.
14. Boutigny, P-H. *Etudes sur les corps a l'etat spheroidale.* Paris, 1844.

15. Tomlinson, C. *On the spheroidal condition of liquids at common temperatures.* Phil Mag 26, (1863), pp. 437-441.
16. Leidenfrost, J.G. *De aquæ communis nonnullis qualitatibus, tractatus.* Duisburg, 1765.
17. Reynolds, O. *On drops floating on the surface of water.* Proc.Manchester Lit & Phil Soc 21, (1882) see also Chem. News 44, (1881), pp. 211-212
18. Maltézos, C. *Les microglobules lenticulaires liquides. Conditions de l'équilibre.* Comptes Rendus 115, (1892). pp. 717-720, and, *Conditions d'équilibre et de formations des microglobules liquides* Comptes Rendus 115, (1892). pp. 796-9.
19. Hauksbee, F. *An account of an experiment touching the direction of a drop of oil of oranges, between two glass planes, towards any side of them that is nearest press'd together.* Phil Trans 27, no. 332, (1710-1712), pp. 395-396.
20. Hauksbee, F. *An account of an experiment concerning the angle requir'd to suspend a drop of oyl of oranges, at certain stations, between two glass planes, placed in the form of a wedge.* Phil Trans 27, no 334, (1710-1712), pp. 473-474.
21. Jurin, J. *An account of some experiments shown before the Royal Society; with an enquiry into the cause of ascent of water in capillary tubes.* Phil Trans 30, no. 355, (1717), pp. 739-747.
22. Jurin, J. *An account of some new experiments, relating to the action of glass tubes upon water and quicksilver.* Phil Trans 30, no. 363, (1719), pp. 1083-1096.
23. Young, T. *An Essay on the Cohesion of Fluids.* Phil Trans 95, (1805), pp. 65-87.
24. Laplace, P.S. *Mechanique Celeste.* V. 10, supp. (1806).
25. Gauss, C.F. *Principia generalia Theoriæ Fluidorum in Statu Æquilibrii.* Gottingen, (1830).
26. Plateau, J.A.F. *Statique Experimentale et théorique des liquides soumis aux seules forces moléculaires.* Paris/Gand (Ghent), (1873).
27. Van der Mensbrugghe, G. *Sur la Tension Superficielle des Liquides consid*érée *au point de vue de certains mouvements observés a leur surfaces.* Mem. cour. de l'Ac. Roy. De Belgique (Savants Étranger), 37, (1873), pp. 3-32.
28. Maxwell, J.C. Article *Capillary Action*, Encycl. Brit. 9th ed, v.5, (1876) pp. 56-71.
29. Boys, C.V. *Soap Bubbles, and the Forces which Mould Them.* S.P.C.K., (1890).
30. Worthington, A.M. *A Study of Splashes.* Longmans, Green & Co., (1908).
31. Adam, N.K. *The Physics and Chemistry of Surfaces.* Oxford, (1930), p.212.
32. Mahajan, L.D. *The effect of the surrounding medium on the life of floating drops.* Phil. Mag. 10, (1930). p383.
33. Mahajan, L.D. *Liquid drops on the same liquid surface.* Nature 126, 1930, p.761.
34. Benedicks & Sederholm. Ark. Mat. Astr. Fys. 'B'. 30(5), (1944).
35. Prokhorov, P.S. *The effects of humidity defecit on coagulation processes and the coalescence of liquid drops.* Disc. Faraday Soc. (18), (1954), pp. 41-51.

36. Baird, M.H.I. *The stability of inverse bubbles.* Disc. Faraday Soc. (1959), pp. 213-219.
37. Scriven, L.E. and Sternling, C.V. *The Marangoni effects.* Nature 187 (4733) (1960), pp. 186-188.
38. Thompson, J. *On certain curious motions observable on the surface of wine and other alcoholic liquors.* Brit. Assos. Report for 1855, Part II, pp. 16-17.
39. Schotland, R.M. *Experimental results relating to the coalescence of water drops with water surfaces.* Disc. Faraday Soc. (30) (1960), pp. 72-77.
40. Hickman, K.C.D. *Floating drops and boules.* Nature 201 (4923) (1964), pp. 985-987.
41. Hickman, K.C.D., Maa, J.R., Davidhazy, A. & Mady, O. *Floating Drops and Liquid Boules.* Ind. and Eng. Chem. 59(10) (1967), pp. 18-41.
42. Stong, C.L. (Ed.) *Curious bubbles in which a gas encloses a liquid instead of the other way round.* Scientific American 230(4), (1974), pp. 116-120.
43. Dell'Aversana, P., Monti, R. & Gaeta, F.S. *Marangoni flows and coalescence in microgravity.* Adv. Space Res. 16(7), (1995), pp.95-98.
44. Dell'Aversana, P., Banavar, J. & Koplik, J. *Suppression of coalescence by shear and temperature gradients.* Phys. Fluids 8(1), (1996), pp. 15-28.
45. Dell'Aversana, P., Tontodonato, V. & Carotenuto, L. *Suppression of coalescence and of wetting: the shape of the interstitial film.* Phys. Fluids 9(9), (1997), pp. 2475-2485.
46. Dell'Aversana, P & Neitzel, G.P. *When fluids stay dry.* Physics Today, (Jan. 1998), pp. 38-41.
47. Nahmias, J., Téphany, H. & Méjanelle, P. *Long lifetime floating drops.* J. Colloid Int. Sci. 190 (1997), pp. 497-498.
48. Téphany, H., Nahmias, J. *Lifetime of floating drops under low pressure.* J. Colloid Int. Sci. 217 (1999), pp. 214-215.
49. Savino, R., Paterna, D. & Lappa, M. *Marangoni floatation in liquid droplets.* J. Fluid Mech. 479 (2003), pp. 307-326.
50. Amarouchene, Y., Christbal, G. & Kellay, H. *Noncoalescing drops.* Phys. Rev. Letters 87(20) (2001), art. 206104, 4pp.
51. Rayleigh (Lord). *On the capillary phenomena of jets.* Proc. Roy. Soc., 29 (1879), pp. 71-97.
52. Rayleigh (Lord). *On the tension of recently formed liquid surfaces.* Proc. Roy. Soc., 47 (1890), pp. 281-287.
53. Allan, R.S. & Mason, S.G. *Effects of electric fields on coalescence in liquid + liquid systems.* Trans. Faraday Soc., 57. (1961), pp. 2027-2040.
54. Jayaratne, O.W. & Mason, B.J. *The coalescing and bouncing of drops at an air/water interface.* Proc. Roy. Soc. 'A', 280(1383), (1964), pp. 545-565.
55. Mason, B.J., Jayaratne, O.W. & Woods, J.D. *An improved vibrating capillary device for producing uniform water droplets of 15 to 500μm radius.* J. Sci. Instruments 40, (1963), pp. 247-249.
56. Brazier-Smith, P.R., Jennings, S.G. & Latham, J. *The interaction of falling water drops: coalescence.* Proc. Roy. Soc.,'A' 326 (1972), pp. 393-408.

57. Stong, C.L. (Ed) *Water drops that float on water.* Scientific American, 229(8), 1973, pp. 104-109.
58. Walker, J. *Drops of liquid can be made to float on the liquid. What enables them to do so?* Scientific American, 238(6) (1978), pp. 123-129.
59. Ochs, H.T. & Czys, R.R. *Charge effects on the coalescence of water drops in free fall.* Nature 327 (1987), pp. 606-608.
60. Orme, M. *Experiments on droplet collisions, bounce, coalescence and disruption.* Prog. in Energy & Comb. Sci., 23 (1997) pp. 65-79.
61. Ahern, J.C. & Balachandran, W. *Some basic phenomena of water boules.* Proc. ESA Annual Meeting, Brock University. (2000), pp. 195-203.
62. Spencer, H.M. *Laboratory methods for maintaining constant humidity.* International Critical Tables, McGraw-Hill/NRC, (1926-33).
63. Franks, F. *Water.* Royal. Society of Chemistry (1984), p.10.
64. Taylor, R.J. *Water.* Unilever Advanced Educational booklet (1969).
65. Bjerrum, N. *Structure and properties of ice.* Science 115 (1952), pp. 385-390.
66. Eigen, M & de Maeyer, L. *Self-dissociation and protonic charge transport in water and ice.* Proc. Roy. Soc. 'A' 247 (1958), pp. 505-533.
67. Helmholtz, H. *Studiern uber electrisshe Grenzschichten.* Weid. Ann. Phys. 7, (1879), pp. 337-382.
68. Guoy, G. *Constitution of electrical charge at surface of an electrolyte.* J. Physique 9 (1910), p.457.
69. Chapman, D.L. *Theory of electrocapillarity.* Phil. Mag. 25 (1913) pp. 475-485.
70. Stern, O. *Theory of the electrical double layer.* Z. Electrochem. 30 (1924), p.508.
71. Butler, J.A.V. *Electrical phenomena at interfaces.* Methuen (1951), p.52.
72. Cross, J.A. *Electrostatics.* Adam Hilger (1987), p.68.
73. Loeb, L.B. *Static Electrification.* Springer Verlag, Berlin. (1958), pp. 65-74.
74. McTaggart, H.A. *On the electrification at the boundary between a liquid and a gas.* Phil. Mag. 44, (1922), pp. 386-395.
75. Quincke, G.H. Pogg. Ann. 113, (1861), p.513.
76. Alty, T. *The cataphoresis of gas bubbles in water.* Proc. Roy. Soc. 'A' 106, (1924), pp. 315-340.
77. Chalmers, J.A. & Pasquill, F. Phil. Mag. 23. (1937), p.88.
78. Lenard, P. *Über die elektrizität der Wasserfalle*. Ann. Phys. Lpz. 46, (1892), p. 584.
79. Lenard, P. *Über wasserfalleelektrizität und über die oberflächen-beschaffenheit der flüssigkeiten.* Ann. Phys. Lpz. 47, (1915), pp. 463-524.
80. Levin, Z & Hobbs, P.V. *Splashing of water drops on solid and wetted surfaces: hydrodynamics and charge separation.* Phil. Trans. 269 (1971), pp. 555-585.
81. Wang Y.Y. & Bailey, A.G. *Drop charging during liquid dispersion.* Inst. Phys. Conf. Ser. 163 (1999), pp. 167-170.
82. Efimov, N.A, Zvonov, V.A & Efimova, L.Ya. *Investigation of the effect of the nature of an applied voltage on the flow of benzine.* Electron. Obrab. Math. USSR Vol 1(1979), pp.45-47.

83 Sato, M, Kudo, N & Saito, M. *Surface tension reduction of liquid by applied electric field using vibrating jet method.* IEEE Trans. Ind. Apps. 34(2) (1998), pp. 294-300.
84. Schmidt, G.M, Hurd, R.M & Snavely, E.S. *Effect of electrostatic field on the surface tension of salt solution.* J. Electroche. Soc. 109(9) (1962) pp.852-858.
85. Leob, L.B. *The basic mechanisms of static electrification.* Science 102 (1945), pp. 573-576.
86. Bowden, F.P. *The amount of hydrogen and oxygen present on the surface of a metallic electrode.* Proc. Roy. Soc. 'A' 125 (1929), pp. 446-462.
87. Elton, G.A.H. *Electroviscosity.II. Experimental demonstration of the electroviscous effect.* Proc. Roy. Soc. 'A' 194 (1948), pp. 275-287.
88. Frankel, S.P & Mysels, K.J. *On the dimpling during the approach of two interfaces.* J. Phys. Chem. 66 (1962), pp. 190-191.
89. Chen, J-D. *Effects of London-van der Waals and electrical double layer forces on the thinning of a dimpled film between a small drop or bubble and a horizontal solid plane.* J. Coll. Int. Sci. 98(2) (1984), pp. 329-341.
90. Schulze H.J. *Einige untersuchungen ueber das zerreissen duenner fluessigkeitsfilme auf feststoffoberflaechen. (Rupture studies of thin liquid films on solid surfaces).* Colloid. Polym. Sci. 253 (1975) pp. 730-737.
91. Yiantsios, S.G. & Davis, R.H. *On the buoyancy-driven motion of a drop towards a rigid surface or a deformable interface.* J. Fl. Mech. 217 (1990), pp. 547-573.
92. Yiantsios, S.G. & Davis, R.H. *Close approach and deformation of two viscous drops due to gravity and van der Waals forces.* J. Coll. Int. Sci. 144(2) (1991), pp. 412-433.
93. Wilson, M.A, Pohorille, A & Pratt, L.R. *Molecular dynamics of the water liquid-vapor interface.* J. Phys. Chem. 91 (1987), pp. 4873-4878.
94. Wilson, M.A, Pohorille, A & Pratt, L.R. *Surface potential of the water liquid-vapor interface.* J. Chem. Phys. 88(5) (1987), pp. 3281-3285.
95. Edgerton, H.E, & Killian, J.R. *Flash! Seeing the unseen by ultra high speed photography.* Hale, Cushman & Flint, Boston (1939).
96. Macklin, W.C. & Hobbs, P.V. *Subsurface phenomena and the splashing of drops on shallow liquids.* Science. 166. (1969), pp. 107-108.
97. Dooley, B.S, Warncke, A.E, Gharib, M & Tryggvason, G. *Vortex ring generation due to the coalescence of a water drop at a free surface.* Exp. in Fluids. 22 (1997), pp. 369-374.
98. Manzello, S.L. & Yang, J.C. *An experimental study of a water droplet impinging on a liquid surface.* Exp. in Fluids. 32 (2002), pp. 580-589.
99. Ochs, H.T, Beard, K.V, Laird, N.F, Schaufelberger, D.E, & Holdridge, D.J. *Collisions between small precipitation drops.* J. Atmos. Sci., 52(12) (1995) pp.2258 - 2275.
100. Ochs, H.T, Beard, K.V, Laird, N.F, Schaufelberger, D.E, & Holdridge, D.J. *Effects of relative humidity on the coalescence of small precipitation drops in free fall.* J. Atmos. Sci., 52(21) (1995) pp.3673-3680.
101. Jones, A.F & Wilson, S.D.R. *The film drainage problem in droplet coalescence.* J. Fluid Mech. 87(2) (1978) pp. 263-288.

102. Jeelani, S.A.K & Hartland, S. *Effect of surface mobility on collision of spherical drop.* J. Coll. Interface Sci. 206(1998) pp. 83-93.
103. Kumar, K, Nikolov, A.D & Wasan, D.T. *Effect of film curvature on drainage of thin liquid films.* J. Coll. Interface Sci. 256 (2002) pp. 194-200.
104. Lindblad, N.R. *Effects of relative humidity and electric charge on the coalescence of curved water surfaces*. J. Colloid Sci.,19 (1964) pp. 729-743.
105. Taylor, G.I. *The coalescence of closely spaced drops when they are at different electric potentials.* Proc. Roy. Soc. 'A'., 306 (1968) pp. 423-434.
106. Newton, F.H & Searle, V.H.L. *The General Properties of Matter – Chapter 6*. Arnold, London, 1950.
107. Du Nouy, P (Lecomte) J. Gen. Physiol (1) 521 (1919).
108. Langmuir, I. *The evaporation of small spheres*. Phys. Rev., 12(5) (1918), pp. 368-370.
109. O'Brien, R.N & Savill, P. *Investigation of liquid drop evaporation by laser interferometry.* Langmuir, 3 (1987) pp. 41-45.
110. Ray, A.K, Lee, J & Tilley, H.L. *Direct measurements of evaporation rates of single droplets at high Knudsen numbers.* Langmuir, 4 (1988), pp. 631-637.
111. Ivchenko, I.N & Muradyan, S.M. *Ов Испарении Сферических Капель Бинарной Газовой Смеси При Ироизвольлых Числах Кнудсена.* Izv. Akad. Nauk. SSSR, Mekh. Zhidk. Gaza. (1982) (1), pp. 112-118.
112. Birdi, K.S., Vu, D.T. & Winter, A. *A study of the evaporation rates of small water drops placed on a solid surface.* J. Phys. Chem., 93 (1989), pp. 3702-3703.
113. Nolan, J.J. Proc. *The breaking of water drops by electric fields.* Roy. Irish Acad. 37 (1926), pp. 28-39.
114. Macky, W.A. *Some investigations on the deformation and breaking of water drops in strong electric fields.* Proc. Roy. Soc. 'A'., 133 (822) (1931), pp. 565-587.
115. Latham, J & Roxburgh, I.W. *Disintegration of pairs of water drops in an electric field.* Proc. Roy. Soc. 'A'., 295 (1966), pp. 84-97.
116. Wilson, C.T.R & Taylor, G.I. *The bursting of soap bubbles in a uniform electric field.* Proc. Camb. Phil. Soc. 22 (1925), pp.728-730.
117. Davis, M.H. *Two charged spherical conductors in a uniform electric field: Forces and field strength.* Quart. J. Mech. and Appl. Maths. 17(4) (1964), pp. 499-511.
118. Worthington, A.M. *On impact with a liquid surface.* Proc. Roy. Soc. 34 (1882/3),, pp.201-230.
119. Worthington, A.M, & Cole, R.S. *Impact with a liquid surface studied by the aid of instantaneous photography.* Phil. Trans. 'A' 189 (1897), pp. 137-148.
120. Worthington, A.M, & Cole, R.S. *Impact with a liquid surface studied by the aid of instantaneous photography: paper II.* Phil. Trans 'A' (1900), pp. 175-199.
121. Rayleigh (Lord). *On the equilibrium of liquid conducting masses charged with electricity.* Phil. Mag. (Series 5), 14 (1882) pp. 184-186.

122. Zeleny, J.*On the conditions of instability of electrified drops, with applications to the electrical discharge from liquid points.* Proc. Camb. Phil. Soc. 18 (1915), pp. 71-83.
123. Taylor, G.I. *Disintegration of water drops in an electric field.* Proc. Roy. Soc. 'A' 280 (1964), pp. 383-397.
125. Taylor, G.I. & Mc.Ewan, A.D. *The stability of a horizontal fluid interface in a vertical electric field.* J. Fluid Mech. 22 (1965), pp.1-15.
125. Taylor, G.I. *Instability of jets, threads and sheets of viscous fluid.* Proc. 12th Int. Congress of App. Mech. (Springer Verlag 1969), pp. 382-388.
126. Eow, J.S. & Ghadiri, M. *The behaviour of a liquid-liquid interface and drop-interface coalescence under the influence of an electric field* Colloids & Surfaces 'A' 215 (2003), pp. 101-123.
127. Eow, J.S, Ghadiri, M. & Sharif, A. *Experimental studies of deformation and break-up of aqueous drops in high electric fields.* Colloids and Surfaces 'A' 225 (2003) pp.193-210.
128. Ahern, J.C. & Balachandran, W. *Influence of relative humidity on the electrical field strength to promote coalescence between two water drops.* J.Electrostatics (2003 – in press)
129. Granick, S. *Motions and relaxations of confined liquids.* Science 253 (1991) pp. 1374-1379.
130. Koplik, J & Banavar, J.R. *Molecular structure of the coalescence of liquid interfaces.* Science 257 (1992), pp. 1664-1666.
131. Miller, A.H, Shelden, C.E & Atkinson, W.R. *Spectral study of the luminosity produced during coalescence of oppositely charged falling water drops.* Phys. Fluids 8 (11) (1965), pp. 1921-1928.
132. Phelps, C.T, Griffiths, R.F & Vonnegut, B. *Corona produced by the splashing of water drops on a water surface in a strong electric field.* J.App.Phys. 44 (7) (1973) pp. 3082-3086.
133. Matsui, M, Murasaki, N, Fujibayashi, K, Bao, P-Y, & Kishimoto, Y. *Electrification of pure water flowing down a trough set up with a resin sheet.* J.Electrostatics 31 (1993), pp. 1-10.

AUTHOR'S PUBLICATIONS.

Ahern, J.C & Balachandran, W. *Some basic Phenomena of Water Boules.* Proc. ESA Annual Meeting, Brock University, Ontario. 2000.

Ahern, J.C & Balachandran, W. *Some Electrical Phenomena accompanying Drop Coalescence.* DRC2000 Doctoral Research Conference, Brunel University, 2000.

Ahern, J.C & Balachandran, W. *An Electrical Event accompanying Drop Coalescence.* Proc. ESA Annual Meeting, Michigan State University, Lansing Michigan, 2001

Balachandran, W, Ahern, J.C. & Kulon, J. *Electrohydrodynamic Micro and Nano Spray.* 7th ILASS-Asia Conference, Tainan, Taiwan, 2002.

Ahern, J.C & Balachandran, W. *Electrohydrodynamic Nanospray production using Drawn Glass Capillaries.* Proc. ESA-IEEE Joint Meeting, University of Arkansas at Little Rock, 2003.

Ahern, J.C & Balachandran, W. *Influence of Relative Humidity of the Electric Field Strength to promote Coalescence between two Water Drops.* J.Electrostatics, 2003 (in press).

Ahern, J.C & Balachandran, W. *Experimental Electrohydrodynamic Nanospray Production using Drawn Glass Capillaries.* Particulate Science and Technology: An International Journal. 2003 (submitted).